Distribution Agreement

In presenting this thesis or dissertation as a partial fulfillment of the requirements for an advanced degree from Emory University, I hereby grant to Emory University and its agents the non-exclusive license to archive, make accessible and display my thesis or dissertation in whole or in part in all forms of media, now or hereafter known, including display on the world wide web. I understand that I may select some access restrictions as part of the online submission of this thesis or dissertation. I retain all ownership rights to the copyright of the thesis or dissertation. I also retain the right to use in future works (such as articles or books) all or part of this thesis or dissertation.

Signature:

Avanti Gokhale

_____ _____

Student's Name Date

Regulation of ciliary dynein by the axonemal protein kinase CK1

By

Avanti Gokhale
Doctor of Philosophy

Graduate Division of Biological and Biomedical Science
Biochemistry, Cell and Developmental Biology

_____

Winfield S.Sale, Ph.D.
Advisor

_____

Victor Faundez, M.D, Ph.D.
Committee Member

_____

Maureen Powers, Ph.D.
Committee Member

_____

Karl Saxe, III, Ph.D.
Committee Member

_____

Steve L'Hernault, Ph.D.
Committee Member

Accepted:

_____

Lisa A. Tedesco, Ph.D.
Dean of the Graduate School

_____

Date

Regulation of ciliary dynein by the axonemal protein kinase CK1

By

Avanti Gokhale
B.Sc University of Madras
M.S Pondicherry Central University

Advisor: Winfield S. Sale, Ph.D.

An abstract of
a dissertation submitted to the Faculty of the Graduate School of Emory University in partial fulfillment of the requirements for the degree of
Doctor of Philosophy

Graduate Division of Biological and Biomedical Science
Biochemistry, Cell and Developmental Biology

2009

Abstract

Regulation of ciliary dynein by the axonemal protein kinase CK1

By Avanti Gokhale

Cilia are highly conserved organelles that play essential motile and sensory roles required for normal development and function of most organs in the adult. The goal of my work is to study mechanisms that regulate dynein motor activity and control ciliary/flagellar motility. Genetic and functional studies revealed ciliary dynein is regulated by phosphorylation, and that a CK1-like kinase is located in the axoneme and thought to phosphorylate the intermediate chain IC138 of the inner dynein arm isoform I1. I postulated that CK1 is targeted and anchored on the outer doublet microtubules, near I1 dynein, to regulate dynein-driven microtubule sliding and control ciliary movement. To test this, I cloned and characterized the axonemal CK1 in *Chlamydomonas*, and confirmed it is a highly conserved member of the CK1 family of kinases. Analysis of ciliary structural mutants and immunofluorescence analysis revealed that CK1 is anchored on the outer doublet microtubules, along the entire length of the axonemes. Consistent with this localization, chemical crosslinking in axonemes revealed that CK1 directly interacts with tubulin.

To study the physiologocial role of axonemal CK1, I took advantage of an in vitro microtubule sliding assay to measure dynein activity in mutant axonemes lacking the radial spoke structures (*pf17).* Importantly, in absence of the radial spokes, axonemal CK1 activity is misregulated resulting in global inhibition of dynein-driven microtubule sliding. Consistent with this conclusion, CK1 inhibitors rescued dynein activity in *pf17* axonemes. Using a novel approach, to produce CK1-depleted axonemes, I tested the idea that removal of CK1 would restore dynein activity. As predicted, CK1 depletion restored dynein-driven microtubule sliding, mimicking the effect of CK1 inhibitors. Using a purified, recombinant CK1, I reconstituted the CK1-depleted *pf17* axonemes and restored inhibition of dynein activity, in a CK1 kinase-inhibitor sensitive manner. Furthermore, reconstitution of CK1-depleted axonemes with a purified, recombinant "kinase-dead" CK1 did not restore the inhibition of dynein activity. These results demonstrated that CK1 kinase activity is required for regulation of dynein-driven microtubule sliding.

This work addresses fundamental aspects of signal transduction and regulation of dynein motors in cilia. The data are consistent with the model that CK1 is a structural component of the axoneme, localized on the outer doublet microtubules in position to regulate phosphorylation of IC138 and control microtubule sliding. Additional challenges include identifying the precise location of CK1 in the axoneme and identifying interacting proteins that anchor and localize CK1. One prediction is that CK1 is located adjacent to I1 dynein, anchored by a novel class of CK1-anchoring proteins (CKAPs). Further tests also include identification of key phosphorylated residues in IC138 to directly test how IC138 contributes to regulation of dynein activity and ciliary motility.

Regulation of ciliary dynein by the axonemal protein kinase CK1

By

Avanti Gokhale
B.Sc University of Madras
M.S Pondicherry Central University

Advisor: Winfield S. Sale, Ph.D.

A dissertation submitted to the Faculty of the Graduate School of Emory University in partial fulfillment of the requirements for the degree of
Doctor of Philosophy

Graduate Division of Biological and Biomedical Science
Biochemistry, Cell and Developmental Biology

2009

Acknowledgements

The last six years have been an education not only in the fundamentals of biology, but in the philosophy of life. For his instinctive belief in me, incredible patience and fortitude, breadth of knowledge and generosity of spirit I thank Win Sale – mentor, colleague and lifelong friend. He has taught me the best lessons in life by living them.

Sincere gratitude to my committee members – Victor Faundez, Steve L'Hernault, Maureen Powers and Karl Saxe- for there support, guidance and conversations. They are the finest examples that committee meetings can be hugely productive, rigorous, and fun.

Much thanks to my lab family- to Laura- who taught me to think with my hands, to Maureen- for being generous with her time and mind, to Candice- for being quintessentially, Candice, to Rasagnya- for being a fearless questioner and to Tal and Feifei- for being young, enthusiastic scientists. I could not have asked for a more fertile and nourishing environment.

I am grateful to be a part of my batch of classmates- especially Marie (class mom), Rob (class drinker), Seth (class brewer), Dina (class jester) and Emma (class spirit). We have shared and survived a similar path and experiences and in their individual unique way they have enriched my graduate experience.

Atlanta has become home to me because of a great circle of friends– my Georgia tech companions, Amisha, Chirag, Anu and Farzan. Thank you for giving me a life outside the lab. I am particularly indebted to Srini- for being my first friend here, whose constant prodding literally drove me to Emory, to this Ph.D. I have not forgotten.

I am blessed with a strong genetic pool. To my grandfathers – Appa - the orginal philanthropist and Nana- the original curious scientist- although I could not find a way to cite your scientific contributions, this is a formal, written acknowledgement of your contribution to me as an individual. I would only be so lucky to have a generous portion of your genes.

To my dad and mom, educationists and parents extraordinaire – for endeavoring, being models of strength, resilience, perseverance and passion. You make me want to do so much more. This is as much your achievement as it is mine.

And to Sumegha- for everything she is, and more importantly, everything she is not.

Table of contents:

List of Figures and Tables:

Chapter 1:

Chapter 2:

Chapter 3:

Figure 2: Model for localized regulation of CK1 activity, I1 dynein and axonemal bending:

Figure 3: CK1 is assembled in *pf27* axonemes

Figure 4: *pf27* axonemes slide at the same rate as wild-type axonemes

Figure 5: IC138 is abnormally phosphorylated in *pf27* axonemes

Figure 6: Mapping of CK1 and *pf27*, and strategy for cloning *PF27* using BACs and transformation – rescue of *pf27*

List of abbreviations:

AKAP - A-kinase anchoring protein

BAC - Bacterial artificial chromosome

BBS- Bardet-biedl syndrome

CK1-7- N-(2-aminoethyl)-5-chloroisoquinoline-8-sulfonamide

CKAP – CK1-anchoring protein

CP – Central pair

CSC – Calmodulin and spoke associated complex

DEAE - Diethylaminoethyl cellulose

DFDNB - 1, 5-Difluoro-2,4-dinitrobenzene

DMP- Dimethyl pimelimidate•2 HCl

DMSO – Dimethyl sulfoxide

DRB - 5,6-dichloro-1-beta-D-ribofuranosylbenzimidazole

DRC- Dynein regulatory complex

DSS - Disuccinimidyl suberate

DTT - Dithiothreitol

EDC - 1-Ethyl-3-[3-dimethylaminopropyl]carbodiimide hydrochloride

EDTA - Ethylenediaminetetraacetic acid

EGTA- Ethylene glycol tetraacetic acid

FPLC – Fast pressure liquid chromatography

HC – Heavy chain

IC – Intermediate chain

IDA- Inner dynein arm

IFT – Intraflagellar transport

IPTG- Isopropyl β-D-1-thiogalactopyranoside

KHD- Kinesin homology domain

LC – Light chain

MC- Microcystin-LR

NLS – Nuclear localization signal

ODA – Outer dynein arm

ODA-DC – Outer dynein arm – docking complx

PCD - Primary ciliary dyskinesia

PKA - Protein kinase A

PKD- Polycystic kidney disease

PKI- Protein kinase inhibitor

PMSF- Phenyl-methane-sulphonyl-fluoride

PVDF- Polyvinylidene Fluoride

rCK1 – Recombinant CK1

rCK1-KD – Recombinant CK1-kinase dead

RS – Radial spoke

Chapter 1: Introduction.

I. Overview and Significance:

The overall objective of this dissertation work is to determine mechanisms that regulate the molecular motor dynein and control of ciliary/flagellar motility (in this dissertation, the terms cilia and flagella will be used interchangeably). We are particularly interested in defining a ciliary signaling pathway that ultimately controls dynein motor activity by phosphorylation. Importantly, the key components of this signaling pathway are physically anchored in the "9+2" axoneme, a conserved microtubule scaffold that includes the molecular motor dynein, and structures called the central pair apparatus and the radial spokes, as well as highly conserved protein kinases and phosphatases (reviewed in Porter and Sale, 2000). The main focus of this thesis is an axonemal kinase CK1 (formerly known as casein kinase 1), and its role in regulating dynein activity by phosphorylation of dynein subunits. I will demonstrate that an axonemal phospho-regulatory mechanism impinges on a single dynein isoform called "I1 dynein", and its regulatory intermediate chain IC138, for control of dynein-driven microtubule sliding (Wirschell *et al.*, 2007; Bower *et al.*, 2009; Wirschell *et al.*, 2009). Together, the central pair apparatus, radial spokes and I1 dynein define a network of conserved structures and enzymes – the "CP/RS/I1 regulatory mechanism"- that controls the size and shape of the ciliary bend. My goal was to determine the functional role of CK1 in the CP/RS/I1 regulatory mechanism. The general hypothesis is that the protein kinase, CK1, is localized in the axoneme, near I1 dynein, and is a "downstream" regulator of dynein-driven microtubule sliding in the CP/RS/I1 regulatory mechanism.

To better understand the mechanisms that control ciliary motility, I will define the axonemal structures responsible for regulation including the central pair apparatus, radial

spoke structures and the inner dynein arm- I1 dynein. I will also define axonemal kinases, particularly CK1, and the axonemal phosphatases responsible for control of axonemal protein phosphorylation. As emphasized in this dissertation, the catalytic subunit of CK1, and other signaling proteins, are highly conserved across species, including in *Chlamydomonas,* and physically anchored to the axoneme (Porter and Sale, 2000; Wirschell *et al.*, 2007). Thus, the key question is: How are these ubiquitous enzymes targeted and anchored in the microtubule based axoneme?

Significance: My work is focused on the molecular mechanism that regulates dynein motors and ciliary motility. The dyneins are a family of large, complex, highly conserved microtubule-associated molecular motors responsible for a wide range of cellular functions, including movement of cilia, "retrograde" movement of organelles and protein cargo, assembly and function of the Golgi and assembly and function of the mitotic spindle (Karki and Holzbaur, 1999; Vallee *et al.*, 2004; Oiwa and Sakakibara, 2005; Hook and Vallee, 2006; Brokaw, 2009). As illustrated in Fig. 1, common features of dyneins include a conserved motor domain, found in characteristically large heavy chains, intermediate chains and light chains. The ciliary axoneme bears at least 8 distinct dyneins, each targeted to a specific, unique position on the microtubule "cargo" and each appears to play unique, albeit overlapping roles for generation and control of ciliary motility. Major questions about all dynein motors include: What is the mechanism of ATP force generation? What is the mechanism of targeted anchoring to cellular cargo? And how is dynein motor activity regulated?

Major advances in structural and biophysical approaches have led to a new understanding of the force generating mechanism in the dyneins, a topic beyond the

scope of this thesis (Oiwa and Sakakibara, 2005; Carter *et al.*, 2008; Gennerich and Vale, 2009; Kon *et al.*, 2009; Roberts *et al.*, 2009). However, we still have a limited understanding of how the dynein motors are targeted to cargo or how dynein activity is regulated. This thesis focuses on regulation of axonemal dynein activity, taking advantage of the model system *Chlamydomonas,* and is based on diverse studies indicating that dynein-driven microtubule sliding is regulated by phosphorylation of specific dynein subunits in cilia (Habermacher and Sale, 1997).

Cilia or flagella are microtubule based structures that are highly conserved in both protein composition as well as structural organization (Satir and Christensen, 2007; Basu and Brueckner, 2008; Christensen *et al.*, 2008). Recent research has revealed the presence of cilia on nearly all differentiated cells in metazoa, and, in addition to motility, cilia display an extraordinary range of vital signaling roles required for normal control of cell division cycle, sensory transduction required for vertebrate development and adult functions. Cilia are typically characterized either as playing mechano-sensory roles as immotile, sensory "primary cilia", or in locomotion required for cell movement. Examples of motility include- movement of sperm cells or protozoa, or the directed motility on apical surface epithelia. Such epithelia are found in the embryonic node, airways, oviducts and brain ventricles of the vertebrates. Consequently, defects in either assembly or function of cilia can result in a wide spectrum of diseases, termed "ciliopathies", listed in Table 1 (Snell *et al.*, 2004; Christensen *et al.*, 2007; Marshall, 2008b; Sharma *et al.*, 2008; Gerdes *et al.*, 2009). Examples include Bardet-Bieldl syndrome (BBS) resulting in a range of defects (obesity, polycystic kidney disease, blindness), primary cilia dyskinesia (PCD) often resulting in defects in Left-Right pattern

formation (Kartaganer's syndrome), hydrocephaly, airway infections and male infertility, polycystic kidney disease (PKD) and retinal degeneration. Much of the recent fundamental work that has led to better understanding of the genetic and physiological basis of the ciliopathies has been carried out using the model genetic system *Chlamydomonas reinhardtii. Chlamydomonas* is a powerful experimental system for study of ciliary motility and recent genomic and proteomic studies have directly revealed the conserved genes and proteins required for normal health (reviewed in Pazour and Witman, 2009). The focus of this dissertation work is on motile cilia and the regulation of ciliary motility, taking advantage of the genetic and biochemical model system *Chlamydomonas reinhardtii*. One of the key questions is: How is ciliary motility controlled?

The experimental system: Chlamydomonas has become the champion system for study of the assembly, structure and mechanism of cilia and is a very powerful experimental system for discovery of conserved genes required for normal ciliary assembly and function in all organisms, including humans (Pazour and Witman, 2009). Indeed, much of our understanding of the ciliopathies is a direct result of studies in *Chlamydomonas* (Merchant *et al.*, 2007; Pazour and Witman, 2009). *Chlamydomonas* is a biflagellate alga, primarily used to study basal body assembly and ciliary motility. *Chlamydomonas* is also a powerful genetic and molecular system for study of chloroplast and mitochondrial biology. The most commonly used laboratory species is *Chlamydomonas reinhardtii,* a haploid cell that can reproduce vegetatively or sexually. Each cell is 10 μm in diameter and they use their two flagella to swim, often in response to light stimuli, in a process termed phototaxis. In addition, the flagella are critical for

cell-cell recognition and mating during sexual reproduction (Snell, 1976). The flagella in *Chlamydomonas* are not required for viability. Thus, mutants that exhibit flagellar defects, including paralyzed flagella or organisms that completely lack flagella, are viable and can be easily isolated by simple motility or taxis screens (Pazour *et al.*, 1995; King and Dutcher, 1997). Motility-defective mutants can be then grown on agar plates or in liquid culture using simple, minimal media (Harris, 2009).

Chlamydomonas has several advantages as a model genetic system. *Chlamydomonas* is normally haploid, and has two mating types, "+" and "-" that, when differentiated, can mate, undergo zygote formation and meiosis. Meiotic progeny allow genetic mapping by tetrad analysis in mapping strains. Thus, like yeast and other haploid organisms, *Chlamydomonas* is amenable to efficient genetic analysis and mapping of genes by relatively simple approaches. The cells can also be transformed by exogenous DNA and stable diploid cells can be isolated by taking advantage of useful auxotrophic mutations for selection (Ebersold, 1967). Notably, zygotes produced after mating form temporary quadriflagellate dikaryons useful for complementation rescue assay and analysis of flagellar assembly (e.g. Luck et al., 1977). To date, *Chlamydomonas* is the only organism that allows for transformation of the nuclear, chloroplast and mitochondrial genome. The nuclear genome has been sequenced and a well annotated genomic database has been produced and maintained, founded on a nearly complete sequence (http://genome.jgi-psf.org/Chlre4/Chlre4.home.html). Additionally, BAC, cDNA and nuclear genomic libraries, and mutant maps, are available in a very useful public database (http://www.chlamy.org/chlamydb.html). The database includes description of mutant strains and reagents important for *Chlamydomonas* research. Using

these molecular tools, we can often directly map and clone genes starting with protein or genomic sequence (see discussion of flagellar proteome below) or identify mutants corresponding to a particular region in a chromosome using a positional mapping approach.

An additional major advantage is that *Chlamydomonas* cells can be grown in large quantities to produce sufficient ciliary proteins suitable for biochemical and structural analysis (Witman, 1986). Thus, *Chlamydomonas* offers a valuable combination of genetic and biochemical approaches that have revealed the composition and function of most ciliary axonemal structures. The *Chlamydomonas* strain collection includes flagellar structural mutants useful for localization of proteins in specific axonemal structures (see Table 2). The library of structural and motility mutants is maintained in the *Chlamydomonas* core collection that enables study of genetic interactions (http://www.chlamy.org/). In addition, Pazour and Witman have published a comprehensive ciliary proteome made possible due to the isolation of significant amounts of ciliary and axonemal proteins with high degree of purity (Pazour et al., 2005). Notably, with limited exceptions, all the proteins described in the *Chlamydomonas* proteome are highly conserved in ciliary cells and many are targeted to, and enriched in, the ciliary compartment.

As a consequence of the genome and ciliary proteome many of fundamental studies that defined the ciliopathies, listed in Table 1, were based on studies in *Chlamydomonas*. This includes conserved proteins required for assembly of both primary and motile cilia using a mechanism called intraflagellar transport (IFT; reviewed in Rosenbaum, 2002; Pedersen *et al.*, 2006; Scholey and Anderson, 2006). The process of

IFT and the proteins involved have been defined by detailed biochemical analysis of the membrane-matrix fraction of the *Chlamydomonas* flagellum and functional studies in *C.elegans*, zebrafish and mouse (Pazour *et al.*, 2000; Insinna *et al.*, 2008; Omori *et al.*, 2008). Defective IFT machinery has been implicated in many disease phenotypes including BBS, polycystic kidney disease, and other diseases and syndromes listed in Table 1. Therefore, *Chlamydomonas* is not only successfully used to study mechanisms of ciliary motility, it has also been useful in delineating fundamental mechanisms of ciliary assembly and signaling pathways that are common to both motile and primary cilia and defining genes required for normal human development and adult functions.

Major questions in the field include: How are cilia assembled? How is ciliary motility regulated? How does the microtubule-based molecular motor dynein contribute to ciliary motility and, how is dynein activity regulated in cilia? This thesis describes a chemical and structural signaling pathway that is implicated in controlling dynein activity by phosphorylation. The phospho-regulatory pathway is inherent to the axoneme; each component, including the kinase CK1 and the phosphatases PP1 and PP2A, are physically anchored in the "9+2" structure. Thus, a key principle and foundation for my study is that each regulatory component is physically assembled in a single, complex structure, the axoneme, which includes the dynein motors and the regulatory structures and conserved signaling proteins. Importantly, isolated axonemes can be reactivated to move when suspended in buffers containing ATP (Gibbons and Gibbons, 1972; Kamiya and Witman, 1984). Thus, the machinery required for movement is physically built into this complex, conserved, "solid-state machine". As developed in this thesis, the signaling proteins are also built directly into the structure, and include calcium-binding proteins

(Kamiya and Witman, 1984; Dymek and Smith, 2007) and the kinases and the phosphatases discussed here.

II: Structure and mechanism of motile cilia:

Motile cilia contain a bundle of nine outer doublet and two central microtubules called the 9+2 axoneme (Fig. 2A). While the length of the ciliary axoneme can vary between 10 and 100 μm, the diameter of the axoneme is remarkably constant across species at 0.18 μm. The axoneme is surrounded by the ciliary membrane, which is continuous with, but distinct from, the plasma membrane. For example, the protein polycystin is exclusively found in the ciliary membrane (Pazour et al., 2002). Additionally, the ciliary membrane also contains specialized ion channels, including voltage-sensitive calcium channels, that regulate calcium influx in response to change in voltage and control calcium concentration in the ciliary compartment (Dunlap, 1977; Quarmby, 2009) and detergent resistant domains (Iomini *et al.*, 2006). Unresolved issues include determining how the membrane and ciliary matrix proteins targeted to the cilium (Tyler et al., 2009) and are segregated from proteins and lipids in the plasma membrane (see ciliary "necklace"; Gilula and Satir, 1972).

Cilia can be easily isolated from *Chlamydomonas* and the membrane/matrix can be removed by non-ionic detergents (Triton x-100 or Nonidet-P40) for proteomic or biochemical analysis (Pazour *et al.*, 2005). This procedure allowed identification of the intraflagellar transport machinery (IFT) that is responsible for ciliary assembly (Cole et al., 1998; Piperno et al., 1998). Moreover, this procedure resulted in sufficient pure membrane-matrix proteins for analysis by tandem mass spectrometry revealing other

components cataloged in the *Chlamydomonas* flagellar proteome (Pazour et al., 2005). Thus, the proteome provides a catalog of membrane-matrix and axonemal components, and in total ~600 proteins have been identified in the intact cilium (Pazour et al., 2005), a number consistent with computational, genomic analysis (Dutcher, 2000; Li *et al.*, 2004).

The ciliary axoneme originates from the basal body, which provides a template for microtubule growth and is required for assembly of all cilia (Dutcher, 2003; Hiraki *et al.*, 2007; Nakazawa *et al.*, 2007; Marshall, 2008a). The basal body is a barrel shaped structure derived from the centriole and composed of 9 triplet microtubules; the A tubule that is attached to an incomplete B tubule that is in turn attached to an incomplete C tubule. A and B tubules of the basal body continue as the A and B microtubules of the axoneme while the C tubule terminates between the basal body and the origin of the axoneme, a region termed as the "transition zone" (O'Toole et al., 2003). Like the axoneme, the basal bodies / centrioles are highly conserved (Fig. 2B)

The motile axoneme is typically characterized by a 9+2 arrangement of microtubules: 9 peripheral outer doublets, continuous with the basal body A and B microtubules, and a pair of central singlet microtubules that originate near the transition zone (Fig. 2B). The central pair microtubules, as well as the 9 outer doublet microtubules, are continuous throughout the length of the axoneme. The A microtubule is a complete structure made of 13 protofilaments, while B microtubule is a partial structure made of 10 protofilaments; together they form an outer doublet microtubule. Each outer doublet appears to be associated with the adjacent outer microtubule by structures called nexins (Warner and Satir, 1974; Goodenough, 1989; Bozkurt and Woolley, 1993; Nicastro *et al.*, 2006). The precise role and composition of the nexin structure is not yet known, but it is

thought that these structures play roles in generation of a ciliary bend by maintaining interactions between the outer doublets, thus preserving the integrity of the 9-fold structure during microtubule sliding. Consistent with this model, protease treatment, important for the in-vitro microtubule sliding assays described below, appears to disrupt nexin structures (Summers and Gibbons, 1971, 1973). Recent advances in structural analysis indicate that the nexin structure repeats at 96 nm and is associated with a part of the dynein regulatory complex (DRC; see below).

The 9+2 structural configuration is highly conserved among all ciliated eukaryotes (Li *et al.*, 2003; Avidor-Reiss *et al.*, 2004; Li *et al.*, 2004; Pazour *et al.*, 2005), and the basis of this conservation appears to be related to the conservation of basal body organization. When observed in cross section, most key conserved structures are revealed (Fig. 2A). These include the inner and outer dynein arms, which are firmly attached to the A microtubule and project toward the B microtubule of the adjacent outer doublet; the radial spokes, also anchored to the A microtubule and project towards the central apparatus; and the central pair complex composed of the "C1" and "C2" microtubules and associated structures (Mitchell and Sale, 1999; Wargo *et al.*, 2005; Lechtreck and Witman, 2007; Lechtreck *et al.*, 2008). The asymmetric structure of the central pair is founded on the distinct composition of components associated with C1 and C2 (Mitchell, 2009).

The axoneme has a physical and functional axis relative to the bending plane and direction. For example, in *Chlamydomonas,* one doublet, labeled #1 lacks the outer dynein arm (Hoops and Witman, 1983). As in all axonemes, other doublets are numbered in the direction the dynein arms point, #2-#9 (Fig. 2A). This asymmetry defines an axis:

doublets #1, #5 and #6 sit in the plane of the bend and doublet #1 leads the forward, effective bend (Hoops and Witman, 1983). Moreover, although the central pair twists and rotates along the length of the *Chlamydomonas* axonemes (Omoto et al., 1999), the axonemal bend is tightly coupled to the orientation of the central pair (Mitchell, 2003; Wargo and Smith, 2003), and recent tomographic study of the axoneme reveals an asymmetry in doublet microtubule structures across the axis (Bui *et al.*, 2009). As discussed below, this axonemal axis is relevant to the mechanism of bending, the pattern of microtubule sliding and a "sliding microtubule- switching model" for oscillatory bends.

When viewed along the long axis, the complexity of the axonemal structures is appreciated in much greater detail as illustrate in Fig. 3. Each component associated with the outer doublet microtubule is organized in regular, repeating 96 nm units. This axonemal organization was revealed by thin section analysis of the axonemes and negative stain of doublet microtubule throughout the 1960s and 1970s (Warner and Satir, 1974; Sale and Satir, 1976; Dentler and Cunningham, 1977). Our understanding of the axonemal structure was greatly advanced in the 1980s by Goodenough and Heuser, using a rapid freeze deep-etch rotary shadow approach that revealed the 96 nm repeat organization in greater detail, and also revealing new details of dynein organization and substructures (Goodenough and Heuser, 1982, 1985; Sale *et al.*, 1985; Burgess *et al.*, 1991a). The next major advance in structural analysis of the axoneme occurred in the 1990s when image averaging was applied to analysis of thin sections, and was coupled to analysis of axonemes from *Chlamydomonas* mutants lacking specific structures (Kamiya et al., 1991; Mastronarde et al., 1992). This approach led to identification of the position

of the DRC (Gardner, 1994) and new detail of inner arm dyneins (Kamiya *et al.*, 1991; Porter *et al.*, 1992; Bower *et al.*, 2009). The most recent advance has been achieved using cryoEM tomography of intact axonemes (Nicastro *et al.*, 2005; Nicastro *et al.*, 2006; Oda *et al.*, 2007; Bui *et al.*, 2008, 2009) which revealed additional detail in axonemal morphology as well as the inherent asymmetry of the 9+2 scaffold (discussed below).

As illustrated, the electron microscopy analysis of structural mutants reveals that within each 96 nm axonemal repeat in *Chlamydomonas* there are four outer arm dyneins that repeat at 24 nm, two radial spokes (spoke #1(S1) is most proximal) and a surprisingly complex collection of different inner dynein arm structures, including the inner dynein arm called "I1 dynein", or the f dynein. For example, failure in assembly of I1 dynein results in a repeating 96 nm gap in structure (Piperno *et al.*, 1990; Porter *et al.*, 1992; Smith and Sale, 1992b; Perrone *et al.*, 1998; Nicastro *et al.*, 2006). This result alone indicates each inner arm dynein structure assembles independent of the others and that each structure is targeted to a precise position. Although the 96 nm repeat organization is highly conserved, the molecular basis that establishes this organization is unknown. It is likely this repeat organization is so fundamental that mutations in genes that encode proteins responsible for establishment of the 96 nm repeat result in complete failure of cilia assembly. Such mutations could result in "bald" phenotype- cells lacking flagella (Goodenough and StClair, 1975). Understanding the basis for the 96 nm repeat structure is a very high priority since it not only establishes the precise location of inner dynein arms, radial spokes and DRC, but likely dictates the position of the protein kinase CK1, the topic of this dissertation.

Central pair apparatus: Detailed structural analysis of the central pair apparatus has been made possible due to availability of *Chlamydomonas* mutants that specifically lack the various central pair apparatus structures (Adams et al., 1981; Dutcher et al., 1984; Mitchell and Sale, 1999; Rupp et al., 2001; Wargo et al., 2005). For example, gel analysis comparing axonemal protein composition from wild-type and central pair mutants revealed that the central pair apparatus is composed of at least 23 separate proteins (Adams et al., 1981; Dutcher et al., 1984). The central pair apparatus is composed of two single microtubules- C1 and C2, made up of 13 protofilaments each and associated structures including the central pair projections, central pair bridges and central pair caps. C1 and C2 are associated with distinct proteins- at least 10 that are unique to C1 and at least 7 unique to C2 (Adams et al., 1981; Dutcher et al., 1984; Mitchell and Sale, 1999; Rupp et al., 2001; Wargo et al., 2005). As indicated above, the different associated proteins in each central pair microtubule define a structural and biochemical asymmetry shown to be related to the mechanism of bending (Mitchell, 2003; Nakano *et al.*, 2003; Wargo and Smith, 2003; Wargo *et al.*, 2004). C1 has two prominent projections termed 1A and 1B measuring 18 nm in length. C2 on the other hand has two projections 2A and 2B of shorter length – 8 nms (Fig. 2A). Lesser prominent projections on both C1 and C2 - 1C, 1D and 2C- have also been resolved. The C2 microtubule projections repeat every 16 nm, while the C1 microtubule projections appear to have 16 and 32 nm repeating structures. Availability of a large variety of central pair mutants has aided in understanding the precise role and composition of the central apparatus. Some of the mutants and associated phenotypes are listed in Table 2.

Chlamydomonas mutants defective in central pair assembly are paralyzed (Smith and Yang, 2004). Therefore, the central pair apparatus is essential for normal ciliary motility. The central pair apparatus is thought to function as a scaffold where it provides anchoring positions for important signaling molecules that regulate dynein activity by directing signals, through spokes, to specific doublet microtubules. For example, the catalytic subunit of the axonemal phosphatase PP1 is a part of the C1 microtubule (Yang et al., 2000). Notably, paralysis in central pair assembly mutants can be rescued by extragenic suppressor mutations (Porter et al., 1992). For example, one such suppressor mutant is *pf9-2* that has a mutation in a component of the inner dynein arm I1, implicating the central pair, radial spokes and I1 dynein in a pathway that controls ciliary motility. This signaling model provides much of the foundation for this thesis and the concept will be discussed and developed further below and in Chapter 5.

Radial spokes: Radial spokes are a highly conserved collection of proteins found in all ciliated organisms and required for motility (Luck *et al.*, 1977; Witman *et al.*, 1978; Sturgess *et al.*, 1979; Huang *et al.*, 1981; Piperno *et al.*, 1981). Radial spokes contain at least 23 proteins, many of which are conserved in all ciliated organisms (Yang *et al.*, 2001; Yang *et al.*, 2006). Structure and morphology of the radial structure complex has been defined by biochemical as well as microscopy techniques. For example, the composition of the radial spokes was identified by comparing 2D gels containing purified axonemal fractions of wild-type and radial spoke deficient mutant strains and successful isolation of intact radial spokes provided important additional advances (Yang *et al.*, 2001; Yang *et al.*, 2004; Yang and Yang, 2006).

Radial spokes are T-shaped structures, anchored on the A microtubule, that extend from the outer doublets towards the central apparatus. The spokes are composed of a "stalk" that anchors the entire structure to the outer doublets, near the base of the inner dynein arms. The radial spokes terminate in a spokehead that transiently interacts with the central pair projections (Warner and Satir, 1974; Curry and Rosenbaum, 1993; Smith and Yang, 2004). Like the outer and inner dynein arms, the radial spokes are also precisely positioned and targeted in the axoneme. In *Chlamydomonas,* a pair of radial spokes (termed S1 and S2) repeats every 96 nms throughout the length of the axoneme. I1 dynein, localized by electron microscopy as well as cryoEM tomography, is present at the base of spoke S1 towards the proximal end of the 96 nm repeat (Piperno *et al.*, 1990; Porter *et al.*, 1992; Nicastro *et al.*, 2006). Therefore, the radial spokes are ideally positioned to transmit signals from the central pair apparatus to I1 dyneins on the outer doublets.

One radial spoke protein (RSP3) is the most proximal protein at the stalk and anchors the radial spokes to the A-microtubule (Diener et al., 1993). Moreover, RSP3 has been identified as an A-kinase anchoring protein (AKAP; Gaillard et al., 2001; Gaillard et al., 2006). Therefore, one predicted function of RSP3 is to anchor the protein kinase, PKA, in the axoneme, in position to regulate the kinase activity by physically localizing it near its substrate (Gaillard et al., 2006). The AKAP model for localization of otherwise ubiquitous kinases provides an important general model for my thesis, and the prediction is that the axoneme contains a CK1-anchoring protein (CKAP) that targets CK1 near its dynein substrate. This model could define one basis for regulating CK1 activity and

thereby ciliary motility or other CK1-dependent cellular functions. This concept will be discussed in detail in Chapter 3.

Dynein regulatory complex (DRC): Apart from the dynein motors, suppressor analysis of central pair and radial spoke mutants indicated that the DRC is a part of a mechano-chemical pathway that regulates dynein activity (Brokaw *et al.*, 1982; Huang *et al.*, 1982; Piperno *et al.*, 1992; Porter *et al.*, 1992; Gardner, 1994; Piperno *et al.*, 1994; Rupp and Porter, 2003). The DRC comprises of at least 7 proteins and electron microscopy analysis has positioned the DRC such that it is in contact with the inner dynein arms, outer dynein arms as well as the nexin structure and located near the base of the S2 spoke (Gardner, 1994; Nicastro et al., 2006). Given its location, one prediction, is that the DRC plays a role in mediating signals between this spoke and the dynein motors. Additionally, DRC subunits have been shown to interact or provide the foundation of the nexin structure and this interaction is thought to maintain axonemal organization during ciliary bend formation (Nicastro et al., 2006). The exact functions of each of the DRC subunits are only just beginning to be defined (Piperno *et al.*, 1992; Piperno *et al.*, 1994; Rupp and Porter, 2003), and *Chlamydomonas* mutants that do not assemble one DRC subunit, PF2, exhibit altered waveform as well as slow motility phenotypes (Table 2; Piperno *et al.*, 1992; Piperno *et al.*, 1994). Orthologs of PF2 have been identified in humans where it may play non-ciliary functions in cell cycle control (Rupp and Porter, 2003; Colantonio *et al.*, 2006). Furthermore, it has also been shown that the DRC proteins also play roles in ciliary motility and in various zebrafish developmental pathways (Colantonio et al., 2009). Currently, the challenges include identification and

functional characterization of individual DRC subunits and to determine their precise role with respect to regulation of dynein activity.

The dynein motors: each has a place; each has a purpose. Critical to this thesis is an understanding of the location and functional role of more than 8 different axonemal dynein motors (reviewed in King and Kamiya, 2009). Most generally, the dynein arm structures are categorized in two rows – the outer dynein arms (ODA) and the inner dynein arms (IDA; Fig. 2A). The outer and inner rows of dyneins are structurally and functionally distinct: the outer dynein arms are homogenous in composition and structure, whereas, the inner dynein arms are complex, composed of at least 7 distinct dynein isoforms each localized in a fixed pattern in the 96 nm repeat (Fig. 3). These conclusions are based on study of mutant *Chlamydomonas* axonemes that have defects in assembly of single dynein subforms. For example, mutants leading to a failure in assembly of I1 dynein results in a gap in the structure that repeats every 96 nm (Piperno *et al.*, 1990; Nicastro *et al.*, 2006; Bower *et al.*, 2009).

The dynein motors were discovered in cilia by Ian Gibbons in the 1960s (Gibbons, 1963; Gibbons and Rowe, 1965). Although the ODA is not the main focus of this dissertation, it is helpful to briefly describe the structure, composition and assembly since these features provide the foundation for understanding I1 dynein. The ODA is bound to the A microtubule towards the periphery of each doublet microtubule, therefore the designation- outer dynein arm (Fig. 2A). Outer dynein arms are homogenous complexes of 15 different protein subunits that are uniformly distributed at 24 nm intervals along the length of the axoneme (Goodenough and Heuser, 1982; Burgess *et al.*, 1991a; Nicastro *et al.*, 2006; Oda *et al.*, 2007; Bui *et al.*, 2008). In *Chlamydomonas,* the

ODA is found on all outer doublets except doublet #1, (Hoops and Witman, 1983; Bui *et al.*, 2009). Based on mutant analysis (Kamiya and Okamoto, 1985; Mitchell and Rosenbaum, 1985), the ODA is chiefly responsible for controlling beat frequency and producing the power to generate a normal ciliary beat (reviewed in Kamiya, 2002; Brokaw, 2009; King and Kamiya, 2009). Therefore, *Chlamydomonas* mutants that are defective in ODA assembly or function beat with a lower frequency and swim slowly with a characteristic "jerky" phenotype compared to wild-type cells (Kamiya and Okamoto, 1985; Mitchell and Rosenbaum, 1985; Brokaw and Kamiya, 1987; Kamiya, 1988). These easily observable phenotypes have allowed extensive screening for ODA mutants that permit further genetic, biochemical and functional analysis. The ODA mutants also revealed that the inner dynein arms are sufficient to generate oscillatory bends and normal waveform, albeit at reduced beat frequency and reduced power (Kamiya and Okamoto, 1985; Mitchell and Rosenbaum, 1985). When viewed in the axoneme (Goodenough and Heuser, 1982; Burgess *et al.*, 1991b; Nicastro *et al.*, 2006; Oda *et al.*, 2007; Bui *et al.*, 2008) or as isolated complexes (Goodenough and Heuser, 1982; Johnson and Wall, 1983; Burgess *et al.*, 1991b) the dyneins display large head domains that bear the ATP and motor structures. The outer dynein arm is composed of either two or three heavy chains (depending on species), and a number of intermediate and highly conserved light chains (reviewed in King and Kamiya, 2009). In *Chlamydomonas,* the ODA is comprised of three heavy chains (α, β, γ), two intermediate chains (IC1, IC2) and at least 10 known light chains. The heavy chains contain the ATPase and motor activities as well as microtubule binding domains, where as the intermediate and most light chains are organized at the "base" of the ODA.

The intermediate and light chains play roles in assembly of the outer dynein arms onto the axonemes. The intermediate chain proteins typically contain WD-repeat domains, important for protein-protein interactions and required for assembly of multiple subunits of dynein (Wilkerson et al., 1995; Yang and Sale, 1998). For example, IC1 was shown to bind to tubulin and is predicted to play a role in dynein- microtubule interaction required for anchoring the arm structure (King et al., 1991). Intermediate chains of I1 dynein are also responsible for docking the inner dynein arms as discussed below. Light chain proteins associated with ODA are also well characterized in *Chlamydomonas* and represent a group of proteins that are not always exclusive to the ODA, but also perform as light chains in other dyneins. For example, LC8 is a highly conserved light chain subunit that is also a part of cytoplasmic dynein, I1 dynein and the radial spokes (King and Patel-King, 1995; DiBella *et al.*, 2001; Yang *et al.*, 2001; Yang *et al.*, 2009). Light chains of the ODA can be characterized functionally into two groups (Kamiya, 2002). One set of light chains interact with the heavy chains and act as signal transducers (example LC1, LC3 LC4, LC5). The second group of proteins associate with the intermediate chains at the base and have roles in ODA assembly in the axoneme (example LC6 and LC8). Notably, LC1 has been shown to interact with the motor domain of the γ-heavy chain (Benashski et al., 1999) and regulate dynein activity (Patel-King and King, 2009). It is possible that similar regulatory light chains are yet to be defined in other dynein structures.

Assembly, transport and docking of the ODA is achieved through a surprisingly complex series of molecular mechanisms and cellular events (King and Kamiya, 2009). A model is shown in Fig. 4. Assembly begins in the cytoplasm (Fowkes and Mitchell, 1998)

and recent evidence indicates this process requires additional non-dynein proteins including the *PF13* gene product (step 1, Fig. 4; Omran et al., 2008). PF13 is found to have an identical role in *Chlamydomonas,* zebrafish and in humans, indicating a conserved function and mechanism required for ODA assembly. Once the ODA complex is assembled in the cytoplasm, it is then loaded onto the IFT system, for directed transport into the ciliary compartment (step 2, Fig. 4). Although loading of cargo onto the IFT transit system is not well understood, the IFT protein IFT46 (Hou et al., 2007) along with Oda16p (Ahmed and Mitchell, 2003) is required for transport of ODA into the axoneme (step 3, Fig. 4). Thus, the ODA maybe one of the best understood IFT cargoes to date, and predictably other axonemal dyneins, including I1 dynein, are transported in a similar manner, possibly using similar specialized adaptor proteins for assembly and IFT. Once in the ciliary compartment, the ODA complex is then unloaded from the IFT transporters (step 4, Fig.4), a process also not well understood, where it can then bind to the axoneme. Precise binding of the ODA at 24 nm intervals is mediated by the outer dynein arm docking complex (ODA-DC; Koutoulis *et al.*, 1997; Takada *et al.*, 2002; Casey *et al.*, 2003a; Casey *et al.*, 2003b) as well as a complex that includes Oda5 (step 5, Fig. 4; Wirschell et al., 2004). Mutations in any of the docking complex proteins lead to a failure in ODA assembly in the axonemes. Predictably, based on reconstitution approaches (Smith and Sale, 1992b), each inner arm, also I1 dynein, requires separate and unique docking mechanisms similar to ODA-DC. However, to date no I1 dynein docking mechanism has been identified. This is a particularly relevant problem since, as developed below, I predict the mechanism that targets and docks I1 dynein may also target and anchor axonemal CK1 and this concept is discussed further in Chapter 3.

Inner dynein arms (IDA): The regulatory mechanism, defined and focused upon in this dissertation, impinges on the inner arms, in particular I1 dynein, also known as "dynein f". I will briefly review the inventory of inner arm dynein isoforms, and then focus on review of relevant features of I1 dynein structure and function. The inner dynein arms and I1 dynein in particular, are important for controlling the axonemal waveform (Kamiya, 2002; Brokaw, 2009; King and Kamiya, 2009). As stated above, the IDAs are bound on the A tubule, towards the interior of the structure and anchored near the radial spoke structures (Fig. 2). Inner arm dyneins are heterogeneous, comprising of at least 7 distinct species that are distinct in localization and function (King and Kamiya, 2009). Structural analysis and biochemical fractionation of wild-type and mutant axonemes has been essential in defining the composition and arrangement of the various IDA isoforms. Additionally, resolution and identification of heavy chain, intermediate chain and light chain composition of the 7 different dynein complexes has depended upon sensitive biochemical techniques, such as 2D gels and fast protein liquid chromatography (FPLC) using ion exchange chromatography. The FPLC approach utilizes salt extracts from axonemes lacking the ODA that are fractionated into 7 distinct dynein peaks and, the different inner arm dynein isoforms were designated a, b, c, d, e, f and g (Kagami *et al.*, 1990; Kagami and Kamiya, 1995). Among the chief challenges has been associating each dynein isoform a-g with specific heavy chain gene, mutant cells and dynein structure within the 96 nm repeat.

Recent progress has resulted in partial resolution of this problem and I summarize the protein complexes, structures, genes and mutant cells in Table 2. Notably, in some cases, specific inner arm dyneins are localized toward the proximal or distal end of the

axonemes (Piperno and Ramanis, 1991; Yagi et al., 2009). In contrast, I1 dynein is localized along the length of the axoneme on each outer doublet microtubule (Bui *et al.*, 2009). Thus, it is predicted that each inner dynein arm isoform is individually targeted to a unique position and that each dynein plays a different, but likely overlapping, role in control of the size and the shape of the axonemal bend. The best understood inner arm dynein is the two-headed I1 dynein.

I1 Dynein: The major challenge of understanding ciliary motility is to determine mechanisms that locally control dynein activity on specific outer doublets. Here, I describe I1 dynein and explain the use of I1 dynein as a model to study dynein regulation by phosphorylation and build a model indicating that CK1 is an important regulator of I1 dynein phosphorylation (Yang and Sale, 2000). Diverse data has revealed I1 dynein displays unusual properties and is required for the normal control of the size and shape of the flagellar bend (Brokaw and Kamiya, 1987; Wirschell et al., 2007). Unlike the other inner dynein arms, which are single-headed dyneins, I1 dynein is a two headed structure, and was originally identified as a "triad" structure in the axoneme localized to the base of spoke S1 at the proximal region of the 96 nm repeat (Goodenough and Heuser, 1985). As mentioned above, I1 dynein was also localized by comparing axonemes from wild-type strains and mutant strains that do not assemble I1 dynein (Piperno et al., 1990; see Table 1). This analysis revealed specific and repetitive gaps in electron densities in positions where I1 dynein is predicted to localize and repeat in a 96 nm period. This conclusion was supported by numerous subsequent studies (Porter *et al.*, 1992; Smith and Sale, 1992b; Nicastro *et al.*, 2006; Bower *et al.*, 2009). Failure of I1 dynein assembly does not affect assembly of other inner arm dynein

isoforms, indicating that each inner arm dynein is assembled independently. Furthermore, fully functional I1 dyneins could be reconstituted in-vitro to the original positions in every 96 nm repeat (Smith and Sale, 1992b; Yamamoto et al., 2006). Clearly, I1 dynein must be precisely targeted and anchored to a specific position in the axoneme and assembly involves an I1 dynein intermediate chain, IC140 (Perrone et al., 1998; Yang and Sale, 1998). However, to date, we do not understand the docking mechanism for I1 dynein.

As illustrated in Fig. 5, I1 dynein is a heterodimer composed of the 1α and 1β heavy chains and contains three intermediate chains IC140, IC138 and IC97, FAP120 and multiple light chains, including LC7a, LC7b, LC8, Tctex1 and Tctex2 (Fig.5; Piperno *et al.*, 1990; Porter *et al.*, 1992; Myster *et al.*, 1997; Harrison *et al.*, 1998; Perrone *et al.*, 1998; Yang and Sale, 1998; Myster *et al.*, 1999; Perrone *et al.*, 2000; DiBella *et al.*, 2004a; DiBella *et al.*, 2004b; Hendrickson *et al.*, 2004; Ikeda *et al.*, 2009; Wirschell *et al.*, 2009). Sequence and structural analysis has revealed that the 1α and 1β heavy chains contain the same signature domains that characterize the nucleotide binding and microtubule binding in all dyneins (Myster et al., 1997; Myster et al., 1999; Perrone et al., 2000), and in unpublished high resolution structural analysis, each motor domain has the same structural features as other dyneins (unpublished data, Sale, Porter, Oiwa labs). However, based on studies of mutants lacking one or the other I1 dynein heavy chain motors, the two heavy chains are not identical in function (Myster et al., 1999; Perrone et al., 2000). Biophysical analysis of isolated I1 dynein complexes reveal that compared to other dyneins, I1 dynein only generates slow microtubule translocation activity also implying unique function (Smith and Sale, 1991; Kotani *et al.*, 2007).

Furthermore, biophysical measurements using purified I1 dynein complexes indicate I1 dynein can inhibit translocation of microtubules driven by other inner arm dyneins (Kotani et al., 2007). These, and other data, have led to the important model that I1 dynein can locally inhibit microtubule sliding in the axoneme and thus alter axonemal bending (Kotani et al., 2007; Wirschell et al., 2007). This model is discussed further below as I consider the mechanism of I1 dynein and control of microtubule sliding by phosphorylation.

Before discussing the intermediate and light chains in I1 dynein, it is important to discuss additional features of the 1α and 1β heavy chains, since as discussed above, they each display different motor functions. Two mutants called *ida1* and *ida2* (Table 2) are defective in the genes for the 1α and 1β heavy chains and lead to failure in assembly of I1 dynein (Myster et al., 1997; Myster et al., 1999; Perrone et al., 2000). Mutants such as *ida1* and *ida2* (as well as *ida3, ida7* and *bop5*) display reduced swimming speeds, altered flagellar waveform and defective phototaxis (Brokaw and Kamiya, 1987; King and Dutcher, 1997; Okita et al., 2005). Taking advantage of *ida1, ida2* and DNA mediated transformation, new mutant strains were recovered that express truncated 1α and 1β heavy chains lacking the individual motor domains but retaining the tail domain and assembling the remaining I1 dynein subunits in the axonemes (Myster et al., 1999; Perrone et al., 2000; unpublished analysis, W.S. Sale and L.A. Fox). These mutants offered the opportunity to examine the role of each motor domain separately in regulation of axonemal bending. Unpublished data from the Sale, Sakakibara, Porter and Oiwa labs reveals that the 1β heavy chain motor is an effective microtubule motor, where as the 1α heavy chain is not an effective motor (S. Toba, L.A. Fox, H. Sakakibara, M.E. Porter, K.

Oiwa and W.S. Sale, unpublished data). The results indicate the 1α heavy chain motor domain may play a role in inhibition of microtubule sliding, a feature of I1 dynein that may be required for control of bending.

Additional informative mutants and biochemical analysis revealed that, similar to the ODA, the intermediate and light chains collectively play roles in cargo binding, regulation of motor activity as well as assembly of I1 dynein onto the axoneme. The IC140 subunit is required for assembly of the complete structure and data has implicated IC140 in anchoring I1 dynein to the axoneme (Perrone et al., 1998; Yang and Sale, 1998). For example, the *Chlamydomonas* mutant *ida7*, defective in the *IC140* gene does not assemble I1 dynein in the axoneme and IC140 can compete with I1 dynein rebinding in in-vitro experiments using isolated axonemes lacking I1 dynein (Yang and Sale, 1998). This result is consistent with a role for IC140 in anchoring I1 dynein to the outer doublet microtubules. Additionally, as shown in Table 2, a number of mutations in genes that encode I1 dynein subunits can result in partial I1 dynein assembly (Perrone et al., 1998; Hendrickson *et al.*, 2004; Bower *et al.*, 2009; Wirschell *et al.*, 2009). In each case, IC140 is required for assembly of the intact or partial I1 dynein complex further indicating that among the I1 dynein subunits, IC140 is critical for I1 dynein assembly.

Since genetic and biochemical analysis reveals that the key I1 dynein regulatory subunit is IC138, much of our focus has been devoted to its study (Habermacher and Sale, 1997; King and Dutcher, 1997; Yang and Sale, 2000; Hendrickson *et al.*, 2004; Bower *et al.*, 2009; Wirschell *et al.*, 2009). *Chlamydomonas* mutants that exhibit hyperphosphorylated IC138 are defective in phototaxis- a process by which cells either move towards or away from light (King and Dutcher, 1997; Okita et al., 2005). In

response to a light stimulus, the two flagella behave differently, indirectly altering their waveform to turn the cell (Witman, 1993). Light is detected by the eyespot, an asymmetrically localized organelle, and a signal is transmitted to the flagellum that regulates voltage-gated ion channels. Phototaxis affects the waveform of the two flagella coordinately. Therefore, it is predicted that inner dyneins, particularly I1 dynein, in the two flagella are differentially regulated (King and Dutcher, 1997; Iomini *et al.*, 2006). Based on mutant analysis, this differential regulation is likely to be via chemical signaling pathways that ultimately impinge upon I1/IC138 phosphorylation. Consistent with this prediction, mutants with hyperphosphorylated IC138 are defective in the phototaxis response (King and Dutcher, 1997). However, the exact mutation in these phototactic defective strains is unknown. One of the possibilities is that the axonemal kinases, including CK1 or phosphatases that control the phosphorylation state of IC138 are not properly regulated or assembled in the axoneme.

The third intermediate chain is called IC97 and unlike all other dynein intermediate chains, IC97 is not a WD repeat protein (Wirschell et al., 2009). Multiple lines of evidence including immunoprecipitation and blot overlays, EDC cross-linking have demonstrated that IC97 interacts with α and β tubulin and may also play a role in docking I1 dynein to the microtubules. Another idea, discussed in Wirschell et.al., (2009) is that the IC97-tubulin interaction could operate as a "sensor" that detects change in curvature of the cilia, thus playing a role in control of microtubule sliding (see next section). Additional evidence has also indicated that IC97 interacts with IC138, LC7 and FAP120 in a regulatory complex- the "IC138 regulatory sub-complex" (Bower et al., 2009) required for I1 dynein- mediated control of dynein-driven microtubule sliding

(Wirschell et al., 2009). The evidence indicates that microtubule sliding is controlled by phosphorylation of IC138, but that assembly of IC97 is also important for function of IC138.

Recently, a novel I1 dynein associated protein has been identified-FAP120. FAP120 is an ankyrin-repeat protein and is missing from mutants that do not assemble I1 dynein or IC97 (Ikeda et al., 2009; Wirschell et al., 2009). Preliminary studies indicate that FAP120 is associated with IC138 presumably via one of its ankyrin repeat domains and plays a role in regulation of I1 dynein function. The precise role of FAP120 is not yet determined. One possibility is that FAP120 recruits signaling kinases or phosphatases near the I1 dynein structure in order to phosphorylate IC138. This hypothesis will be addressed further in Chapter 3.

A "sliding microtubule – switching" model for ciliary motility: Seminal work, using multiple experimental systems including isolated motile axonemes, has revealed that the basis for ciliary motility lies in controlled dynein-driven microtubule sliding- a "sliding microtubule" model for ciliary bending (Satir, 1968; Brokaw, 1972). This model is supported by a variety of experimental data and founded upon Satir's original electron micrograph analysis of cilia captured in known bend positions (Satir, 1963; Satir and Rosenbaum, 1965; Satir, 1967, 1968) revealing a process analogous to a "sliding filament" model for muscle contraction. Satir (1968) reasoned that electron microscopy study of the tips of cilia captured in each bend position could be used to determine if microtubules are contractile- i.e. elastic or rigid and inextensible. Cilia beating in metachronal waves were captured by chemical fixation and Satir demonstrated both qualitatively and quantitatively that microtubule displacement during bending exactly fits

the geometry predicted if microtubules are inextensible and slide. Therefore, to generate a ciliary bend, the adjacent microtubules must slide across each other and Satir formally proposed a "sliding-microtubule" model for bending (Fig. 6).

In 1971, Summers and Gibbons reported the first direct observation of dynein-driven microtubule sliding in isolated axonemes (Summers and Gibbons, 1971). This was a pioneering study that, for the first time, showed that the interdoublet sliding is generated by dynein motors interposed between adjacent doublet microtubules. Innovations of Gibbons work also included introduction of dark field light microscopy for direct, real time observation of microtubules and microtubule sliding. This assay, that is, observation and measurement of microtubule sliding in axonemes using dark field and video, was subsequently adapted for the study of dynein-driven motility in wild-type and mutant axonemes from *Chlamydomonas* (Okagaki and Kamiya, 1986). Emphasized below, this motility assay has become the central approach for study of regulation of dynein activity in axonemes (Smith and Sale, 1992a). Briefly, microtubule sliding activity can be measured in isolated axonemes, treated with a mild protease (a process that does not affect dynein structure or activity, but disrupts interdoublet nexin linkages) and ATP. In this in-vitro analysis, since the nexin linkages are disrupted and the cilia are not attached to the cell body, ciliary bending is uncoupled from microtubule sliding activity (Fig. 7) and the outer doublet microtubules can slide apart. As microtubule sliding is produced by the molecular motor dynein, in-vitro microtubule sliding velocities can be measured and used as a reliable assay to quantify dynein activity, or change in dynein activity that results from regulation or change induced by exogenous treatment with pharmacological inhibitors of kinases or phosphatases. In-vitro microtubule sliding

assays have been used experimentally to delineate signaling pathways that regulate dynein activity as well as identify the key components involved. Results from such assays provide the basis for my study and overall hypothesis, and will be referred to throughout this thesis.

In addition to the studies of Satir (1968) and Summers and Gibbons (1971), the sliding microtubule model is also supported by data from two other classical papers from the Shingyoji and Brokaw labs (Shingyoji *et al.*, 1977; Brokaw, 1991). In both studies, motility was assessed in axonemes reactivated to move in ATP containing buffers using a classical approach pioneered by Gibbons and Gibbons (1972). In this approach, illustrated in Fig. 7, cells or flagella were demembranated with the non-ionic detergent Triton-X-100 for subsequent ATP reactivation studies (interestingly, this 1972 paper was the first introduction of non-ionic detergents, such as Triton-X-100, for permeabilization of cells). Shingyoji et al., (1977) applied low concentrations of ATP by micropipette and ionophoresis to the middle region of an axoneme using and ATP concentration below the concentration threshold required to induce regular, oscillatory bending. This procedure resulted in generation of two equal bends but opposite in direction, and located on opposite sides of the ATP-containing pipette tip. This important experiment and result was considered direct evidence for a sliding microtubule model for ciliary bending (the 1977 Shingyoji et al., paper also contains additional important experiments critical for our understanding of axonemal motility). In 1991, Brokaw demonstrated, for the first time, microtubule sliding during bending by attaching colloidal gold to the sides of the microtubules in demembranated axonemes, and then using high resolution dark field and video measurements of bead oscillation during ATP-induced reactivation of flagellar

bending. These data also strongly support a dynein-driven, sliding microtubule model for ciliary/flagellar bending.

The immediate challenges were to determine if microtubules could actively slide in both directions, that is, determine if dyneins could produce force in both directions relative to microtubule structure. This question was addressed by Sale and Satir (1977) and led to the discovery that dynein motors generate force in one direction (minus-end direction) relative to microtubule polarity (Sale and Satir, 1977; Fox and Sale, 1987). The 1977 paper was the first demonstration that dynein was a minus-end motor, and the observation directly led to a "switching" model for alternating effective (principal/forward) and recovery (reverse) bending (Fig. 8). For example, if dyneins on all outer doublets are active at the same time, and since they are all minus-end directed motors, predictably no net sliding can occur and, therefore, no movement. Thus, a "switching model" was proposed where dyneins on one side of a structural and functional axis of the axoneme are active for bending in one direction (Fig. 8). Predictably, when the direction of bending changes or "switches", there is a switch in activity where the previously inactive dyneins, on one side of the axis, are activated, and the formerly active dyneins on the opposite side, are turned off (see Smith 2007 for commentary). The axis of the axoneme refers to the plane of the axonemal bend and is defined both structurally and functionally. For example, in *Chlamydomonas,* structurally this plane passes through doublet #1 and between #5 and #6 (Hoops and Witman, 1983; Bui *et al.*, 2009). Furthermore, recent work by Lechtreck et al. (2007; 2008) has shown that a conserved protein called hydin, which is localized to the central pair apparatus, plays an important role in the "switch-point" mechanism. Thus, although the dynein mutants and doublet

microtubules can drive oscillatory bending, the "switch point" mechanism appears to also be controlled by second messengers and the central pair-radial spoke structure. The "switching" model for oscillatory bending is founded in the original observation that all dyneins are minus-end directed motors. Additional experimental observations and genetic analyses of mutant cells also support a switching model (Satir and Sale, 1977; Lechtreck and Witman, 2007; Lechtreck *et al.*, 2008). The precise mechanism for sensing the end point of each bend direction is not understood. However, diverse experimental evidence indicates oscillatory movements and switches in bend direction are inherent properties of the dynein motors involving microtubule curvature. For example, in-vitro reactivation studies reveal as few as a pair of doublet microtubules independent of the central pair, are sufficient to generate repetitive bends (Aoyama and Kamiya, 2005). Indeed, using altered buffer conditions, alternating bends can be generated in reactivated axonemes lacking the central pair structures (reviewed in Smith and Yang, 2004). The best evidence for bending or curvature control of dynein activity and switching of activity comes from the elegant biophysical studies of Shingyoji and colleagues (Morita and Shingyoji, 2004; Hayashi and Shingyoji, 2009). Together, the data indicates switching of dynein activity between opposite sides of the axonemal axis is regulated in part by sensing curvature. The sensor is not known, but Patel-King and King (2009) propose a model in which the outer dynein arm plays a role as a sensor of microtubule curvature (see also Hayashibe et al., 1997). Further discussion of the biophysical properties of the dyneins goes well beyond the scope of this dissertation and will only be considered further in the context of regulation by phosphorylation.

The mechanical feedback mechanism cited above does not require the CP/RS regulatory system. As developed further in the next section, the CP/RS regulation appears to be superimposed on the basic mechanically and motor controlled switching mechanism to modulate either microtubule sliding or possibly the "switch point" mechanism. Presumably, the CP/RS system is controlled by second messengers including calcium, and leading to altered axonemal phosphorylation. Consistent with the idea that calcium and the CP/RS system can modulate the switch point, Satir and colleagues demonstrated in in-vitro studies that changes in calcium concentration result in stopping of ciliary beating at the end point/switch point of the beat cycle (Satir and Matsuoka, 1989).

III. Focus of the thesis

A variety of studies have revealed the central pair apparatus and radial spokes are required for normal ciliary motility and regulate microtubule sliding. For example, mutations in *Chlamydomonas* and humans genes encoding for the central pair and radial spoke structures, result in a defective spoke assembly and ciliary paralysis (Witman *et al.*, 1978; Sturgess *et al.*, 1979; Smith and Yang, 2004). Taking advantage of the microtubule sliding assay using isolated axonemes, Witman (1978) determined that, despite paralysis, dynein-driven microtubule sliding still occurred. However, Smith and Sale (1992a) went a step further and determined that the velocity of dynein-driven microtubule sliding is greatly reduced in axonemes deficient in central pair and radial spoke assembly. They postulated that dynein activity is inhibited in axonemes from paralyzed flagellar mutants. To test this idea, they combined a novel in-vitro reconstitution approach (of re-binding dynein arms with dynein-depleted axonemes) and then measured microtubule sliding in reconstituted axonemes (Smith and Sale, 1992b). As predicted, they determined the

reduced dynein activity in the axonemes from radial spoke deficient mutants was due to a reversible post-translational modification and that the alteration occurred in the inner dynein arms.

To test this idea further, Howard et al., (1994) took a pharmacological approach to test the hypothesis that the post-translational modification was phosphorylation and that the key phospho-protein was found in the inner arm dyneins. Howard and colleagues found that protein kinase inhibitors including HA1008 and PKI, "rescued" microtubule sliding velocity in paralyzed flagellar axonemes from radial spoke mutants. The results implied an axonemal protein kinase A (PKA), and possibly additional axonemal kinases, when unregulated in the paralyzed flagellar axonemes, lead to inhibition in motility, presumably due to abnormal phosphorylation in an inner dynein arm component. These results also indicate that in wild-type axonemes, the assembled central pair and radial spoke structure operate, in part, to tightly control axonemal protein kinases for precise control of flagellar motility.

Since protein kinase inhibitors rescued microtubule sliding in axonemes, the axonemes must contain protein phosphatases required for dephosphorylation of key axonemal dyneins phospho-proteins and rescue of microtubule sliding (Habermacher and Sale, 1995). Consistent with this prediction, Habermacher and Sale (1996), determined that phosphatase inhibitors, including microcystin LR and okadaic acid, when applied before or with the kinase inhibitor, block kinase inhibitor-dependent rescue of microtubule sliding. At that time, it was postulated that an axonemal PP1 was critical for rescue of microtubule sliding, and, indeed, further biochemical analysis revealed the axonemes contains a highly conserved PP1 (Yang et al., 2000). However, in these same

and subsequent studies, Yang and Fox determined that the axoneme also bears a protein phosphatase PP2A that localizes to the outer doublet microtubules. The current model, being tested by Candice Elam in the Sale lab, is that PP2A is anchored in the outer doublet microtubules, by a B-subunit, near the inner dynein arms. Notably, Candice Elam and W. Sale working in collaboration with Dr. Susan Dutcher (Washington University, St. Louis) have determined that the *pf4* mutant is defective in the gene for the PP2A B-subunit. Phenotypic analysis has revealed the *pf4* mutant phenocopies the I1 dynein mutants, consistent with a direct role for PP2A in regulation of I1 dynein. Elam and Sale also determined that the C-subunit of PP2A also fails to assemble in the *pf4* axonemes, consistent with a model that the B-subunit mediates PP2A targeting and anchoring in the axoneme and that PP2A is required for normal I1 dynein function. In this thesis, I will also test the idea that assembly and function of CK1 is regulated and mediated by specific proteins and is required for normal I1 dynein function.

Shortly after I1 dynein was identified and characterized, Porter *et al.* (1992) determined that mutations in I1 dynein could suppress paralysis of motility in a central pair mutant. These results implicated I1 dynein in a regulatory pathway that involves the central pair and the radial spokes. Genetic analysis using double mutants defective in radial spoke assembly (*pf14* or *pf17*), and lacking selected subsets of dynein arms revealed that I1 dynein assembly is required for rescue of microtubule sliding (Habermacher and Sale, 1997; Yang and Sale, 2000). Subsequent analysis confirmed that I1 dynein is critical and assembly of the IC138 sub-complex is required for rescue of microtubule sliding in paralyzed flagellar mutants (King and Dutcher, 1997; Yang and Sale, 2000; Bower *et al.*, 2009). Further biochemical analysis revealed the critical

regulatory phospho-protein in I1 dynein is IC138 (Habermacher and Sale, 1997; King and Dutcher, 1997; Yang and Sale, 2000; Hendrickson *et al.*, 2004; Bower *et al.*, 2009; Wirschell *et al.*, 2009). Indeed, functional analyses demonstrated a tight correlation between IC138 phosphorylation and regulation of microtubule sliding: inhibition of microtubule sliding correlated with phosphorylation of IC138; active or rescued microtubule sliding correlated with dephosphorylation of IC138 (Fig. 9). Importantly, and relevant to the model developed below, the requirement for assembly of I1 dynein and IC138, with IC138 in a dephosphorylated state, indicated I1 dynein plays a "positive" and active role in rescue and regulation of microtubule sliding. This conclusion is critical for discussion of models of I1 dynein function and regulation of motility.

To more directly test whether an axonemal PKA regulates IC138 phosphorylation, specific PKA inhibitors were used to determine if they block phosphate incorporation into IC138 (Yang and Sale, 2000). Surprisingly, although PKI rescues microtubule sliding in the paralyzed flagellar axonemes, PKI failed to completely block phosphorylation of IC138. Therefore, it was postulated that the axoneme must contain additional kinases important for control of IC138 phosphorylation. Using inhibitors that block the activity of the CK1 class of protein kinases, Yang found that these inhibitors also rescued sliding in paralyzed radial spoke defective axonemes (Yang and Sale, 2000). The results of these functional assays are shown in Fig 10 and include discovery that I1 dynein assembly is required for rescue of microtubule sliding. These results implicated an axonemal CK1, possibly in addition to PKA, in regulation of I1 dynein-dependent control of microtubule sliding (Yang and Sale, 2000). Yang and Sale went on to use "in-gel" kinase assays, immunoblots and peptide specific substrates to directly determine whether

the axoneme bears a CK1-like kinase. They demonstrated that the CK1-like kinase is localized in the outer doublet microtubules and that this CK1-like kinase is a relatively abundant axonemal protein. Furthermore, the CK1 inhibitors block phosphate incorporation into IC138 demonstrating a correlation between IC138 phosphorylation and regulation of microtubule sliding (Fig. 9).

The data from Yang and Sale (2000) indicated that a CK1-like protein kinase is localized to the axoneme and appears to regulate phosphorylation of IC138 and control of microtubule sliding. A model derived from the data is shown in Fig. 9, and indicates that unregulated CK1 activity (in paralyzed axonemes from radial spoke mutants) phosphorylates IC138 leading to inhibition of microtubule sliding. Pharmacological and biochemical data also revealed the phosphatase PP2A is present in the axoneme and likely responsible for dephosphorylation of IC138 and rescue or activation of microtubule sliding (Habermacher and Sale, 1996, 1997; Yang *et al.*, 2000; Elam, Wirschell, Fox and Sale, unpublished data). Notably, all of these studies were performed with isolated axonemes, thus the kinase - CK1 - and phosphatase- PP2A, like the dynein motors and regulatory structures, are physically built into and localized in the axonemal structure. The focus of this thesis is on CK1 and to specifically define the role of CK1 in the CP/RS phospho-regulatory pathway and determine its function in controlling the size and shape of the axonemal bend.

The critical question is: How does the CP/RS/I1 dynein regulatory mechanism control the size and shape of the axonemal bend in wild-type axonemes? The general hypothesis that provides the foundation for this thesis is that CK1 is a “downstream” component of the CP/RS/I1 regulatory mechanism that controls IC138 phosphorylation.

Key questions include: What is the gene that encodes the axonemal CK1, and what is the amino acid sequence of the predicted protein? At the beginning of this work, the axonemal CK1 had only been characterized pharmacologically and enzymatically (Yang and Sale, 2000). I predicted CK1 would be a conserved member of the CK1 family of protein kinases (see Chapter 2 for a brief review of CK1). Cloning and characterization of the *CK1* gene and axonemal CK1 is described in Chapter 2.

Where does the *CK1* gene map? Although it remained possible that mutations in the *CK1* gene resulted in flagellar phenotypes, most likely a mutation in the gene would be lethal since CK1 is likely responsible for a range of vital functions (reviewed in Chapter 2). Nevertheless, it remained possible that *Chlamydomonas* bears more than one *CK1* gene and the CK1 responsible for control of axonemal function is dispensable.

Inherent in my model and based on the "solid state" nature of the axoneme, CK1 must be precisely localized. Therefore, questions include: What is the location of CK1 in the axonemes? Predictably, based on the physical interaction of CK1 with the axoneme, the hypothesis is that CK1 must be localized to the outer doublet microtubules, along the length of the axonemes, anchored near I1 dynein. Localization of CK1 is also addressed in Chapter 2. What is the molecular mechanism for localizing and anchoring CK1 on the outer doublet microtubule? Predictably, again based on the model, CK1 must be localized by another specific protein that repeats at 96 nm. It is possible that I1 dynein and CK1 are targeted and anchored by a common scaffold-docking protein or protein complex. Additionally, identification of such a putative CK1-anchoring protein (CKAP) could define a more general class of proteins (or protein domains) that localize CK1 in the cytoskeleton, or to organelles, to direct and regulate CK1 function. This model is

analogous to AKAPs (A-Kinase anchoring proteins) responsible for localizing and regulation of otherwise ubiquitous PKA (Wong and Scott, 2004). This question will be addressed in Chapter 3.

My main goal was to determine the physiological role of CK1 in the axonemes. The discovery of the CP/RS/I1 phospho-regulatory pathway was made possible due to the failure in regulation of the protein kinase and phosphatases in paralyzed flagellar axonemes defective in radial spokes and resulting in a global, but reversible inhibition of dynein-driven microtubule sliding. Thus, the microtubule sliding assay was an extremely effective and reliable means of detection of regulation. In Chapter 4, I address this question using novel in-vitro reconstitution and functional assays to determine CK1 kinase activity is critical for regulation of microtubule sliding and test whether I1 dynein assembly is required for regulation of dynein-driven microtubule sliding. The results of these in-vitro functional studies are also described in Gokhale *et al.*, (2009)

One related question is: Is CK1 actively regulated by the radial spokes in wild-type axonemes? This is a problem that is not directly addressed in this thesis, but predictably structural strain in the radial spokes can alter protein interactions at the base of the spoke near inner dynein arms. As discussed in Chapter 5, this regulatory mechanism must be highly controlled in wild-type axonemes, directly and locally regulating I1 dynein. Such a mechano-sensitive signal transduction mechanism could also alter kinase activity, but at this time, I do not have the tools or approach to test this important idea. Models for chemical and mechanical regulation of the radial spokes in discussed in Chapter 5.

Fig.1

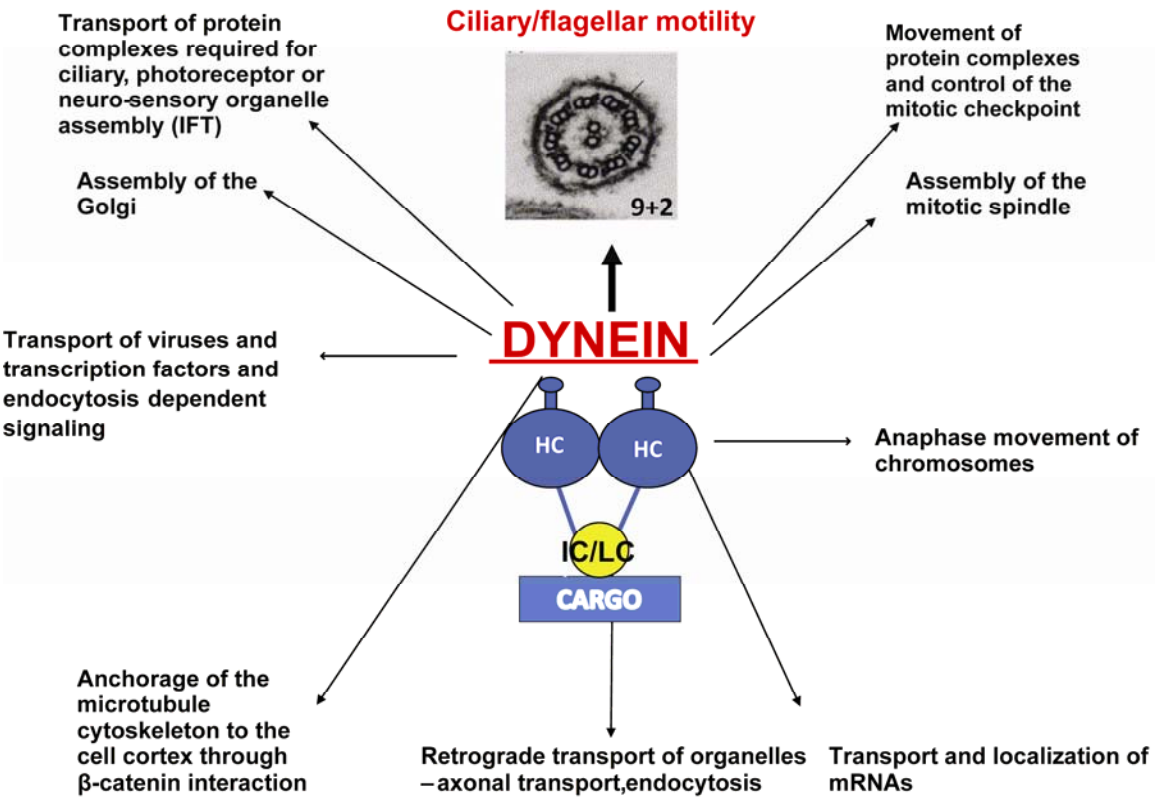
Ciliary/flagellar motility
Transport of protein complexes required for ciliary, photoreceptor or neuro-sensory organelle assembly (IFT)
Movement of protein complexes and control of the mitotic checkpoint
Assembly of the Golgi
Assembly of the mitotic spindle
9+2
DYNEIN
Transport of viruses and transcription factors and endocytosis dependent signaling
HC
HC
Anaphase movement of chromosomes
IC/LC
CARGO
Anchorage of the microtubule cytoskeleton to the cell cortex through β-catenin interaction
Retrograde transport of organelles –axonal transport,endocytosis
Transport and localization of mRNAs

Figure 1: Common features and functions of cytoplasmic and axonemal dyneins:

Dyneins play diverse and vital functions in every cell. Common features include motor domains (globular domains consist of conserved regions of the heavy chains – HC, indicated in blue), tail domains and associated intermediate (IC) and light chain (LC) domains (yellow) required for cargo docking and regulation. All dyneins are minus (-) end motors (i.e. they move with cargo towards the minus-end of the microtubule). Cargoes can range from membrane vesicles (e.g. endocytic vesicles) to kinetochores to microtubules of the ciliary axoneme. Among the most important questions are: How are dynein motors targeted to cargo? And, how is dynein activity regulated?

Fig.2A

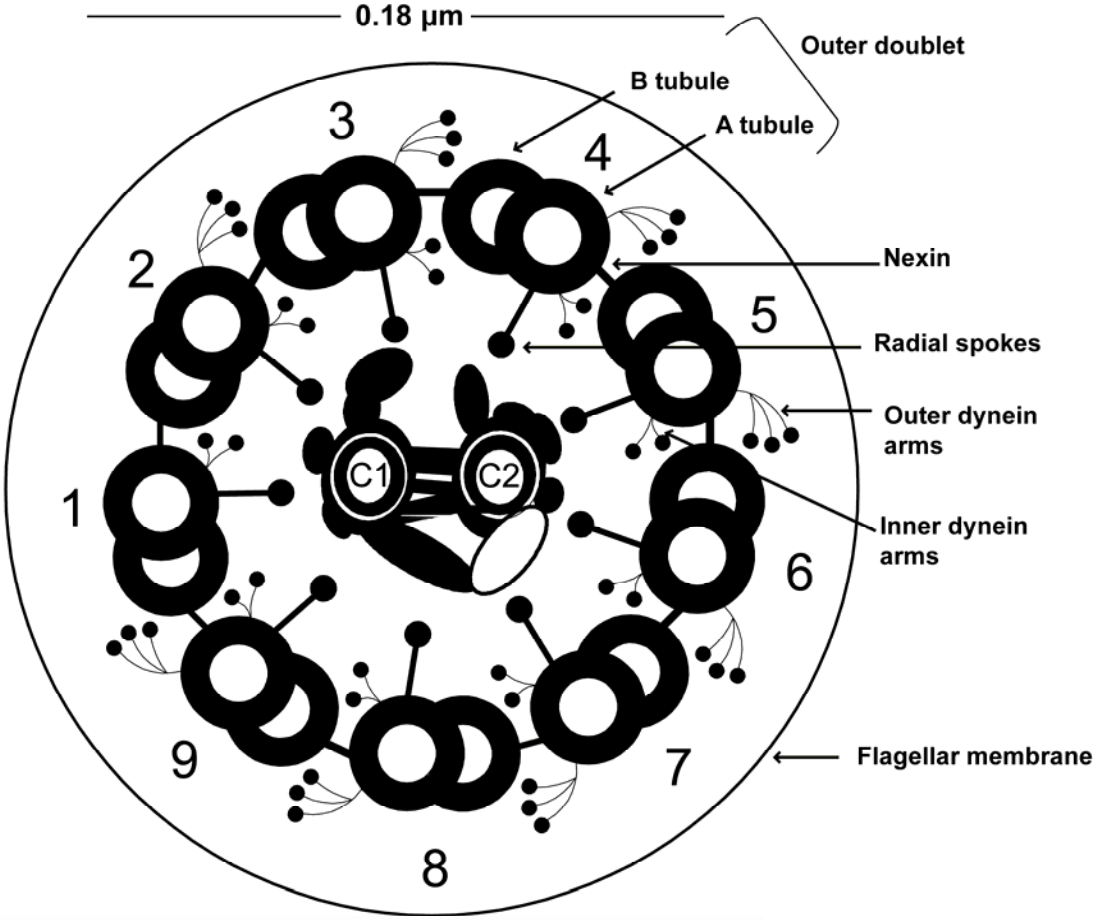
0.18 µm
Outer doublet
B tubule
A tubule
Nexin
Radial spokes
Outer dynein arms
Inner dynein arms
Flagellar membrane
1
2
3
4
5
6
7
8
9
C1
C2

Fig.2B

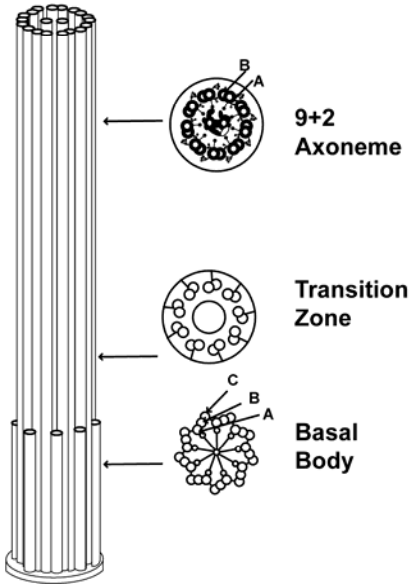
B
A
9+2 Axoneme
Transition Zone
C
B
A
Basal Body

Figure 2: Cross-sectional diagram of a typical motile cilia or flagellum depicting the 9+2 arrangement of microtubules in the axoneme. (A)The motile axoneme is composed of nine sets of outer "doublet" microtubules, surrounding a "central pair" of single microtubules (C1 and C2). Dynein arms are arranged in two rows- outer dynein arm (ODA) and inner dynein arm (IDA) - on the outer doublet microtubules, pointing in a clockwise direction, indicating the axoneme is viewed from base toward the tip. The ODAs and IDAs generate sliding between the outer doublet microtubules that is constrained by interdoublet linkages called nexins. The radial spokes (RS) and central pair (CP) regulate dynein-driven microtubule sliding to generate sophisticated flagellar bends. The axoneme is surrounded by a membrane. (B) The 9+2 axonemal structure originates at the basal body, a cartwheel-like structure characterized with a 9+3 arrangement of microtubules. While the A and B microtubules of the basal body are continuous with the axonemal A and B microtubules, the C microtubule of the basal body terminates at a region called the transition zone. Additionally, pair of central singlet microtubules originates at the transition zone.

Fig. 3

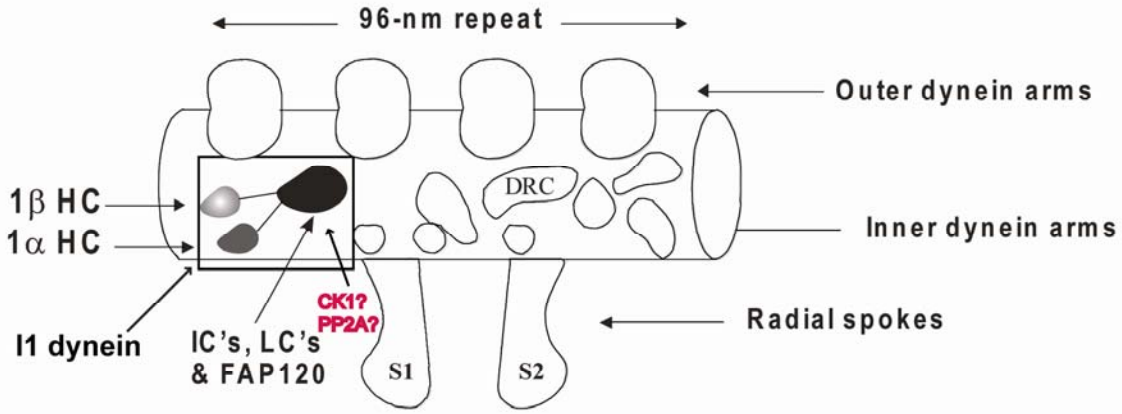
96-nm repeat
Outer dynein arms
1β HC
1α HC
DRC
Inner dynein arms
CK1?
PP2A?
I1 dynein
IC's, LC's
& FAP120
S1
S2
Radial spokes

Figure 3: Longitudinal view of the axonemal outer doublet microtubule depicting regular arrangement of key axonemal structures in discrete 96 nm repeating units. The proximal end of the axoneme is on the left. The 96 nm repeating structure comprises of four outer dynein arms, two radial spokes (S1 and S2) as well as inner dynein arms. I1 dynein (box) is a trilobed structure localized towards the proximal end of the 96 nm repeat, at the base of spoke S1. Each I1 domain has been directly localized, taking advantage of structural mutants in *Chlamydomonas,* using high resolution electron microscopy and image averaging. Hypothetically, CK1 and PP2A are targeted and anchored near the base of I1 dynein by the intermediate and light chains.

Fig.4

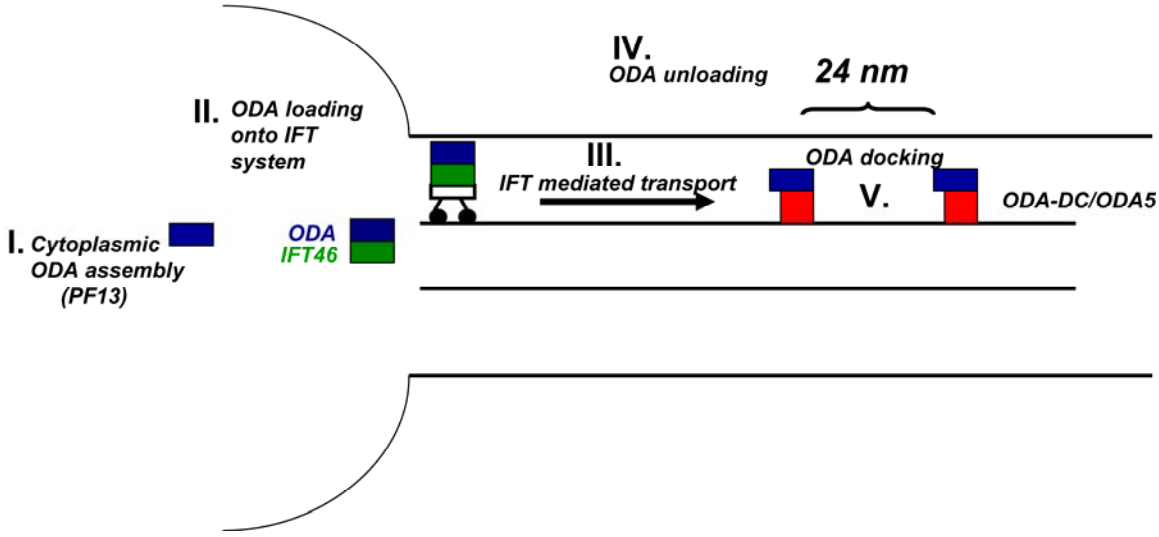
IV.
ODA unloading
24 nm
II. ODA loading onto IFT system
III.
IFT mediated transport
ODA docking
V.
ODA-DC/ODA5
I. Cytoplasmic ODA assembly (PF13)
ODA
IFT46

Figure 4: Model describing the complex, step-wise assembly, transport and docking of the ODA in the flagellum. The outer dynein arm complex (blue box) is preassembled in the cytoplasm and this process requires pf13p **(Step I)**. This complex is then loaded onto the IFT complex, a process involving IFT46 and Oda16p **(Step II)** and transported into the flagellar compartment **(Step III).** In the flagella, ODA are unloaded **(Step IV)** and bound to the axoneme via interactions with outer dynein arm docking complex (ODA-DC) and an axonemal protein Oda5p **(Step V)**. We postulate that I1 dynein assembles by a similar step-wise pathway requiring IFT.

Fig.5

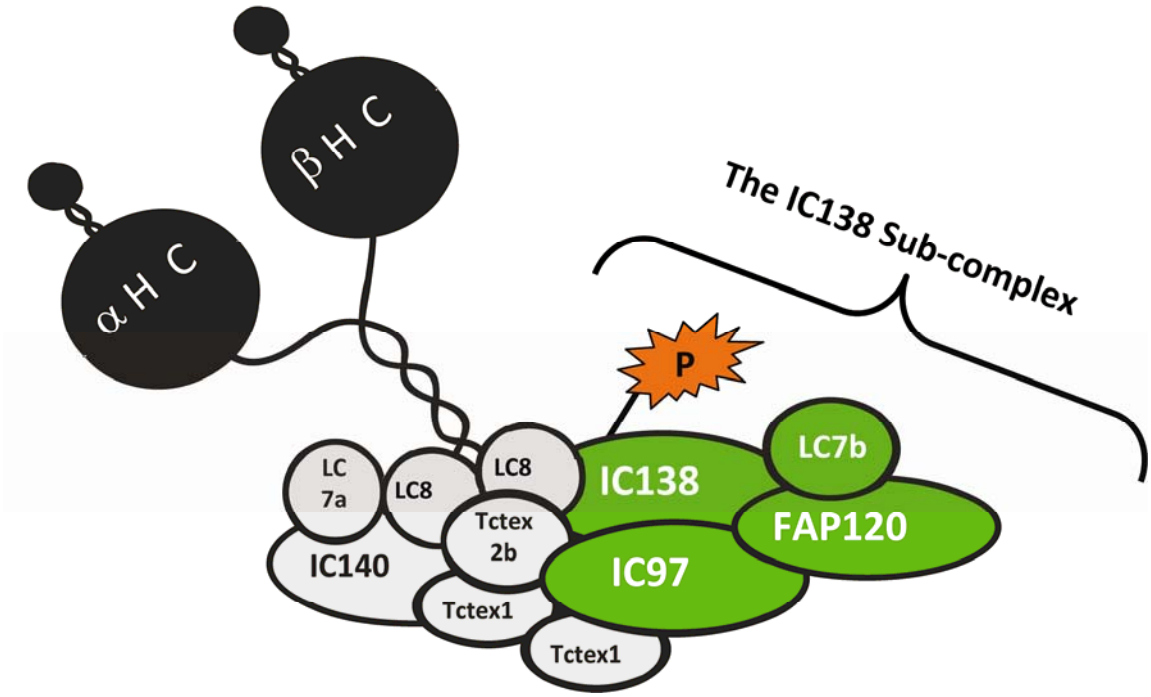
βHC
αHC
The IC138 Sub-complex
P
LC
7a
LC8
LC8
Tctex
2b
IC138
LC7b
FAP120
IC140
IC97
Tctex1
Tctex1

Figure 5: I1 dynein complex. The I1 dynein complex is composed of two heavy chains (1α HC and 1β HC), three intermediate chains (IC140, IC138, and IC97—also called IC110), and several light chains (LC8, LC7a, LC7b, Tctex1, and Tctex2b). An additional subunit, FAP120, has recently been identified and is thought to associate with the IC138 intermediate chain. IC138 is a key regulatory phospho-protein, and together with IC97, FAP120 and LC7b forms an "IC138 sub-complex" that plays a critical role in regulating dynein-driven microtubule sliding.

Fig.6

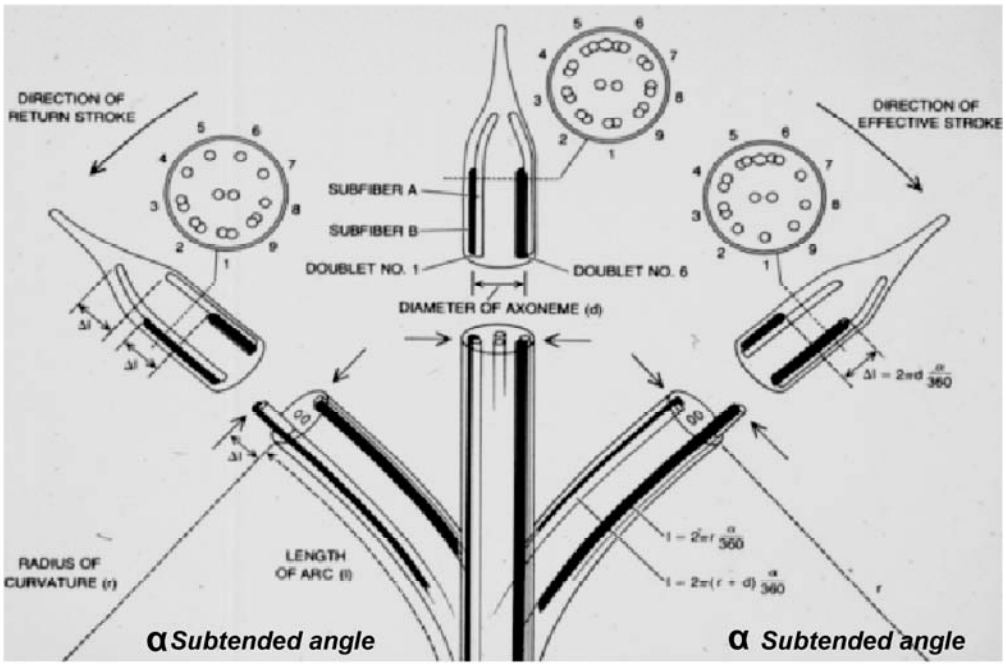
DIRECTION OF RETURN STROKE
DIRECTION OF EFFECTIVE STROKE
SUBFIBER A
SUBFIBER B
DOUBLET NO. 1
DOUBLET NO. 6
DIAMETER OF AXONEME (d)
RADIUS OF CURVATURE (r)
LENGTH OF ARC (l)
α Subtended angle
α Subtended angle

Figure 6: Sliding model for ciliary bending and motility. The "sliding filament" or "sliding microtubule" model of ciliary bending, illustrating the geometry of microtubule displacement for bends in the effective and reverse direction. The model illustrates that microtubules on the inner edge of the bend must slide relative to microtubules on the outer edge of the same bend and predicts that the amount of sliding could be measured as displacement, Δl, at the tips of cilia (adapted from Satir, 1968).

Fig.7

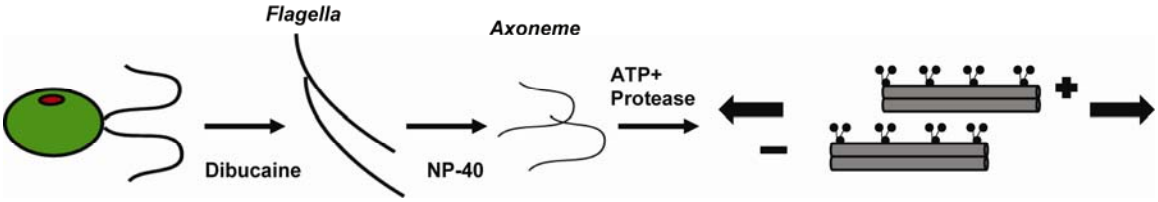

Figure 7: Axonemal isolation and the microtubule sliding assay. Flagella from *Chlamydomonas* cells are obtained after dibucaine treatment, demembranated with non-ionic detergents, such as NP-40, to generate isolated axonemes. Axonemes can then be reactivated to beat in ATP containing buffers or exposed to ATP and proteases to induce interdoublet sliding. Sliding can then be viewed by dark field microscopy and recorded by video for measurement of sliding velocity. The microtubule sliding velocity measurements provide an assay for quantifying dynein activity.

Fig.8

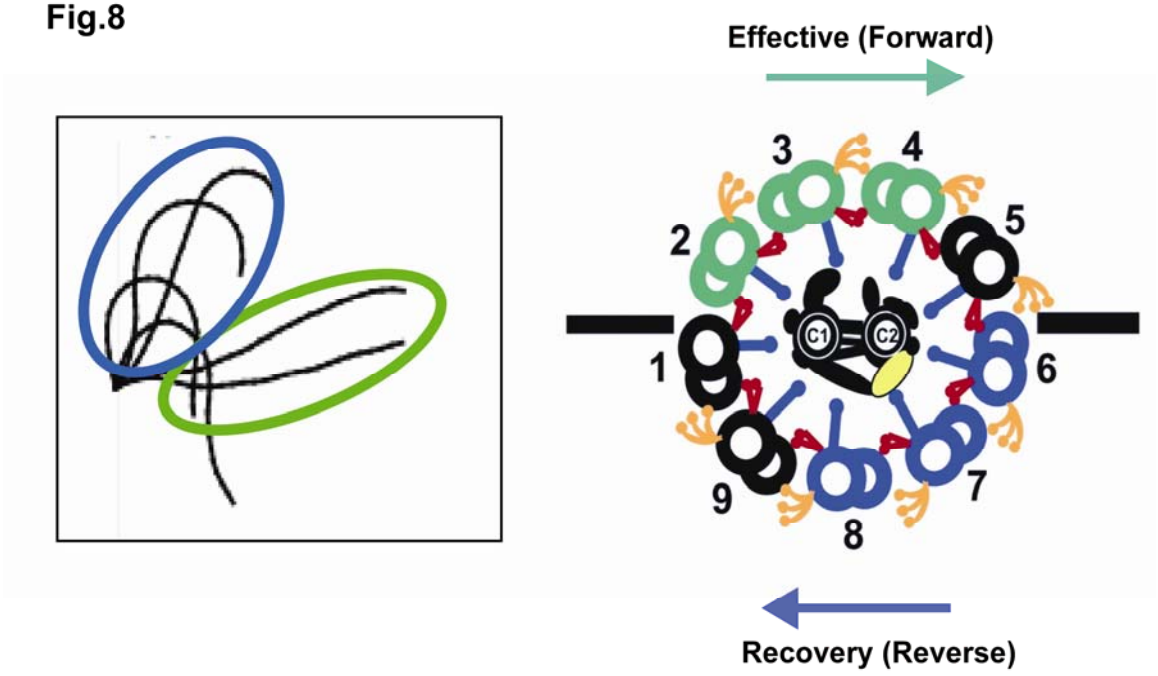

Figure 8: Axis of the axoneme and the "switching model for alternating forward and reverse bends. The axoneme is an asymmetrical structure that beats in a plane defined by the black line that passes through doublet #1 and between doublet #5 and 6. Since dyneins are minus-end directed motors, if all the dyneins on the outer doublet microtubules are simultaneously active, there is no net ciliary movement. Therefore, dynein activity must be tightly and locally regulated on each outer doublet microtubule. According to the "switching hypothesis", dyneins on one side of the functional axis, (i.e. dyneins on doublet #2, 3 and 4) when active, generate an effective or forward bend (left panel, green). When the direction of bending reverses, dyneins on doublets #2, 3, 4 are switched off and dyneins on doublets #6, 7 and 8 are switched on, thus generating a recovery or reverse bend (left panel, blue).

Fig. 9

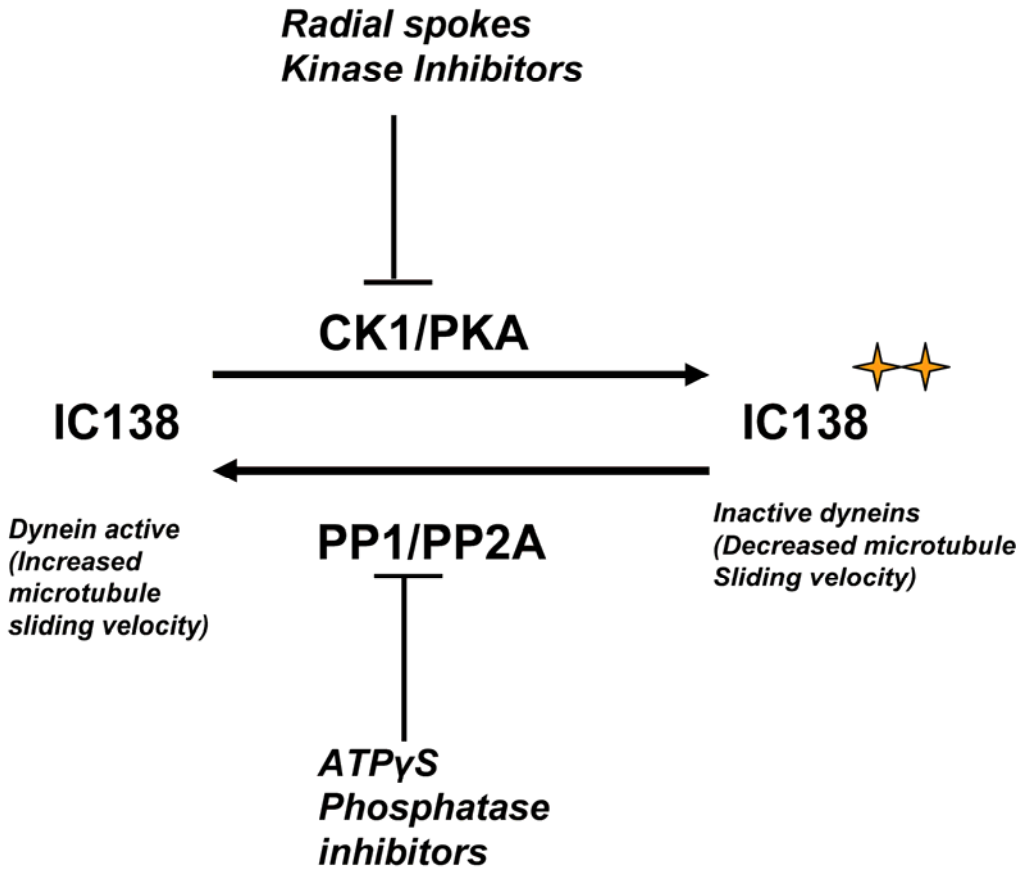
Radial spokes
Kinase Inhibitors
CK1/PKA
IC138
IC138
Dynein active
(Increased
microtubule
sliding velocity)
PP1/PP2A
Inactive dyneins
(Decreased microtubule
Sliding velocity)
ATPγS
Phosphatase
inhibitors

Figure 9: Model for I1 dynein control of microtubule sliding: Previous experimental evidence, using the *Chlamydomonas* model system, has demonstrated that the key regulatory phospho-protein in I1 is the intermediate chain IC138. This pathway was revealed in paralyzed flagellar mutants where the kinases are apparently misregulated leading to a global phosphorylation of IC138. IC138 when phosphorylated by axonemal kinase CK1 (or PKA), results in inhibition of dynein activity as revealed by a decrease in microtubule sliding velocity observed in motility assays. This inhibition can be relieved by specific kinase inhibitors. Furthermore, in wild-type axonemes, radial spokes regulate axonemal kinase activity, thus allowing normal ciliary waveform and movement. IC138 can be dephosphorylated by an axonemal phosphatase PP2A, resulting in activation of dyneins and therefore increases microtubule sliding velocity.

Fig.10

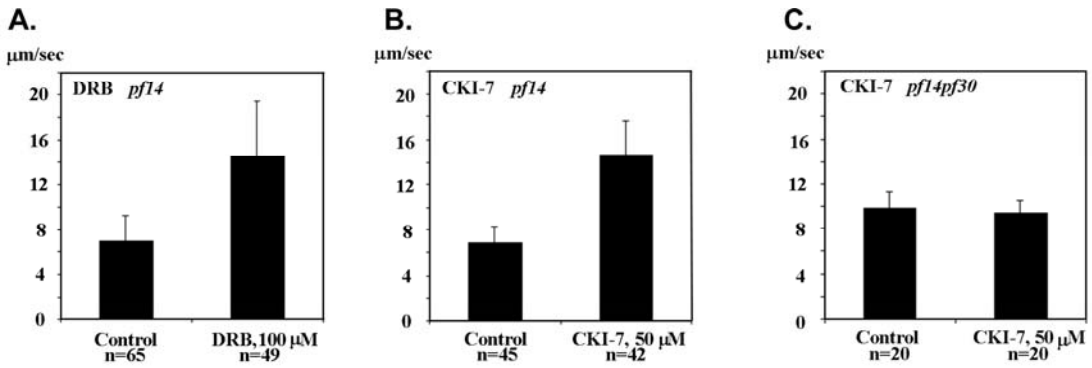
A.
μm/sec
DRB pf14
20
16
12
8
4
0
Control
n=65
DRB,100 μM
n=49
B.
μm/sec
CKI-7 pf14
20
16
12
8
4
0
Control
n=45
CKI-7, 50 μM
n=42
C.
μm/sec
CKI-7 pf14pf30
20
16
12
8
4
0
Control
n=20
CKI-7, 50 μM
n=20

Figure 10: CK1 inhibitors restore dynein activity in paralyzed axonemes lacking the radial spokes. In-vitro microtubule sliding assays reveal that dynein activity is greatly reduced in paralyzed axonemes lacking the radial spokes (*pf14*). When these axonemes were treated with CK1 inhibitors DRB (A) and CK1-7(B) dynein-driven microtubule sliding velocity is restored. CK1-7 or DRB fail to rescue dynein activity in a double mutant lacking the radial spokes as well as I1 dynein (C; *pf14pf30*) indicating an essential, positive role for I1 dynein in the regulatory pathway and control of microtubule sliding. I find the same result from another paralyzed flagellar mutant, *pf17* (Chapter 4). These results provide part of the foundation for my study and hypothesis.

Table 1: Examples of "ciliopathies"

Ciliopathy	Genes affected	Protein	Major symptoms	References
Alstrom syndrome	*ALMS1*	Unknown	Retinal degeneration, hearing loss, heart failure	(Badano et al., 2006; Joy et al., 2007)
Bardet-Biedl syndrome	*BBS1-BBS12*	BBS proteins-involved in IFT transportation, ciliogenesis and ciliary function	Retinal degeneration, polydactyly, obesity, mental retardation and diabetes.	(Ansley et al., 2003; Badano et al., 2006; Blacque et al., 2004)
Hydrocephaly	*Hydin3*	Axonemal central pair protein playing a role in ciliary motility	Accumulation of CSF within the brain ventricles	(Lechtreck et al., 2008; Lechtreck and Witman, 2007)
Joubert syndrome	*AHI1, CEP290, NPHP1*	Unknown	Polydactyly, hyperpnea, hypotonia, ataxia, nephronophthisis	(Badano et al., 2006; Saraiva and Baraitser, 1992)
Meckel-Gruber Syndrome	*MKS1, MKS3*	MKS1, meckelin	Renal failure, polydactyly	(Badano et al., 2006; Dawe et al., 2007)
Nephronopthisis	*NPHP1-NPHP8*	Nephrocystins-localize to the cilia	Polyuria, renal failure	(Hildebrandt and Zhou, 2007; Saunier et al., 2005)
Orofaciodigital syndrome	*OFD1*	OFD1 localizes to both centrosomes and basal bodies	Malformations of the face, oral cavity, and digits with polycystic kidney disease	(Badano et al., 2006)
Polycystic kidney disease	*PKD1 PKD2, PKHD1*	PKHD1, polycystin 1 and 2, IFT88 (polaris in the mouse)	Kidney failure	(Pazour, 2004)
Polycystic liver disease	*DNAI1, DNAH5*	Ciliary outer dynein arm proteins	Liver disease	(Badano et al., 2006)
Primary cilia dyskinesia	*DNAI1, DNAH5,*	Ciliary outer dynein arm	Defective mucus clearance and	(Badano et al., 2006; Nonaka

	DNAH11	proteins, ciliary motility defects	respiratory illness, *situs inversus,* infertility, hydrocephalus	et al., 1998; Nonaka et al., 2005; Zariwala et al., 2001)
Retinal degeneration		Nephrocystin, IFT57	Blindness	(Besharse et al., 2003)
Senior-loken syndrome	*NPHP1*	Nephrocystin-functions in signal transduction in renal cilia	Nephronophthisis and progressive eye disease	(Badano et al., 2006; Otto et al., 2005; Schuermann et al., 2002)

Table 2: List of Chlamydomonas structural mutants

A. Mutations that affect the outer dynein arm

Gene	Protein	Mutant phenotype	References
ODA1	DC2 Docking complex coiled-coil protein	Required for outer arm assembly, Slow swimming	(Kamiya, 1988; Takada *et al.*, 2002)
ODA2	γDHC ATPase and MT motor	Required for outer arm assembly, Slow swimming	(Mitchell and Rosenbaum, 1985)
ODA3	DC1 Docking complex coiled-coil protein	Required for outer arm assembly, Slow swimming	(Kamiya, 1988; Koutoulis *et al.*, 1997)
ODA4	βDHC ATPase and MT motor	Required for outer arm assembly, Slow swimming	(Kamiya, 1988; Sakakibara *et al.*, 1993; Porter *et al.*, 1994)
ODA5	Coiled-coil protein	Required for outer arm assembly, Slow swimming	(Kamiya, 1988; Wirschell *et al.*, 2004)
ODA6	IC2 (IC69/70) WD repeat protein, regulatory	Required for outer arm assembly, Slow swimming	(Kamiya, 1988; Mitchell and Kang, 1991)
ODA9	IC1 (IC78/80) WD repeat protein, binds α-tubulin	Required for outer arm assembly, Slow swimming	(Kamiya, 1988; King *et al.*, 1991)
ODA11	αDHC ATPase and MT motor	Not required for assembly of other outer arm components except LC5. Swims slightly slower than wild-type	(Sakakibara *et al.*, 1991)
ODA14	DC3 Docking complex, Ca^{2+} binding protein	Partial *oda*; some arms assemble, slow swimming, speed in between wild-type and complete *oda* mutants	(Casey *et al.*, 2003a; Casey *et al.*, 2003b)
ODA15	LC7a, Roadblock, bithoraxoid homolog	Required for outer arm assembly, Slow swimming. Also associates with Inner arm I1 (IC138) and may interact with LC7b.	(Pazour and Witman, 2000; DiBella *et al.*, 2004)
ODA16	WD repeat protein	Required for IFT transport of ODA. Partial assembly of ODA's observed	(Ahmed and Mitchell, 2003; Ahmed *et al.*, 2008)
PF13	?	Required for cytoplasmic pre-assembly of ODA, short flagella	(Huang *et al.*, 1979; Omran *et al.*, 2008)

B. Mutations that affect the inner dynein arm.

Gene	Protein	Mutant phenotype	References
IDA1 (PF9,PF30)	1αHC	Lacks inner arm I1, slow swimming	(Kamiya *et al*., 1991) (Myster, 1997) (Porter *et al*., 1992)
IDA2	1βHC	Lacks inner arm I1, slow swimming	(Kamiya *et al*., 1991) (Perrone, 2000)
IDA3	?	Lacks inner arm I1, slow swimming	(Kamiya *et al*., 1991)
IDA4	p28	Lacks inner arm subtypes a, c, and d	(Kamiya *et al*., 1991)
IDA5	Actin	Lacks inner arm subtypes a, c, d, and e	(Kato, 1993)
IDA6	?	Lacks inner arm subtype e	(Kato, 1993)
IDA7	IC140	Lacks arm I1, slow swimming	(Perrone, 1998; Yang and Sale, 1998)
IDA8	?	Slow swimming, structural defects in inner arm region	M. Porter personal communication
IDA9	Dynein C Heavy chain	Lacks inner arm subtype c, Kamiya cloned dynein c HC; found defective in *ida9*	(Yagi *et al.*, 2005)
BOP2	?	Slow swimming, abnormal waveform, missing part of DRC, projection, and *ida4* density.	(Piperno *et al.*, 1992; King *et al.*, 1994)
BOP5-1	IC138	Point mutation in IC138 of I1. Truncates the last WD-repeat. LC7b fails to assemble into I1 complex.	(King and Dutcher, 1997)
G41A	Truncated 1αHC oda+	Missing motor domain, still assembles I1	(Myster *et al.*, 1999)
D11	Truncated 1βHC oda+	Missing motor domain, still assembles I1	(Perrone *et al.*, 2000)
5A	Truncated IC140	Missing N-terminus of IC140. Still assembles I1. IC97 association with I1 is unstable.	(Perrone *et al*., 2000)
6F5 (bop5-2)	IC138 null	Axoneme is missing IC138 and IC97, but assembles IC140, FAP120 and presumably LC7b and rest of I1.	(Bower *et al.*, 2009)
mia1	72-kD	Hyperphosphorylated IC138.	(King and Dutcher, 1997)

		Missing 74-and 34-a polypeptides and reduced levels of a 35-kD polypeptide.	
mia2	?	Hyperphosphorylated IC138. Missing 34- and 35-kD polypeptides. IC138 defect can be rescued with Calcineurin.	(King and Dutcher, 1997)

C. Mutations affecting the central pair apparatus

Gene	Protein	Mutant phenotype	References
PF18	?	The *pf18* mutant has a central pair defect that causes the flagella to be rigid. Motility is completely impaired	(Bloodgood *et al.*, 1979; Adams *et al.*, 1981)
PF6	PF6	The *pf6* mutant lacks the C1a projection and is deficient in three central pair proteins. Paralyzed, twitching flagella. The PF6 protein is predicted to form a scaffold that is required for the assembly and/or stability of the C1a central pair projection	(Dutcher *et al.*, 1984; Wargo *et al.*, 2005)
PF15	Katanin p80 subunit	The *pf15* mutants lack the central pair of microtubules and are deficient in 18 axonemal polypeptides.	(Bernstein *et al.*, 1994; Dymek *et al.*, 2004)
PF16	CP14	The *pf16* mutants have an unstable central pair C1 tubule.	(Dutcher *et al.*, 1984; Smith and Lefebvre, 1996)
PF19	?	The *pf19* mutant lacks the central pair of microtubules in the flagellar axoneme. Flagella are paralyzed and rigid.	(Witman *et al.*, 1978; Adams *et al.*, 1981)
PF20	?	The *pf20* mutant partially lacks the central pair microtubules of the flagellar axonemes. Paralyzed, rigid flagella, but cultures contain some motile cells	(Adams *et al.*, 1981; Smith and Lefebvre, 1997)
CPC1	CPC1	Disrupted C1 projections, reduced beat frequency	(Mitchell and Sale, 1999)
HY3	Hydin	Deficient in C2 and C3 projections. Abnormal motility with flagella arrested at switch position.	(Lechtreck and Witman, 2007; Lechtreck *et al.*, 2008)

D. Mutations that affect the radial spokes

Gene	Protein	Mutant phenotype	References
pf14	RSP3	Lacks entire spoke. AKAP	(Diener *et al.*, 1990; Gaillard *et al.*, 2001)
pf17	RSP9	Lacks spoke head (RSP1, 4, 6, 8 and 10)	(Curry and Rosenbaum, 1993)
pf24	?	Reduced amounts of RSP2, 16, 23 and spoke head proteins; calmodulin-binding protein	(Yang *et al.*, 2004)
pf25	RSP11	Absence of RSP11 (spoke structure appears normal), abnormal motility	(Huang *et al.*, 1981)
pf26	RSP6	-	(Curry *et al.*, 1992)
pf27	Unknown. Not considered a spoke component itself. Required for phosphorylation of 5 spoke proteins (2,3,5,13 and 17)	Paralyzed flagella.	(Huang *et al.*, 1981)

E. Mutations that affect the DRC

Gene	Protein	Mutant phenotype	References
pf3	DRC1	Abnormal waveform; slow; missing DRC 1,2,5 and 6	(Huang *et al.*, 1982; Piperno *et al.*, 1992; Piperno *et al.*, 1994)
pf2	DRC4 (Gas8/11 homolog)	Abnormal waveform, slow, missing DRC 3-7	(Piperno *et al.*, 1994)
sup-pf4	DRC5	Wild-type like motion, missing DRC 5, 6	(Piperno *et al.*, 1994)
sup-pf3	?	Wild-type like motion, DRC 3-6 reduced	(Piperno *et al.*, 1992)

Chapter 2: Cloning and characterization of the *Chlamydomonas* protein kinase CK1

Introduction:

The overall goal is to study the role of the axonemal kinase, CK1, in the regulation of dynein activity and control of ciliary motility. As described in Chapter 1, flagellar dynein activity is controlled by a phospho-regulatory pathway that involves the central pair, radial spokes and a network of axonemal kinases and phosphatases (reviewed in Porter and Sale, 2000; Wirschell et al., 2009a). The general idea is that second messengers, including calcium, impinge on proteins in the central pair apparatus, or other positions in the axoneme, and relay mechanical and/or chemical signals through the radial spokes to the outer doublet microtubules for control of protein kinase activity, regulation of I1 dynein and microtubule sliding. For convenience, I will refer to this regulatory mechanism as the, – "CP/RS/I1 regulatory pathway"- a conserved mechanism that controls axonemal bending. Major challenges include identification of axonemal kinases and phosphatases that are directly responsible for regulating dynein activity and their direct substrates. As indicated in Chapter 1, one critical "downstream" kinase identified is CK1 (Yang and Sale, 2000). Here, I will briefly revisit key features that provide the foundation and rationale for the study of axonemal CK1.

Most of our understanding of the CP/RS/I1 dynein regulatory pathway is founded on functional and biochemical analysis of isolated axonemes. This observation indicates the signaling proteins, regulatory substrates and the dynein motors are physically anchored to the microtubules of the axoneme and that each unit must be precisely localized (Porter and Sale, 2000). The localization of kinases and phosphatases in the axoneme is a central theme of my lab's work and this thesis and almost all functional and biochemical studies take advantage of isolated axonemes. For example, pharmacological

and functional analysis has determined the presence of kinase activity in *Chlamydomonas* axonemes. As reviewed in Chapter 1, the reduced microtubule sliding rates in isolated, paralyzed axonemes (e.g. axonemes lacking the radial spokes including the mutants' *pf14* and *pf17*) can be rescued to wild-type velocities upon treatment with relatively specific inhibitors of CK1 or PKA (Howard et al., 1994; Yang and Sale, 2000). These types of in-vitro functional assays provided the first evidence for the presence of CK1 in motile axonemes. Taking advantage of structural *Chlamydomonas* mutants that do not assemble I1 dynein, it was also determined that rescue of microtubule sliding velocity in paralyzed axonemes requires assembly of I1 dynein, and in particular, the regulatory phospho-protein IC138, a key target of the regulatory pathway and IC97(Bower et al., 2009; Wirschell et al., 2009b; Yang and Sale, 2000). Again, since the kinase inhibitors presumably inhibited CK1 and PKA activity in isolated axonemes, the kinases must be localized and anchored in the axoneme. Consistent with this model, Yang and Sale (2000) used immunoblot analysis and biochemical fractionation to confirm that CK1 is an axonemal protein. However, at that time the genome and flagellar proteome databases had not been completed for *Chlamydomonas* and the *CK1* gene and protein were not identified.

As explained in detail in Chapter 1, one critical phospho-protein substrate is the I1 intermediate chain subunit IC138 (reviewed in Wirschell et al., 2007). Phosphorylation of IC138 by axonemal kinases correlates with inhibition of dynein-driven microtubule sliding (Habermacher and Sale, 1997; Yang and Sale, 2000; Fig 1). In-vitro biochemical analysis revealed that CK1 inhibitors, but not PKA inhibitors, specifically block the phosphorylation of IC138 in a manner that correlates with control of microtubule sliding

(Yang and Sale, 2000). Therefore, the simplest interpretation is that in the paralyzed axonemes, CK1 activity is not regulated and CK1 directly phosphorylates IC138 resulting in inhibition of dynein-driven microtubule sliding.

The data described above provides part of the foundation for our overall hypothesis that flagellar CK1 is a downstream component of the CP/RS/I1 regulatory pathway and is anchored on the axonemal outer doublet microtubules, in position to phosphorylate IC138 and control dynein-driven microtubule sliding. From this model, we also predict that CK1 is localized in a 96 nm repeat pattern and is anchored by specific CK1 anchoring proteins- "CKAPs", analogous to AKAPs- A-Kinase anchoring proteins (see Chapter 3).

To test these hypotheses and predictions, it was first necessary to identify the *CK1* gene as well as characterize the CK1 protein in *Chlamydomonas*. Identification and cloning the *CK1* gene will enable new tests and production of CK1-specific reagents, including antibodies or epitope-tagged proteins permitting localization and protein interaction studies. Therefore, the first goal was to identify the gene that encodes the axonemal CK1 protein, and produce the tools required to define the function of CK1 in the axoneme (Chapter 4) and define mechanisms for targeting and anchoring CK1 to the microtubule cytoskeleton (Chapter 3).

Identification of CK1, in the axoneme, was facilitated by the proteomic database published by Pazour et al., (2005). This large scale proteomics analysis of the *Chlamydomonas* flagellum revealed the identity of >600 proteins including the CK1 protein that is encoded by a single gene in the *Chlamydomonas* genomic database. The

strategy was to use peptide sequence to define the gene. Here, I will discuss the cloning of *Chlamydomonas CK1* gene, characterization of the predicted protein, generation a CK1-specific antibody and definitive localization of CK1 in the axonemes.

The *Chlamydomonas* CK1 protein is highly conserved and biochemical and enzymatic characterization of the axonemal CK1 correlates with previously characterized CK1 proteins. These results confirm the *Chlamydomonas CK1* gene and protein belongs to the CK1 family of protein kinases. Using a *Chlamydomonas* specific CK1 antibody, I used biochemical analysis of axonemes from mutants, and direct localization, to determine that axonemal CK1 is localized along the length of each axoneme and positioned on the outer doublet microtubules. Together, this data supports our overall hypothesis that CK1 is an axonemal protein, anchored in position to regulate phosphorylation of IC138. The CK1 clones, fusion protein and antibody are fundamental for defining the properties of axonemal CK1 and provide the tools required for study of CK1 targeting as well as CK1 function as described in Chapters 3 and 4.

Materials and Methods:

Strains and culture conditions: *Chlamydomonas reinhardtii* strains used in this study include CC125 (wild-type), *pf17* (paralyzed, lacks radial spoke head), *pf18* (paralyzed, lacks central pair apparatus), *pf28pf30ssh1* (paralyzed, lacks outer dynein arms and I1 dynein), *pf3* (abnormal motility, defective in the dynein regulatory complex- DRC) and *pf27* (paralyzed, defective in radial spokes). All strains were obtained from the *Chlamydomonas* Genetics Center (University of Minnesota, St. Paul, MN) with the exception of *pf28pf30ssh1* which was generated by crossing *pf28* with *pf30* and containing a new mutation called "suppressor of short" (Freshour et al., 2007; Piperno, 1990). For most experiments, cells were grown in tris-acetate phosphate (TAP) medium with aeration on a 14:10 hr light: dark cycle.

Identification of CK1 in the Chlamydomonas flagellar proteome and genomic analyses: To identify a candidate CK1 protein in the axoneme, I took advantage of the proteomic database provided by Gregory Pazour and George Witman (University of Massachusetts Medical Centre) prior to publication (Pazour et al., 2005). As discussed in the Results, each of the 15 peptides identified by MS/MS analysis defined the same candidate *CK1* gene, in the JGI genomic database (http://genome.jgi-psf.org/Chlre3/Chlre3.home.html). The gene model C_70149 (JGI version 2.0) defined a predicted protein and provided the basis for cloning and mapping the gene and predicting a polypeptide antigen for antibody production. The gene also provided the basis for design of fusion proteins expressed in bacteria and purified for work described in Chapter 3 and 4.

Cloning and sequencing of the full length genomic CK1 from wild-type and pf27 DNA:

DNA was isolated from wild-type and *pf27* strains as follows: cells were grown to a density ~$1.3x10^7$ cells. The cells were centrifuged to yield ~0.2-0.4 ml of packed cells that were then resuspended in a lysis buffer (20 mM Tris pH 7.5, 20 mM EDTA, 5% SDS and 1 mg/ml Proteinase K) and incubated at 50 °C for 12-16 hours. 0.1 ml of 7.5 M ammonium acetate pH 7.5 was added and the samples extracted once with phenol:chloroform:isoamyl alcohol (1:1:1) followed by chloroform extraction. The aqueous phase was transferred to a new tube to which 1 ml of 100% ethanol was added and mixed by inversion, followed by centrifugation at 10 K RPM for 5 minutes. The pellet was then washed with 80% ethanol and air dried. The DNA pellet was resuspended in 100 µl deionized water. The isolated DNA was used for restriction digests and PCR sequencing. The primer design and cloning strategy is described in the legend and illustrated in Fig. 2.

Antibody preparation: Based on the cDNA sequence, a unique polypeptide was predicted at the C-terminus and used as an antigen for antibody preparation. A restriction fragment containing nucleotides 739-1385 of the cDNA was used as a template for PCR amplification using the following primers: forward primer CTCAAGCAC CAGTCTAGAGGGACG and reverse primer CGGTTCGACTTCTAAAAGCTTGCACGC (*Xba1* and *HindIII* restriction sites are respectively underlined). The resulting PCR product, containing the last 102 base pairs of the CK1 cDNA, was cloned into the pCR2.1 vector (Invitrogen, Carlsbad, CA) to yield plasmid pAGCK1 and transformed into XL1-blue cells (Stratagene, La Jolla CA). The insert sequence was verified, excised with *Xba1* and *HindIII* and subcloned into the

pMAL-c expression vector (New England Biolabs, Ipswich, MA) to obtain the plasmid pAGCK1-MBP. The expression construct was transformed into bacterial strain BL21 (DE3) pLysS (Stratagene, La Jolla CA) and expression of the recombinant protein induced with 1 mM IPTG. The MBP-tagged fusion protein includes the C-terminal 34 amino acids of the CK1 protein. The MBP-CK1 protein was purified by amylose affinity chromatography according to manufacturer's instructions (New England Biolabs, Ipswich, MA) and was used as an antigen for production of a polyclonal CK1-specific antiserum in two rabbits (Spring Valley Laboratories, Woodbine MD).

Rabbits were chosen after pre-screening. The strategy for antibody production and selection of rabbits is illustrated in Fig. 3. Briefly, axonemal proteins were prepared for immunoblot analysis, as described below, and incubated with serum from candidate non-immunized rabbits diluted 1:500. Some of the candidate rabbits (for e.g. rabbit 8 in Fig. 3D) showed cross-reactivity with axonemal proteins and were not selected. Only rabbits that showed little to no cross-reactivity were chosen to be immunized with the CK1 antigen (rabbit 10, Fig.3D).

Cloning and expression of epitope tagged CK1: The CK1 coding sequence was amplified from a cDNA library ("library 7", Gregory Pazour) using the following primers- forward primer: CCTTTGGGACTGAGAAGCAC and reverse primer: CTGGCAGCTGTCTGTTCAAA and cloned into the pCR 2.1 TOPO cloning vector according to the manufacturer's instructions (Invitrogen, Carlsbad, CA) to yield plasmid pAGCK1-FL. The insert in pAGCK1-FL was amplified with the following primers to containing restriction sites: forward primer: CAGCGAGGATCCATGGCGTTGGACATT and reverse primer

GCGATTAAGCTTTTAGAAGTCGAACCGGCCG (*BamH1* and *Hind III* restriction sites, respectively, are underlined). The PCR product containing full length CK1 sequence was digested with *BamH1* and *HindIII* and cloned into the pet28A expression vector (Novagen, San Diego, CA). The resulting construct, pAGHisCK1, was transformed into strain BL21(DE3) pLysS (Stratagene, La Jolla, CA) and expression of the His-tagged fusion protein was induced with 1 mM Isopropyl β-D-1-thiogalactopyranoside (IPTG). The His-tagged CK1 protein was purified using Talon metal affinity resin (Clontech, Mountain View, CA).

Affinity Purification of CK1 antibodies: Antibodies were affinity purified using a modification of the original method of Olmsted (1981). Purified His-CK1 fusion protein was separated by SDS-PAGE and transferred to a nitrocellulose membrane as described above. The membrane was stained with Ponceau the HisCK1 band excised and incubated with blocking buffer (5% nonfat dry milk in TBS). The strip was then incubated with CK1 antiserum diluted 1:10 in 5% nonfat dry milk overnight at 4°C. The strip was washed 3X in 1x TBS buffer and the antibody was eluted in a buffer containing 0.2M glycine and 1mM EDTA and immediately neutralized in an equal volume of buffer containing 1% BSA, 50µl 1M Tris pH 9.0 in 1x TBS. Affinity-purified CK1 antibodies were subsequently used for immunoblotting as well as immunofluorescence microscopy.

***Isolation of axonemes*:** Flagella were isolated as described previously using a combination of laminar filtration and differential centrifugation to harvest cells, dibucaine for flagellar excision and differential centrifugation for flagellar isolation (Witman, 1986). Flagella were demembranated in buffer (10 mM Hepes, 5 mM $MgSO_4$, 1 mM DTT, 0.5 mM EDTA, 0.1 M PMSF, and 0.6 TIU aprotinin, pH 7.4) containing 1%

Nonidet-P40 to yield purified axonemes. For some experiments, CK1 was extracted from axonemes (1 mg/ml) with a buffer containing 0.3 M NaCl for 20 min on ice. Axonemal fractions were prepared for SDS-PAGE at a concentration of 1 mg/ml and typically either 10 or 20 μg of total protein was used for immunoblot analysis. Protein concentrations were determined using the Bradford assay (Biorad, Hercules CA) and BSA used as a standard. Unless otherwise stated, all reagents were obtained from Sigma-Aldrich and deionized H_2O was used throughout.

Immunoblotting: Axonemal protein samples were separated by SDS-PAGE and either stained by Coomassie blue or transferred to a nitrocellulose membrane (Bio-Rad, Hercules, CA) for immunoblot analysis. The membrane was blocked with 5% nonfat dry milk in TBS followed by incubation with primary antibodies (anti-CK1 serum diluted 1:10,000–1:20,000 or affinity purified antibodies diluted as cited in the below), then HRP-conjugated goat anti-rabbit secondary antibodies (1:10,000, Bio-Rad). The antibody reactivity was detected with the Pierce Western ECL blotting substrate (Thermo Scientific, Waltham, MA).

DEAE Chromatography: DEAE chromatography was carried out as previously described (Yang and Sale, 2000) with modification. The 0.3 M NaCl extract was dialyzed into DEAE buffer (20 mM Tris, pH 8, 2 mM EGTA, 2 mM EDTA, 5 mM dithiothreitol, 10% glycerol), loaded onto a DEAE column (3-5 ml) (Sigma), and washed with 30 ml of DEAE buffer, and 0.5-ml fractions were collected at a flow rate of 0.3 ml/min from 15 ml of a linear 0.0-0.7 M NaCl gradient in DEAE buffer.

Protein Kinase Assay: Protein kinase assays were performed using specific CK1 peptide substrates (C2335, Sigma-Aldrich). For CK1 activity, 2 µl samples from chromatography fractions or purified recombinant CK1 fractions were added to a reaction mixture to a final volume of 20 µl containing reaction buffer (50 mM Tris, pH 8, 0.1 mM EDTA, 0.2% β- mercaptoethanol, 7 mM magnesium acetate, 0.02% Brij 35, 20 mM NaCl, and 100 mM sodium orthovanadate), 0.5 µg/µl CKI specific substrate, and 40 µM [γ-32P] ATP (2000 cpm/pmol). After 30 min at 30 °C, the reactions were terminated by adding 1 µl of 100% trichloroacetic acid. 10µl samples from each reaction were applied in duplicate to discs of P-81 filter paper (Whatman), washed extensively with 75 mM phosphoric acid, and rinsed with acetone. The radioactivity of the dried P-81 paper discs was measured by scintillation counting (Beckmann LS 6500 Multi-purpose scintillation counter).

α-Casein-affinity Purification: Affinity purification of CKI was performed using α-casein conjugated to an agarose matrix (Sigma) and as described previously (Yang and Sale, 2000). α-Casein-conjugated agarose beads (40 µl) were added to 200 µl of the DEAE CKI-containing fraction that was diluted with an equal volume of 2× CK reaction buffer (50 mM Tris, pH 8, 0.1 mM EDTA, 0.2% β-mercaptoethanol, 7 mM magnesium acetate, 0.02% Brij 35, 20 mM NaCl, and 100 µM sodium orthovanadate). The mixture was incubated at 4 °C overnight, and after washing with CK buffer, the proteins sedimenting with the agarose beads were extracted and fixed by suspension in 30 µl of 1× SDS-PAGE sample buffer.

Immunoprecipitation: Dialyzed axonemal 0.3M NaCl extracts were obtained at a final concentration of 2 mg/ml as described above. This lysate was diluted 1:20 in an

immunoprecipitation buffer (IP buffer; 1x PBS, 1% Nonidet-P40, 0.05% Tween and PMSF). The diluted lysate was then incubated with protein A Sepharose beads (Sigma) (washed 5X with IP buffer) for 2 hours following by centrifugation to recover the supernatant (referred to as the "pre-cleared lysate"). Pre-clearing helps reduce non-specific binding of proteins to the Sepharose beads. The pre-cleared lysate was then mixed with either immune or pre-immune serum and placed on a shaker at 4°C overnight. Protein A Sepharose beads were washed 5X in IP buffer followed by blocking with 3% BSA for 1 hour. After blocking, the protein A Sepharose beads were again washed with IP buffer and then incubated with the antibody+lysate mixture for 5 hours. Beads were then washed 5X with IP buffer and supernatants collected for analysis. Proteins bound to the beads were eluted with 1x SDS-PAGE sample buffer.

Immunofluorescence microscopy: Isolated flagella or axonemes were immobilized on polylysine-L coated cover slips and fixed by immersion in -20°C methanol for 10 minutes (Yang and Sale, 1998). Following methanol fixation, cover slips were placed into 4°C PBS and then transferred to blocking buffer (2% BSA, 1% fish skin gelatin, 0.02% saponin, and 15% horse serum in PBS) at room temperature. Slides were incubated with affinity purified CK1 antibodies and acetylated alpha tubulin antibody (611B1) diluted 1:100 and 1:500 respectively in the blocking buffer at 4°C overnight. Cover slips were washed three times in blocking buffer followed by a 1 hour incubation in Alexa-fluor secondary antibodies (Invitrogen, Carlsbad, CA) diluted 1:1000 in blocking buffer for 1 hour. Images were captured and processed with Simple PCI software (Hamamatsu Corporation) using a wide-field fluorescence microscope (model DMR-E; Leica, Wetzlar, Germany) and a digital camera (model OrcaER; Hamamatsu Corporation,

Sewickley, PA). Image brightness and contrast were adjusted using Photoshop 9.0 (Adobe), and figures were assembled using Illustrator CS2 (Adobe).

Results:

Identification of axonemal CK1: As discussed in Chapter 1 and the Introduction, pharmacological and biochemical data have revealed the presence of a functional axonemal CK1 in *Chlamydomonas* (Yang and Sale, 2000), but the corresponding gene and protein had not been identified. Taking advantage of the *Chlamydomonas* nuclear genome (http://genome.jgi-psf.org/Chlre3/Chlre3.home.html; Merchant et al., 2007) as well as a comprehensive flagellar proteome (Pazour et al., 2005; Rolland et al., 2009; http://labs.umassmed.edu/chlamyfp/index.php), a candidate CK1 protein was identified. Fifteen separate peptides spanning the entire protein were found in the salt soluble KCl fraction from isolated axonemes that defined a conserved CK1 (Pazour et al., 2005; Fig 4). Each peptide defined the same gene located on scaffold 7 in JGI v2 (http://genome.jgi-psf.org/cgi-bin/browserLoad?db=chlre2&position=scaffold_7:199090-202756). Taking advantage of the availability of mapped BAC clones that contain the *CK1* gene, I determined that the *CK1* gene maps to linkage group (LG) XII/XIII, near the *Chlamydomonas* flagellar mutant *pf27* (Fig. 5; discussed below).

The *Chlamydomonas,* CK1 is highly conserved with a predicted mass of 38.4 kD and a high degree of homology to other CK1 isoforms, particularly mammalian CK1δ and CK1ε (Fig. 6). *Chlamydomonas* CK1 contains the domains characteristic of other CK1 isoforms including the NLS (nuclear localization sequence), the KHD (kinesin homology domain) and the ATP and the substrate binding domains (Fig. 3A). However the C- terminal 34 amino acids are unique to the *Chlamydomonas* isoform and unique within *Chlamydomonas*. I also identified an additional candidate *CK1* gene model (C_20325) in the genomic database (http://genome.jgi-psf.org/Chlre3/Chlre3.home.html).

However, the predicted protein from this gene did not contain any peptides found in the flagellar proteome, nor contained any of the signature motifs that characterize the CK1 family of proteins (Table 1). Thus, not only is the protein predicted for C_20325 not found in the flagella, but is likely not in the CK1 family of protein kinases. Therefore, based on homology as well as proteomic analysis, I conclude that there is only one *CK1* gene in *Chlamydomonas*: C_70149 (http://genome.jgi-psf.org/cgi-bin/dispGeneModel?db=chlre2&id=170052). Together, these results demonstrate that *Chlamydomonas* CK1 is a highly conserved protein that is likely to be a stable component of the axoneme and identical to the CK1 defined in our earlier study (Yang and Sale, 2000). Therefore, all studies in this thesis are focused on this gene and protein.

Biochemical characterization of Chlamydomonas CK1: To confirm that the CK1 we identified is an axonemal protein, a polyclonal antibody was produced to a purified MBP-tagged fusion protein containing the unique C-terminal polypeptide (Fig. 3). The antibody detected a single 36.5 kD band in isolated flagella or axonemes, with negligible amounts found in the detergent-soluble membrane-matrix fraction (Fig. 7A). This result indicates that CK1 is nearly completely targeted and anchored to the axoneme, consistent with our earlier biochemical analysis (Yang and Sale, 2000).

As previously demonstrated by Yang and Sale (2000), I also found that CK1 could be solubilized from the axonemes with 0.3M NaCl buffer (Fig. 7B), and remained soluble in physiological buffers permitting further fractionation and/or characterized by enzymatic and biochemical means. Thus, as a further test of specificity, 0.3M salt extract was dialyzed and fractionated by DEAE ion exchange. The peak fractions, identified by immunoblots, (Fig. 8A), correlated with peak CK1 kinase activity, determined by an in-

vitro assay using CK1 peptide substrates (Fig. 8B). To further characterize axonemal CK1 as well as test the specificity of the CK1 antibody, the dialyzed axonemal salt extracts and DEAE fractions were analyzed by immunoprecipitation and α-casein-agarose affinity precipitation respectively. Earlier studies had shown that α-casein agarose could be used to selectively precipitate the Casein Kinase family of kinases (Allocco et al., 2006; Zhai et al., 1995). CK1 was specifically enriched by α-casein-agarose affinity precipitation (Fig. 8C). CK1 antibodies immunoprecipitated CK1 from salt extracts (Fig. 9), providing a possible means to study interacting proteins.

Based on the biochemical properties I conclude that the gene model identified (C_70149; http://genome.jgi-psf.org/cgi-bin/dispGeneModel?db=chlre2&id=170052) is the functional axonemal *CK1* gene. This conclusion is founded on the following: [1] mass spectroscopy analysis of axonemal fractions containing CK1; [2] immunoblot analysis using a new and specific CK1 antibody; [3] solubility with a 0.3M NaCl buffer and co-purification of the CK1 kinase and biochemical activities; [4] kinase activity using CK1-specific peptide substrates; [5] selective purification and enrichment by α- casein-affinity precipitation and immunoprecipitation. Thus, the axonemal CK1 protein behaves exactly as previously characterized CK1 kinases (Hathaway et al., 1983; Kameshita and Fujisawa, 1989). These results also correlate with our previous biochemical analysis (Yang and Sale, 2000). The extracted CK1 remains soluble, an important feature for the biochemical studies described in Chapter 3 and the functional studies described in Chapter 4.

Localization of CK1: One of the advantages of the *Chlamydomonas* experimental system for study of ciliary/flagellar proteins is the availability of a library of axonemal mutants

that fail to assemble specific axonemal structures. For example, the *pf18* mutant fails to assemble the central pair apparatus; the *pf14* mutant fails to assemble the radial spokes; the *pf3* mutant fails to assemble the dynein regulatory complex and the *pf28pf30* double mutant fails to assemble the inner dynein isoform I1 and the outer dynein arms. Therefore, by a process of elimination and comparison of wild-type axonemes with mutant axonemes by immunoblots, we can determine if CK1 is associated with any of these axonemal structures. Using this strategy, I determined that CK1 is not missing in flagellar mutants that fail to assemble the central pair, radial spokes (Fig.10A). Therefore, CK1 is likely localized in the outer doublets microtubules. Furthermore, CK1 is not missing in mutants lacking the dynein regulatory complex (DRC) and the inner or outer dynein structures (Fig.10A). Therefore, we presume that CK1 must be associated with the outer doublet microtubules, and that its assembly in the axoneme does not require the radial spokes, central pair apparatus, DRC, I1 dynein or the outer dynein arms. As discussed below, this localization is consistent with targeting and anchoring CK1 near I1 dynein.

As an additional test, and to determine the distribution of CK1 in the axoneme, immunofluorescent localization using affinity purified CK1 antibodies was performed. As illustrated in Fig. 11 (intact axonemes), CK1 is uniformly distributed along the length of isolated axonemes. Since all axonemes in the field of view stain with the CK1 antibody and co-stain with the tubulin antibody, we conclude that CK1 is localized on both flagellar axonemes in *Chlamydomonas*.

Consistent with the biochemistry, axonemes depleted of CK1 with 0.3M NaCl buffer do not react with the CK1 antibody by immunofluorescence (Fig.11, “extracted

axonemes"). These data, showing CK1 is distributed along each axoneme, is consistent with our hypothesis that CK1 is a relatively abundant axonemal protein present in amounts at least equal to that of the I1 dynein complexes that are localized in every 96 nm repeat along the axoneme and on all 9 outer doublet microtubules. As described below, biochemical data from the proteome and axonemal fractionation is also consistent with this model, indicating that CK1 is relatively abundant. However, we have not yet directly localized CK1 at the electron-microscope level, and we have not yet determined if CK1 is localized along all nine outer doublet microtubules. As discussed below, experiments are planned to more directly localize CK1 on the outer doublet microtubules. Also, in the experiments described in Chapter 4, I take advantage of the "CK1-depleted" axonemes to test the role of CK1 in regulation of dynein.

The Chlamydomonas pf27 is not defective in the CK1 gene and CK1 is fully assembled in pf27 axonemes: As described above, I took advantage of BAC clones containing the *CK1* gene, and mapped the *CK1* gene near the previously mapped *Chlamydomonas* flagellar mutant *pf27* (Fig. 5). Mapping was made possible due to availability of an indexed BAC library composed of ~15,000 clones representing the *Chlamydomonas* nuclear genome with 10-12 fold coverage (Lefebvre and Silflow, 1999). The overlapping BAC clones are aligned with the large contigs of genomic DNA sequence and subsequently associated with molecular markers, previously characterized mutants and genetic maps. In this case, BAC clones containing the *CK1* gene mapped to an area on linkage group XII/XIII, close to a previously mapped flagellar mutant *pf27* (Fig. 5). *pf27* is a paralyzed mutant that is defective in axonemal spoke assembly and exhibits reduced phosphorylation of radial spoke proteins 2, 3, 5, 13 and 17 (Huang et al., 1979). Genetic

analysis indicates that the *pf27* gene product is extrinsic to the radial spokes, that is the gene product affects assembly and phosphorylation of radial spoke proteins but is not itself a radial spoke protein (Huang et al., 1979). Thus, the *pf27* gene product may play a role in assembly, trafficking or post-translational modification of radial spoke components in the axoneme.

Based on the mapping analysis, I postulated that *pf27* is defective in the *CK1* gene or defective in the transport or targeting of CK1 to the axoneme. To test these hypotheses, I sequenced the *CK1* gene in *pf27* and performed immunoblot analysis on isolated *pf27* axonemes. Genomic sequencing (Fig. 2) and immunoblot analysis (Fig. 12) revealed that there is no mutation in the *CK1* gene and the CK1 protein is intact and fully assembled in *pf27* axonemes. Further functional and biochemical analysis of *pf27* axonemes is described in Chapter 4, but we have yet to identify the gene and gene product for *pf27*.

Discussion:

Primary Conclusions

Although pharmacological and functional studies determined the presence of CK1 activity in the axoneme, the *Chlamydomonas CK1* gene and corresponding protein had not been identified at the beginning of my study. The goal of the work described in this chapter was to clone and characterize the *Chlamydomonas* axonemal CK1. In this work, I have demonstrated that: [1] *Chlamydomonas* CK1 is encoded by a single gene located on LG XII/XIII near *pf27* and it is highly conserved, sharing a high degree of homology to other CK1 isoforms; [2] immunoblot analysis and immunofluorescent localization using *Chlamydomonas* specific CK1 antibodies confirmed that CK1 is an axonemal protein located on the outer doublet microtubules, and along the length of both axonemes; [3] the axonemal CK1 is soluble in 0.3M NaCl buffers and CK1 co-purifies with CK1 kinase activity; [4] CK1 can be selectively enriched by immunoprecipitation as well as α-casein-agarose affinity precipitation; [5] *pf27* is not a mutation in the *CK1* gene.

These data support the model shown in Fig. 3, Chapter 1 indicating CK1 is targeted and anchored on the outer doublet microtubules. Predictably, CK1 is localized near I1 dynein repeating at 96 nm on each outer doublet microtubule in position to directly and effectively regulate phosphorylation of IC138 (Fig. 1).

***Chlamydomonas* CK1 is a highly conserved protein kinase**

As described in the Introduction, CK1 belongs to a family of serine/threonine kinases that have diverse and vital cellular functions including cell cycle control, control of circadian rhythm, regulation of apoptosis as well as regulation of developmental pathways such as the *Wnt* pathway (Bryja et al., 2007; Gross and Anderson, 1998;

Knippschild et al., 2005). CK1 kinases are monomeric, constitutively active enzymes that utilize ATP exclusively as a phosphate donor and are co-factor independent (Knippschild et al., 2005). Several isoforms of CK1 have been characterized in yeast as well as mammalian model systems. Based on homology analysis, signature domains have been identified that are common to all isoforms and they include- ATP and substrate binding domains, the catalytic triad, nuclear localization signals (NLS) and the kinesin-homology domain (KHD; Knippschild et al., 2005). The *Chlamydomonas* CK1 contains each of these signature domains.

Evidence from my study also indicates that *Chlamydomonas* bears only a single gene. Therefore, CK1 must be quite a versatile protein kinase responsible for functions in the cytoplasm, nucleus, eyespot and flagella (Schmidt et al., 2006). However, we do not know the molecular mechanism of how CK1 becomes targeted to these compartments and organelles. Several functions of CK1 involve its specific interactions with the microtubules, but as discussed in Chapter 3, we do not yet know the mechanisms.

To further confirm that the gene model identified belonged to the CK1 family of proteins, I took biochemical and enzymatic approaches to characterize the *Chlamydomonas* CK1. Polyclonal antibodies generated to the unique C-terminus identified a single 36.5 kD band in isolated flagella and axonemes . Solubility (CK1 is soluble in physiological buffers), biochemical fractionation, substrate-specific kinase assays as well as selective purification by α-casein-affinity precipitation and immunoprecipitation of axonemal CK1 was consistent with previously characterized CK1 proteins (Allocco et al., 2006; Hathaway et al., 1983; Kameshita and Fujisawa, 1989). Together this data confirms that C_70149 encodes the functional axonemal CK1

and that antibodies to the C-terminal polypeptide are specific to CK1. As indicated above, the predicted mass of CK1 is 38.5 kD, yet on SDS-PAGE gels, the axonemal CK1 migrates more quickly at 36.5 kD. The reason for this difference is not known but is commonly seen with other axonemal proteins.

To identify *Chlamydomonas* mutants that do not assemble CK1 in the axoneme, I compared the map position of CK1 to known motility mutants. The *CK1* gene was mapped using known mapped BAC clones that contained the entire *CK1* gene (Kathir et al., 2003). These BAC clones mapped the *CK1* gene to linkage group XII/XIII near the mutant *pf27*. I postulated that *pf27* was defective in the *CK1* gene; however, genomic sequencing and immunoblot analysis confirmed that *pf27* is not defective in the *CK1* gene and that CK1 is fully assembled in axonemes from *pf27*.

To date we have been unable to identify CK1 mutants. This is likely due to additional essential functions in cell growth and circadian rhythm (Schmidt et al., 2006). Furthermore, CK1 siRNA strains are defective in flagellar assembly (Schmidt et al., 2006) and, therefore, not useful for testing the role of CK1 in axonemal motility. These data also predict a fundamental role for CK1 in processes of flagellar assembly, possibly implicating CK1 in regulation of IFT (intra-flagellar transport), the mechanism for transport of axonemal components from the cytoplasm to the flagellar compartment for assembly (reviewed in Rosenbaum and Witman, 2002; Scholey, 2008; Scholey and Anderson, 2006). This is an appealing idea since little is known about regulation and loading of cargo or motors on the IFT complexes or how directed IFT motility is regulated.

CK1 is targeted and anchored in the flagellar axoneme

Here, we cloned the *Chlamydomonas CK1* gene starting with peptides identified in the axonemal fractions of the flagellar proteome (Pazour et al, 2005). These data alone indicated that the CK1 protein is axonemal and identical to the same protein identified in an earlier study (Yang and Sale, 2000). The *CK1* gene (C_70149 in JGI version 2.0) encodes a highly conserved protein that contains all the signature CK1 domains described above. However, the C-terminal 34 amino acids are unique to *Chlamydomonas* CK1 and we presume that this C-terminal domain could have a species-specific function. *Chlamydomonas* CK1 shares a high degree of homology with mammalian CK1δ and CK1ε (Fig. 6). Interestingly, CK1δ is enriched in ciliated cells of the mouse respiratory tract and rat testis, suggesting CK1 has analogous functions in mammalian cilia and flagella (Lohler et al., 2009). Differences in C-terminal amino acid sequences cannot, therefore, define a common structure used to target and anchor CK1 to microtubules. Rather, if the mammalian isoforms are also located in the cilia and flagella and targeted to the axonemes, it is more likely a conserved structure responsible for interaction with axonemal microtubules or microtubules in general. It has been proposed that the "KHD" domain in CK1 mediates microtubule interactions (Behrend et al., 2000). However, microtubule interactions and tubulin binding alone cannot explain the precise localization of CK1. Proper localization likely involves other domains and putative "CKAPs" (see Chapter 3). It will be important to localize mammalian CK1 isoforms in ciliated cells and determine if they are located in the axoneme.

Previous data predicted that axonemal CK1 is a relatively abundant protein present in possible equal amounts to I1 dynein (Yang and Sale, 2000). This conclusion is

based on protein stains of partially purified CK1 derived from axonemes. Thus, a more precise estimate of CK1 stoichiometry in the axonemes is required. This remains a difficult, but high priority goal. I1 dynein has been shown to localize to the proximal position of the 96 nm repeating module that is found along the length of both axonemes and on every outer doublet microtubules (Fig. 3, Chapter 1). Direct immunofluorescent localization using affinity purified CK1 antibodies revealed that CK1 is localized uniformly along the entire length of both axonemes, consistent with localization near I1 dynein. Analysis of flagella and axonemes from mutants that do not assemble specific axonemal structures revealed that CK1 is associated with outer doublet microtubules. Thus, the simplest model is that CK1 is localized in a 96 nm repeat pattern along each outer doublet microtubule (see below).

One fundamental question is: How is CK1 targeted and anchored to the outer doublet microtubules? Based on our hypothesis, CK1 is localized with a 96 nm periodicity and therefore, tubulin interaction alone cannot explain this precise localization. Thus, we predict the axoneme contains a specific CK1 interacting protein ("CKAP") or a "docking complex" (analogous to AKAPs) that localize CK1 near I1 dynein. Discovery of CK1 interacting proteins remains a very high priority and is discussed in the next chapter.

Model for CK1 localization in the axoneme and the prediction that CK1 must be localized by a specialized docking protein or "CKAP".

In keeping with our overall hypothesis, and the predicted dynein regulatory function, we propose that CK1 is positioned near I1 dynein and the IC138 sub-complex at

regular intervals of 96 nm and on every outer doublet (Fig. 3, Chapter 1). Demonstration of the periodic spacing will require direct localization by immunoelectron microscopy. Immunogold localization in whole mount, negative stained, "splayed" axonemes could reveal the periodic arrangement of CK1 along the outer doublet microtubules. Immunogold offers sufficient resolution to reveal the 96 nm repeat module or multiples of a 96 nm repeat (Bernstein et al., 1994). I anticipate that the colloidal gold will be localized near the base of the radial spoke 1 (S1) as indicated in Fig.3, Chapter 1.

Although immunoblot analysis of axonemes from structural mutants indicates CK1 is located on the outer doublet microtubules and immunofluorescent microscopy reveals CK1 is located along the length of the axoneme, I have not yet determined whether CK1 is localized to all nine outer doublet microtubules. This is an important future goal and the results are important irrespective of the outcome.

One strategy that we can use is illustrated in Fig. 13. In this experiment, axonemal microtubules can be induced to slide with ATP and protease (method of Okagaki and Kamiya, 1986) to extrude the central pair and induce individual outer doublets to extend along one another. This method is further described in the legend, and doublet #1 can be identified using antibodies to outer arm dynein, since the outer arm dynein arms do not assemble on doublet #1. It is possible that CK1 is present on all nine outer doublets. However, one intriguing possibility is that CK1 is asymmetrically distributed on the 9 outer doublet microtubules. For example, CK1 maybe localized to doublet microtubules on one side of the bending axis **(**Fig 8, Chapter 1). If this is the case, it is likely that CK1 could affect bending by locally altering I1-dynein activity on specific doublet microtubules and affecting microtubule sliding on a one side of the "axis" of the

axoneme, and modulating the form of the bend. Models of axonemal bending are described in Chapter 1 and Chapter 5.

Fig.1

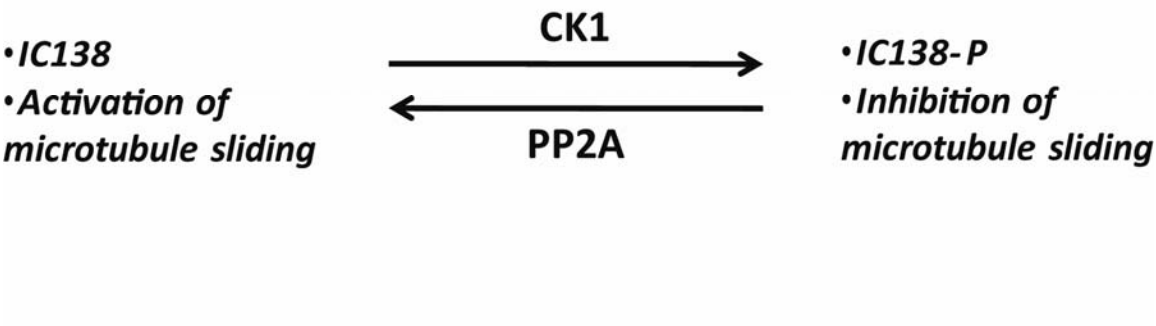
•IC138
•Activation of microtubule sliding
CK1
PP2A
•IC138-P
•Inhibition of microtubule sliding

Figure 1: Model for regulation of I1 dynein and the CK1 protein. Analysis of wild-type and mutant axonemes has revealed that microtubule sliding activity is regulated by phosphorylation of the I1 dynein subunit IC138 (Wirschell et al., 2007). Pharmacological data predicts that IC138 is phosphorylated by the axonemal kinase CK1, and that phosphorylation inhibits dynein-driven microtubule sliding. Evidently, in paralyzed axonemes defective in central pair or radial spoke assembly, CK1 activity is unregulated, leading to a uniform phosphorylation of IC138 and inhibition of dynein. The model also indicates an axonemal phosphatase, PP2A, is required for active microtubule sliding (Yang and Sale, 2000).

Fig. 2

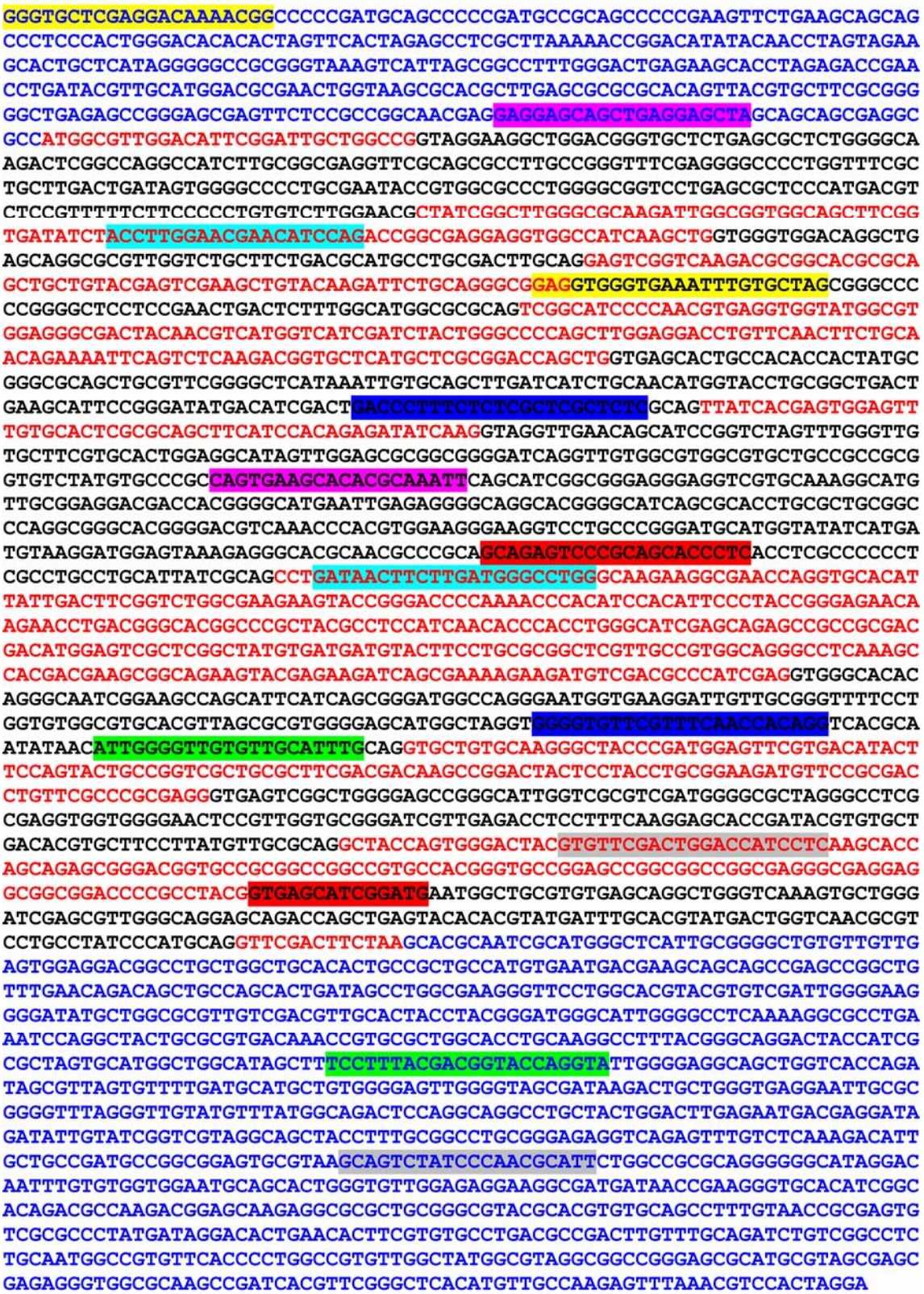
GGGTGCTCGAGGACAAAACGGCCCCCGATGCAGCCCCCGATGCCGCAGCCCCCGAAGTTCTGAAGCAGCAG
CCCTCCCACTGGGACACACACTAGTTCACTAGAGCCTCGCTTAAAAACCGGACATATACAACCTAGTAGAA
GCACTGCTCATAGGGGGCCGCGGGTAAAGTCATTAGCGGCCTTTGGGACTGAGAAGCACCTAGAGACCGAA
CCTGATACGTTGCATGGACGCGAACTGGTAAGCGCACGCTTGAGCGCGCGCACAGTTACGTGCTTCGCGGG
GGCTGAGAGCCGGGAGCGAGTTCTCCGCCGGCAACGAGGAGGAGCAGCTGAGGAGCTAGCAGCAGCGAGGC
GCCATGGCGTTGGACATTCGGATTGCTGGCCGGTAGGAAGGCTGGACGGGTGCTCTGAGCGCTCTGGGGCA
AGACTCGGCCAGGCCATCTTGCGGCGAGGTTCGCAGCGCCTTGCCGGGTTTCGAGGGGCCCCTGGTTTCGC
TGCTTGACTGATAGTGGGGCCCCTGCGAATACCGTGGCGCCCTGGGGCGGTCCTGAGCGCTCCCATGACGT
CTCCGTTTTTCTTCCCCCTGTGTCTTGGAACGCTATCGGCTTGGGCGCAAGATTGGCGGTGGCAGCTTCGG
TGATATCTACCTTGGAACGAACATCCAGACCGGCGAGGAGGTGGCCATCAAGCTGGTGGGTGGACAGGCTG
AGCAGGCGCGTTGGTCTGCTTCTGACGCATGCCTGCGACTTGCAGGAGTCGGTCAAGACGCGGCACGCGCA
GCTGCTGTACGAGTCGAAGCTGTACAAGATTCTGCAGGGCGGAGGTGGGTGAAATTTGTGCTAGCGGGCCC
CCGGGGCTCCTCCGAACTGACTCTTTGGCATGGCGCGCAGTCGGCATCCCCAACGTGAGGTGGTATGGCGT
GGAGGGCGACTACAACGTCATGGTCATCGATCTACTGGGCCCCAGCTTGGAGGACCTGTTCAACTTCTGCA
ACAGAAAATTCAGTCTCAAGACGGTGCTCATGCTCGCGGACCAGCTGGTGAGCACTGCCACACCACTATGC
GGGCGCAGCTGCGTTCGGGGCTCATAAATTGTGCAGCTTGATCATCTGCAACATGGTACCTGCGGCTGACT
GAAGCATTCCGGGATATGACATCGACTGACCCTTTCTCTCGCTCGCTCTCGCAGTTATCACGAGTGGAGTT
TGTGCACTCGCGCAGCTTCATCCACAGAGATATCAAGGTAGGTTGAACAGCATCCGGTCTAGTTTGGGTTG
TGCTTCGTGCACTGGAGGCATAGTTGGAGCGCGGCGGGGATCAGGTTGTGGCGTGGCGTGCTGCCGCCGCG
GTGTCTATGTGCCCGCCAGTGAAGCACACGCAAATTCAGCATCGGCGGGAGGGAGGTCGTGCAAAGGCATG
TTGCGGAGGACGACCACGGGGCATGAATTGAGAGGGGCAGGCACGGGGCATCAGCGCACCTGCGCTGCGGC
CCAGGCGGGCACGGGGACGTCAAACCCACGTGGAAGGGAAGGTCCTGCCCGGGATGCATGGTATATCATGA
TGTAAGGATGGAGTAAAGAGGGCACGCAACGCCCGCAGCAGAGTCCCGCAGCACCCTCACCTCGCCCCCCT
CGCCTGCCTGCATTATCGCAGCCTGATAACTTCTTGATGGGCCTGGGCAAGAAGGCGAACCAGGTGCACAT
TATTGACTTCGGTCTGGCGAAGAAGTACCGGGACCCCAAAACCCACATCCACATTCCCTACCGGGAGAACA
AGAACCTGACGGGCACGGCCCGCTACGCCTCCATCAACACCCACCTGGGCATCGAGCAGAGCCGCCGCGAC
GACATGGAGTCGCTCGGCTATGTGATGATGTACTTCCTGCGCGGCTCGTTGCCGTGGCAGGGCCTCAAAGC
CACGACGAAGCGGCAGAAGTACGAGAAGATCAGCGAAAAGAAGATGTCGACGCCCATCGAGGTGGGCACAC
AGGGCAATCGGAAGCCAGCATTCATCAGCGGGATGGCCAGGGAATGGTGAAGGATTGTTGCGGGTTTTCCT
GGTGTGGCGTGCACGTTAGCGCGTGGGGAGCATGGCTAGGTGGGGTGTTCGTTTCAACCACAGGTCACGCA
ATATAACATTGGGGTTGTGTTGCATTTGCAGGTGCTGTGCAAGGGCTACCCGATGGAGTTCGTGACATACT
TCCAGTACTGCCGGTCGCTGCGCTTCGACGACAAGCCGGACTACTCCTACCTGCGGAAGATGTTCCGCGAC
CTGTTCGCCCGCGAGGGTGAGTCGGCTGGGGAGCCGGGCATTGGTCGCGTCGATGGGGCGCTAGGGCCTCG
CGAGGTGGTGGGGAACTCCGTTGGTGCGGGATCGTTGAGACCTCCTTTCAAGGAGCACCGATACGTGTGCT
GACACGTGCTTCCTTATGTTGCGCAGGCTACCAGTGGGACTACGTGTTCGACTGGACCATCCTCAAGCACC
AGCAGAGCGGGACGGTGCCGCGGCCGGCCGTGCCACGGGTGCCGGAGCCGGCGGCCGGCGAGGGCGAGGAG
GCGGCGGACCCCGCCTACGGTGAGCATCGGATGAATGGCTGCGTGTGAGCAGGCTGGGTCAAAGTGCTGGG
ATCGAGCGTTGGGCAGGAGCAGACCAGCTGAGTACACACGTATGATTTGCACGTATGACTGGTCAACGCGT
CCTGCCTATCCCATGCAGGTTCGACTTCTAAGCACGCAATCGCATGGGCTCATTGCGGGGCTGTGTTGTTG
AGTGGAGGACGGCCTGCTGGCTGCACACTGCCGCTGCCATGTGAATGACGAAGCAGCAGCCGAGCCGGCTG
TTTGAACAGACAGCTGCCAGCACTGATAGCCTGGCGAAGGGTTCCTGGCACGTACGTGTCGATTGGGGAAG
GGGATATGCTGGCGCGTTGTCGACGTTGCACTACCTACGGGATGGGCATTGGGGCCTCAAAAGGCGCCTGA
AATCCAGGCTACTGCGCGTGACAAACCGTGCGCTGGCACCTGCAAGGCCTTTACGGGCAGGACTACCATCG
CGCTAGTGCATGGCTGGCATAGCTTTCCTTTACGACGGTACCAGGTATTGGGGAGGCAGCTGGTCACCAGA
TAGCGTTAGTGTTTTGATGCATGCTGTGGGGAGTTGGGGTAGCGATAAGACTGCTGGGTGAGGAATTGCGC
GGGGTTTAGGGTTGTATGTTTATGGCAGACTCCAGGCAGGCCTGCTACTGGACTTGAGAATGACGAGGATA
GATATTGTATCGGTCGTAGGCAGCTACCTTTGCGGCCTGCGGGAGAGGTCAGAGTTTGTCTCAAAGACATT
GCTGCCGATGCCGGCGGAGTGCGTAAGCAGTCTATCCCAACGCATTCTGGCCGCGCAGGGGGGCATAGGAC
AATTTGTGTGGTGGAATGCAGCACTGGGTGTTGGAGAGGAAGGCGATGATAACCGAAGGGTGCACATCGGC
ACAGACGCCAAGACGGAGCAAGAGGCGCGCTGCGGGCGTACGCACGTGTGCAGCCTTTGTAACCGCGAGTG
TCGCGCCCTATGATAGGACACTGAACACTTCGTGTGCCTGACGCCGACTTGTTTGCAGATCTGTCGGCCTC
TGCAATGGCCGTGTTCACCCCTGGCCGTGTTGGCTATGGCGTAGGCGGCCGGGAGCGCATGCGTAGCGAGC
GAGAGGGTGGCGCAAGCCGATCACGTTCGGGCTCACATGTTGCCAAGAGTTTAAACGTCCACTAGGA

Figure 2: Cloning strategy for sequencing genomic DNA. The above sequence denotes the genomic CK1 sequence based on gene model C_70149 (JGI version 2.0). To verify the sequence and clone the gene, primers were designed for PCR. Matching colored sequences (boxed) are regions to which primers were designed for genomic sequencing analysis. The primers were designed in order to ensure complete coverage and accurate sequencing of genomic DNA from both wild-type as well as *pf27* strains. Base pairs in red denote coding sequence (exons), while base pairs in black are non-coding introns. Base pairs in blue are overhangs on the 5' and 3' end.

Fig.3

A. Schematic diagram of axonemal CK1

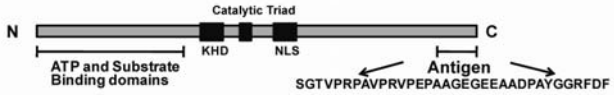

B. Antigenic sequence cloned into pMAL-C to give MBP-tagged polypeptide

C. Solubilization and purification of MBP-tagged CK1 fusion protein.

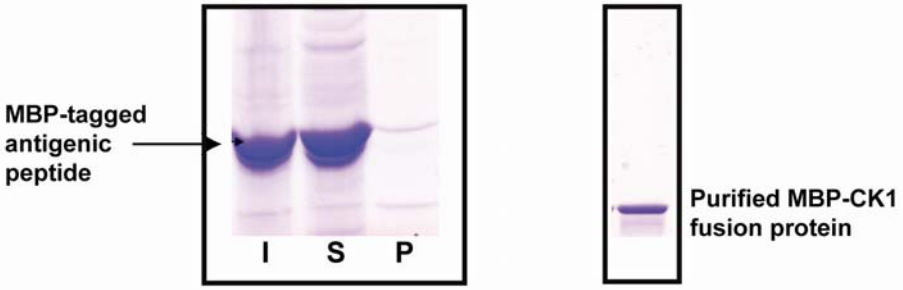

D. Prescreening non-immune sera from candidate rabbits

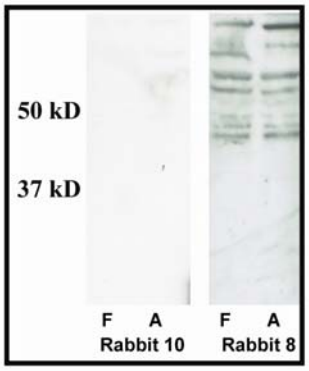

E. Testing immune-sera for antigenicity

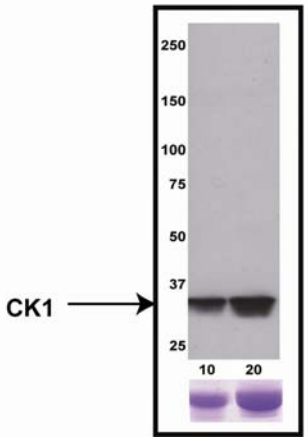

Figure 3: Strategy to produce Chlamydomonas CK1-specific antibody: (A) *Chlamydomonas* CK1 is highly conserved and contains characteristic CK1 domains including the N-terminal ATP and substrate binding domains, the kinesin homology domain (KHD), the catalytic triad and the nuclear localization signal (NLS). A CK1 specific antibody was made to a unique polypeptide at the C-terminus. (B) DNA encoding the C-terminal peptide was cloned into the pMAL-c vector to produce a MBP-tagged fusion protein to be used as an antigen.(C) MBP-tagged fusion protein was expressed (I) and was found to be almost completely soluble (S) with very little protein found in the insoluble pellet (P) fraction (left panel). MBP-CK1 peptide was purified over an amylose- resin column (right panel) (D) Non-immune rabbit serum was tested for antibodies to axonemal proteins in the 37-50 kD size range (predicted molecular weight for CK1). Immunoblots containing axonemal proteins were probed with non-immune rabbit sera from candidate rabbits (diluted 1:500). Rabbit #8 exhibits several background bands, while rabbit #10 shows minimal background bands, and was chosen for antibody production (E) The CK1 antiserum identifies a single 36.5 kD band in isolated axonemes. The two lanes contain 10 and 20 μg of axonemal proteins, and the Coomassie stain below shows tubulin as a loading control.

Fig. 4

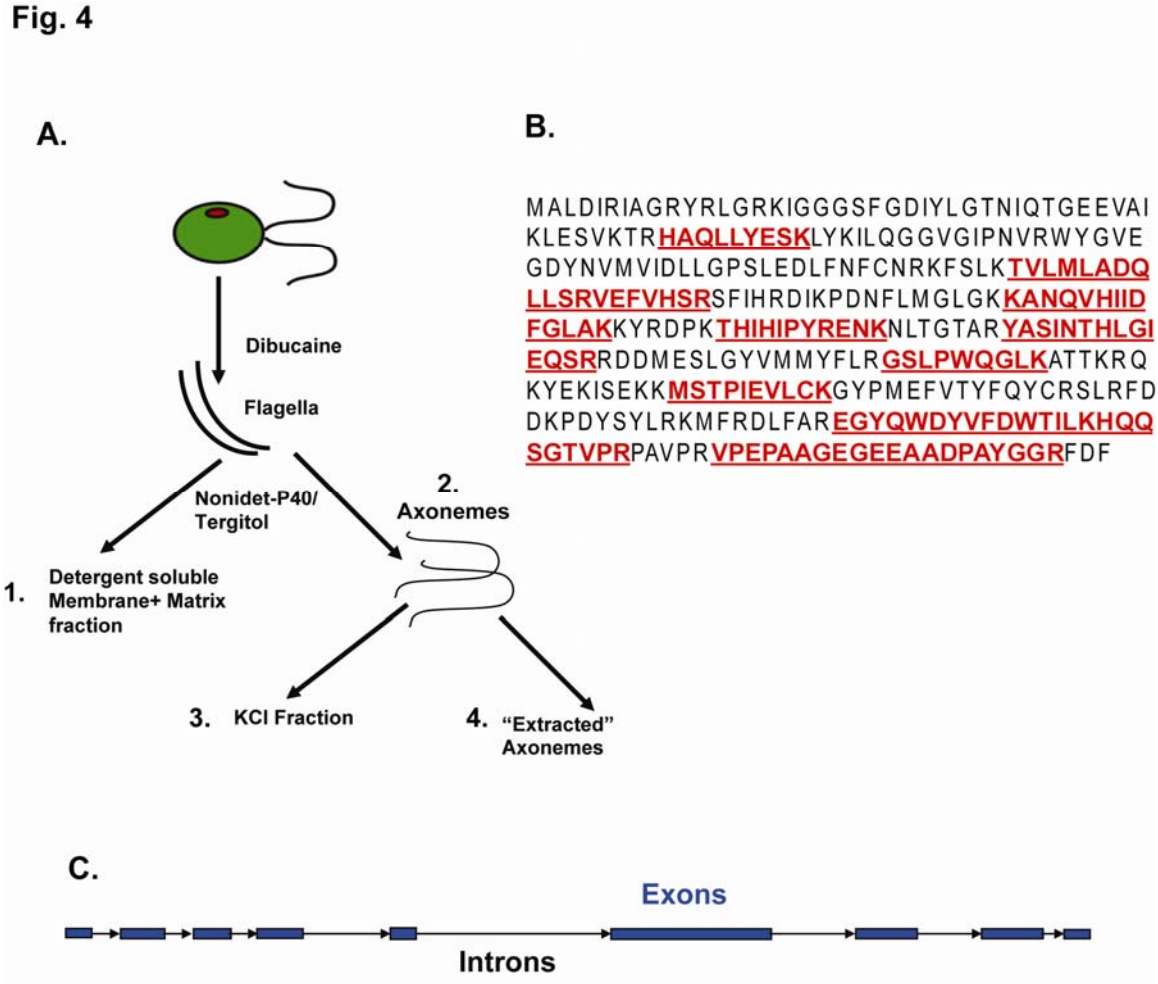
A.
Dibucaine
Flagella
Nonidet-P40/
Tergitol
2.
Axonemes
1.
Detergent soluble
Membrane+ Matrix
fraction
3.
KCl Fraction
4.
"Extracted"
Axonemes
B.
MALDIRIAGRYRLGRKIGGGSFGDIYLGTNIQTGEEVAI
KLESVKTRHAQLLYESKLYKILQGGVGIPNVRWYGVE
GDYNVMVIDLLGPSLEDLFNFCNRKFSLKTVLMLADQ
LLSRVEFVHSRSFIHRDIKPDNFLMGLGKKANQVHIID
FGLAKKYRDPKTHIHIPYRENKNLTGTARYASINTHLGI
EQSRRDDMESLGYVMMYFLRGSLPWQGLKATTKRQ
KYEKISEKKMSTPIEVLCKGYPMEFVTYFQYCRSLRFD
DKPDYSYLRKMFRDLFAREGYQWDYVFDWTILKHQQ
SGTVPRPAVPRVPEPAAGEGEEAADPAYGGRFDF
C.
Exons
Introns

Figure 4: Identification of Chlamydomonas CK1. (A) Flow chart for isolation of flagellar fractions used for MS analyses (Pazour et al., 2005). Purified flagella were isolated from *Chlamydomonas* cells and demembranated with the non-ionic detergents (tergitol or Nonidet-P40) to obtain "membrane+matrix" fraction and demembranted axonemes. Axonemes were resuspended in 0.6 M KCl and the mixture was centrifuged to yield a supernatant containing the "KCl extract" and a pellet containing the "extracted axonemes". The proteins in the (1) "membrane+matrix", (2) axonemal, (3)"0.6 KCl extract" and (4)"extracted axoneme" fractions were analyzed by tandem mass spectroscopy (B) CK1 amino acid sequence: 15 separate peptides (red, underlined) identified in the KCl/axonemal fraction in the *Chlamydomonas* flagellar proteome span the entire sequence (C) The axonemal *CK1* gene identified (C_70149) is composed of 9 exons (blue) and 8 introns (black).

Fig. 5.

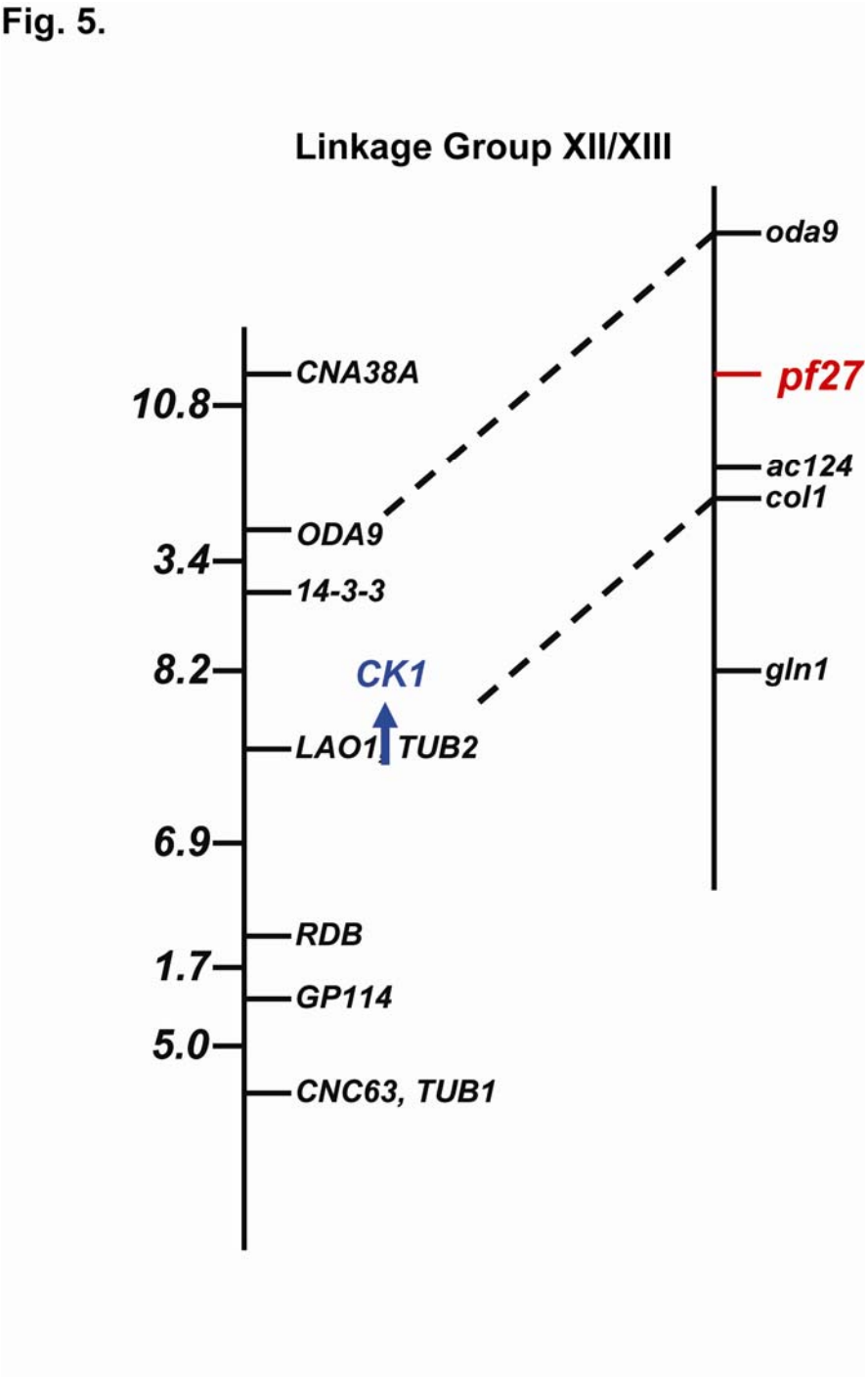
Linkage Group XII/XIII
oda9
pf27
ac124
col1
gln1
CNA38A
10.8
ODA9
3.4
14-3-3
8.2
CK1
LAO1, TUB2
6.9
RDB
1.7
GP114
5.0
CNC63, TUB1

Figure 5: Chlamydomonas CK1 gene maps near pf27: BAC clones containing the entire *CK1* gene map to linkage group XII/XIII, near a previously mapped *Chlamydomonas* mutant called *pf27*.

Fig. 6

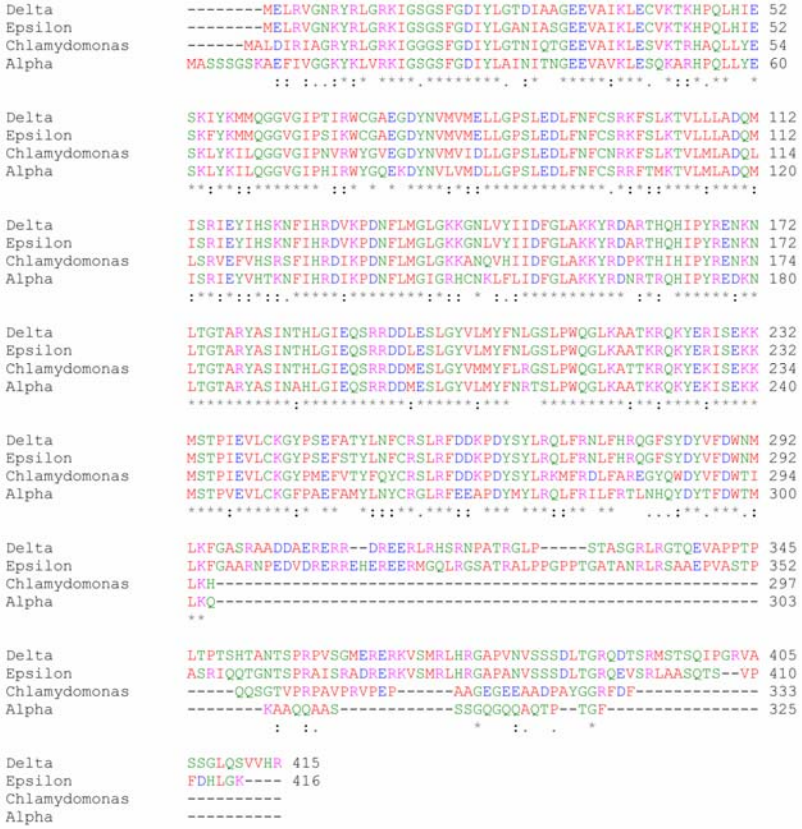
Delta --------MELRVGNRYRLGRKIGSGSFGDIYLGTDIAAGEEVAIKLECVKTKHPQLHIE 52
Epsilon --------MELRVGNKYRLGRKIGSGSFGDIYLGANIASGEEVAIKLECVKTKHPQLHIE 52
Chlamydomonas ------MALDIRIAGRYRLGRKIGGGSFGDIYLGTNIQTGEEVAIKLESVKTRHAQLLYE 54
Alpha MASSSGSKAEFIVGGKYKLVRKIGSGSFGDIYLAINITNGEEVAVKLESQKARHPQLLYE 60
Delta SKIYKMMQGGVGIPTIRWCGAEGDYNVMVMELLGPSLEDLFNFCSRKFSLKTVLLLADQM 112
Epsilon SKFYKMMQGGVGIPSIKWCGAEGDYNVMVMELLGPSLEDLFNFCSRKFSLKTVLLLADQM 112
Chlamydomonas SKLYKILQGGVGIPNVRWYGVEGDYNVMVIDLLGPSLEDLFNFCNRKFSLKTVLMLADQL 114
Alpha SKLYKILQGGVGIPHIRWYGQEKDYNVLVMDLLGPSLEDLFNFCSRRFTMKTVLMLADQM 120
Delta ISRIEYIHSKNFIHRDVKPDNFLMGLGKKGNLVYIIDFGLAKKYRDARTHQHIPYRENKN 172
Epsilon ISRIEYIHSKNFIHRDVKPDNFLMGLGKKGNLVYIIDFGLAKKYRDARTHQHIPYRENKN 172
Chlamydomonas LSRVEFVHSRSFIHRDIKPDNFLMGLGKKANQVHIIDFGLAKKYRDPKTHIHIPYRENKN 174
Alpha ISRIEYVHTKNFIHRDIKPDNFLMGIGRHCNKLFLIDFGLAKKYRDNRTRQHIPYREDKN 180
Delta LTGTARYASINTHLGIEQSRRDDLESLGYVLMYFNLGSLPWQGLKAATKRQKYERISEKK 232
Epsilon LTGTARYASINTHLGIEQSRRDDLESLGYVLMYFNLGSLPWQGLKAATKRQKYERISEKK 232
Chlamydomonas LTGTARYASINTHLGIEQSRRDDMESLGYVMMYFLRGSLPWQGLKATTKRQKYEKISEKK 234
Alpha LTGTARYASINAHLGIEQSRRDDMESLGYVLMYFNRTSLPWQGLKAATKKQKYEKISEKK 240
Delta MSTPIEVLCKGYPSEFATYLNFCRSLRFDDKPDYSYLRQLFRNLFHRQGFSYDYVFDWNM 292
Epsilon MSTPIEVLCKGYPSEFSTYLNFCRSLRFDDKPDYSYLRQLFRNLFHRQGFSYDYVFDWNM 292
Chlamydomonas MSTPIEVLCKGYPMEFVTYFQYCRSLRFDDKPDYSYLRKMFRDLFAREGYQWDYVFDWTI 294
Alpha MSTPVEVLCKGFPAEFAMYLNYCRGLRFEEAPDYMYLRQLFRILFRTLNHQYDYTFDWTM 300
Delta LKFGASRAADDAERERR--DREERLRHSRNPATRGLP-----STASGRLRGTQEVAPPTP 345
Epsilon LKFGAARNPEDVDRERREHEREERMGQLRGSATRALPPGPPTGATANRLRSAAEPVASTP 352
Chlamydomonas LKH---------- 297
Alpha LKQ---------- 303
Delta LTPTSHTANTSPRPVSGMERERKVSMRLHRGAPVNVSSSDLTGRQDTSRMSTSQIPGRVA 405
Epsilon ASRIQQTGNTSPRAISRADRERKVSMRLHRGAPANVSSSDLTGRQEVSRLAASQTS--VP 410
Chlamydomonas -----QQSGTVPRPAVPRVPEP------AAGEGEEAADPAYGGRFDF---------- 333
Alpha --------KAAQQAAS-----------SSGQGQQAQTP--TGF---------- 325
Delta SSGLQSVVHR 415
Epsilon FDHLGK---- 416
Chlamydomonas ----------
Alpha ----------

Figure 6: Chlamydomonas CK1 is a highly conserved protein: Multiple sequence analysis (ClustalW) revealed that *Chlamydomonas* CK1 is a highly conserved protein with high degree of homology to mammalian CK1 isoforms, particularly CK1δ (79% identity) and CK1ε (78% identity). NCBI accession numbers: CK1α: NP_666199, CK1δ: NP_620690, CK1ε: NP_038795.

Fig. 7

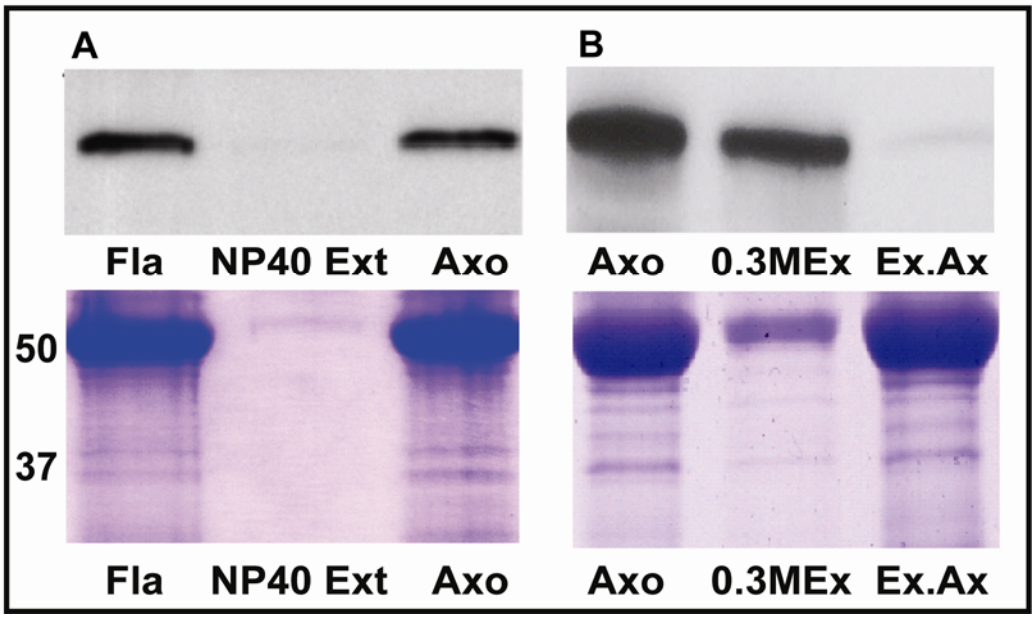
A
B
Fla
NP40 Ext
Axo
Axo
0.3MEx
Ex.Ax
50
37
Fla
NP40 Ext
Axo
Axo
0.3MEx
Ex.Ax

Figure 7: CK1 is an axonemal protein and is extractable in 0.3M NaCl buffers. (A) Flagella (Fla) were fractionated into a Nonidet-P40 soluble membrane/matrix fraction (NP-40 Ext) and axonemal fraction (Axo) then analyzed by immunoblot probed with the anti-CK1 antibody. The antibody shows that CK1 is present in the flagella and axonemal fractions but a negligible amount of CK1 is detected in the membrane+matrix fraction, verifying that CK1 is an axonemal protein. (B) Axonemes (Axo) were extracted with 0.3M salt to yield a 0.3M salt extract (0.3M Ex) and extracted axonemes (Ex.Ax) and the fractions were analyzed by immunoblots. The CK1 antibody detects CK1 in the axonemes and 0.3M extracts but not in the extracted axonemes, indicating that CK1 is solubilized from axonemes by 0.3M salt treatment. Lower panels are coomasie stained gels used as load controls.

Fig.8

A.

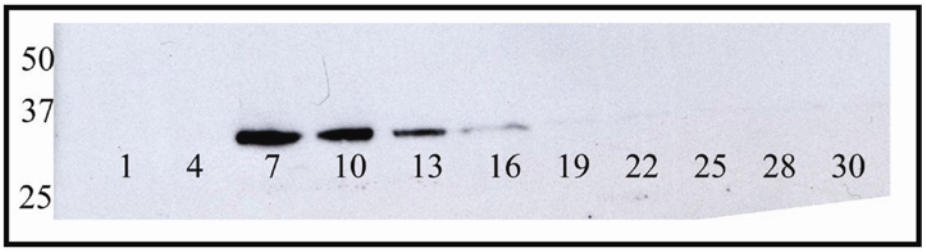
50
37
25
1
4
7
10
13
16
19
22
25
28
30

B.

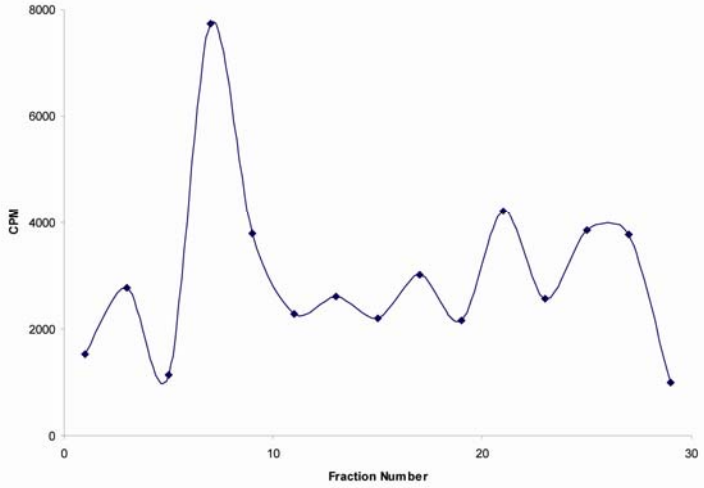
8000
6000
4000
2000
0
CPM
0
10
20
30
Fraction Number

C.

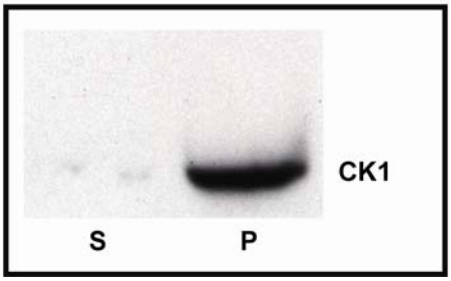
CK1
S
P

Figure 8: Biochemical fractionation and characterization of axonemal CK1- Co-purification of CK1 kinase activity and immunoreactivity. (A) A 0.3M salt extract from isolated wild-type axonemes was fractionated by DEAE ion-exchange chromatography and peak CK1 fractions were identified by immunoblot analysis using the CK1 antibody (peak 7-13). (B) Each DEAE fraction (2 µl) was then analyzed for CK1-kinase activity using CK1-specific peptide substrates and [γ-32P] ATP. Peak kinase activity correlated with the peak CK1 fractions identified in panel A. (C) Peak CK1 fractions obtained from DEAE chromatography were further fractionated by α-casein-affinity precipitation. Immunoblot analysis revealed that CK1 was enriched by α-casein affinity.

Fig. 9

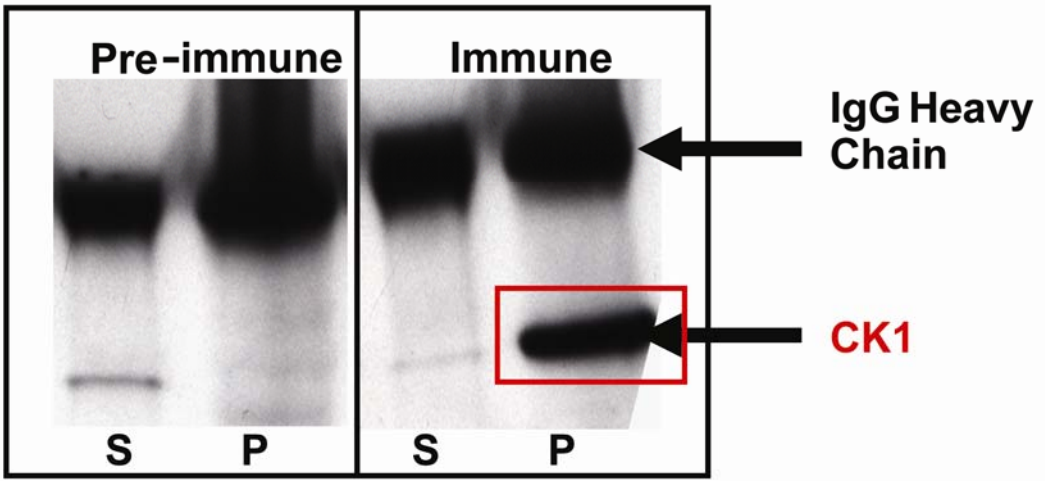

Figure 9: The CK1 antibody immunoprecipitates CK1 from axonemal salt extracts.

Analysis of immunoprecipitation experiments using the CK1 antibody conjugated with protein A Sepharose beads for precipitation of proteins in axonemal salt extracts, reveals that CK1 is precipitated, thus additionally confirming the specificity of the CK1 antibody. The left panel shows a mock immunoprecipitation using preimmune serum in which no CK1 is pulled down. The upper bands represent the IgG heavy chains.

Fig.10

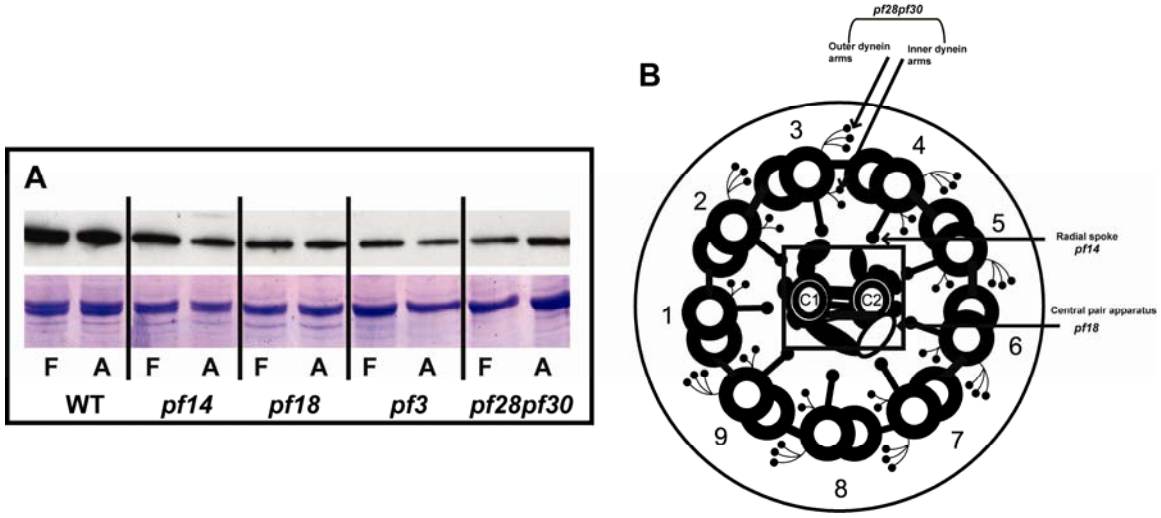
A
F A F A F A F A F A
WT
pf14
pf18
pf3
pf28pf30
B
pf28pf30
Outer dynein arms
Inner dynein arms
Radial spoke
pf14
Central pair apparatus
pf18
C1
C2
1
2
3
4
5
6
7
8
9

Figure 10: Axonemal CK1 is associated with the outer doublet microtubules. *(A)* Flagellar (F) and axonemal (A) fractions from wild-type and structural mutants were probed with the CK1 antibody. CK1 is present in nearly the same amount in all flagella and axonemes indicating CK1 is not located in the central pair (*pf18*); radial spokes (*pf14*), DRC (*pf3*) or I1 dynein or outer dynein arms (*pf28pf30*). Therefore, CK1 must be localized to the outer doublet microtubules and CK1 assembly does not require these axonemal structures. Coomassie stain of tubulin (lower panel) was used as a loading control. (B) Diagram illustrating axonemal structure and corresponding structural mutants.

Fig.11

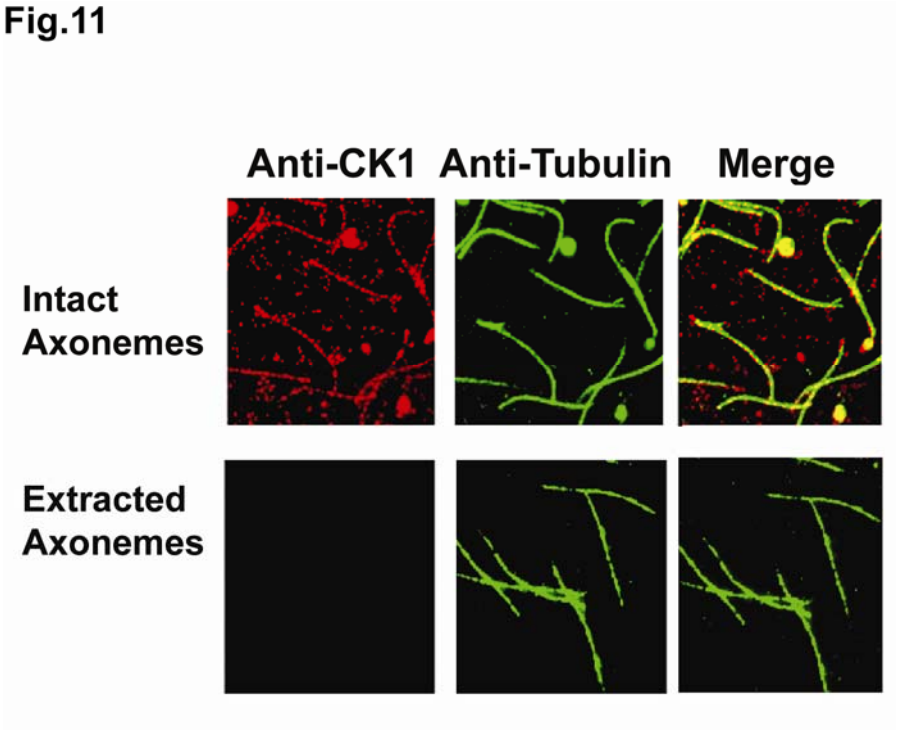
Anti-CK1
Anti-Tubulin
Merge
Intact Axonemes
Extracted Axonemes

Figure 11: Axonemal CK1 is localized along the length of the axoneme and on both flagella. CK1 localizes along the length of the axoneme (top panel; Intact Axonemes, red). Biochemical depletion of CK1 removes all detectable CK1 (bottom panels; Extracted Axonemes, red). Co-staining with tubulin was performed to label all axonemes (green).

Fig. 12

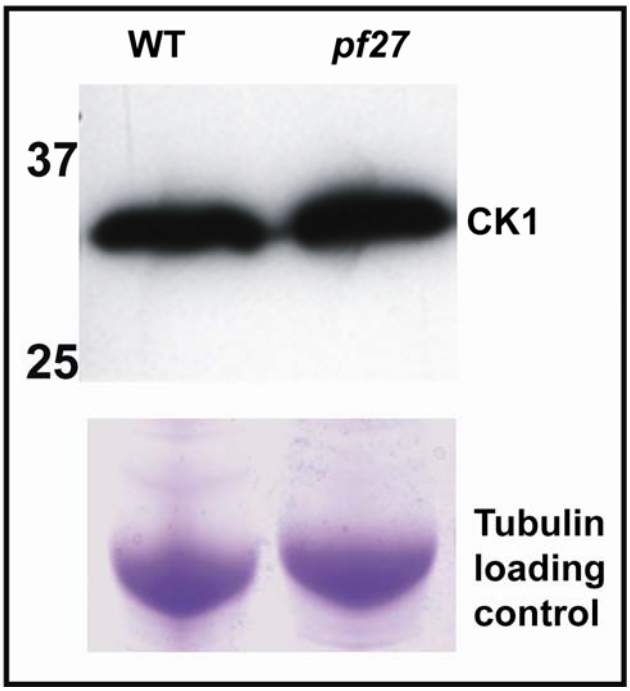

Figure 12: CK1 is fully assembled in axonemes from pf27. Blots of wild-type (WT) and *pf27* axonemes were probed with the CK1 antibody. CK1 is fully assembled in *pf27*, similar to wild-type axonemes. Coomasie stain (lower panel) serves as a loading control.

Fig.13

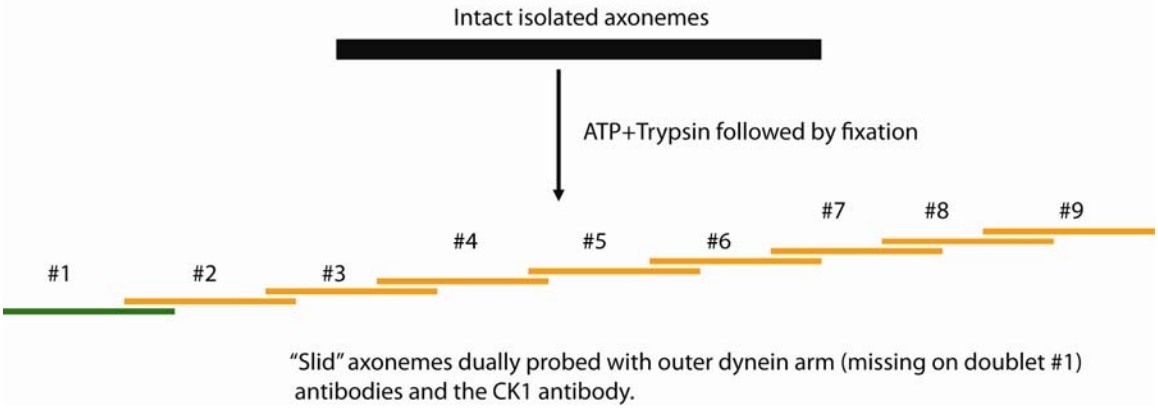

"Slid" axonemes dually probed with outer dynein arm (missing on doublet #1) antibodies and the CK1 antibody.

Figure 13: Strategy for localizing CK1 on each of the nine outer doublet microtubules by immunofluorescence. Isolated axonemes are treated with ATP and a protease (e.g. trypsin). This treatment induces individual outer doublets of the axoneme to slide across each other. "Slid" axonemes are then fixed and prepared for immunofluorescence as described in Materials and Methods and dually stained with outer dynein arm antibodies as well as CK1 antibodies. The outer dynein arm structure is missing on doublet #1. Our prediction is that CK1 is present on all nine outer doublets. In this case, doublet #1 should react only with the CK1 antibody (denoted in green) and the remaining doublets should be dually stained (denoted in orange). Alternately, CK1 could be localized to only a subset of doublet microtubules.

***Table 1: Candidate Chlamydomonas CK1 gene models identified in the flagellar proteome: Chlamydomonas* contains a single *CK1* gene – "C_70149"**

Gene models (JGI Version 2)	Predicted molecular weight (kD)	Characteristic CK1 domains (NLS, KHD, catalytic)	Homology (BLAST) analysis	Peptides identified in the *Chlamydomonas* flagellar proteome
C_20325	38.2	All absent	Serine/Threonine kinase	All absent
C_70149	**38.5**	**All present**	**CK1**	**All present**

Chapter 3: Identification of CK1-interacting proteins in the axoneme

Introduction:

As described in Chapter 1, the protein kinase, CK1, is a versatile kinase involved in a number of vital cellular functions (reviewed in Knippschild et al., 2005). For example, CK1 can be targeted to the nucleus, eyespot, cytoskeleton or flagella in *Chlamydomonas* (Behrend et al., 2000; Fu et al., 2001; Schmidt et al., 2006; Yang and Sale, 2000). Furthermore, in *Chlamydomonas* there appears to be only one *CK1* gene; thus CK1 is particularly versatile in this organism. In several experimental systems, it has been shown that CK1 is targeted to the microtubule cytoskeleton (Behrend et al., 2000; Hanger et al., 2007; Li et al., 2004). However, little is known about how CK1 is regulated and/or targeted to specific locations, to perform specific regulatory functions. Therefore, one important general goal is to determine CK1-interacting proteins and test the hypothesis that classes of CK1 anchoring proteins ("CKAPs") play a role in targeting and anchoring CK1 family members. The ciliary/flagellar axoneme provides an excellent model for identifying candidate CK1-interacting proteins. In particular, *Chlamydomonas* flagellar axonemes provide a powerful system for study due to biochemical, structural and genetic advantages.

The motile axoneme is a highly ordered, "solid-state structure" comprised of >400 proteins (Dutcher, 1995; Pazour et al., 2005). The isolated axonemes, and each axonemal component, is not soluble in physiological buffers; and motility can be reactivated and regulated in buffers containing ATP and various concentrations of calcium, cyclic nucleotides or pharmacological reagents. Thus, the axoneme bears components for regulated movement- the motors and the signaling proteins required for control.

Axonemal protein structures are organized in discrete, uniform repeating units, along the length of the axoneme. Detailed studies of axonemal organization have been made possible by advances in image acquisition and analysis as well as due to the availability of a large library of *Chlamydomonas* structural mutants missing specific axonemal components. Electron microscopy, and stable structural mutants, has revealed that the key axonemal components required to generate coordinated ciliary motility are organized in regular, repeating 96 nm units along each outer doublet microtubule – the "96 nm repeat". The organization of the 96 nm repeat was initially recognized by thin section electron microscopy (Warner and Satir, 1974) and further was elucidated by rapid freeze, deep-etch rotary shadow approach developed by Goodenough and Heuser (1985a;1985b) in which structures were resolved in shadow replica of rapidly frozen axonemes. In fact, Goodenough and Heuser (1985a) originally identified the I1 dynein as a structure they called the "triad" in the inner dynein arm structures. Analysis of inner arm mutants further defined the regular repeat of inner arm dynein structures in the 96 nm repeat and revealed each inner dynein arm assembles in a specific position, independent of other inner arms (Piperno et al., 1990). The next advances in image analysis of thin sections (Kamiya et al., 1991; Mastronarde et al., 1992) revealed that the inner dynein arm structures are very complex and also defined the location of the DRC (Gardner, 1994). Most recently, advances in cryoEM-tomography have provided a major advance in resolution of native axonemal structures and a refined view of the 96 nm repeat (Bui et al., 2008; Ishikawa et al., 2007; Nicastro et al., 2006; Oda et al., 2007). These analyses demonstrated that within each 96 nm axonemal repeat are four outer dynein arms that repeat at 24 nms, two radial spokes, and a collection of inner dynein arm

structures, including I1 dynein that repeats once every 96 nms (Fig.1). Analysis of structures in a range of organisms by electron microscopy shows that this overall organization of axonemal outer doublet components is highly conserved in all motile cilia ranging from protozoa to humans. Fundamental questions include: [1] What is the molecular basis for the 96 nm organization? [2] How are axonemal proteins, including CK1, specifically targeted and anchored to specific positions in the axoneme with a defined periodicity?

My overall hypothesis is that axonemal CK1 is targeted and anchored in the axoneme, near I1 dynein, to directly control IC138 phosphorylation and regulate dynein activity and ciliary motility. Based on this hypothesis, we predict that axonemal CK1 activity is regulated by its specific proximity to its substrate and, therefore, must be anchored near IC138, presumably with a 96 nm periodicity. Supporting evidence for this model comes from data discussed in Chapter 2 and suggests that CK1 is localized uniformly along the length of the axoneme and on both flagella, consistent with localization with I1 dynein and IC138. Furthermore, we also propose that the predicted CK1 position and periodicity is determined by its interaction with a putative "anchoring protein" or "docking complex" that we postulate would define a class of putative "CKAPs" designed to localize CK1 (Fig.1). Conceptually, this model is based on the AKAP model for localization and regulation of otherwise ubiquitous PKA (Gaillard et al., 2001; Scott, 2003; Wong and Scott, 2004). The general idea is that the ubiquitous, catalytic subunit of a kinase is targeted and anchored by specific members of a class of anchoring proteins.

Previous studies have indicated that many axonemal complexes are targeted and anchored to a specific position in the 96 nm repeat including each dynein structure and each radial spoke. For example, the position and 24 nm periodicity of the outer dynein arm is defined by a complex of proteins including the outer dynein arm docking complex (ODA-DC) as well as a complex that includes the Oda5 protein, that can assemble independent of the dynein complex but is required for correct assembly and localization of the outer dynein arms in the axonemes (Casey et al., 2003; Koutoulis et al., 1997; Takada et al., 2002; Wakabayashi et al., 2002a; Wakabayashi et al., 2002b; Wakabayashi et al., 2001; Wirschell et al., 2004). Mutations in any of the above mentioned proteins leads to a failure in assembly of the axonemal outer dynein arm. Presumably there is an analogous I1-docking complex and a CK1-docking complex that is responsible for targeting I1 to the proximal region of the 96 nm repeat and targeting CK1 near the I1 complex. For example, failure in assembly of inner arm dyneins, including I1 dynein results in a regular 96 nm gap in structure (Nicastro et al., 2006; Piperno et al., 1990). This result alone implied each inner arm dynein component is targeted and anchored independent of other axonemal components such as other inner dynein isoforms. Smith and Sale (1992) used an in-vitro reconstitution approach to show that I1 dynein is targeted to its unique position by additional factors, and that these putative docking proteins are not soluble in 0.6M NaCl buffer. Furthermore, the results of Diener et al., (1993) also showed that the radial spokes are targeted to their unique position and that the mechanism involves interaction of a putative radial spoke docking protein and the radial spoke protein 3 (RSP3). Interestingly, and relevant to my study of CK1 localization, RSP3- has been identified as an A-Kinase-Anchoring-Protein (AKAP, as reviewed

above). Proteins belonging to the AKAP family have been shown to anchor protein kinase A (PKA) in proximity to its substrate, thus regulating PKA activity (Gaillard et al., 2001; Scott, 2003). Based on these data and evidence for axonemal docking/anchoring complexes that localize dyneins, radial spokes and other proteins, we predict the axoneme must bear a specialized CKAP that will localize and anchor CK1, an otherwise ubiquitous and versatile kinase, near I1 dynein and the phospho-protein, IC138.

In order to identify and define the mechanisms responsible for targeting and anchoring CK1 to the axoneme, I sought to identify CK1-interacting proteins in the axoneme using the following experimental approaches:

[1] Chemical cross-linking: Since the axoneme is a multi-protein, "solid-state system", the proteins are highly ordered and in close apposition to each other making it amenable to covalent cross-linking techniques. Several cross-linkers have been designed and synthesized for the study of protein-protein interactions and include, EDC, DSS, DFDNB and DMP (reviewed in Benashski and King, 2000). These cross-linkers have been useful in identifying specific axonemal inter-protein interactions between dynein subunits and tubulin (King et al., 1991; Wirschell et al., 2009) as well as protein interactions within dyneins (Hendrickson et al., 2004) or radial spokes (Wirschell et al., 2008). One of the most commonly used covalent cross-linker is EDC; a "zero-length" cross-linker. EDC cross-links proteins that directly interact with each other and the mechanism is illustrated in Fig. 2. EDC is a high stringency cross-linker requiring close interactions of very specific amino-acids and thus reducing the chances of spurious, background interactions. Using EDC, and a combination of cross-linking in the axoneme as well as axonemal salt extracts, I determined that CK1 interacts with α and β tubulin.

[2] Affinity chromatography using epitope-tagged His-CK1 To identify additional CK1-interacting proteins, I used an in-vitro method taking advantage of soluble, epitope-tagged HisCK1, conjugated to cobalt-Sepharose beads, and dialyzed axonemal salt extracts. This mixture was then incubated with an axonemal salt extract (0.6M KI). The proteins were then eluted with an imidazole-based buffer and candidate proteins identified by protein stain or immunoblot analysis. The strategy is illustrated in Fig. 3 and this method will be referred to as a "pull down" approach. Surprisingly, preliminary data from these experiments suggest that CK1 may interact with I1 subunits, particularly IC138 and FAP120. Therefore, the simplest interpretation is that CK1 is localized in the axoneme by its interaction with tubulin and I1 dynein. This result would explain the specific localization and predicted periodicity of CK1 in the axoneme and suggests a highly efficient "solid-state" regulatory interaction of CK1 with components of the I1 regulatory sub-complex (Bower et al., 2009).

The goal of the work, described here, is to define proteins that anchor CK1 in the axoneme. By identifying such mechanisms and the specific protein interactions between CK1 and docking proteins, we can also define universal mechanisms of CK1 docking to the microtubule cytoskeleton.

Materials and Methods:

Strains and culture conditions: The *Chlamydomonas reinhardtii* strain used in this study was CC125 (wild-type, 137 mating type (+) plus) and obtained from the *Chlamydomonas* Genetics Center (University of Minnesota, St. Paul, MN). For most experiments, cells were grown in tris-acetate phosphate (TAP) medium with aeration on a 14:10 hr light: dark cycle.

Isolation of axonemes: Flagella were isolated as described previously using a combination of laminar filtration and differential centrifugation to harvest cells, dibucaine for flagellar excision and differential centrifugation for flagellar isolation (Witman, 1986). Flagella were demembranated in buffer (10 mM Hepes, 5 mM $MgSO_4$, 1 mM DTT, 0.5 mM EDTA, 0.1 M PMSF, and 0.6 TIU aprotinin, pH 7.4) containing 1% Nonidet-P40 to yield purified axonemes. For some experiments, CK1 was extracted from axonemes (1 mg/ml) with a buffer containing 0.3 M NaCl for 20 min on ice. Axonemal fractions were fixed for SDS-PAGE at a concentration of 1 mg/ml. 10 or 20 μg of total protein was used for immunoblot analysis. Protein concentrations were determined using the Bradford assay (Biorad, Hercules CA) and BSA used as a standard. Unless otherwise stated, all reagents were obtained from Sigma-Aldrich and deionized H_2O was used throughout.

Cross-linking experiments: Axonemes were isolated as described above and resuspended in a buffer without DTT at a concentration of 1 mg/ml and as reviewed in (Benashski and King, 2000) and increasing amounts of EDC was added (0.5, 1, 1.5, 2 and 2.5 mM from a 100 mM stock). Cross-linking was performed at room temperature for 1 hour and the reaction was quenched with a 20-fold molar excess of β-mercaptoethanol. Samples were

then centrifuged at 12 K RPM for 20 minutes (SS34 rotor, Sorvall) and the axonemal pellets were resuspended at 2 mg/ml in HMDEN buffer (10 mM Hepes, 5 mM $MgSO_4$, 1 mM DTT, 0.5 mM EDTA, 25 mM NaCl and 0.1 M PMSF, and 0.6 TIU aprotinin, pH 7.4).

In some experiments, after cross-linking, axonemes were centrifuged at 12 K RPM for 20 minutes (SS34 rotor, Sorvall) and the resulting pellet was resuspended in the HMDEN buffer with 0.6M KI. This mixture was kept on ice for 20 minutes and then centrifuged at 12 K for 20 minutes (SS34 rotor, Sorvall). The resulting supernatant ("0.6M KI extract") was either fractionated or analyzed by immunoblot analysis. For cross-linking in salt extracts, 0.3 M axonemal salt extracts were prepared as described above, either in presence or absence of 40 μM taxol and at 5 mg/ml of axonemal protein. EDC cross-linking was performed as described but at higher concentrations of EDC (10, 20 and 30 mM of EDC from a 100 mM stock added to the dialyzed extracts). Higher concentrations of EDC were chosen as proteins are more dilute in the axonemal salt extracts and, therefore, more EDC was required for cross-linking neighboring proteins.

Immunoblotting: Axonemal protein samples were separated by SDS-PAGE and either stained by Coomassie blue or transferred to a nitrocellulose membrane (Bio-Rad, Hercules, CA) for immunoblot analysis. The membrane was blocked with 5% nonfat dry milk followed by incubation with primary antibodies (anti-CK1 serum diluted 1:10,000–1:20,000), then HRP-conjugated goat anti-rabbit secondary antibodies (1:10,000, Bio-Rad). The antibody reactivity was detected with the Pierce Western ECL blotting substrate (Thermo Scientific, Waltham, MA).

Sucrose density gradients: Sucrose density gradient centrifugation was carried out as described previously (Tang et al., 1982) using a 11.2 ml linear 5–20% sucrose density gradient prepared in HMDEN buffer containing 0.6M KI. 0.6 ml of 0.6M KI axonemal extracts were overlaid on the top of the gradients and were centrifuged in a SW41 swinging bucket rotor at 35,000 for 16 hours at 4 °C. Twenty one fractions (500 µl each) were collected from the bottom of the tube and prepared for SDS-PAGE. Approximate sedimentation rates on sucrose density gradients were determined by reference to dynein marker proteins, located at ~20S and ~12S, or tubulin dimers (8S).

Cloning full-length His-CK1: The CK1 coding sequence was PCR cloned from a cDNA library ("library 7", Gregory Pazour, University of Massachusetts) using the following primers: forward primer- CCTTTGGGACTGAGAAGCAC and reverse primer- CTGGCAGCTGTCTGTTCAAA into the pCR 2.1 TOPO cloning vector according to the manufacturer's instructions (Invitrogen, Carlsbad, CA) to yield plasmid pAGCK1-FL. The insert in pAGCK1-FL was amplified with the following primers to engineer restriction sites: forward primer: CAGCGAGGATCCATGGCGTTGGACATT and reverse primer GCGATTAAGCTTTTAGAAGTCGAACCGGCCG (*BamH1* and *Hind III* restriction sites, respectively, are underlined). The amplified full length CK1 sequence was digested with *BamH1* and *HindIII* and cloned into the pet28A (Novagen, San Diego, CA). The resulting expression construct, pAGHisCK1, was transformed into strain BL21(DE3) pLysS (Stratagene, La Jolla, CA) and expression of the His-tagged fusion protein was induced with 1 mM Isopropyl β-D-1-thiogalactopyranoside (IPTG). The fusion protein was solubilized from bacterial cells using Bugbuster (Novagen, Darmstadt, Germany). HisCK1 was found in the soluble fraction and was purified using Talon metal

affinity resin (Clontech, Mountain View, CA). A Coomasie stained gel of expressed, soluble and purified HisCK1 is illustrated in Fig.4.

Purification of HisFAP120: HisFAP120 has previously been cloned and expressed (Ikeda et al., 2009); the clone was obtained from Dr. R. Kamiya (University of Tokyo). Expressed HisFAP120 is soluble and was purified using Talon metal affinity resin per manufacturer's instructions (Clontech, Mountain View, CA). Fractions containing pure HisFAP120 were identified by Coomasie staining and verified using an affinity purified FAP120 antibody, also generously provided by R.Kamiya (Ikeda et al., 2009). A Coomasie stained gel of expressed, soluble and purified HisFAP120 is illustrated in Fig. 5.

Affinity purification of axonemal proteins using purified HisCK1 or HisFAP120: HisCK1 or HisFAP120 recombinant proteins were expressed and purified as described above. Purified fractions were identified by Coomasie staining and were pooled together and dialyzed against an equilibration buffer (50 mM phosphate buffer, 300 mM NaCl at pH 8.0) to remove imidazole and facilitate rebinding to the cobalt-Sepharose resin. HisCK1 or HisFAP120 was conjugated to 0.5 ml of cobalt-Sepharose resin (Clontech, Mountain View, CA) at room temperature for 2 hours, followed by washing 2X with equilibration buffer and 1X with equilibration buffer containing 100 mM NaCl.

0.6M KI axonemal extracts were obtained as described above and dialyzed in a buffer (10 mM Hepes, 5 mM $MgSO_4$, 1 mM DTT, 0.5 mM EDTA, 100 mM NaCl and 0.1 M PMSF, and 0.6 TIU aprotinin, pH 7.4) for 1 hour at 4°C followed by a clarifying spin at 6000 RPM for 1 minute. The supernatants from the clarifying spin were then incubated with cobalt-Sepharose resin that was conjugated with HisCK1 or HisFAP120.

This mixture was kept at 4°C overnight. The mixture was then spun at 6000 RPM for 5 minutes and the cobalt-Sepharose resin was washed 5X with equilibration buffer containing 100 mM NaCl. The beads were then incubated with elution buffer (50 mM phosphate buffer, 300 mM NaCl and 150 mM Imidazole at pH 7.0) for 10 minutes. The mixture was then spun at 6000 RPM for 5 minutes. The supernatant was saved for SDS-PAGE and used for immunoblot analysis as well as protein stain analysis using silver staining. Controls included: (1) cobalt-Sepharose bead matrix conjugated to purified bacterial fractions containing HisCK1 or HisFAP120, to identify contaminating co-purifying, bacterial proteins that bind non-specifically to the cobalt-Sepharose beads and (2) cobalt-Sepharose bead matrix directly incubated with the dialyzed 0.6M KI axonemal salt extracts to identify axonemal proteins that non-specifically and directly bind to the cobalt-Sepharose beads.

Results:

CK1 directly interacts with tubulin: To identify CK1-interacting axonemal proteins, I took a chemical cross-linking approach using the zero-length cross-linker EDC (see Introduction). The EDC cross-linker couples carboxyl groups and primary amines of proteins that are directly in contact with each other (Fig. 2). EDC cross-linking was performed in wild-type axonemes with increasing concentration of EDC for a fixed time. Immunoblots probed with the CK1 antibody demonstrated a prominent and stable cross-linked product doublet at ~85-90 kD (Fig.6). Therefore, a candidate CK1 interacting protein(s) was predicted to be ~50-55 kD.

In order to identify the ~50-55 kD protein, my next goal was to purify it in sufficient amounts for MS/MS analysis. The cross-linked product was extremely stable and could be solubilized from the axoneme using 0.6M KI (Fig.6) - a condition in which the axonemal structure is partially disrupted (Yang et al., 2001). Following extraction, the 0.6M KI salt extracts were further fractionated by velocity sedimentation on a sucrose gradient (5-20%) with the goal to purify the cross-linked product. The cross-linked product migrated at about 11S, in a complex, separated from uncross-linked CK1 that sediment near the top of the gradient (Fig.7). This is an encouraging result, consistent with CK1 complex formation. However, further attempts to sufficiently purify the CK1 complex were not successful. For example, immunoprecipitation using CK1 antibodies did not yield the cross-linked product(s) in sufficient quantity for MS/MS analysis. Thus, alternate approaches were taken.

As described in Chapter 2, CK1 is solubilized from the axoneme at a relatively low salt concentration – 0.3M NaCl. The first question was whether the 50-55 kD cross-

linked product is also soluble in 0.3M NaCl and then detectable by EDC cross-linking. I obtained axonemal salt extracts (0.3M) and performed cross-linking with increasing amounts of EDC. Immunoblot analysis revealed the same cross-linked product doublet that migrates at ~85-90 kD, was obtained in 0.3M NaCl extracts (Fig.8). This result suggested that the ~50-55 kD interacting protein(s) is at least partially soluble with 0.3M NaCl and continued to interact with CK1 as assessed by EDC cross-linking and immunoblotting.

I next took a candidate approach to identify the 50-55 kD protein. Based on my overall hypothesis, the CK1- anchoring protein must be at least as abundant as CK1. Therefore, on the basis of relative abundance as well as predicted molecular weight of the CK1-cross-linked product (~50 kD), tubulin was a candidate. As a simple test of this hypothesis, I used immunoblots to determine if the 85-90 kD cross-linked product contains either or both α and β tubulin. However α and β tubulin antibodies do not react with the 85-90 kD cross-linked product.

This negative result however could be due to disruption of epitopes after EDC cross-linking rendering the tubulin antibodies unable to identify the cross-linked product. As an alternate approach, I prepared axonemal salt extracts in the presence and absence of taxol. The prediction was that taxol would prevent tubulin solubilization and, therefore, remove the candidate CK1 interacting 50-55 kD proteins from the extracts and block formation of the ~85-90 kD cross-linked product in the 0.3M NaCl extract (strategy illustrated in Fig.9). As predicted, taxol prevented solubilization of tubulin (Fig. 10) and cross-linking in 0.3M NaCl extracts obtained in the presence of taxol, failed to generate the 85-90 kD cross-linked product (Fig.11). As a control, and to confirm that taxol does

not interfere with EDC cross-linking, I performed cross-linking in axonemes in the presence of taxol and obtained the ~85-90 kD cross-linked product (Fig. 12). Therefore, based on these data, the simplest interpretation is that CK1 interacts with α and/or β tubulin. Since EDC cross-linking generated closely spaced doublet bands, CK1 possibly interacts with both α and β tubulin. However, based on our original hypothesis, and since tubulin is a ubiquitous axonemal protein, this result cannot explain the predicted specific and periodic localization of CK1 near I1 dynein. Although this result provides definitive evidence for a physical and close interaction between CK1 and tubulin, there must be additional CK1-interacting proteins that direct the targeting of CK1 to a precise position near I1 dynein. Therefore, I used an alternate approach to identify additional interacting proteins, including candidate CK1-anchoring proteins.

CK1 interacts with I1 proteins: Given that the full length, epitope tagged CK1 is soluble (Fig. 4), an alternate approach to define CK1 interacting proteins is through affinity purification using the expressed, purified HisCK1 and dialyzed 0.6M KI axonemal extracts as illustrated in Fig.3. The 0.6M KI extracts were used since at this salt concentration most of the axonemal proteins are soluble. However, among the major pitfalls, it is also possible that under these harsh extraction conditions protein-protein interactions will not be restored after dialysis. This possible weakness in the approach will be discussed below.

Epitope tagged HisCK1 was solubilized and purified using cobalt-Sepharose beads as described above. The purified HisCK1 fractions were dialyzed in order to remove imidazole and permit subsequent successful re-conjugation of purified HisCK1 to cobalt-Sepharose beads. This mixture was then incubated with 5 mg/ml of dialyzed 0.6M

KI extracts. Following overnight incubation, the resin was washed, and proteins were then eluted off the beads with an imidazole-based buffer and analyzed by both immunoblots, as well as protein stains. Controls included: (1) cobalt-Sepharose resin conjugated to purified bacterial fractions containing HisCK1 or HisFAP120, to identify contaminating and co-purified, bacterial proteins that bind non-specifically to the cobalt-sepharose beads and (2) cobalt-Sepharose resin directly incubated with the dialyzed 0.6M KI axonemal salt extracts to identify axonemal proteins that non-specifically and directly bind to the cobalt-Sepharose beads.

Silver stains of control fractions and "pulldown" fractions identified bands that are not present in the controls, but present in the "pulldowns" fractions" (Fig. 13). However, since the protein bands are not sufficiently enriched or purified, this method needed to be refined further to obtain protein bands suitable for MS/MS analysis and I thus focused on a "candidate approach" to identify CK1-interacting proteins. For example, we can narrow down candidates based on predicted molecular weights of the bands identified in the silver stain, and comparing it with the proteins identified in the flagellar proteome.

One of the predictions is that CK1 interacts either directly or indirectly with I1 proteins. Using specific antibodies and immunoblot analysis of pull-down fractions I determined that IC138 and FAP120 interacted with CK1 (Fig. 14). FAP120 is a novel I1 component that is thought to be associated with IC138. It is also missing in mutants that do not assemble I1 proteins and is found in reduced amounts in mutants that are deficient in IC138 and the amount of FAP120 in the axonemes correlates with IC138 (Ikeda et al., 2009). However, the precise function of FAP120 is yet to be determined.

Based on this preliminary analysis, I postulated that FAP120 interacts with CK1. To further examine the CK1-FAP120 interaction, I performed reciprocal pull-downs with recombinant His-tagged FAP120 and dialyzed 0.6M KI extracts. Immunoblot analysis using specific antibodies revealed that HisFAP120 pulls down IC140, IC138, CK1 and IC97 (Fig. 15). The simplest initial interpretation is that CK1 interacts either directly or indirectly with IC138 and/or FAP120, consistent with the hypothesis that CK1 is targeted to I1 dynein and FAP120, or another associated protein that is responsible for anchoring CK1.

Discussion:

Primary conclusions:

One of the principal mechanisms by which CK1 activity is regulated in the cell is by its specific proximity to its substrate. For example, the centrosomal anchoring protein AKAP450 specifically localizes CK1δ to the centrosomes during interphase, where its proximity regulates access to substrate (Sillibourne et al., 2002). Predictably, since CK1 is physically associated with the axoneme, it must be localized precisely adjacent to its substrates, and, therefore, there must be an interacting protein or proteins that targets CK1. In this study, I predicted that CK1 is localized and regulated by its proximity to I1 dynein, and in particular to the base of I1 dynein where the IC138 regulatory sub-complex is localized (Bower et al., 2009; Nicastro et al., 2006). I postulated that CK1 is localized near I1 dynein by means of an axonemal CKAP and speculated that such a protein could define a novel class of anchoring proteins. Thus the goal of the work described here is to identify CK1-interacting proteins in the axoneme and determine the mechanisms that target and anchor CK1 to the axoneme.

Using biochemical approaches to study CK1 interactions in isolated axonemes, I have demonstrated that CK1 directly interacts with tubulin and that CK1 interacts with I1 dynein, through a direct or indirect, interaction with IC138 and FAP120. These results indicate that CK1 is anchored in the axoneme by association with microtubules and possibly localized by I1 dynein, or more likely, by proteins associated with both I1 dynein and tubulin. This is a very appealing model, consistent with a close localization of CK1 with I1 dynein and particularly the IC138 sub-complex of proteins, resulting in a convenient means of regulating access of CK1 to one or few substrates. Although these

data supports the model that CK1 is targeted to the axoneme near I1 dynein, I have not yet identified a CKAP. Further tests are required to determine alternate CK1-interacting proteins and will be discussed below.

CK1 directly interacts with tubulin:

One of the most common methods of determining protein-protein interactions in the axoneme is by covalent cross-linking using various chemical cross-linkers including EDC, DSS, DMP and DFDNB. As discussed above, EDC is a "zero-length" cross-linker that does not incorporate itself into the cross-linked product. EDC cross-linking of axonemes revealed a prominent cross-linked product at about ~85-90 kD and therefore a CK1-interacting protein of about ~50-55 kD. I also determined the cross-linked product could be solubilized in a 0.6M KI buffer and fractionated by zonal centrifugation on a sucrose gradient revealing the complex sediments at about 11S. I also observed that the cross-linked product was a closely spaced pair of doublets suggesting that CK1 interacts with two different proteins of nearly the same size or a single protein with two distinct post-translational modifications. I was not able to obtain sufficient, purified cross-linked product for MS/MS analysis and, therefore, took alternate approaches to identify the CK1 cross-linked product, including a candidate approach predicting the cross-linked product contains tubulin.

As described in Chapter 2, CK1 is solubilized from the axonemes with 0.3 M NaCl buffers (Yang and Sale, 2000). Therefore, one question is whether the 50-55 kD CK1-interacting protein is also solubilized under the same buffer conditions. The idea was to determine if the same cross-linked product could be found following extraction. EDC addition to dialyzed 0.3M axonemal extracts resulted in the formation of the ~85-90

kD cross-linked product, also appearing as a doublet and suggesting that the same ~50-55 kD interacting protein(s) is at least partially soluble in 0.3M NaCl buffers and, based on properties of EDC, continues to interact with CK1 by the same residues. Based on the molecular weight and the appearance of the cross-linked product as a doublet, I predicted that α and β tubulin are candidate CK1-interacting proteins. Tubulin antibodies failed to identify the ~85-90 kD CK1 cross-linked product. However, this is clearly a negative result and could be due to disruption of tubulin eptiopes after cross-linking, a phenomenon also observed for the IC97-tubulin cross-linked product (Wirschell et al., 2009). Therefore it was necessary to take alternate approaches to test whether tubulin was the CK1 cross-linked product.

Taxol is an antibiotic drug found to stabilize tubulin in microtubules (Parness and Horwitz, 1981) and in axonemal microtubules (Sale et al., 1985). Predictably, if the CK1 cross-linked products are α and β tubulin, then treatment of axonemes with taxol should block tubulin solubilization and result in the failure to form the EDC cross-linked product when performed in the 0.3M salt extracts. I prepared 0.3M axonemal salt extracts in the presence and absence of taxol. As predicted, formation of the cross-linked product was prevented when salt extracts were prepared in the presence of taxol. Control experiments confirmed that taxol does not interfere in the EDC-cross-linking reaction. Therefore, based on these data, the simplest interpretation is that CK1 directly interacts with tubulin and the formation of a cross-linked product doublet also suggests that CK1 interacts with both α and β tubulin. However, another possibility is that Taxol prevents solubilization of other axonemal proteins, similar in size to tubulin, that contribute to the formation of the

~85-90 kD CK1 cross-linked product. Thus, additional independent tests are required to confirm that α and β tubulin directly interacts with CK1.

Since tubulin is found throughout the length and breadth of each axonemal microtubule, the interaction of CK1 with tubulin cannot explain how CK1 is specifically targeted in the axoneme. Indeed, CK1 is present in only a small fraction compared to the amount of tubulin in the axonemes, yet CK1 is localized along the entire length of the axoneme. Therefore, like dynein structures and the radial spokes, CK1 must be more precisely localized, presumably repeating at 96 nm intervals. As discussed below, a "CKAP" could influence the exact position of CK1 along each outer doublet microtubule.

Another possible mechanism that dictates specificity of CK1 localization in the axoneme could involve localized differences in post-translational modification of tubulin. Axonemal microtubules undergo a wide range of post-translational modifications including acetylation, polyglutamylation and polyglycylation (Bre et al., 1998; L'Hernault and Rosenbaum, 1983; Redeker et al., 1994; Redeker et al., 2005; Rosenbaum, 2000). Indeed failure in tubulin glutamylation or glycylation can result in failure in axonemal assembly (Dave et al., 2009; Lechtreck and Geimer, 2000; Million et al., 1999). However, although possible, to date no one has documented a periodicity associated with post-translationally modified tubulin. Therefore, the CK1 localization cannot yet be explained by periodic tubulin heterogeneity. One interesting test of CK1 interacting with modified tubulin would be to use antibodies that recognize the glutamylated or glycylated domains. Additional key questions then include whether, CK1 interacts with both α and β tubulin, consistent with EDC cross-linking data, and whether CK1 interacts with equal stoichiometry with both α and β tubulin.

Previous studies in other systems have shown that CK1 directly interacts with the microtubule cytoskeleton. For example, Behrend et al., have shown by biochemical and microscopy methods, that CK1 interacts stably with tubulin in mammalian cell cultures in a cell cycle specific manner. Furthermore, CK1 isoforms also phosphorylate tubulin isoforms, as well as microtubule associated proteins including tau, stathmin and MAP4 (Behrend et al., 2000; Kuret et al., 1997; Li et al., 2004). Interestingly, there appears to be a correlation between phosphorylation of CK1 substrates and cell-cycle progression, possibly dictated by regulated targeting to the microtubule cytoskeleton. Given this evidence, CK1 activity must be tightly controlled and we predict the mechanism must include localization of CK1 by a postulated microtubule interacting protein. However, mechanisms of CK1-tubulin interaction have not been determined and it is not known if this interaction occurs directly or is mediated by an intermediate "linking" protein. Thus, one of the important future goals is to determine the precise mechanism of CK1-tubulin interactions as well as identifying key, possibly conserved, domains in CK1 involved in these interactions. These studies could provide a universal mechanism for targeting CK1 to the microtubule cytoskeleton in other cellular compartments and model systems.

I have not yet fully investigated a wide range of chemical cross-linkers for study of axonemal CK1 interacting proteins. As indicated, EDC is a very stringent cross-linker. Thus, all CK1-protein interactions will not be revealed using this one approach. Previous studies have shown that alternate cross-linkers can be used to study protein-protein interactions in the axoneme (reviewed in Benashski and King, 2000) including DSS, DFDNB and DMP. Unlike EDC, these are not "zero-length" cross-linkers and do not require the interacting proteins to be in direct contact with each other and the mechanism

utilizes amino acids other than those involved in EDC cross-linking. Therefore, although DSS, DFDNB and DMP are not "high stringency" cross-linkers and may identify non-specific, background proteins as potential CK1 interactors, we might be able to identify alternate cross-linked products, whose epitopes might otherwise be concealed or disrupted by EDC cross-linking. Additionally, these cross-linked products might be soluble at lower salt concentrations, making it more amenable for purification by immunoprecipitation.

Evidence that CK1 interacts with I1 proteins:

To date, only preliminary experiments were performed to identify additional CK1-axonemal interacting proteins, but as discussed, the results are quite promising. To identify alternate CK1 interacting axonemal proteins that could define the exact localization of CK1 on the microtubules, I took advantage of soluble, purified, epitope-tagged CK1 to develop a new method involving CK1 affinity. A key feature permitting development of this assay was the solubility of expressed HisCK1. Purified HisCK1 was conjugated to cobalt-Sepharose beads and then incubated with dialyzed 0.6M KI axonemal salt extracts. As explained above, 0.6M KI results in solubilization of most axonemal proteins potentially facilitating interactions with CK1 by the in-vitro affinity approach. Protein stain analyses, using silver stain, revealed several candidate CK1-interacting protein bands that were associated with the HisCK1-Sepharose but were not present in control samples. This initial analysis is promising and further refinement of the technique will reveal axonemal CK1 proteins in the axoneme. As a next step I will use MS/MS analysis to determine the identity of these candidate interacting proteins. This method can also be used with cytoplasmic extracts or 0.6M NaCl extracts from axonemes

to identify possible proteins that target CK1 to the flagellar compartment, including IFT proteins or axonemal anchoring proteins.

The main caveat of this method, as used so far, is the harsh salt conditions used to produce axonemal extracts. Although these salt extracts are dialyzed to a more physiologically relevant salt concentration (100 mM), it is likely that many protein-protein interactions as well as protein structures are either irreversibly altered or disrupted by 0.6M KI treatment or lost in subsequent dialysis steps. Therefore, the immediate goal would be to repeat these experiments with dialyzed 0.6M NaCl salt extracts from axonemes or using cytoplasmic extracts produced by physiological buffers. At a lower salt concentration, fewer axonemal proteins will be and solubilized, presumably, resulting in fewer background bands. Furthermore, we can also take advantage of the *Chlamydomonas* mutants that continue to assemble axonemal CK1 but fail to assemble other less relevant structures that are not likely to include a candidate CKAP. In-vitro pull-downs using axonemal extracts from mutants as well as dialyzed 0.6M NaCl extract may thus reveal and enrich protein bands with sufficient purity and abundance for MS/MS analysis.

In spite of these caveats, I took a candidate approach and produced very exciting preliminary results, indicating an interaction between CK1 and I1 dynein subunits. One of the advantages of the *Chlamydomonas* model system is the availability of a large collection of axoneme specific antibodies as well as specific mutants that lead to failure in assembly of structures. Taking advantage of several antibodies, and using immunoblot analysis, I sought to determine if well known candidate proteins were specifically pulled down in the assays. Importantly, these analyses revealed that CK1 interacts with I1

proteins – IC138 and FAP120. This result was further confirmed by reciprocal pull-downs using the recombinant HisFAP120-Sepharose matrix that revealed FAP120 interacts not only with the I1 dynein proteins (IC140, IC138 and IC97) but also CK1. These results were unexpected, indicating CK1 directly or indirectly interacts with proteins in the IC138/FAP120 sub-complex, and therefore are the foundation of immediate further investigation.

While these experiments indicate that CK1 interacts with FAP120 and IC138, we do not know if these interactions are direct or indirect and alternate approaches are required to test this idea and are described below. It is unlikely that this CK1-IC138 or CK1-FAP120 interaction is direct since *Chlamydomonas* flagellar mutants that do not assemble I1 dynein or IC138 or FAP120, continue to assemble axonemal CK1. Therefore, based on this data, it appears that CK1 is localized to the axoneme, near I1 dynein, by interactions involving CK1 and tubulin, CK1 and IC138/FAP120 as well as CK1 and an additional anchoring protein that may localize CK1 every 96 nm at the I1 dynein docking site (Fig.16). One exceptionally intriguing idea is that such a CKAP is also a long sought I1 dynein docking protein.

Based on these exciting new data, the highest priority is to continue to define axonemal CK1 interacting proteins as a postulated CKAP. This model is attractive, since it defines CK1 periodicity in the axoneme and also specifies a position for CK1 near I1 dynein for local and tight control of I1 dynein activity. Several approaches that have been previously successful in identifying protein-protein interactions in the axoneme have yet to be explained. These include blot overlay experiments using either an epitope tagged CK1 or radioactively labeled CK1 and/or “far western” for identification of candidate

CKAP proteins using specific antibodies. Blot overlays have been useful for studying protein-protein interactions in the axoneme. For example, Wargo et al., 2005 used Calmodulin (CaM)-blot overlays to determine CaM interacting proteins within the central pair complex. Gaillard et al., 2001 used radioactively labeled "RII" blot overlays to identify the axonemal AKAPs-RSP3 and a 240 kD central pair protein. The blot overlay technique involves fractionating axonemal proteins on SDS-PAGE, transferring to a nitrocellulose or PVDF membrane and then incubating with a probe of interest. In this case the probe would be the soluble, epitope tagged HisCK1. Alternatively, the probe can be radiolabeled or visualized with a specific antibody (in this case, the commercially available His antibody or the *Chlamydomonas* CK1 antibody). This method can be used to identify unknown protein–protein interactions as well as confirm previously characterized interactions. Moreover, the blot overlay approach can be used to determine the domain in CK1 responsible for CK1 binding. This approach was used to identify the RII binding domain in the RSP3 AKAP.

Once we identify a CK1 domain responsible for binding CK1 in the axoneme, such a domain or a candidate domain could be used as bait for yeast-2-hybrid. Yeast-2-hybrid has been successfully used to study IFT protein interactions (Lucker et al., 2005) as well as for identifying Oda16, a cargo-specific adaptor required for axonemal outer dynein assembly (Ahmed et al., 2008). Taking advantage of the high degree of similarity between *Chlamydomonas* CK1 and mammalian CK1 isoforms, we would choose the CK1 mouse homologue (CK1δ or CK1ε) as a bait to screen a mouse testis–derived cDNA library. Once candidate mammalian interacting proteins are identified, we would look for the corresponding ortholog in *Chlamydomonas* to identify additional CK1 interacting

proteins in the axoneme. This technique could also define proteins and mechanisms that target CK1 to specific cellular compartments in the mammalian system.

Recently, we have refined methods for purifying the CK1 antibody. For example, the CK1 antibody was generated against a MBP-tagged CK1 peptide (Chapter 2) and affinity purification using this antigen was inefficient and not suitable to identify CK1-interacting proteins in the axoneme. However, currently we have a soluble, full length CK1, tagged with a "His" epitope. Using this as an antigen, we can affinity purify the CK1 antibody. Preliminary analysis has indicated that blot affinity purification of the CK1 antiserum using the HisCK1 antigen provides us with a highly purified fraction of anti-CK1. Combining a higher quality affinity purified CK1 antibody with more sophisticated immunoprecipitation methods, (e.g. using Dynabeads (Invitrogen) as a matrix instead of protein A-sepharose beads to reduce background contamination) might prove to be suitable to identify CK1-interacting proteins from axonemal extracts. The challenge continues to be to produce an axonemal extract that results in soluble and native proteins suspended in physiological buffers. One alternative is to perform CK1 immunoprecipitation in cytoplasmic extracts prepared in physiological buffers. Although this approach could yield a number of CK1-interacting proteins, among them could be components also enriched in the axonemes or in the IFT compartment.

Fig.1

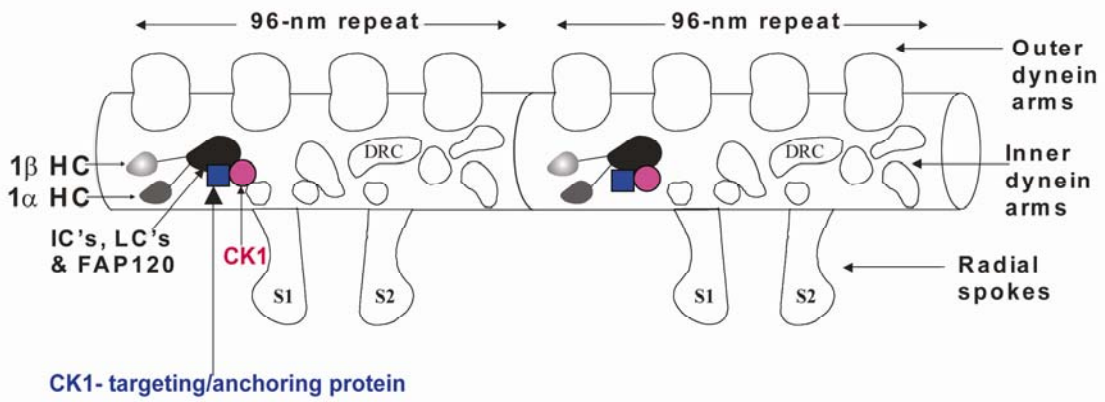
96-nm repeat
96-nm repeat
Outer dynein arms
Inner dynein arms
Radial spokes
1β HC
1α HC
IC's, LC's & FAP120
CK1
DRC
DRC
S1
S2
S1
S2
CK1- targeting/anchoring protein

Figure 1: The axoneme is a highly ordered structure comprising of repeating 96 nm modules: The motile axoneme is organized into 96 nm repeating structures, each of which comprise of 4 outer dynein molecules, 2 radial spokes (S1 and S2), DRC and each of the inner dynein arm isoforms including I1 dynein. I1 dynein is located to the proximal region of the 96 nm repeat. The regulatory IC138-FAP120 sub-complex is specifically localized to the base of spoke S1. The prediction is that CK1 is also targeted to the base of S1 near the IC138-FAP120 sub-complex by means of an "anchoring protein", predictably once every 96 nms.

Fig.2

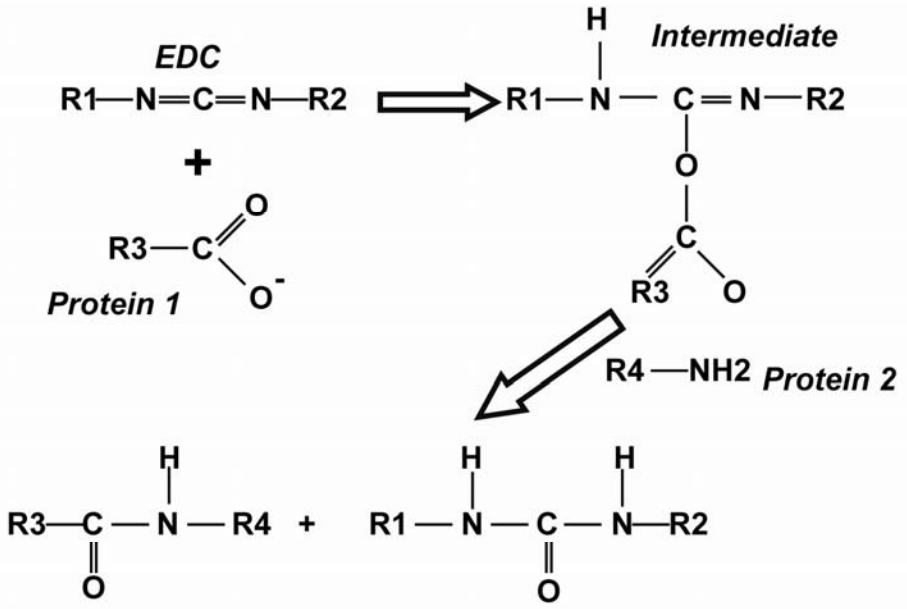

R1 = CH3CH2
R2 = (CH3)2 N (CH2)3
R3 = PROTEIN 1 WITH REACTIVE CARBOXYLATE FROM Asp OR Glu
R4 = PROTEIN 2 WIH REACTIVE ε- AMINO FROM Lys

Figure 2: Chemical mechanism of EDC cross-linking: EDC reacts with the carboxylic acid group from a Asp or Glu side chain on protein 1 giving rise to an intermediate by-product with an activated carboxyl group that can then be coupled to the amine group from a lysine residue on protein 2. The result of EDC treatment is that the two proteins are directly joined via an isopeptide bond. Importantly, the cross-linking reagent itself does not contribute to this covalently linked protein–protein product. Rather, EDC is released as a soluble urea derivative after displacement by the nucleophile R4-NH2.

Fig.3

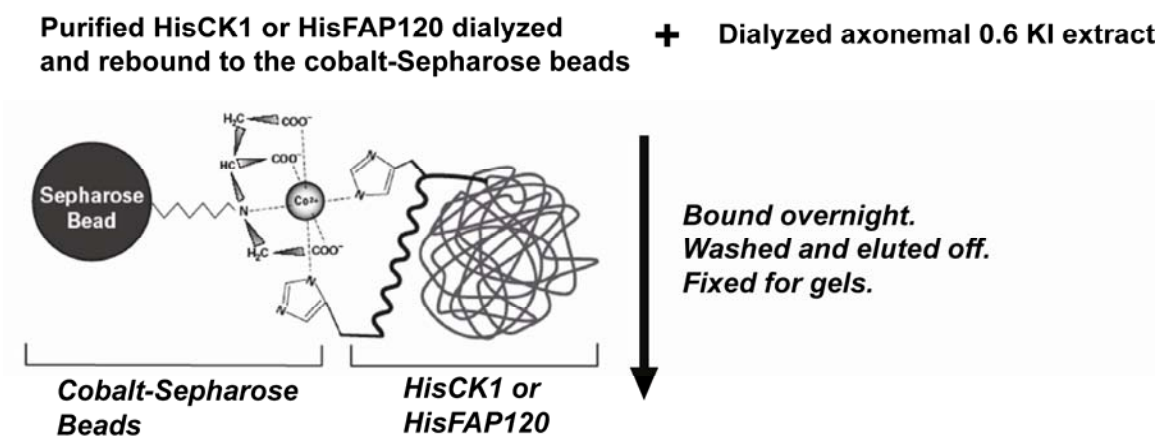
Purified HisCK1 or HisFAP120 dialyzed and rebound to the cobalt-Sepharose beads
+
Dialyzed axonemal 0.6 KI extract
Sepharose Bead
Bound overnight.
Washed and eluted off.
Fixed for gels.
Cobalt-Sepharose Beads
HisCK1 or HisFAP120

Figure 3: Strategy for "in-vitro pull-downs": Cobalt-Sepharose beads are conjugated with purified His-tagged proteins (CK1 or FAP120) and then incubated with dialyzed 0.6M KI extracts. Proteins that interact with the His-tagged proteins are then eluted off the beads with an imidazole-based buffer.

Fig.4

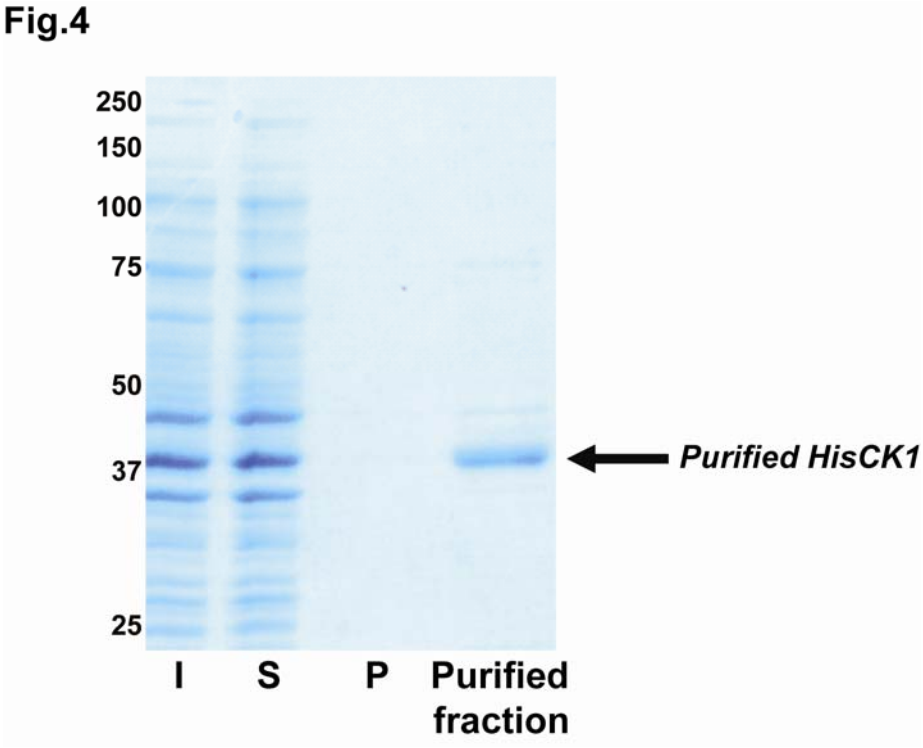
250
150
100
75
50
37
25
Purified HisCK1
I
S
P
Purified fraction

Figure 4: Expression and purification of HisCK1: Coomasie stained gel of recombinant HisCK1 expressed in bacterial cells (I). Almost all of the expressed HisCK1 is found in the soluble fraction (S) with little to none in the insoluble pellet (P). HisCK1 is then batch affinity purified using the cobalt-Sepharose matrix and a single band is obtained in the "purified fraction".

Fig.5

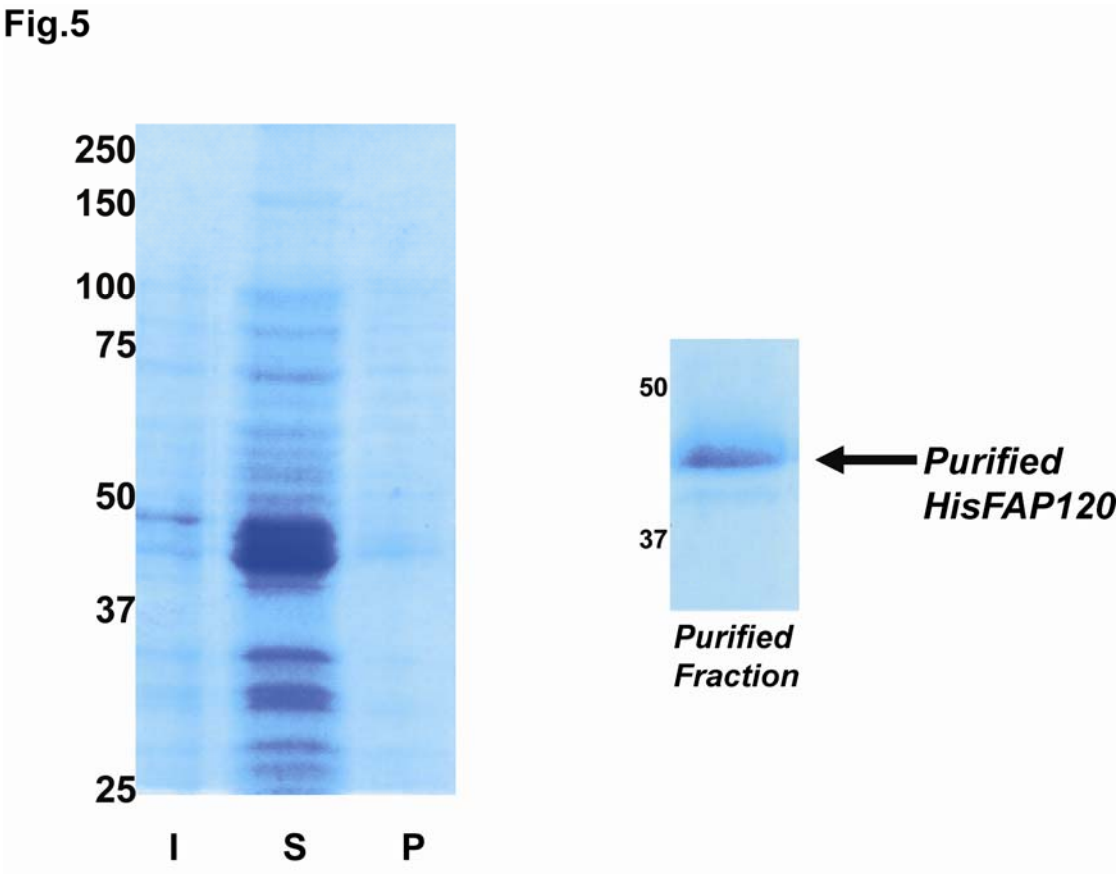
250
150
100
75
50
37
25
I
S
P
50
37
Purified
HisFAP120
Purified
Fraction

Figure 5: Expression and purification of HisFAP120: Coomasie stained gel of recombinant HisFAP120 (obtained from R. Kamiya, University of Tokyo) expressed in bacterial cells (I). A majority of the expressed protein is found in the soluble fraction (S) with negligible amounts found in the insoluble fraction (P). HisFAP120 is then batch affinity purified using the cobalt-Sepharose matrix and a single band is obtained in the "purified fraction".

Fig.6

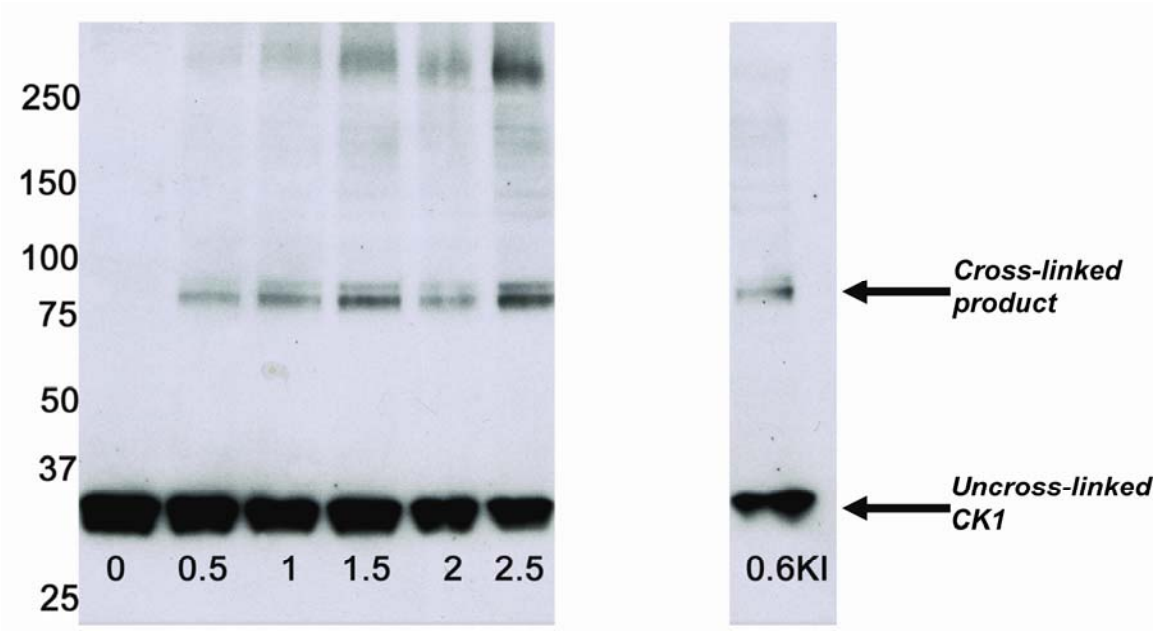
250
150
100
75
50
37
25
0
0.5
1
1.5
2
2.5
0.6KI
Cross-linked product
Uncross-linked CK1

Figure 6: EDC cross-linking in wild-type axonemes reveals a ~85-90 kD cross-linked product that is soluble in 0.6M KI buffer: Axonemes are isolated from wild-type *Chlamydomonas* and increasing concentration of EDC (0-2.5 mM) is added for 1 hour and the samples are prepared for SDS-PAGE. Immunoblots of cross-linked samples probed with the CK1 antibody reveal a ~85-90 kD CK1 interacting protein(s). The cross-linked product is solubilized from the axonemes with a 0.6M KI buffer.

Fig.7

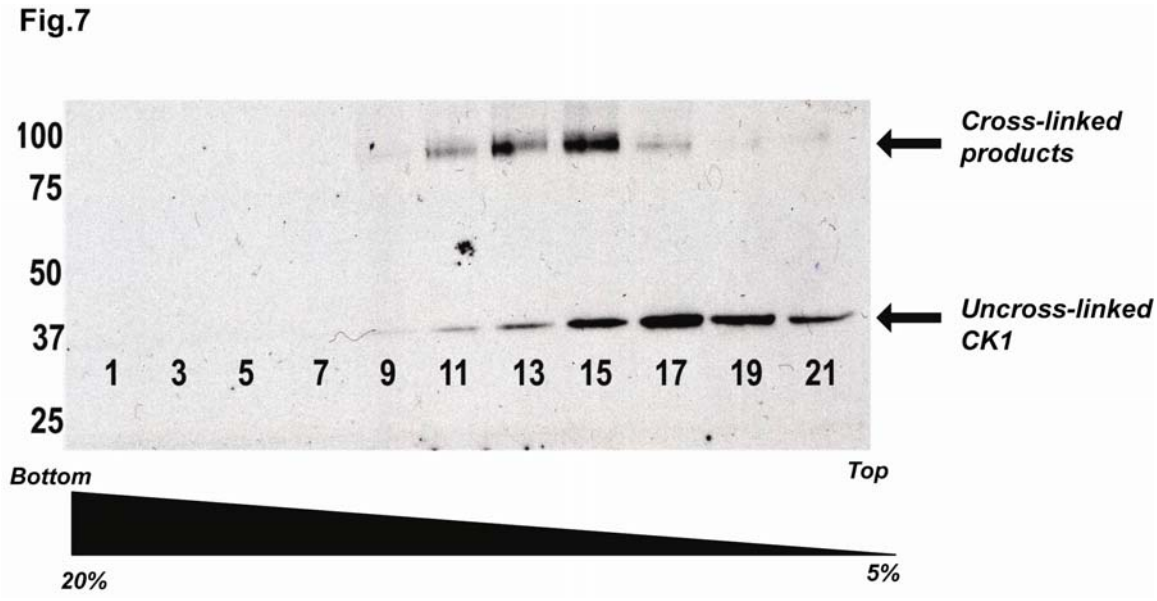
100
75
50
37
25
1 3 5 7 9 11 13 15 17 19 21
Cross-linked products
Uncross-linked CK1
Bottom
Top
20%
5%

Figure 7: Solubilized (0.6KI) CK1- cross-linked product can be fractionated by sucrose-density centrifugation: The solubilized CK1 cross-linked product is fractionated on a 5-20% sucrose gradient and 0.5ml fractions are collected and prepared for SDS-PAGE. Immunoblot analysis using the CK1 antibody reveals that uncross-linked CK1 fractionates near the top of the gradient, while cross-linked CK1 migrates at ~11S (as determined by dynein markers that fractionate at 12S and 20S).

Fig.8

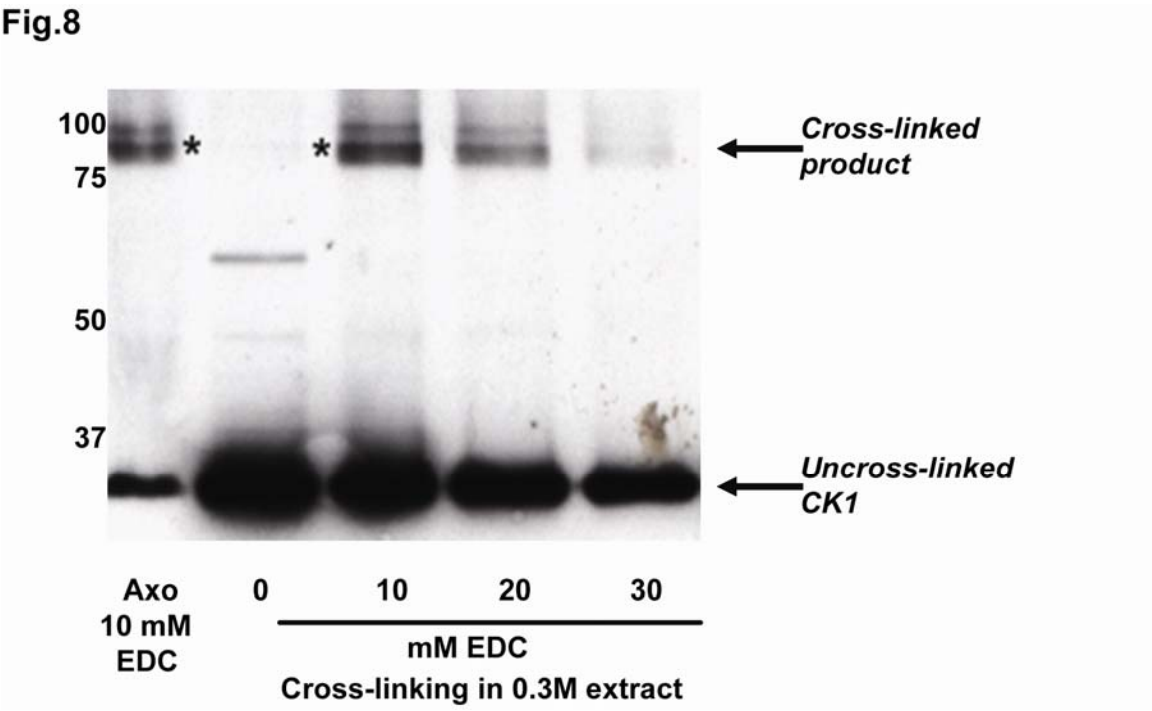
100
75
50
37
*
*
Cross-linked product
Uncross-linked CK1
Axo
10 mM EDC
0
10
20
30
mM EDC
Cross-linking in 0.3M extract

Figure 8: CK1 cross-linked product is obtained in a 0.3M axonemal salt extract:

Increasing amounts of EDC (10-30 mM) are added to the dialyzed axonemal 0.3M salt extracts. Immunoblot analysis using the CK1 antibody reveal that the ~85-90 kD product is formed in the salt extracts identical to the cross-linked product in the axonemes ("Axo, 10 mM EDC")

Fig.9

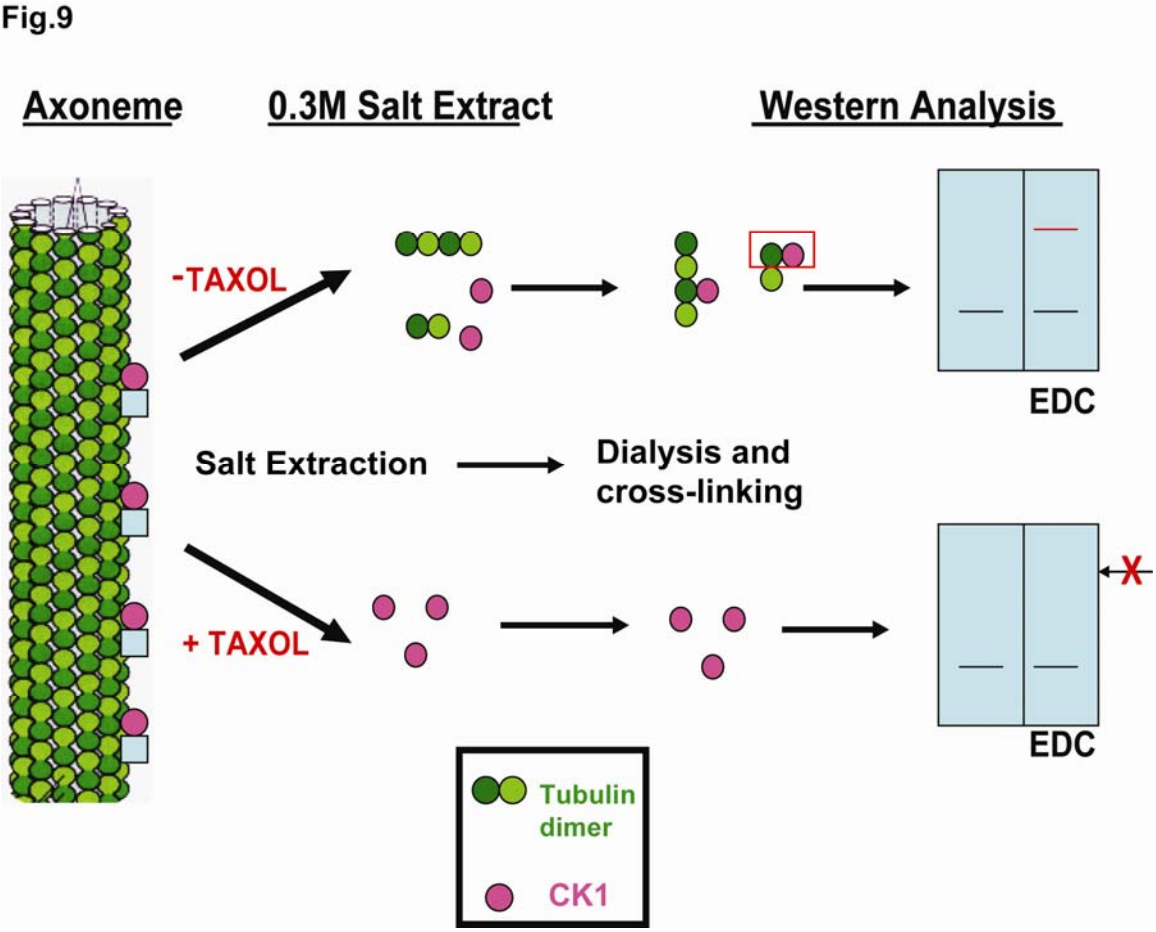
Axoneme
0.3M Salt Extract
Western Analysis
-TAXOL
EDC
Salt Extraction
Dialysis and
cross-linking
+ TAXOL
X
EDC
Tubulin
dimer
CK1

Figure 9: Strategy to test if the ~85-90 kD cross-linked product is tubulin: 0.3M salt extracts are obtained in the presence and absence of taxol. In the absence of taxol, CK1 and tubulin are solubilized and therefore cross-linking in these salt extracts would predictably generate the ~85-90 kD cross-linked product as seen by immunoblot analysis using the CK1 antibody. Salt extracts produced in the presence of taxol predictably does not contain tubulin, but does contain CK1, and therefore, cross-linking in these extracts would not generate the ~85-90 kD cross-linked product when analyzed by immunoblots using the CK1 antibody.

Fig .10

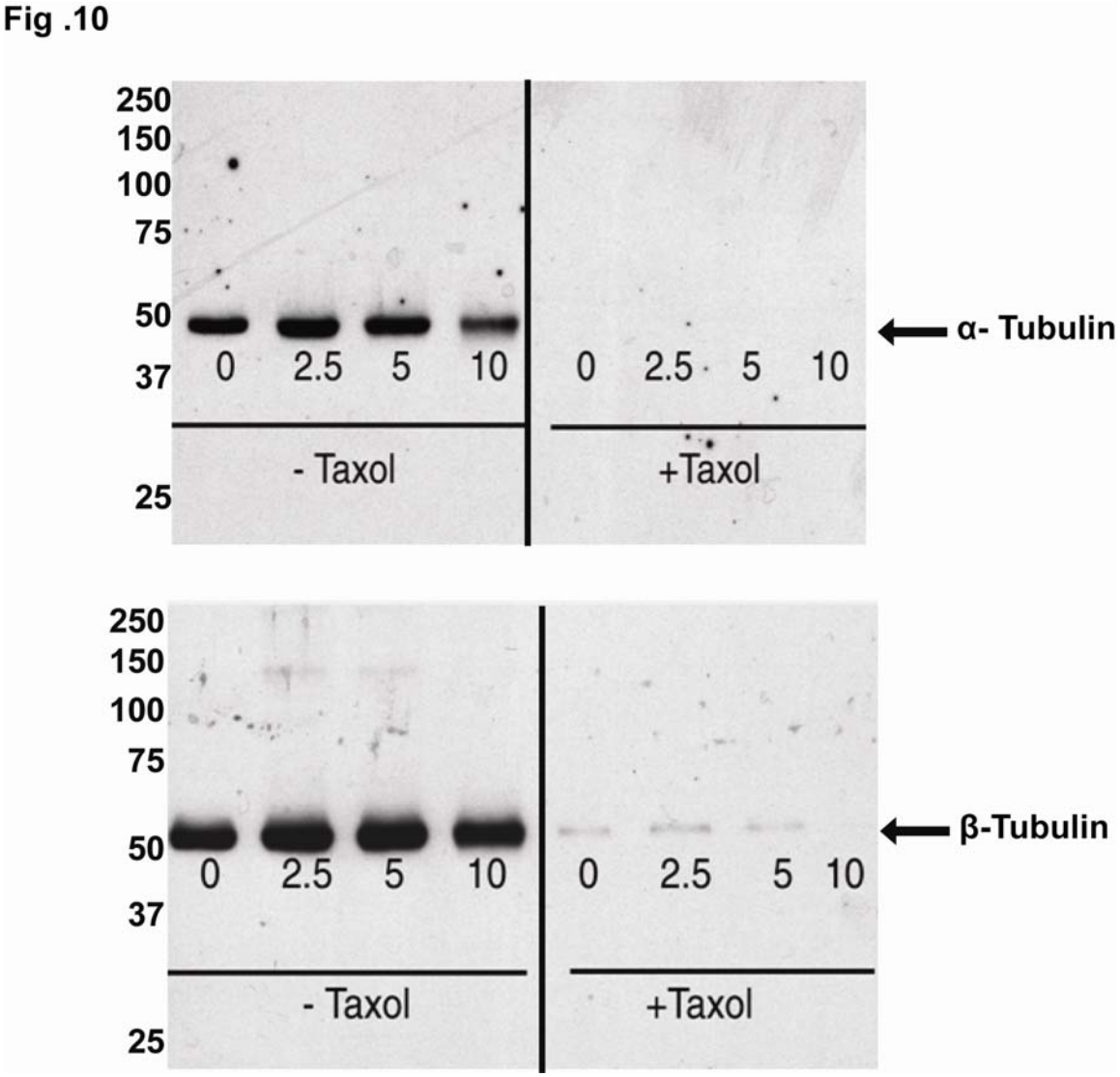
250
150
100
75
50
37
25
0
2.5
5
10
0
2.5
5
10
- Taxol
+Taxol
α- Tubulin
β-Tubulin

Figure 10: Taxol stabilizes tubulin in the axoneme and prevents solubilization of both α and β tubulin with 0.3M NaCl buffer: 0.3M NaCl axonemal salt extracts are prepared in the absence and presence of taxol followed by cross-linking with increasing concentrations of EDC (0-10 mM). Immunoblots probed with antibodies to α and β tubulin reveals that in the presence of taxol, both α and β tubulin are not extracted with a 0.3M NaCl buffer.

Fig.11

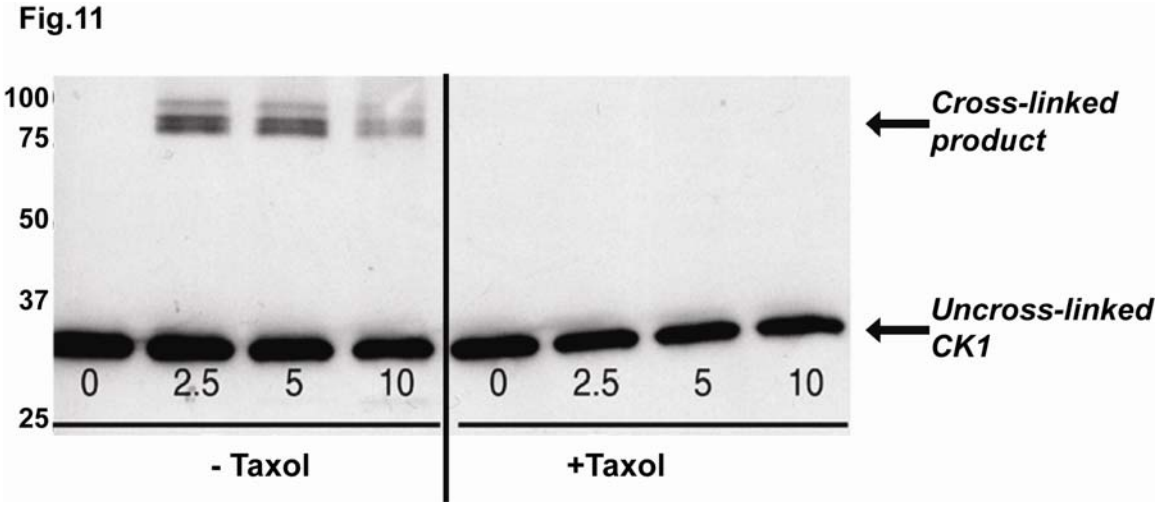
100
75
50
37
25
0
2.5
5
10
0
2.5
5
10
- Taxol
+Taxol
Cross-linked product
Uncross-linked CK1

Figure 11: CK1-EDC cross-linked product is tubulin: 0.3M NaCl axonemal salt extracts are prepared in the absence and presence of taxol and increasing amounts of EDC is added (0-10 mM) for 1 hour and the samples are prepared for SDS-PAGE. Immunoblot analysis using the CK1 antibody reveals that cross-linking in dialyzed 0.3M NaCl axonemal extracts prepared in the presence of taxol fails to produce the ~85-90 kD cross-linked product.

Fig. 12

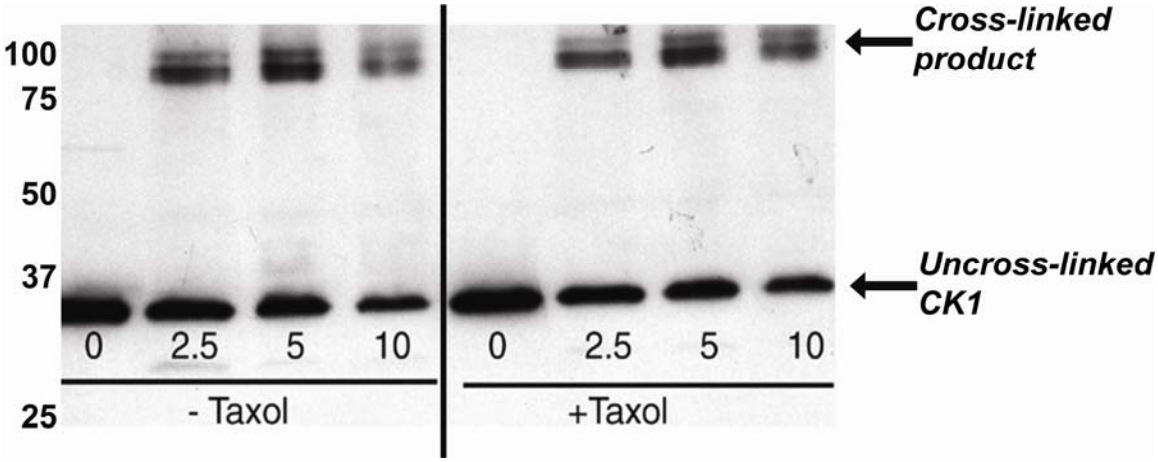
100
75
50
37
25
0
2.5
5
10
0
2.5
5
10
- Taxol
+Taxol
Cross-linked product
Uncross-linked CK1

Figure 12: Taxol does not interfere with the EDC cross-linking mechanism: Cross-linking is performed in the axonemes in the absence and presence of taxol with increasing concentrations of EDC (0-10 mM). Immunoblot analysis using the CK1 antibody reveals that the original ~85-90 kD CK1-cross-linked product continues to form in the presence or absence of taxol. Therefore, the conclusion is that taxol does not interfere in the EDC cross-linking mechanism.

Fig. 13

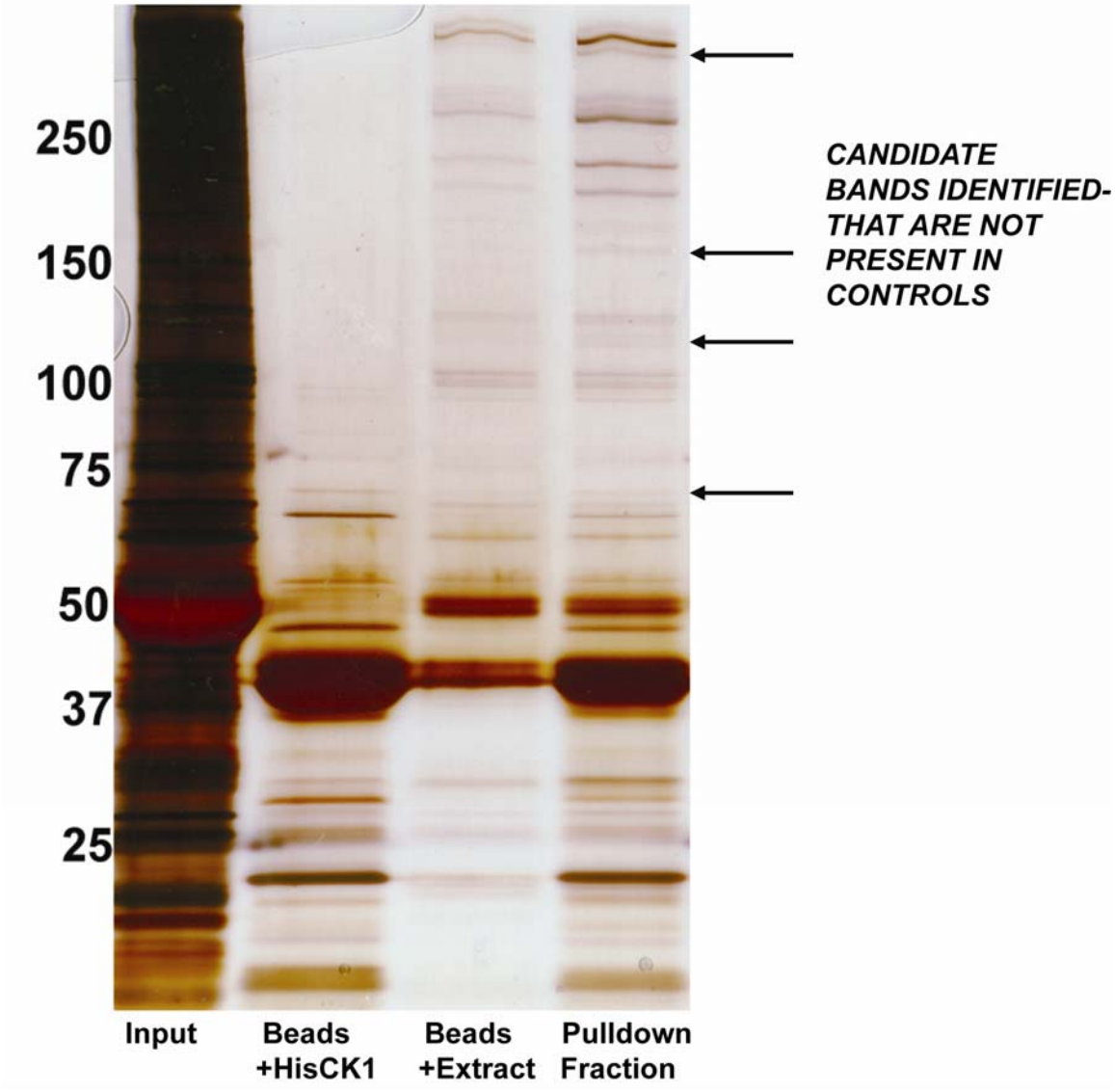
250
150
100
75
50
37
25
CANDIDATE BANDS IDENTIFIED- THAT ARE NOT PRESENT IN CONTROLS
Input
Beads +HisCK1
Beads +Extract
Pulldown Fraction

Figure 13: Identification of candidate-CK1 interacting proteins by silver-staining:

Silver stain analysis of fractions obtained from the in-vitro pull-down experiment using HisCK1 reveals candidate protein bands present in the "pulldown fraction" that are not present in the control fractions ("Beads+HisCK1" and "Beads+Extract"). The first lane ("input") contains the dialyzed 0.6M KI axonemal extracts that were originally incubated with the cobalt-Sepharose beads.

Fig.14

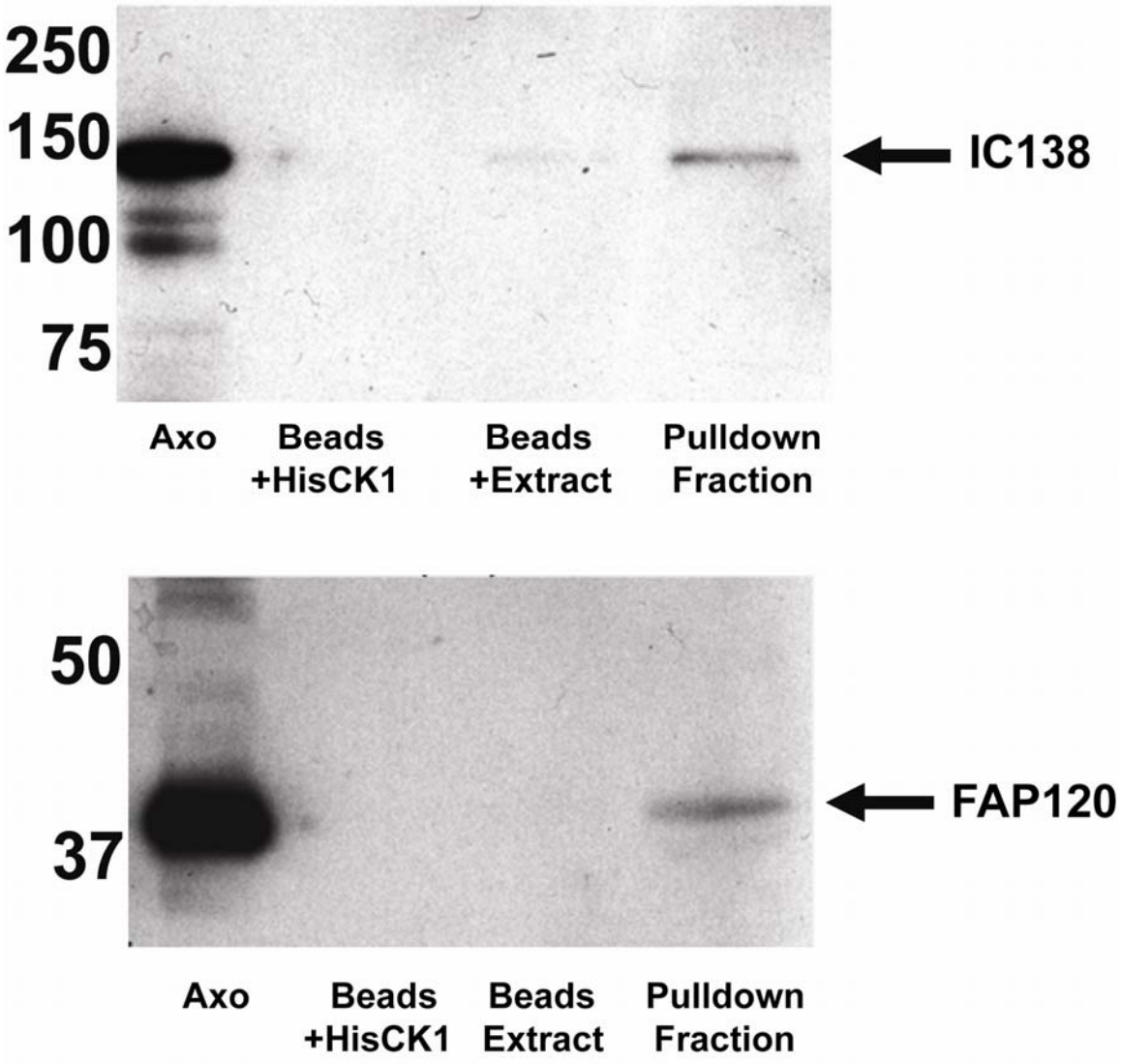
250
150
100
75
IC138
Axo
Beads +HisCK1
Beads +Extract
Pulldown Fraction
50
37
FAP120
Axo
Beads +HisCK1
Beads Extract
Pulldown Fraction

Figure 14: CK1 interacts with IC138 and FAP120: Fractions from in-vitro pull-downs using HisCK1 are probed with antibodies to IC138 and FAP120. Axonemal (Axo) fractions, controls (including "Beads+HisCK1" and "Beads+Extract") and the "pull-down fractions" obtained from the pull-down assay are prepared for SDS-PAGE and immunblot analysis. IC138 and FAP120 is present in the pull-down fractions but not in the control fractions. Therefore, CK1 must interact directly or indirectly with IC138 and FAP120.

Fig.15

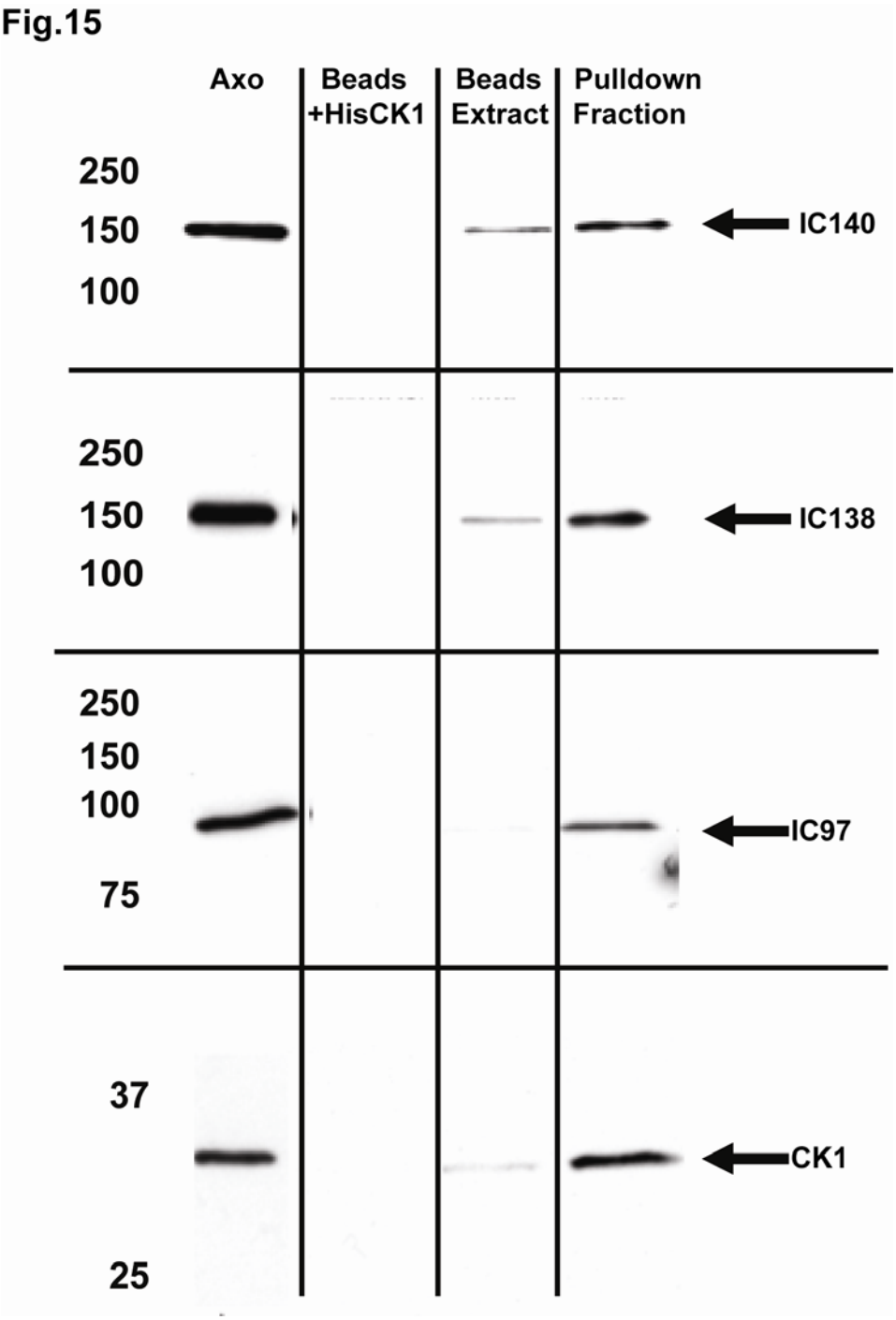
Axo
Beads +HisCK1
Beads Extract
Pulldown Fraction
250
150
100
IC140
250
150
100
IC138
250
150
100
75
IC97
37
25
CK1

Figure 15: FAP120 interacts with IC140, IC138, IC97 and CK1: Fractions from in-vitro pull-downs using HisFAP120 are probed with antibodies to IC140, IC138, IC97 and CK1. Axonemal (Axo) fractions, controls (including "Beads+HisCK1" and "Beads+Extract") and the "pulldown fractions" obtained from the pull-down assay are prepared for SDS-PAGE and immunblot analysis. Although some amount of IC140 and IC138 is seen in the control "Beads+Extract" fraction, these proteins are enriched in the "pulldown fractions". Therefore, the conclusion is that FAP120 interacts with the I1 intermediate chains as well as CK1.

Fig.16

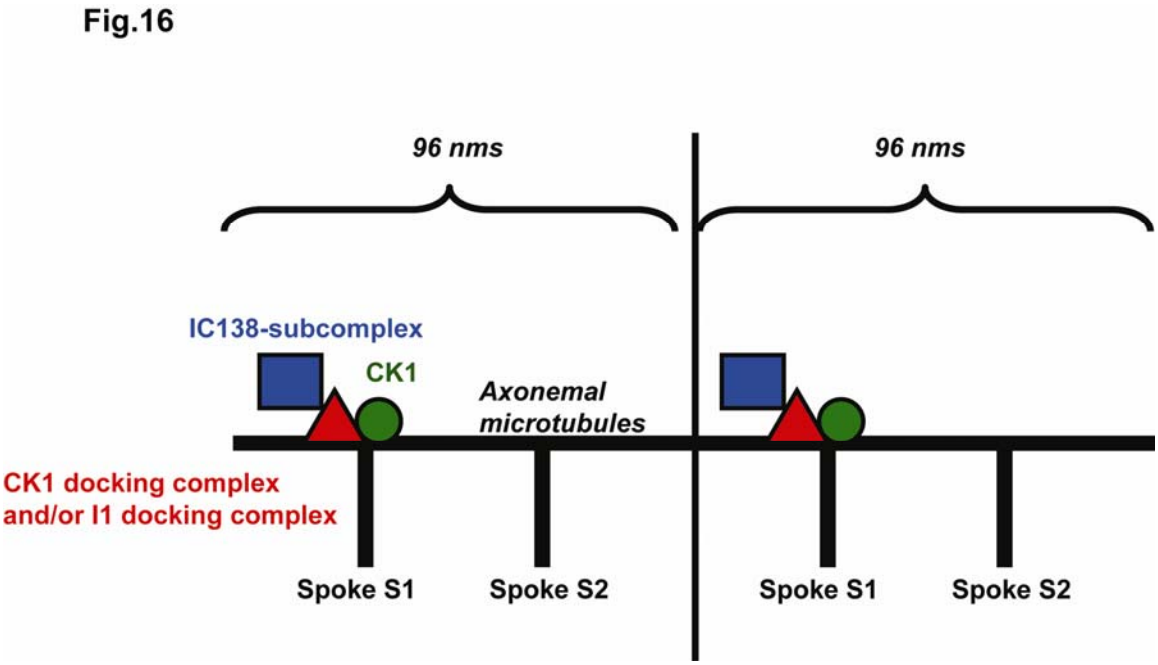
96 nms
96 nms
IC138-subcomplex
CK1
Axonemal microtubules
CK1 docking complex and/or I1 docking complex
Spoke S1
Spoke S2
Spoke S1
Spoke S2

Figure 16: Model for CK1 interactions in the axoneme: The prediction is that CK1 is localized to the axoneme via multiple, possibly independent protein-protein interactions. EDC cross-linking has demonstrated that CK1 directly interacts with tubulin. However, this does not explain specific, predicted periodicity of CK1 within the axoneme. Preliminary in-vitro pull-downs suggest that CK1 interacts with the I1 subunits, IC138 and FAP120. Based on mutant analysis, the prediction is that CK1 interacts indirectly with IC138 and FAP120, possibly via another protein that is responsible for anchoring I1 dynein and CK1 to the axoneme (red triangle). These data support the hypothesis that CK1 is localized along the length of the axoneme and is in proximity to the I1 dynein, particularly the IC138 sub-complex.

Chapter 4: Regulation of dynein-driven microtubule sliding by the axonemal kinase CK1

Introduction:

Motile cilia and flagella are capable of complex, carefully coordinated movements that have diverse roles in embryonic development, fertilization, and function of epithelia (Eggenschwiler and Anderson, 2007; Marshall, 2008; Sharma *et al.*, 2008; Gerdes *et al.*, 2009). Within the axoneme, spatial and temporal regulation of dynein-driven microtubule sliding is required for production of the complex bends that characterize ciliary and flagellar motility (Satir, 1968; Summers and Gibbons, 1971; Shingyoji *et al.*, 1977; Brokaw, 1991b, 2009). However, the mechanisms that regulate dynein and modulate the size and shape of the axonemal bend are poorly understood (Salathe, 2007; Brokaw, 2009). Here, I focus on the specific role of CK1 and its role in control of dynein-driven microtubule sliding in flagella (Yang and Sale, 2000) by development of new in-vitro reconstitution approaches and functional assays to directly test the hypothesis that CK1 regulates dynein-driven microtubule sliding.

As indicated in Chapter 1, genetic and functional analyses of isolated axonemes in *Chlamydomonas* have revealed that the central pair – radial spoke structures (CP/RS) regulate microtubule sliding by a control mechanism involving axonemal protein phosphorylation (Porter and Sale, 2000; Smith and Yang, 2004; Wirschell *et al.*, 2007). Additional evidence for such a control system has come from characterization of bypass suppressor mutations that restore motility to paralyzed CP/RS mutants without restoring the missing structures (Huang *et al.*, 1982; Piperno *et al.*, 1992; Porter *et al.*, 1992; Rupp *et al.*, 1996; Rupp and Porter, 2003). These experiments revealed regulatory systems that, in the absence of the CP/RS, results in inhibition of axonemal dyneins.

Consistent with this interpretation, isolated axonemes lacking the CP/RS can be induced to undergo dynein-driven microtubule sliding using a microtubule sliding disintegration assay, although the rate of microtubule sliding is significantly reduced compared to wild-type axonemes (Witman *et al.*, 1978; Smith and Sale, 1992a). Importantly, in-vitro functional and pharmacological assays and reconstitution experiments, coupled with mutant cells lacking specific dynein subforms, demonstrated that the changes in microtubule sliding velocity are mediated by phosphorylation of the inner dynein arms (Smith and Sale, 1992b; Howard *et al.*, 1994; Habermacher and Sale, 1996, 1997; King and Dutcher, 1997). These studies also revealed that the protein kinases and phosphatases responsible for control of dynein phosphorylation, including CK1, are physically anchored in the axoneme (Porter and Sale, 2000; Yang *et al.*, 2000; Yang and Sale, 2000; Gaillard *et al.*, 2001; Gaillard *et al.*, 2006).

In addition to the central pair and radial spoke structures, the phospho-regulatory pathway also requires the assembly of an inner arm dynein called I1 dynein important for control of flagellar waveform (Wirschell *et al.*, 2007). The key phospho-protein within I1 dynein is the IC138 subunit. This conclusion is based both on direct analysis of IC138 phosphorylation (Habermacher and Sale, 1997; Yang and Sale, 2000; Hendrickson *et al.*, 2004) and recovery of *Chlamydomonas* flagellar mutants defective in either IC138 phosphorylation (King and Dutcher, 1997; Hendrickson *et al.*, 2004; Dymek and Smith, 2007; Wirschell *et al.*, 2009) or in IC138 assembly (Bower *et al.*, 2009). For example, rescue of microtubule sliding by protein kinase inhibitors requires assembly of I1 dynein and the assembly of the IC138 sub-complex (Habermacher and Sale, 1997; Yang and Sale, 2000; Bower *et al.*, 2009; Wirschell *et al.*, 2009). Such pharmacological

experiments also revealed a role for the protein kinase CK1 in the regulatory pathway (Yang and Sale, 2000). These experiments take advantage of specific CK1-inhibitors that can be used in the in-vitro microtubule sliding assay (Yang and Sale, 2000), thus suggesting the presence of CK1 and CK1 kinase activity in the motile axoneme. Subsequent studies revealed that a CKI-like protein is physically anchored in the ciliary/flagellar axoneme, potentially in the exact position required to regulate IC138 phosphorylation (Chapter 2; Yang and Sale, 2000). For example, study of *Chlamydomonas* flagellar structural mutants revealed that CK1 is localized to the outer doublet microtubules (Chapter 2) and biochemical analysis revealed that CK1 is a relatively abundant axonemal protein, consistent with regular localization near the dynein motors (Yang and Sale, 2000; Pazour *et al.*, 2005). Together, these studies have led to the model shown in Fig. 1, implicating an axonemal CK1, and a failure in regulation of CK1, in control of IC138 phosphorylation and microtubule sliding. However, tests of this model require more direct analysis of axonemal CK1.

To test this hypothesis, I took advantage of a biochemical feature of CK1 where CK1 can be solubilized from axonemes in a 0.3M NaCl buffer. Furthermore, this extraction procedure does not solubilize the key microcystin-LR-sensitive axonemal phosphatases, including PP2A, as well as does not disrupt the dynein arm, radial spoke or central pair structures which are required to regulate and rescue microtubule sliding. I took advantage of the solubility of axonemal CK1 to produce "CK1-depleted axonemes", in combination with the in-vitro microtubule sliding assay as well as in-vitro reconstitution of the CK1-depleted axonemes using purified recombinant CK1, to directly test the role of CK1 in control of microtubule sliding (see Fig.2 for strategy). I

demonstrate that CK1 rebinds to the depleted axonemes, that reconstituted CK1 kinase activity is required to inhibit dynein-driven microtubule sliding and assembly of I1 dynein is required for this regulatory pathway.

Materials and methods:

***Strains and culture conditions*:** *Chlamydomonas reinhardtii* strains used include CC125 (wild-type), *pf17* (lacks radial spoke head), *ida1pf17,* (lacks I1 dynein and radial spoke head). All strains were obtained from the *Chlamydomonas* Genetics Center (Univ. of MN, St. Paul, MN) with the exception of *ida1pf17* (recovered from non-parental tetrad). Cells were grown in tris-acetate-phosphate (TAP) medium with aeration on a 14:10 hr light: dark cycle.

Molecular approaches: The CK1 coding sequence was PCR cloned into the pCR 2.1 TOPO cloning vector according to the manufacturer's instructions (Invitrogen, Carlsbad, CA) to yield plasmid pAGCK1-FL. The insert in pAGCK1-FL was excised by digestion with *BamH1* and *HindIII* and cloned into the pet28A (Novagen, San Diego, CA). The resulting expression construct, pAGHisCK1, was transformed into strain BL21(DE3) pLysS (Stratagene, La Jolla, CA) and expression induced with 1 mM Isopropyl β-D-1-thiogalactopyranoside (IPTG). The His-tagged CK1 protein was purified using Talon metal affinity resin (Clontech, Mountain View, CA). Site directed mutagenesis was performed on the pAGCK1-FL plasmid to make the amino acid substitution, K40R, using QuickChange^{TM} in-vitro Site-Directed Mutagenesis System (Stratagene, La Jolla, CA), to produce plasmid pAGCK1-KD. The His-tagged CK1-KD was induced, expressed and purified as described above.

Protein Kinase Assay: Protein kinase assays were performed using specific CK1 peptide substrates (C2335, Sigma-Aldrich). For CK1 activity, 2µl samples from chromatography fractions or purified recombinant CK1 fractions were added to a reaction mixture to a final volume of 20 µl containing reaction buffer (50 mM Tris, pH8, 0.1 mM EDTA, 0.2%

β- mercaptoethanol, 7 mM magnesium acetate, 0.02% Brij 35, 20 mM NaCl, and 100 mM sodium orthovanadate), 0.5 µg/µl CKI specific substrate, and 40 µM [γ-32P] ATP (2000 cpm/pmol). After 30 min at 30 °C, the reactions were terminated by adding 1 µl of 100% trichloroacetic acid. 10 µl samples from each reaction were applied in duplicate to discs of P-81 filter paper (Whatman), washed extensively with 75 mM phosphoric acid, and rinsed with acetone. The radioactivity of the dried P-81 paper discs was measured by scintillation counting (Beckmann LS 6500 Multi-purpose scintillation counter).

Axoneme isolation: Flagella were isolated as described (Witman, 1986). For CK1 extraction, axonemes (1 mg/ml) were treated with buffer (10 mM Hepes, 5 mM $MgSO_4$, 1 mM DTT, 0.5 mM EDTA, 0.1 M PMSF, and 0.6 TIU aprotinin, pH 7.4) containing 0.3 M NaCl. Axonemal fractions were fixed for SDS-PAGE at a concentration of 1 mg/ml and 20 µg of protein was used for analysis.

Kinase inhibitors and reagents: 5, 6-Dichloro-1-b-D-ribofuranosylbenzimidazole (DRB; Biomol, Plymouth Meeting PA) was stored as a 50 mM stock solution in ethanol and *N*-(2-aminoethyl)-5-chloroisoquinoline-8-sulfonamide (CKI-7, Toronto Research Chemicals, North York, Canada) was stored as a 50 mM stock solution in DMSO. Microcystin-LR (Calbiochem, La Jolla, CA) was stored as a 500 µM stock solution in methanol.

Microtubule sliding assay and reconstitution experiments: Measurement of microtubule sliding velocity was performed as described (Okagaki and Kamiya, 1986; Wirschell *et al.*, 2009). Flagella were isolated and demembranated in a motility buffer (10mM HEPES, 5mM magnesium sulphate, 1% polyethylene glycol, 0.1mM EGTA, 50 mM

potassium acetate and 2 mM DTT) containing 1% Nonidet-P40. Axonemes were then applied to the perfusion chamber and nonadherent axonemes were washed away with motility buffer. To initiate microtubule sliding motility buffer with 1 mM ATP and subtilisin (5μg/ml) protease was added by perfusion.

For CK1-depletion experiments, flagella were demembranated and extracted in motility buffer containing 1% Nonidet-P40 and 0.3 M NaCl for ~2 minutes and the axonemes applied to the perfusion chamber (strategy is illustrated in Fig.2). For inhibition studies, DRB (50 μM), CK1-7 (50 μM) or a mixture of DRB/CK1-7 and MC (2 μM) was introduced to the perfusion chamber, and sliding was then initiated with 1 mM ATP and subtilisin (5 μg/ml). For reconstitution experiments, rCK1, rCK1-KD or a mixture of rCK1 and rCK1-KD was flowed through the perfusion chamber containing CK1-depleted axonemes for 2 minutes and unbound fusion protein washed away. The reconstituted axonemes were treated with inhibitors and microtubule sliding induced as described above. Sliding events were observed by dark field microscopy and recorded by SIT camera and converted to a digital image for analysis using Labview 7.1 software (National Instruments, Austin,TX). Microtubule displacement was measured manually using tracings calibrated with a micrometer and used to calculate sliding velocities.

Results:

Depletion of CK1 rescues microtubule sliding in RS mutant axonemes and rescue requires I1 dynein: To test the hypothesis that CK1 inhibits dynein-driven microtubule sliding, we developed a novel approach of measuring microtubule sliding in CK1-depleted axonemes (Fig. 2). We predicted that biochemical removal of CK1 from *pf17* axonemes would mimic treatment with the kinase inhibitors, DRB and CK1-7, and rescue microtubule sliding. As shown in Fig. 3 the CK1 inhibitors restore microtubule sliding velocity in isolated *pf17* axonemes (Fig. 3, compare bar 3 with 4 and 5; Yang and Sale, 2000). The results indicated that flagellar paralysis in *pf17* is a consequence of uniform, CK1-dependent inhibition of dynein activity through phosphorylation (Fig. 1). Consistent with this interpretation, addition of the phosphatase inhibitor, microcystin-LR, blocked the CK1-inhibitor mediated rescue of microtubule sliding in *pf17* axonemes (Fig. 3, bars 6 and 7). Microtubule sliding velocity was also rescued in CK1-depleted *pf17* axonemes (Fig. 3, compare bar 3 with 8), mimicking DRB/CK1-7 treatment and consistent with the hypothesis that failure in regulation of CK1 in *pf17* axonemes results in inhibition of dynein-driven microtubule sliding. The phosphatase inhibitor microcystin-LR blocked rescue of microtubule sliding in the CK1-depleted *pf17* axonemes (Fig.3, compare bar 8 and 9). Depletion of CK1 from wild-type axonemes had no effect on microtubule sliding velocity (Fig. 3, compare bars 1 and 2). This result established the CK1-depletion procedure did not remove the microcystin-LR sensitive phosphatases required for rescue of microtubule sliding (Fig. 1).

Rescue of microtubule sliding also required the assembly of I1 dynein and its regulatory intermediate chain IC138 (Habermacher and Sale, 1997; Yang and Sale, 2000;

Bower *et al.*, 2009; Wirschell *et al.*, 2009). To determine whether I1 dynein assembly is required for rescue of microtubule sliding in the CK1-depletion experiments, we analyzed a double mutant *ida1pf17* defective in I1 dynein and radial spoke assembly. Microtubule sliding in the *ida1pf17* axonemes is slow and neither DRB nor CK1-7 rescues sliding (Fig. 3, bars 11 and 12). Similarly, depletion of CK1 fails to rescue microtubule sliding (Fig. 3, bar 13). Therefore, assembly of I1 dynein is required for rescue of microtubule sliding in the CP/RS pathway, indicating that I1 dynein plays an active and essential role for controlling microtubule sliding.

Exogenous CK1 restores inhibition of microtubule sliding in a DRB/CK1-7 sensitive manner: To determine whether rescue of microtubule sliding is specifically due to CK1 depletion, we reconstituted the CK1-depleted *pf17* axonemes with purified, recombinant CK1 (rCK1, Fig. 4, Fig.5). This was possible in part since the purified rCK1 is soluble. We predicted that the rCK1 will functionally rebind CK1-depleted axonemes and restore inhibition of microtubule sliding to the original slow velocity that is characteristic of *pf17* axonemes. The purified rCK1 rebound to CK1-depleted axonemes (inset, Fig. 4), and inhibition of microtubule sliding velocity was restored (Fig. 4, compare bars 3 and 4). Treatment of the rCK1-reconstituted axonemes with DRB or CK1-7 blocked this restoration of sliding inhibition (Fig.4, bars 5 and 6), and microcystin-LR blocked rescue of microtubule sliding by the kinase inhibitors DRB and CK1-7 in the rCK1-reconstituted axonemes (Fig. 4, bars 7 and 8). These results demonstrated that exogenous CK1 binds to the axoneme and inhibits I1dynein-dependent microtubule sliding velocity in *pf17* axonemes. The results also demonstrate that rescue of microtubule sliding in *pf17* axonemes depends upon an axonemal, microcystin-LR dependent phosphatase (Fig. 1).

CK1 kinase activity is required for inhibition of microtubule sliding: For further investigation, I designed a CK1-KD mutant (based on Gao *et al.*, 2002) that was also soluble and lacked kinase activity but was otherwise capable of binding to the CK1-depleted axonemes (Fig. 5, inset Fig.6). Reconstitution of CK1-depleted axonemes with rCK1-KD did not alter rescued microtubule sliding velocity (Fig. 6, bar 3), and, as expected, DRB or CK1-7 treatment did not have any further effect (Fig. 6, bars 4 and 5). To test whether rCK1-KD functionally rebinds to the CK1-depleted axonemes, we performed competition experiments using a mixture of different ratios of rCK1 and rCK1-KD. We predicted that rCK1-KD would compete with rCK1 for binding to the axoneme and block inhibition of microtubule sliding. As the amount of rCK1-KD protein was increased, there was a corresponding increase in microtubule sliding (Fig.7, bars 3-7).

Discussion:

Primary conclusions:

The main goal of this work is to directly test the role of CK1 in control of dynein-driven microtubule sliding. Here, I present data from a novel in-vitro assay that couples in-vitro reconstitution of purified CK1 with CK1-depleted axonemes and measures microtubule sliding. I have demonstrated that when axonemal CK1 is depleted from paralyzed axonemes, it rescues dynein-driven microtubule sliding activity. Furthermore, inhibition of dynein-driven microtubule motility can be restored by addition of recombinant CK1 to the depleted axonemes but restored inhibition requires CK1 kinase activity. These data demonstrate that unregulated CK1 kinase activity in the radial spoke mutants' results in inhibition of microtubule sliding. Based on these and additional data, I postulate that axonemal CK1 is a "downstream" component of the CP/RS phospho-regulatory pathway that controls normal flagellar waveform.

A novel in-vitro assay to study the role of CK1 in dynein-driven microtubule sliding:

In this study I have taken advantage of a solubilization property of axonemal CK1, where CK1 is easily extracted from axonemes at a relatively low salt concentration. Importantly, at this salt concentration, the dyneins, as well as the phosphatases, stay on the axonemes, enabling us to focus solely on the role of CK1 in the control of microtubule sliding. One important modification in the process of obtaining CK1-depleted axonemes involved combining CK1 extraction with flagellar demembranation. Traditional methods of spinning down the axonemes after demembranating disrupts the core axonemal structure and results in a high percentage of axonemes that do not slide. Thus, combining the demembranation and extraction steps is critical in preserving the

functional integrity of the axonemes and one of the innovations required for success of these experiments.

Depleting CK1 from *pf17* axonemes resulted in the rescue of sliding activity, which is similar to DRB or CK1-7 treatment and microcystin prevented this rescue. We next reconstituted CK1-depleted axonemes with purified, recombinant, CK1 onto the depleted axonemes and this resulted in the restoration of reduced microtubule sliding velocities. The restored, reduced microtubule sliding velocities are rescued with DRB/CK1-7 indicating that the inhibition of microtubule sliding not only requires CK1 rebinding, but also requires CK1 kinase activity. Similarly rCK1-KD also binds to the CK1-depleted axonemes, but does not restore inhibition of microtubule sliding, thus confirming that it is the kinase activity of CK1 that is required for the modification of the sliding activity. Based on this in-vitro analysis, using the CK1-depleted axonemes and rCK1 as well as rCK1-KD, I have confirmed that CK1 inhibits dynein-driven microtubule sliding. Therefore, as discussed below, in wild-type axonemes, CK1 activity must be tightly controlled by the CP/RS mechanism.

Interestingly when I performed competition experiments involving equal amounts of rCK1 and rCK1-KD reconstituted onto a fixed amount of CK1-depleted axonemes, I observed an intermediate microtubule sliding velocity. This result demonstrated that rCK1 and rCK1-KD compete equivalently for axonemal binding and that rCK1-KD can efficiently block the effect of rCK1 kinase activity in restoring inhibition of microtubule sliding. The intermediate sliding velocity is predicted to be a result of a mixture active and inactive I1 dynein. This observation may be consistent with biophysical analysis that

has indicated that I1 dynein can operate, in part, to resist microtubule sliding generated by other dyneins (Kotani *et al.*, 2007).

CK1 as a part of a phospho-regulatory pathway that controls flagellar motility:

Here, I present a novel in-vitro assay that reveals coupling of CK1 kinase activity to the CP/RS phospho-regulatory pathway that controls dynein activity (Fig. 1). The central question is how the CP/RS phospho- regulatory pathway contributes to normal axonemal motility. The CP/RS phospho-regulatory mechanism does not appear to be required for initiation of bending and bend oscillation; features are inherent to the dynein motors and to mechanical feedback control mechanisms that are not well understood (Hayashibe *et al.*, 1997; Lindemann and Hunt, 2003; Morita and Shingyoji, 2004; Aoyama and Kamiya, 2005; Hayashi and Shingyoji, 2008; Brokaw, 2009). Rather, this regulatory mechanism appears to be required for controlling the form (i.e. size and shape of the bend) of forward and reverse bends important for normal flagellar movement. Consistent with this interpretation, mutations that lead to a failure in I1- dynein assembly are defective in flagellar waveform (Brokaw and Kamiya, 1987) and fail to undergo normal phototaxis (King and Dutcher, 1997; Okita *et al.*, 2005). Bypass suppressor mutants that restore motility in the absence of radial spoke assembly fail to generate normal flagellar waveform (Brokaw *et al.*, 1982). In wild-type axonemes, signals from the central pair are presumably asymmetrically distributed to radial spokes anchored on individual or subsets of outer doublet microtubules. Predictably such signals locally regulate dynein activity on individual or groups of outer doublet microtubules, altering the form of the axonemal bend (Wirschell *et al.*, 2007).

It is likely the CP/RS phospho-regulatory mechanism responds to changes in second messengers including cyclic nucleotides and calcium (Walczak and Nelson, 1994; Bannai *et al.*, 2000; Smith, 2002b; Salathe, 2007; Hayashi and Shingyoji, 2009). Consistent with this idea, changes in calcium affect the flagellar waveform, and the mechanism involves direct interaction of calcium with calcium-binding proteins in the axoneme (Bessen *et al.*, 1980; Kamiya and Witman, 1984; Omoto and Brokaw, 1985; Brokaw, 1991a; Yang *et al.*, 2001; Patel-King *et al.*, 2004; Yang *et al.*, 2004). Changes in calcium have been shown to regulate microtubule sliding by a mechanism that involves the central pair (Smith, 2002a; Nakano *et al.*, 2003), and may require assembly of I1 dynein (Smith, 2002b). Dymek and Smith (2007) have identified a calmodulin containing complex called calmodulin-and spoke-associated complex (CSC) that interacts with the radial spokes and functionally interacts with I1 dynein. The CSC could also interact with CK1 and PP2A and mediate signaling from the radial spokes, as well as calcium, for the control of I1 dynein.

Fig. 1

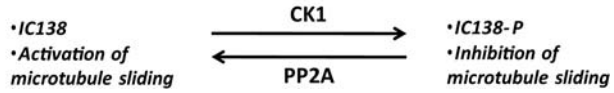
•IC138
•Activation of microtubule sliding
CK1
PP2A
•IC138-P
•Inhibition of microtubule sliding

Figure 1: Model for regulation of I1 dynein and the CK1 protein. Analysis of wild-type (WT) and mutant axonemes has revealed that microtubule sliding activity is regulated by phosphorylation of the I1 dynein subunit IC138 (Wirschell et al., 2007). The data predicts that IC138 is phosphorylated by the axonemal kinase CK1, and that phosphorylation inhibits dynein-driven microtubule sliding activity. The model also indicates axonemal phosphatase PP2A is required to rescue microtubule sliding activity (Yang and Sale, 2000).

Fig. 2

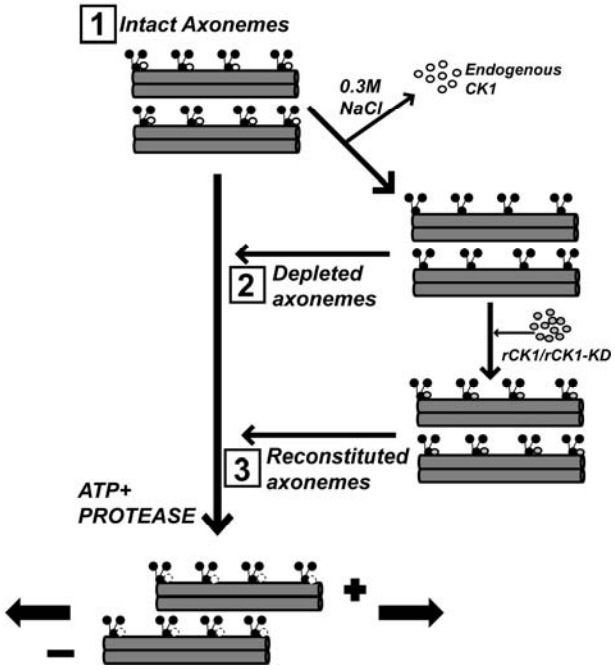
1 Intact Axonemes
0.3M NaCl
Endogenous CK1
2 Depleted axonemes
rCK1/rCK1-KD
3 Reconstituted axonemes
ATP+ PROTEASE
+
−

Figure 2: Experimental strategy to test the role of CK1 in microtubule (1) Isolated axonemes can be induced to slide in the presence of ATP and protease as previously described by the method of Okagaki and Kamiya (1986). (2) Isolated axonemes are obtained from *Chlamydomonas* cells and treated with 0.3M NaCl buffer to generate depleted axonemes. These depleted axonemes can be either induced to slide in presence of ATP and protease or (3) reconstituted with rCK1/rCK1-KD and then induced to slide. This novel method generates functionally null CK1 axonemes and the reconstitution experiments specifically test the precise role of CK1 activity in dynein-driven microtubule sliding.

Fig. 3

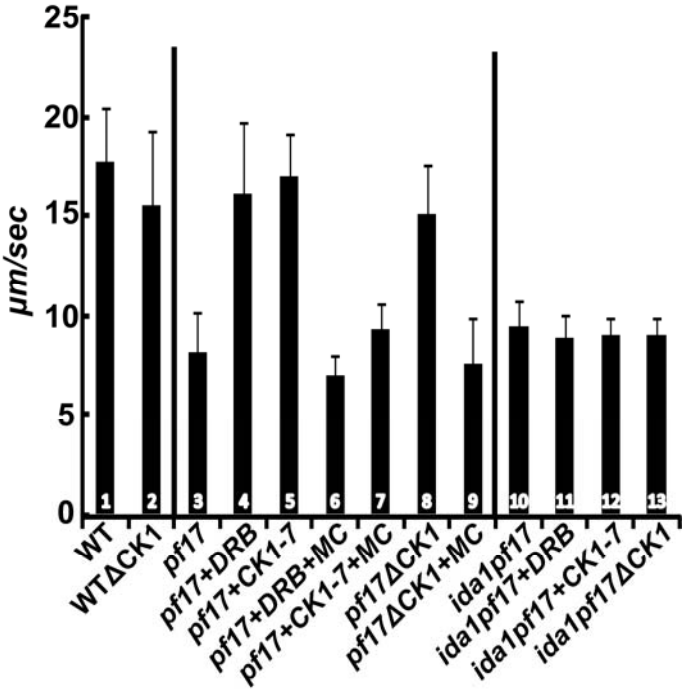
25
20
15
10
5
0
μm/sec
1
2
3
4
5
6
7
8
9
10
11
12
13
WT
WTΔCK1
pf17
pf17+DRB
pf17+CK1-7
pf17+DRB+MC
pf17+CK1-7+MC
pf17ΔCK1
pf17ΔCK1+MC
ida1pf17
ida1pf17+DRB
ida1pf17+CK1-7
ida1pf17ΔCK1

Figure.3: Biochemical depletion of CK1 rescues microtubule sliding in isolated pf17 axonemes and this rescue requires I1 dynein. ATP-induced microtubule sliding velocity was measured in isolated axonemes, CK1-depeleted axonemes or CK1-depleted axonemes reconstituted with purified, recombinant CK1(Okagaki and Kamiya, 1986; Wirschell et al., 2009). The effect of DRB / CK1-7 and phosphatase inhibitor microcystin-LR (MC) was also examined. The bars represent: [1] WT axonemes; [2] WT axonemes depleted of CK1 – note no change in velocity; [3] *pf17* axonemes – note slow, baseline sliding velocity; [4] *pf17* axonemes plus DRB; [5] *pf17* axonemes plus CK1-7; [6] *pf17* axonemes plus DRB and microcystin-LR; [7] *pf17* axonemes plus CK1-7 and microcystin-LR; [8] *pf17* axonemes depleted of CK1 – note rescue of microtubule sliding; [9] *pf17* axonemes depleted of CK1plus microcystin-LR; [10] *ida1pf17* axonemes; [11] *ida1pf17* axonemes plus DRB; [12] *ida1pf17* axonemes plus CK1-7; [13] *ida1pf17* axonemes depleted of CK1- note failure in rescue of sliding. Microtubule sliding velocity is expressed as μm/sec, and averages and standard deviations were calculated from at least three independent experiments with a minimum sample size of 75 axonemes.

Fig. 4

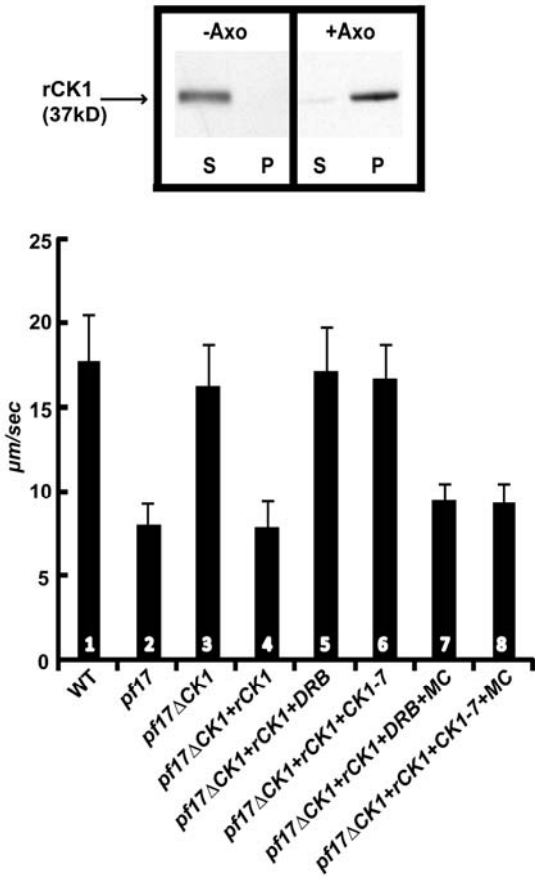
-Axo
+Axo
rCK1
(37kD)
S
P
S
P
25
20
15
10
5
0
µm/sec
1
2
3
4
5
6
7
8
WT
pf17
pf17ΔCK1
pf17ΔCK1+rCK1
pf17ΔCK1+rCK1+DRB
pf17ΔCK1+rCK1+CK1-7
pf17ΔCK1+rCK1+DRB+MC
pf17ΔCK1+rCK1+CK1-7+MC

Figure.4: Recombinant CK1 binds to CK1-depleted axonemes and restores inhibition of dynein-driven microtubule sliding. Addition of rCK1 restores inhibition in CK1-depleted *pf17* axonemes (bars 3 and 4) and rebinds to CK1-depleted *pf17* axonemes (inset). DRB and CK1-7 block restoration of inhibition (bars 5 and 6), and microcystin-LR blocks the effects of the kinase inhibitors (bars 7 and 8).

Fig. 5

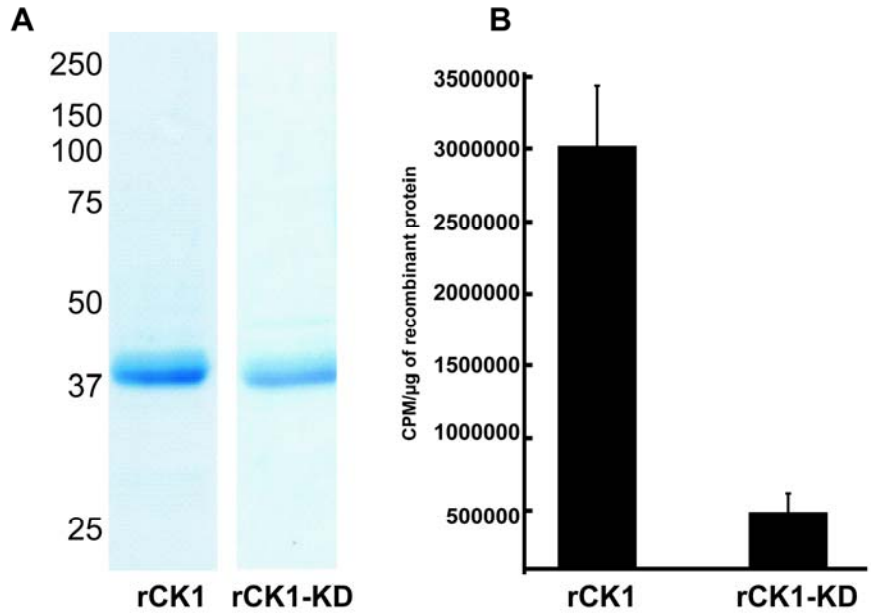
A
250
150
100
75
50
37
25
rCK1
rCK1-KD
B
CPM/µg of recombinant protein
3500000
3000000
2500000
2000000
1500000
1000000
500000
rCK1
rCK1-KD

Figure 5: rCK1 and rCK1-KD are soluble and rCK1-KD is catalytically inactive. (A) Coomassie blue stained gel of soluble, purified recombinant rCK1 and rCK1-KD. The difference in protein levels obtained with rCK1 and rCK1-KD reflect slightly different levels of induction: equal amount of each fusion protein was used in each enzymatic and functional assay. (B) In-vitro kinase assays demonstrated that rCK1 and not rCK1-KD displayed kinase activity. The results are expressed as counts per minute per microgram of protein, and the graphs show the mean of four separate measurements and standard error bars.

Fig. 6

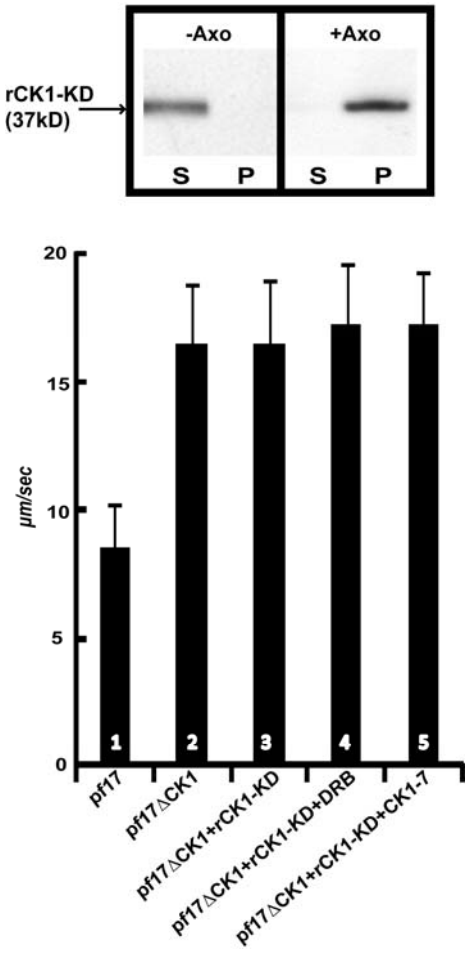
-Axo
+Axo
rCK1-KD
(37kD)
S
P
S
P
20
15
10
5
0
μm/sec
1
2
3
4
5
pf17
pf17ΔCK1
pf17ΔCK1+rCK1-KD
pf17ΔCK1+rCK1-KD+DRB
pf17ΔCK1+rCK1-KD+CK1-7

Figure 6: CK1 kinase activity is required for regulation of microtubule sliding. rCK1-KD rebinds to CK1-depleted *pf17* axonemes (inset) but fails to restore inhibition of microtubule sliding velocity (compare bars 2 and 3). Treatment with CK1 inhibitors had no effect (bars 4 and 5).

Fig. 7

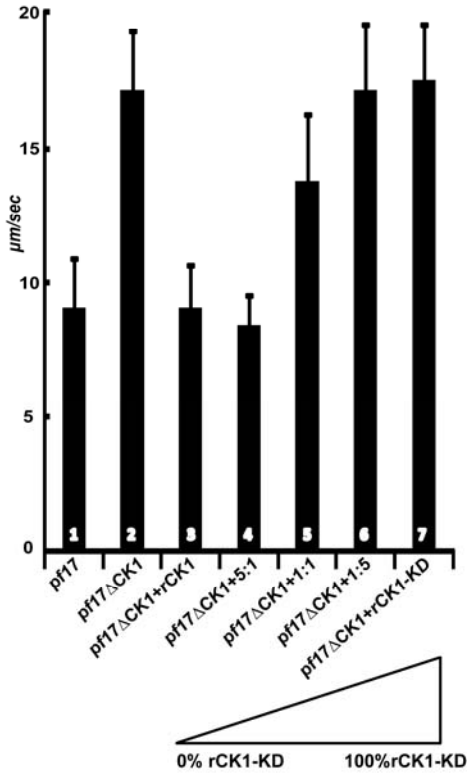
20
15
10
5
0
µm/sec
1
2
3
4
5
6
7
pf17
pf17ΔCK1
pf17ΔCK1+rCK1
pf17ΔCK1+5:1
pf17ΔCK1+1:1
pf17ΔCK1+1:5
pf17ΔCK1+rCK1-KD
0% rCK1-KD
100%rCK1-KD

Figure 7: rCK1-KD can compete with rCK1 for specific binding to the axoneme. rCK1 and rCK1-KD were reconstituted at different ratios to CK1-depleted *pf17* axonemes (illustrated below bars 3-7). With increasing amounts of rCK1-KD, there is a corresponding increase in microtubule sliding velocity indicating rCK1-KD competes for binding and inhibits the effect of rCK1 on microtubule sliding. Microtubule sliding velocity is expressed as μm/sec, and averages and standard deviations were calculated from at least three independent experiments with a minimum sample size of 75 axonemes.

Chapter 5: Significance of results and new questions

Summary and opportunities:

The work presented in this dissertation is founded in pharmacological and functional studies that determined the presence of a CK1-like kinase activity in the axoneme (Yang and Sale, 2000). The goal of this work was to identify the protein kinase CK1 gene that encodes axonemal CK1 and test the role of the axonemal CK1 in regulation of dynein and ciliary motility. My principal objective was to test the hypothesis that CK1 is localized to the axoneme where it inhibits dynein-driven microtubule sliding by phosphorylation of a regulatory protein - IC138. The main results of this work include:

[1] The axonemal CK1 is a highly conserved serine/threonine protein kinase, anchored to the outer doublet microtubules and localized uniformly along the length of the axonemes. I was able to confirm that the CK1 identified in this study was identical to the CK1 identified by Yang and Sale (2000). Interestingly, only one CK1 gene was identified in *Chlamydomonas* and CK1 is shown to be localized to at least three different subcellular sites – the nucleus, eyespot and axoneme. Clearly, CK1 is quite versatile in *Chlamydomonas.* One key question is: How is a single isoform of CK1 targeted to distinct subcellular positions to perform distinct functions? The prediction is that the organelles contain specific proteins required to target and anchor CK1 to the respective organelles. Thus, the axoneme can be used as a model system to define mechanisms by which CK1 may be targeted to the outer doublet microtubules and may involve a common CK1-anchoring protein (CKAP). Two distinct models are shown in Fig.1.

[2] Axonemal CK1 directly interacts with tubulin and directly or indirectly interacts with the I1 proteins IC138 and FAP120. Based on the overall hypothesis, the prediction is that CK1 is localized to the axoneme in precise position by means of the postulated CKAP, and an immediate goal is to identify such a CKAP. The postulated CKAP could also interact with the I1 dynein subunit IC138. The *Chlamydomonas* axoneme, thus, offers opportunities to possibly define a class of proteins that anchor the CK1 family of kinases to the cytoskeleton.

[3] Unregulated axonemal CK1 inhibits dynein-driven microtubule sliding. This advance was made possible by the development of a novel biochemical extraction of axonemal CK1 and functional reconstitution with recombinant CK1 protein combined with an in-vitro microtubule sliding assay. The functional assay is of particular importance since it involves generation of CK1-depleted axonemes to test the specific role of CK1 in absence of a CK1-null *Chlamydomonas* mutant. Based on these data, as well as supporting pharmacological and biochemical evidence, the model is that CK1 phosphorylates IC138, presumably in a highly localized manner on one or few of the nine outer doublets, thereby inhibiting dynein-driven microtubule sliding locally. Immediate goals include: identification of key phospho-residues in IC138 that are phosphorylated by CK1; identification of "upstream" mechanical or chemical signals that regulate CK1 activity (discussed below); and to test the role of CK1 in normal ciliary motility. Each of the above mentioned goals can be addressed using the *Chlamydomonas* model system and the available array of structural mutants as well as the tools and biochemical reagents developed in this work.

Role of CK1 in normal, wild-type ciliary motility:

Among the major challenges is to determine the role of CK1 in controlling I1 dynein activity in wild-type axonemes. Based on analysis of microtubule sliding and motility in mutant cells that fail to assemble I1 dynein, I1 dynein plays an active role in regulation of motility, possibly by locally inhibiting microtubule sliding by other dyneins (Kotani *et al.*, 2007). The current model is that in wild-type axonemes, I1 dynein is locally regulated, that is regulated on single or a small subset of doublet microtubules, in response to chemical or mechanical signals that, presumably, originate at the central pair, and are directed to specific outer doublets by the radial spokes (Fig. 2; reviewed in Wirschell *et al.*, 2007). This prediction is founded on the structural asymmetry inherent to the central pair apparatus, discussed in Chapter 1, and the requirement for central pair and radial spoke assembly and a functional link to I1 dynein (Smith and Yang, 2004; Wirschell *et al.*, 2007). The idea is that an asymmetric signal from one of the central pair microtubules and its associated proteins is transmitted via the radial spokes to the outer doublets. These signals presumably are mediated by CK1, the phosphorylation state of IC138, and consequent changes in I1 dynein activity and microtubule sliding. Predictably, such local changes in microtubule sliding, on one side of an axonemal axis must alter the pattern of bending (Fig. 2).

What is the nature of the "upstream" signals that regulate CK1 activity on each outer doublet for normal wild-type motility? Based on functional data, calcium is a key regulator of the size and shape of the ciliary bend and that calcium alters axonemal bends by direct interaction with axonemal calcium binding proteins (Yang *et al.*, 2001; Smith, 2002; Yang *et al.*, 2004; Wargo *et al.*, 2005). For example, reactivated motility in isolated

axonemes is altered by change in calcium concentration in buffers (Kamiya and Witman, 1984). Furthermore, failure in assembly of the central pair results in inhibition of dynein driven microtubule sliding, but can be rescued by change in calcium concentration (Smith, 2002). Thus, one idea is that calcium signals transmitted from the central pair impinge on single outer doublets to regulate CK1 activity on individual outer doublets. Consistent with this data, calcium binding proteins as well as calcium sensors form an integral part of the central pair apparatus (Yang *et al.*, 2001; Smith, 2002; Yang *et al.*, 2004; Wargo *et al.*, 2005; Dymek and Smith, 2007). One immediate test of this hypothesis is to perform in-vitro functional assays, as described in Chapter 4, with various concentrations of calcium. For example, Smith et al., (2002) have demonstrated in *pf18* axonemes that lack the central pair apparatus, calcium rescues dynein-driven microtubule sliding. Similarly, the CK1 inhibitor DRB also rescues microtubule sliding in *pf18,* and this rescue requires I1 dynein assembly. Therefore, the prediction is that if calcium regulates CK1 activity, calcium will not rescue sliding activity in *pf18* axonemes depleted of CK1. Further, when CK1 is reconstituted with the CK1-depleted *pf18* axonemes, calcium should again rescue microtubule sliding in an I1-dependent manner. These experiments would, for the first time, demonstrate a link between the central pair, CK1 and I1 dynein.

How does the radial spoke regulate CK1 kinase activity on the outer doublet microtubules in wild-type axonemes? The current model is that in absence of radial spokes, CK1 activity is uniformly misregulated, leading to a global inhibition of dynein activity. Consistent with this interpretation, suppressor mutants that rescued motility in radial spoke mutants resulted in a global inhibition of dyneins (Huang *et al.*, 1982). The

idea is that in the absence of radial spokes (or central pairs), the "default" state is dynein inhibition. Predictably, inhibition results from failure in regulation of CK1. Thus for normal motility, the central pair-radial spoke system operates in part to regulate CK1 and provides a permissive "on" state for activation of dyneins.

In addition, one possibility for controlled bending is that radial spokes also generate a structural strain on the axonemal structure that results in displacement of CK1 away from its substrate, IC138, resulting in activation of I1 dynein. Thus, my model is that CK1 kinase activity, in the axoneme, is regulated by its proximity to its substrate. Alternately, the radial spokes may also anchor signaling proteins that in turn regulate CK1 activity. For example, Rsp3, a radial spoke protein, has been identified as an A-kinase-anchoring protein (AKAP; Gaillard *et al.*, 2001; Gaillard *et al.*, 2006). Therefore, predictably, the axonemal PKA is anchored to Rsp3. One possibility therefore is that PKA regulates CK1 activity in wild-type axonemes by either direct control of CK1 or indirect control by pre-phosphorylating IC138 (see below). However, the axonemal PKA is yet to be cloned and characterized, and it is yet to be determined if PKA and CK1 are a part of the same phospho-regulatory pathway or parallel signaling pathways. The current challenge is to develop optical and functional approaches to test the idea that structural and physical strain between the radial spokes and outer doublets controls CK1 activity in wild-type axonemes. We do not yet have the molecular or structural detail required for designing such experiments.

Little is known about how the CK1 kinase activity is regulated. It has previously been shown that the CK1 substrate needs to be pre-phosphorylated for CK1 to phosphorylate the same substrate (Flotow *et al.*, 1990; Meggio *et al.*, 1991). This

requirement for "priming" phosphorylation puts CK1 in a signaling pathway that includes other kinases such as the axonemal PKA (Howard *et al.*, 1994; Gaillard *et al.*, 2006).

Another mechanism of CK1 activity regulation involves inhibitory phosphorylation. For example the C-terminal domain of CK1ε contains a C-terminal sequence, that when phosphorylated, renders CK1 inactive (Cegielska *et al.*, 1998) . This autoinhibition is possibly due to interaction of the phosphorylated C-terminus peptide with the substrate binding domain in CK1 and dephosphorylation by an associated protein phosphatase relieves this inhibition (Gietzen and Virshup, 1999; Swiatek *et al.*, 2004). Perhaps axonemal CK1 is also regulated in an analogous manner by the inherent axonemal phosphatase PP2A. This is an attractive model for CK1 regulation, which together with specific targeting and subcellular localization of CK1 could ensure tight control. The prediction is that CK1 is targeted and anchored near its strate by means of specific anchoring proteins and such an anchoring protein has been identified in the centrosome (Sillibourne *et al.*, 2002). Thus, an important goal is to identify the predicted axonemal CKAP and potentially define mechanisms for trafficking and targeting CK1 to the cytoskeleton (Fig. 1).

Related challenges include determining how changes in IC138 alter I1 dynein activity and control microtubule sliding and to directly test how IC138 controls ciliary bending. Direct tests for how IC138 phosphorylation regulates I1 dynein require a mutagenic approach. Based on published and unpublished data (Gokhale, Fox and Sale; Boesger *et al.*, 2009), we now have candidate serine and threonine residues in IC138 that are phosphorylated by CK1. Thus, one of the immediate projects is to create point mutations in IC138 genomic DNA, transforming the IC138 null strains (see table 2,

Chapter 1) and then examine the motility and phototaxis phenotypes in the mutants. Microtubule sliding assays can also be used to test models for I1 dynein regulation in the new IC138 mutants. Additionally, to directly test the role of CK1 on ciliary motility we can transform wild-type axonemes with a "kinase-dead" CK1 with the assumption that the transformed CK1-KD will assemble in the axoneme and perform as a dominant negative. The prediction is that transformants with CK1-KD will display defects in phototaxis and thus control of flagellar waveform. This dominant-negative technique has been used to characterize the function of dynein light chain LC1, a regulator of the outer dynein arms (Patel-King and King, 2009).

pf27 reveals a new regulatory pathway:

Although, the CP/RS/I1/CK1 phospho-regulatory pathway is of particular importance to the Sale lab, it is likely that alternate parallel pathways also play a role in controlling the size and shape of the bend. As a part of this study, and mapping analysis of the CK1 gene revealed an interesting *Chlamydomonas* mutant *pf27. pf27* is a paralyzed *Chlamydomonas* mutant, defective in both assembly of certain radial spoke components and phosphorylation of specific spoke proteins (RSP 2, 3, 5, 13, 17; Huang *et al.*, 1981). However, it has been determined that *pf27* is not a mutant in any known radial spoke structural protein. Thus, the gene product for *PF27* could affect or control a phosphorylation step.

I postulated that *pf27* is defective in the CK1 gene; however, my analysis of *pf27* axonemes revealed that CK1 is assembled in the axonemes (Fig. 3) and that CK1 is not mutated in the *pf27* cells. Surprisingly, functional analysis of *pf27* axonemes using the in-

vitro microtubule sliding assay revealed that, although the *pf27* axonemes are paralyzed and lack many of the radial spoke components, they still undergo sliding at wild-type velocities (Fig. 4). This is the first instance where a paralyzed flagellar, radial spoke mutant has shown no defect in dynein-driven microtubule sliding. Furthermore, and most striking, analysis of IC138, the key regulatory phospho-protein, revealed that it is hyperphosphorylated, a feature consistent with other radial spoke defective mutants (*pf17)* that correlates with inhibition of microtubule sliding (Fig. 5). This is the only instance where a mutant with hyperphosphorylated IC138 displays normal microtubule sliding velocities. Based on our model, hyperphosphorylated IC138 correlates with reduced dynein-driven microtubule sliding. Therefore, one prediction is that *pf27* reveals a novel mechanism that "bypasses" IC138 phospho-regulation, presumably downstream of I1 dynein/IC138 phosphorylation, resulting in normal in-vitro dynein-driven microtubule sliding, in otherwise paralyzed axonemes.

The pathway revealed in *pf27* maybe a parallel pathway, independent of a CK1-dependent mechanism that results in normal dynein-driven microtubule sliding despite radial spoke defects and abnormal phosphorylation of IC138. Key questions include: What is the *PF27* gene and gene product? This is the primary goal and one approach includes transformations with candidate BACs that span the region where *pf27* is mapped. *pf27* is mapped to chromosome 12, flanked by two previously mapped markers separated by ~1,000,000 base pairs (oda9, tub2; Fig. 6A). This region is covered with candidate BAC clones that can be used for transformation to rescue paralysis in the *pf27* strain (Fig. 6B). Once the BAC clone that rescues the paralyzed phenotype is identified, we can then narrow the complementing DNA and identify the *PF27* gene. Questions

include: What is the role of the *PF27* gene product in regulating radial spoke assembly? And, does the *PF27* gene product affect the phosphorylation of IC138 or does Pf27p define an entirely new mechanism that bypasses IC138? I believe that my new data provides the foundation for an outstanding new project that will reveal an additional, conserved regulatory pathway that controls ciliary motility.

Fig.1

Model 1: Verstaile and universal CKAP model

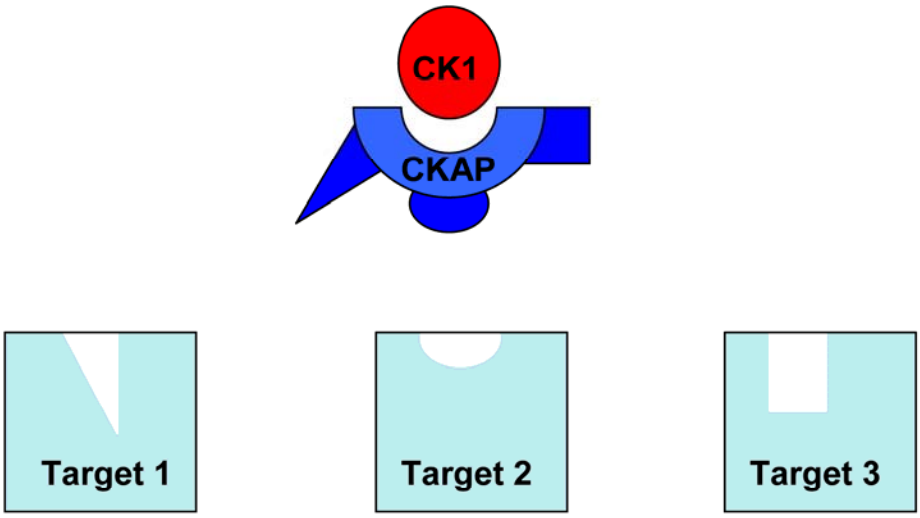

Model 2: AKAP model

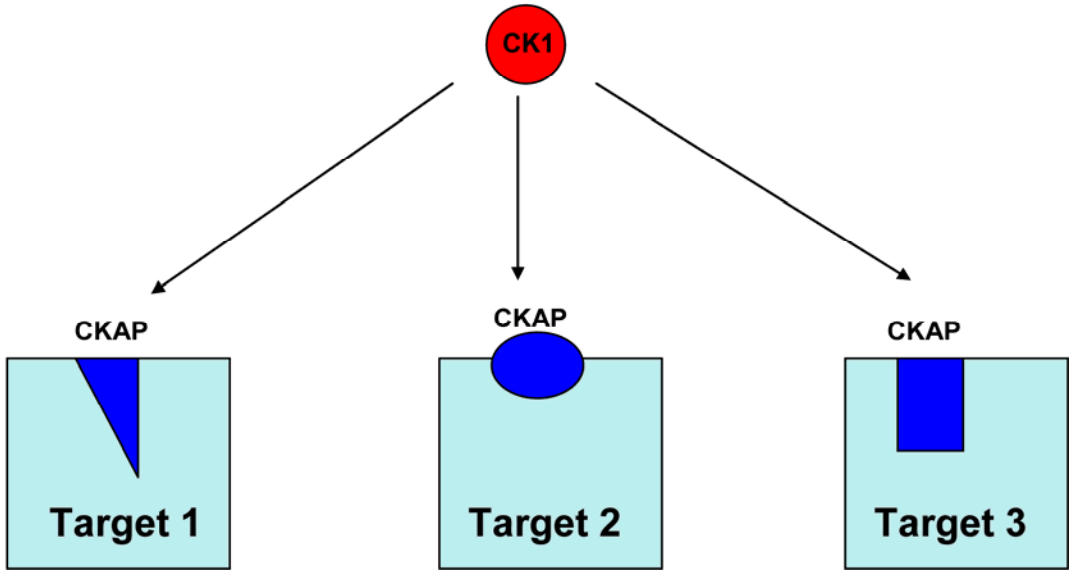

Figure 1: Two models that describe targeting of CK1 to distinct subcellular compartments: Model 1 describes a universal and versatile CK1 anchor (accessory) protein CKAP that contains a common CK1 interacting domain but diverse targeting domains. These targeting domains are target / compartment (e.g. the axoneme) specific. Therefore, the same CKAP can be targeted to different compartments, and anchor CK1 in position to phosphorylate a given, specific substrate such as IC138. Model 2 describes a family of CKAPs (analogous to the AKAP family). Each CKAP is targeted to a distinct compartment by specific domains and anchors CK1 by a common CK1 binding domain (not illustrated here). Therefore, the CKAP anchors CK1 in proximity to its substrate thus regulating CK1 activity.

Fig.2

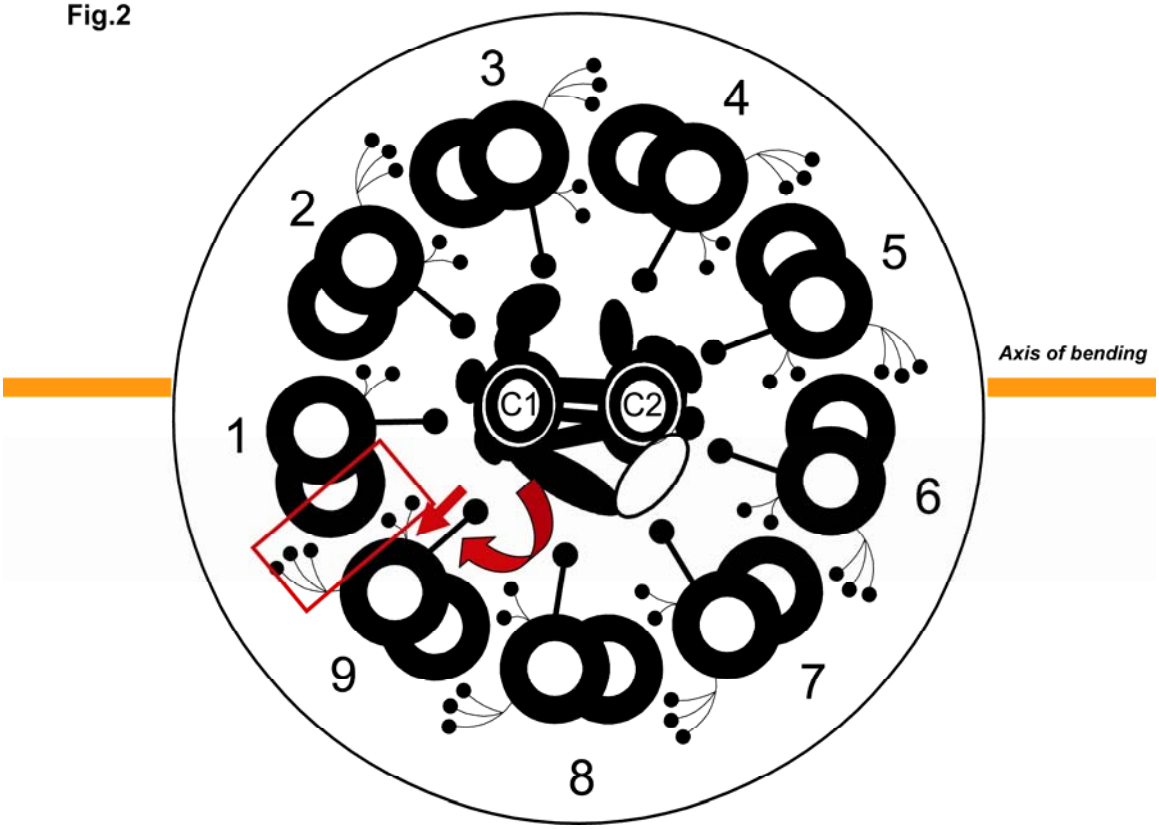

Figure 2: Model for localized regulation of CK1 activity, I1 dynein and axonemal bending: Mechano-chemical signals transmitted from the central pair via the radial spokes, locally regulate CK1 activity on doublet #9. Predictably, IC138 phosphorylation would result in slowed microtubule sliding between doublets #9 and #1 compared to sliding rates between other doublet microtubules. Such a change would result in a change in the size and shape of the bend. Notably, the central pair rotates during the phase of the bend, presumably directly signaling other outer doublet microtubules (Chapter 1). However, we do not know what drives or regulates central pair rotation. Additionally, new data reveal an asymmetry in distribution of the inner dynein arms on the outer doublets (Bui *et al.*, 2009). This important observation may also play a role in control of the direction and the size and shape of the bend.

Fig.3

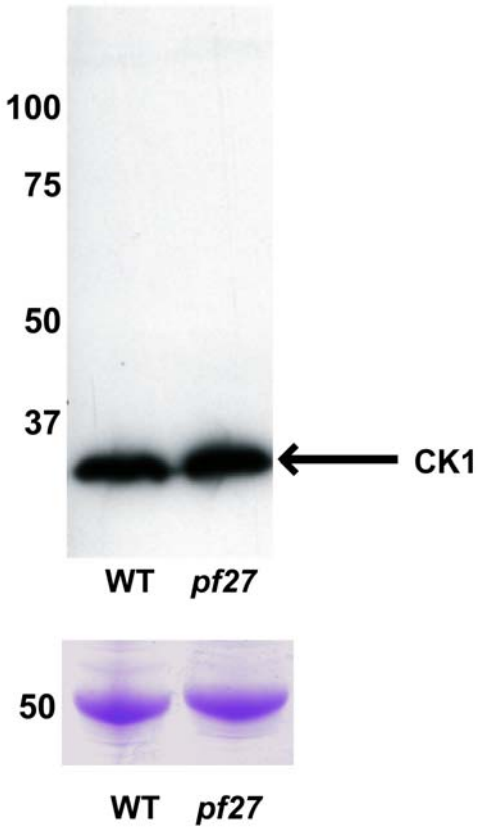

***Figure 3: CK1 is assembled in pf27 axonemes*:** The CK1 antibody identifies a single ~36.5 kD band in isolated axonemes from wild-type and *pf27* axonemes. The coomasie stain (below) shows tubulin as a loading control.

Fig.4

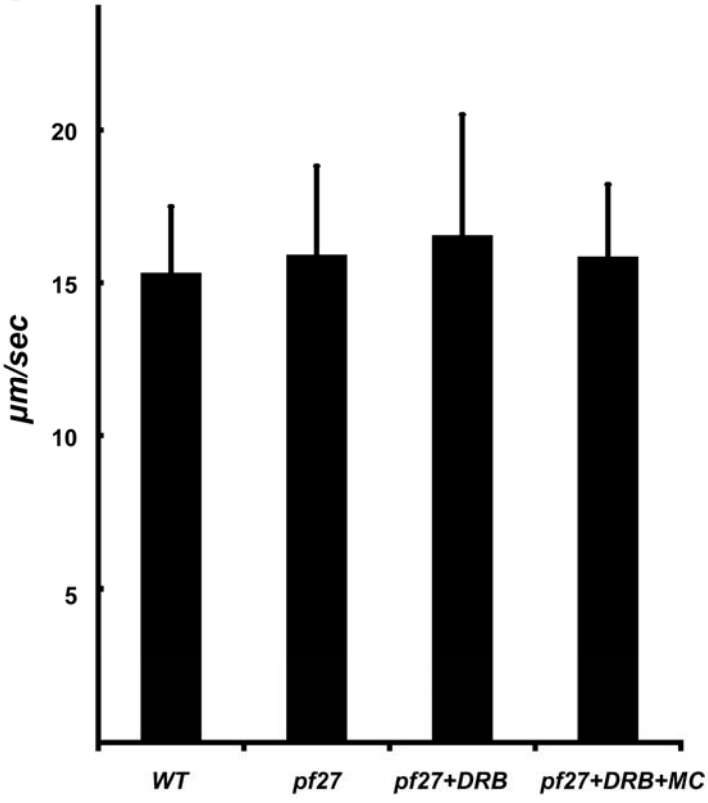

***Figure 4: pf27 axonemes slide at the same rate as wild-type axonemes*:** ATP-induced microtubule sliding velocity was measured in isolated wild-type and *pf27* axonemes. The effect of CK1 inhibitor (DRB) alone and in combination with the phosphatase inhibitor (MC) was also examined. *pf27* axonemes slide at the same rate as wild-type axonemes and the CK1 inhibitor does not have any effect on the rate of microtubule sliding.

Fig.5

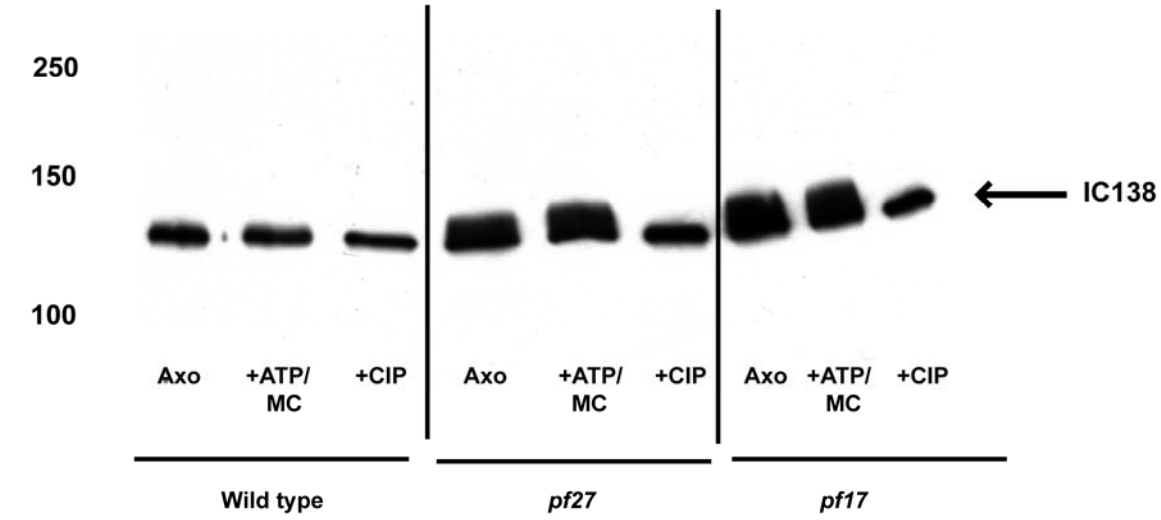
250
150
100
IC138
Axo
+ATP/ MC
+CIP
Axo
+ATP/ MC
+CIP
Axo
+ATP/ MC
+CIP
Wild type
pf27
pf17

***Figure 5: IC138 is abnormally phosphorylated in pf27 axonemes*:** Axonemes were isolated from wild-type, *pf27* and *pf17* strains and either treated with ATP and the phosphatase inhibitor microcystin (MC) or with a phosphatase (calf-intestinal phosphatase CIP). Each of the samples was then probed with the IC138 antibody. Compared to wild-type axonemes, IC138 in *pf27* and *pf17* axonemes is abnormally phosphorylated. This phosphorylated state was relieved by phosphatase treatment.

Fig. 6

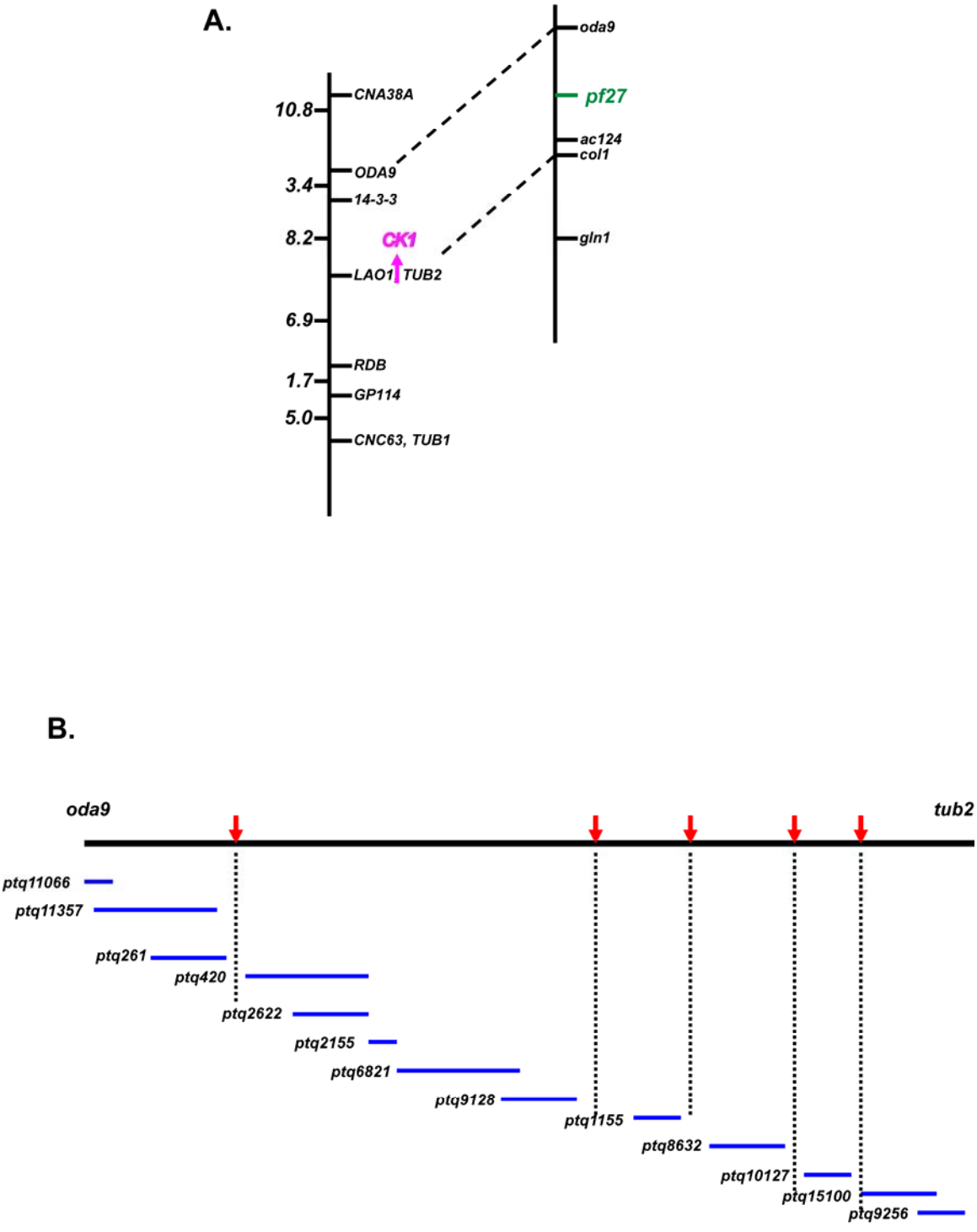
A.
oda9
pf27
ac124
col1
gln1
CNA38A
10.8
ODA9
3.4
14-3-3
8.2
CK1
LAO1
TUB2
6.9
RDB
1.7
GP114
5.0
CNC63, TUB1
B.
oda9
tub2
ptq11066
ptq11357
ptq261
ptq420
ptq2622
ptq2155
ptq6821
ptq9128
ptq1155
ptq8632
ptq10127
ptq15100
ptq9256

Figure 6: Mapping of CK1 and pf27, and strategy for cloning PF27 using BACs and transformation – rescue of pf27: (A) *Chlamydomonas* genes are organized on linkage groups that were originally constructed based on tetrad analysis of crosses between mutants and mapping strains. Molecular advances such as PCR amplification, RFLP analysis and sequencing has led to generation of parallel physical (left) and genetic (right) maps. The genetic map contains the information of the linked genes and the physical map depicts precise physical location of genes characterized to date aligned along the linkage group XII/XIII and chromosome 12. In *Chlamydomonas* BAC libraries have been created that bear most of the genome and in many cases have been mapped within chromosomes. Overlapping BAC clones have been important in generating contigs and therefore, the physical maps. Using a BAC clone that contained the *CK1* gene, I mapped CK1 to linkage group XII/XIII near the previously mapped *Chlamydomonas* mutant *pf27*. The *PF27* gene is not known, and based on the mapping analysis is positioned between the ODA9 and TUB2 markers. (B) Linear diagram of the region between ODA9 and TUB2. The blue lines indicate the various BAC clones that cover the area between the two mapped markers and that may contain the *PF27* gene. The red arrows depict the areas in this region that are not covered by the BAC clones. The idea is to systematically transform *pf27* with BACs until a BAC is found that rescues motility in *pf27*.

References:

1. Adams, G.M., Huang, B., Piperno, G., and Luck, D.J. (1981). Central-pair microtubular complex of *Chlamydomonas* flagella: polypeptide composition as revealed by analysis of mutants. J Cell Biol *91*, 69-76.
2. Ahmed, N.A., and Mitchell, D.R. (2003). *oda*16-1 contains a gene that rescues slow-swimming *Chlamydomonas*. Mol Biol Cell, supplemental *14*, 436a.
3. Ahmed, N.T., C. Gao, B.F. Lucker, D.G. Cole, and D.R. Mitchell. 2008. ODA16 aids axonemal outer row dynein assembly through an interaction with the intraflagellar transport machinery. *J Cell Biol*. 183:313-22.
4. Allocco, J.J., R. Donald, T. Zhong, A. Lee, Y.S. Tang, R.C. Hendrickson, P. Liberator, and B. Nare. 2006. Inhibitors of casein kinase 1 block the growth of Leishmania major promastigotes in vitro. *Int J Parasitol*. 36:1249-59.
5. Ansley, S.J., J.L. Badano, O.E. Blacque, J. Hill, B.E. Hoskins, C.C. Leitch, J.C. Kim, A.J. Ross, E.R. Eichers, T.M. Teslovich, A.K. Mah, R.C. Johnsen, J.C. Cavender, R.A. Lewis, M.R. Leroux, P.L. Beales, and N. Katsanis. 2003. Basal body dysfunction is a likely cause of pleiotropic Bardet-Biedl syndrome. *Nature*. 425:628-33.
6. Aoyama, S., and Kamiya, R. (2005). Cyclical interactions between two outer doublet microtubules in split flagellar axonemes. Biophys J *89*, 3261-3268..
7. Avidor-Reiss, T., Maer, A.M., Koundakjian, E., Polyanovsky, A., Keil, T., Subramaniam, S., and Zuker, C.S. (2004). Decoding cilia function: defining specialized genes required for compartmentalized cilia biogenesis. Cell *117*, 527-539.

8. Badano, J.L., N. Mitsuma, P.L. Beales, and N. Katsanis. 2006. The ciliopathies: an emerging class of human genetic disorders. *Annu Rev Genomics Hum Genet*. 7:125-48.
9. Bannai, H., Yoshimura, M., Takahashi, K., and Shingyoji, C. (2000). Calcium regulation of microtubule sliding in reactivated sea urchin sperm flagella. J Cell Sci *113 (Pt 5)*, 831-839.
10. Basu, B., and Brueckner, M. (2008). Cilia multifunctional organelles at the center of vertebrate left-right asymmetry. Curr Top Dev Biol *85*, 151-174.
11. Behrend, L., M. Stoter, M. Kurth, G. Rutter, J. Heukeshoven, W. Deppert, and U. Knippschild. 2000. Interaction of casein kinase 1 delta (CK1delta) with post-Golgi structures, microtubules and the spindle apparatus. *Eur J Cell Biol*. 79:240-51.
12. Benashski, S.E., and S.M. King. 2000. Investigation of protein-protein interactions within flagellar dynein using homobifunctional and zero-length crosslinking reagents. *Methods*. 22:365-71.
13. Benashski, S.E., Patel-King, R.S., and King, S.M. (1999). Light chain 1 from the *Chlamydomonas* outer dynein arm is a leucine-rich repeat protein associated with the motor domain of the gamma heavy chain. Biochemistry *38*, 7253-7264.
14. Bernstein, M., Beech, P.L., Katz, S.G., and Rosenbaum, J.L. (1994). A new kinesin-like protein (Klp1) localized to a single microtubule of the *Chlamydomonas* flagellum. J Cell Biol *125*, 1313-1326.

15. Besharse, J.C., S.A. Baker, K. Luby-Phelps, and G.J. Pazour. 2003. Photoreceptor intersegmental transport and retinal degeneration: a conserved pathway common to motile and sensory cilia. *Adv Exp Med Biol*. 533:157-64.

16. Bessen, M., Fay, R.B., and Witman, G.B. (1980). Calcium control of waveform in isolated flagellar axonemes of *Chlamydomonas*. J Cell Biol *86*, 446-455

17. Blacque, O.E., M.J. Reardon, C. Li, J. McCarthy, M.R. Mahjoub, S.J. Ansley, J.L. Badano, A.K. Mah, P.L. Beales, W.S. Davidson, R.C. Johnsen, M. Audeh, R.H. Plasterk, D.L. Baillie, N. Katsanis, L.M. Quarmby, S.R. Wicks, and M.R. Leroux. 2004. Loss of C. elegans BBS-7 and BBS-8 protein function results in cilia defects and compromised intraflagellar transport. *Genes Dev*. 18:1630-42.

18. Bloodgood, R.A., Leffler, E.M., and Bojczuk, A.T. (1979). Reversible inhibition of Chlamydomonas flagellar surface motility. J Cell Biol *82*, 664-674.

19. Boesger, J., Wagner, V., Weisheit, W., and Mittag, M. (2009). Analysis of Flagellar Phosphoproteins from *Chlamydomonas reinhardtii* 10.1128/EC.00067-09. Eukaryotic Cell, EC.00067-00009.

20. Bower, R., K. Vanderwaal, E. O'Toole, L. Fox, C. Perrone, J. Mueller, M. Wirschell, R. Kamiya, W.S. Sale, and M.E. Porter. 2009. IC138 Defines a Sub-Domain at the Base of the I1 Dynein That Regulates Microtubule Sliding and Flagellar Motility. *Mol Biol Cell*.

21. Bozkurt, H.H., and Woolley, D.M. (1993). Morphology of nexin links in relation to interdoublet sliding in the sperm flagellum. Cell Motil Cytoskeleton *24*, 109-118.

22. Bre, M.H., V. Redeker, J. Vinh, J. Rossier, and N. Levilliers. 1998. Tubulin polyglycylation: differential posttranslational modification of dynamic cytoplasmic and stable axonemal microtubules in paramecium. *Mol Biol Cell*. 9:2655-65.

23. Brokaw, C.J. (1972). Flagellar movement: a sliding filament model. Science *178*, 455-462.

24. Brokaw, C.J. (1991). Microtubule sliding in swimming sperm flagella: direct and indirect measurements on sea urchin and tunicate spermatozoa. J Cell Biol *114*, 1201-1215.

25. Brokaw, C.J. (1991a). Calcium sensors in sea urchin sperm flagella. Cell Motil Cytoskeleton *18*, 123-130.

26. Brokaw, C.J. (1991b). Microtubule sliding in swimming sperm flagella: direct and indirect measurements on sea urchin and tunicate spermatozoa. J Cell Biol *114*, 1201-1215.

27. Brokaw, C.J. (2009). Thinking about flagellar oscillation. Cell Motil Cytoskeleton *66*, 425-436.

28. Brokaw, C.J., and Kamiya, R. (1987). Bending patterns of Chlamydomonas flagella: IV. Mutants with defects in inner and outer dynein arms indicate differences in dynein arm function. Cell Motil Cytoskeleton *8*, 68-75.

29. Brokaw, C.J., Luck, D.J., and Huang, B. (1982). Analysis of the movement of Chlamydomonas flagella:" the function of the radial-spoke system is revealed by comparison of wild-type and mutant flagella. J Cell Biol *92*, 722-732.

30. Bryja, V., G. Schulte, N. Rawal, A. Grahn, and E. Arenas. 2007. Wnt-5a induces Dishevelled phosphorylation and dopaminergic differentiation via a CK1-dependent mechanism. *J Cell Sci*. 120:586-95.

31. Bui, K.H., Sakakibara, H., Movassagh, T., Oiwa, K., and Ishikawa, T. (2008). Molecular architecture of inner dynein arms in situ in Chlamydomonas reinhardtii flagella. J Cell Biol *5*, 923-932.

32. Bui, K.H., Sakakibara, H., Movassagh, T., Oiwa, K., and Ishikawa, T. (2009). Asymmetry of inner dynein arms and inter-doublet links in Chlamydomonas flagella. J Cell Biol *186*, 437-446.

33. Burgess, S.A., Carter, D.A., Dover, S.D., and Woolley, D.M. (1991a). The inner dynein arm complex: compatible images from freeze-etch and thin section methods of microscopy. J Cell Sci *100 (Pt 2)*, 319-328.

34. Burgess, S.A., Dover, S.D., and Woolley, D.M. (1991b). Architecture of the outer arm dynein ATPase in an avian sperm flagellum, with further evidence for the B-link. J Cell Sci *98 (Pt 1)*, 17-26.

35. Carter, A.P., Garbarino, J.E., Wilson-Kubalek, E.M., Shipley, W.E., Cho, C., Milligan, R.A., Vale, R.D., and Gibbons, I.R. (2008). Structure and functional role of dynein's microtubule-binding domain. Science *322*, 1691-1695.

36. Casey, D.M., Inaba, K., Pazour, G.J., Takada, S., Wakabayashi, K., Wilkerson, C.G., Kamiya, R., and Witman, G.B. (2003a). DC3, the 21-kDa subunit of the outer dynein arm-docking complex (ODA-DC), is a novel EF-hand protein important for assembly of both the outer arm and the ODA-DC. Mol Biol Cell *14*, 3650-3663..

37. Casey, D.M., Yagi, T., Kamiya, R., and Witman, G.B. (2003b). DC3, the Smallest Subunit of the *Chlamydomonas* Flagellar Outer Dynein Arm-docking Complex, Is a Redox-sensitive Calcium-binding Protein. J Biol Chem *278*, 42652-42659.

38. Cegielska, A., Gietzen, K.F., Rivers, A., and Virshup, D.M. (1998). Autoinhibition of casein kinase I epsilon (CKI epsilon) is relieved by protein phosphatases and limited proteolysis. J Biol Chem 273, 1357-1364.

39. Christensen, S.T., Pedersen, L.B., Schneider, L., and Satir, P. (2007). Sensory cilia and integration of signal transduction in human health and disease. Traffic *8*, 97-109.

40. Christensen, S.T., Pedersen, S.F., Satir, P., Veland, I.R., and Schneider, L. (2008). The primary cilium coordinates signaling pathways in cell cycle control and migration during development and tissue repair. Curr Top Dev Biol *85*, 261-301.

41. Colantonio, J.R., Bekker, J.M., Kim, S.J., Morrissey, K.M., Crosbie, R.H., and Hill, K.L. (2006). Expanding the role of the dynein regulatory complex to non-axonemal functions: association of GAS11 with the Golgi apparatus. Traffic *7*, 538-548.

42. Colantonio, J.R., Vermot, J., Wu, D., Langenbacher, A.D., Fraser, S., Chen, J.N., and Hill, K.L. (2009). The dynein regulatory complex is required for ciliary motility and otolith biogenesis in the inner ear. Nature *457*, 205-209.

43. Cole, D.G., Diener, D.R., Himelblau, A.L., Beech, P.L., Fuster, J.C., and Rosenbaum, J.L. (1998). *Chlamydomonas* kinesin-II-dependent intraflagellar transport (IFT): IFT particles contain proteins required for ciliary assembly in *Caenorhabditis elegans* sensory neurons. J Cell Biol *141*, 993-1008.

44. Curry, A.M., and Rosenbaum, J.L. (1993). Flagellar radial spoke: a model molecular genetic system for studying organelle assembly. Cell Motil Cytoskeleton *24*, 224-232.

45. Curry, A.M., Williams, B.D., and Rosenbaum, J.L. (1992). Sequence analysis reveals homology between two proteins of the flagellar radial spoke. Mol Cell Biol *12*, 3967-3977.

46. Dave, D., D. Wloga, N. Sharma, and J. Gaertig. 2009. DYF-1 is required for assembly of the axoneme in Tetrahymena. *Eukaryot Cell*.

47. Dawe, H.R., U.M. Smith, A.R. Cullinane, D. Gerrelli, P. Cox, J.L. Badano, S. Blair-Reid, N. Sriram, N. Katsanis, T. Attie-Bitach, S.C. Afford, A.J. Copp, D.A. Kelly, K. Gull, and C.A. Johnson. 2007. The Meckel-Gruber Syndrome proteins MKS1 and meckelin interact and are required for primary cilium formation. *Hum Mol Genet*. 16:173-86.

48. Dentler, W.L., and Cunningham, W.P. (1977). Structure and organization of radial spokes in cilia of Tetrahymena pyriformis. J Morphol *153*, 143-151.

49. DiBella, L.M., Benashski, S.E., Tedford, H.W., Harrison, A., Patel-King, R.S., and King, S.M. (2001). The Tctex1/Tctex2 class of dynein light chains. Dimerization, differential expression, and interaction with the LC8 protein family. J Biol Chem *276*, 14366-14373.

50. DiBella, L.M., Sakato, M., Patel-King, R.S., Pazour, G.J., and King, S.M. (2004a). The LC7 Light Chains of Chlamydomonas Flagellar Dyneins Interact with Components Required for Both Motor Assembly and Regulation. Mol Biol Cell.

51. DiBella, L.M., Sakato, M., Patel-King, R.S., Pazour, G.J., and King, S.M. (2004). The LC7 Light Chains of Chlamydomonas Flagellar Dyneins Interact with Components Required for Both Motor Assembly and Regulation. Mol Biol Cell.

52. DiBella, L.M., Smith, E.F., Patel-King, R.S., Wakabayashi, K., and King, S.M. (2004b). A novel Tctex2-related light chain is required for stability of inner dynein arm I1 and motor function in the Chlamydomonas flagellum. J Biol Chem *279*, 21666-21676.

53. Diener, D.R., Ang, L.H., and Rosenbaum, J.L. (1993). Assembly of flagellar radial spoke proteins in *Chlamydomonas*: identification of the axoneme binding domain of radial spoke protein 3. J Cell Biol *123*, 183-190.

54. Diener, D.R., Curry, A.M., Johnson, K.A., Williams, B.D., Lefebvre, P.A., Kindle, K.L., and Rosenbaum, J.L. (1990). Rescue of a paralyzed-flagella mutant of *Chlamydomonas* by transformation. Proc Natl Acad Sci U S A *87*, 5739-5743.

55. Dunlap, K. (1977). Localization of calcium channels in Paramecium caudatum. J Physiol *271*, 119-133.

56. Dutcher, S.K. (2000). *Chlamydomonas reinhardtii:* biological rationale for genomics. J Eukaryot Microbiol *47*, 340-349.

57. Dutcher, S.K. (2003). Elucidation of basal body and centriole functions in *Chlamydomonas reinhardtii*. Traffic *4*, 443-451.

58. Dutcher, S.K. 1995. Flagellar assembly in two hundred and fifty easy-to-follow steps. *Trends Genet*. 11:398-404.

59. Dutcher, S.K., Huang, B., and Luck, D.J. (1984). Genetic dissection of the central pair microtubules of the flagella of *Chlamydomonas reinhardtii*. J Cell Biol *98*, 229-236.

60. Dymek, E.E., and Smith, E.F. (2007). A conserved CaM- and radial spoke associated complex mediates regulation of flagellar dynein activity. J Cell Biol *179*, 515-526.

61. Dymek, E.E., Lefebvre, P.A., and Smith, E.F. (2004). PF15p is the chlamydomonas homologue of the Katanin p80 subunit and is required for assembly of flagellar central microtubules. Eukaryot Cell *3*, 870-879.

62. Ebersold, W.T. (1967). *Chlamydomonas reinhardi*: heterozygous diploid strains. Science *157*, 447-449.

63. Eggenschwiler, J.T., and Anderson, K.V. (2007). Cilia and developmental signaling. Annu Rev Cell Dev Biol *23*, 345-373.

64. Flotow, H., Graves, P.R., Wang, A.Q., Fiol, C.J., Roeske, R.W., and Roach, P.J. (1990). Phosphate groups as substrate determinants for casein kinase I action. J Biol Chem 265, 14264-14269.

65. Fowkes, M.E., and Mitchell, D.R. (1998). The role of preassembled cytoplasmic complexes in assembly of flagellar dynein subunits. Mol Biol Cell *9*, 2337-2347.

66. Fox, L.A., and Sale, W.S. (1987). Direction of force generated by the inner row of dynein arms on flagellar microtubules. J Cell Biol *105*, 1781-1787.

67. Freshour, J., R. Yokoyama, and D.R. Mitchell. 2007. Chlamydomonas flagellar outer row dynein assembly protein ODA7 interacts with both outer row and I1 inner row dyneins. *J Biol Chem*. 282:5404-12.

68. Fu, Z., T. Chakraborti, S. Morse, G.S. Bennett, and G. Shaw. 2001. Four casein kinase I isoforms are differentially partitioned between nucleus and cytoplasm. *Exp Cell Res*. 269:275-86.

69. Gaillard, A.R., Diener, D.R., Rosenbaum, J.L., and Sale, W.S. (2001). Flagellar radial spoke protein 3 is an A-kinase anchoring protein (AKAP). J Cell Biol *153*, 443-448.

70. Gaillard, A.R., Fox, L.A., Rhea, J.M., Craige, B., and Sale, W.S. (2006). Disruption of the A-kinase anchoring domain in flagellar radial spoke protein 3 results in unregulated axonemal cAMP-dependent protein kinase activity and abnormal flagellar motility. Mol Biol Cell *17*, 2626-2635.

71. Gao, Z.H., Seeling, J.M., Hill, V., Yochum, A., and Virshup, D.M. (2002). Casein kinase I phosphorylates and destabilizes the beta-catenin degradation complex. Proc Natl Acad Sci U S A *99*, 1182-1187.

72. Gardner, L.C., O'Toole, E., Perrone, C.A., Giddings, T., and Porter, M.E. 1994. Components of a "dynein regulatory complex" are located at the junction between the radial spokes and the dynein arms in *Chlamydomonas* flagella. *J. Cell Biol*. 127:1311-1325.

73. Gennerich, A., and Vale, R.D. (2009). Walking the walk: how kinesin and dynein coordinate their steps. Curr Opin Cell Biol *21*, 59-67.

74. Gerdes, J.M., Davis, E.E., and Katsanis, N. (2009). The vertebrate primary cilium in development, homeostasis, and disease. Cell *137*, 32-45.

75. Gibbons, B.H., and Gibbons, I.R. (1972). Flagellar movement and adenosine triphosphatase activity in sea urchin sperm extracted with triton X-100. J Cell Biol *54*, 75-97.

76. Gibbons, I.R. (1963). Studies on the Protein Components of Cilia from Tetrahymena Pyriformis. Proc Natl Acad Sci U S A *50*, 1002-1010.

77. Gibbons, I.R., and Rowe, A.J. (1965). Dynein: A Protein with Adenosine Triphosphatase Activity from Cilia. Science *149*, 424-426.

78. Gietzen, K.F., and Virshup, D.M. (1999). Identification of inhibitory autophosphorylation sites in casein kinase I epsilon. J Biol Chem 274, 32063-32070

79. Gilula, N.B., and Satir, P. (1972). The ciliary necklace. A ciliary membrane specialization. J Cell Biol *53*, 494-509.

80. Gokhale, A., Wirschell, M., and Sale, W.S. (2009). Regulation of dynein-driven microtubule sliding by the axonemal protein kinase CK1 in Chlamydomonas flagella. J Cell Biol.

81. Goodenough, U.W. (1989). Cilia, flagella and the basal apparatus. Curr Opin Cell Biol *1*, 58-62.

82. Goodenough, U.W., and Heuser, J.E. (1982). Substructure of the outer dynein arm. J Cell Biol *95*, 798-815.

83. Goodenough, U.W., and Heuser, J.E. (1985). Substructure of inner dynein arms, radial spokes, and the central pair/projection complex of cilia and flagella. J Cell Biol *100*, 2008-2018.

84. Goodenough, U.W., and J.E. Heuser. 1985a. Outer and inner dynein arms of cilia and flagella. *Cell*. 41:341-2.

85. Goodenough, U.W., and StClair, H.S. (1975). BALD-2: a mutation affecting the formation of doublet and triplet sets of microtubules in *Chlamydomonas reinhardtii*. J Cell Biol *66*, 480-491.

86. Gross, S.D., and R.A. Anderson. 1998. Casein kinase I: spatial organization and positioning of a multifunctional protein kinase family. *Cell Signal*. 10:699-711.

87. Habermacher, G., and Sale, W.S. (1995). Regulation of dynein-driven microtubule sliding by an axonemal kinase and phosphatase in Chlamydomonas flagella. Cell Motil Cytoskeleton *32*, 106-109.

88. Habermacher, G., and Sale, W.S. (1996). Regulation of flagellar dynein by an axonemal type-1 phosphatase in *Chlamydomonas*. J Cell Sci *109 (Pt 7)*, 1899-1907.

89. Habermacher, G., and Sale, W.S. (1997). Regulation of flagellar dynein by phosphorylation of a 138-kD inner arm dynein intermediate chain. J Cell Biol *136*, 167-176.

90. Hanger, D.P., H.L. Byers, S. Wray, K.Y. Leung, M.J. Saxton, A. Seereeram, C.H. Reynolds, M.A. Ward, and B.H. Anderton. 2007. Novel phosphorylation sites in tau from Alzheimer brain support a role for casein kinase 1 in disease pathogenesis. *J Biol Chem*. 282:23645-54.

91. Harris, E.H. (2009). *Chlamydomonas* in the *Laboratory* In: The *Chlamydomonas* Sourcebook: Introduction to *Chlamydomonas* and Its Laboratory Use, vol. 1, ed. E.H. Harris, Oxford: Academic Press, 241-308.

92. Harrison, A., Olds-Clarke, P., and King, S.M. (1998). Identification of the t complex-encoded cytoplasmic dynein light chain tctex1 in inner arm I1 supports the involvement of flagellar dyneins in meiotic drive. J Cell Biol *140*, 1137-1147.

93. Hathaway, G.M., P.T. Tuazon, and J.A. Traugh. 1983. Casein kinase I. *Methods Enzymol*. 99:308-17.

94. Hayashi, S., and Shingyoji, C. (2008). Mechanism of flagellar oscillation-bending-induced switching of dynein activity in elastase-treated axonemes of sea urchin sperm. J Cell Sci *121*, 2833-2843.

95. Hayashi, S., and Shingyoji, C. (2009). Bending-induced switching of dynein activity in elastase-treated axonemes of sea urchin sperm--roles of Ca2+ and ADP. Cell Motil Cytoskeleton *66*, 292-301.

96. Hayashibe, K., Shingyoji, C., and Kamiya, R. (1997). Induction of temporary beating in paralyzed flagella of Chlamydomonas mutants by application of external force. Cell Motil Cytoskeleton *37*, 232-239.

97. Hendrickson, T.W., C.A. Perrone, P. Griffin, K. Wuichet, J. Mueller, P. Yang, M.E. Porter, and W.S. Sale. 2004. IC138 is a WD-repeat Dynein Intermediate Chain Required for Light Chain Assembly and Regulation of Flagellar Bending. *Mol Biol Cell*. 12:5431-5442.

98. Hildebrandt, F., and W. Zhou. 2007. Nephronophthisis-associated ciliopathies. *J Am Soc Nephrol*. 18:1855-71.

99. Hiraki, M., Nakazawa, Y., Kamiya, R., and Hirono, M. (2007). Bld10p constitutes the cartwheel-spoke tip and stabilizes the 9-fold symmetry of the centriole. Curr Biol *17*, 1778-1783.

100. Hook, P., and Vallee, R.B. (2006). The dynein family at a glance. J Cell Sci *119*, 4369-4371.

101. Hoops, H.J., and Witman, G.B. (1983). Outer doublet heterogeneity reveals structural polarity related to beat direction in *Chlamydomonas* flagella. J Cell Biol *97*, 902-908.

102. Hou, Y., Qin, H., Follit, J.A., Pazour, G.J., Rosenbaum, J.L., and Witman, G.B. (2007). Functional analysis of an individual IFT protein: IFT46 is required for transport of outer dynein arms into flagella. J Cell Biol *176*, 653-665.

103. Howard, D.R., G. Habermacher, D.B. Glass, E.F. Smith, and W.S. Sale. 1994. Regulation of *Chlamydomonas* flagellar dynein by an axonemal protein kinase. *J Cell Biol*. 127:1683-92.

104. Howard, D.R., Habermacher, G., Glass, D.B., Smith, E.F., and Sale, W.S. (1994). Regulation of *Chlamydomonas* flagellar dynein by an axonemal protein kinase. J Cell Biol *127*, 1683-1692.

105. Huang, B., Piperno, G., and Luck, D.J. (1979). Paralyzed flagella mutants of *Chlamydomonas reinhardtii.* Defective for axonemal doublet microtubule arms. J Biol Chem *254*, 3091-3099.

106. Huang, B., Piperno, G., Ramanis, Z., and Luck, D.J. (1981). Radial spokes of *Chlamydomonas* flagella: genetic analysis of assembly and function. J Cell Biol *88*, 80-88.

107. Huang, B., Ramanis, Z., and Luck, D.J. (1982). Suppressor mutations in *Chlamydomonas* reveal a regulatory mechanism for Flagellar function. Cell *28*, 115-124.

108. Ikeda, K., R. Yamamoto, M. Wirschell, T. Yagi, R. Bower, M.E. Porter, W.S. Sale, and R. Kamiya. 2009. A novel ankyrin-repeat protein interacts with the regulatory proteins of inner arm dynein f (I1) of Chlamydomonas reinhardtii. *Cell Motil Cytoskeleton*:epub ahead of print.

109. Insinna, C., Pathak, N., Perkins, B., Drummond, I., and Besharse, J.C. (2008). The homodimeric kinesin, Kif17, is essential for vertebrate photoreceptor sensory outer segment development. Dev Biol *316*, 160-170.

110. Iomini, C., Li, L., Mo, W., Dutcher, S.K., and Piperno, G. (2006). Two flagellar genes, AGG2 and AGG3, mediate orientation to light in Chlamydomonas. Curr Biol *16*, 1147-1153.

111. Ishikawa, T., H. Sakakibara, and K. Oiwa. 2007. The architecture of outer dynein arms in situ. *J Mol Biol*. 368:1249-58.

112. Johnson, K.A., and Wall, J.S. (1983). Structure and molecular weight of the dynein ATPase. J Cell Biol *96*, 669-678.

113. Joy, T., H. Cao, G. Black, R. Malik, V. Charlton-Menys, R.A. Hegele, and P.N. Durrington. 2007. Alstrom syndrome (OMIM 203800): a case report and literature review. *Orphanet J Rare Dis*. 2:49.

114. Kagami, O., and Kamiya, R. (1995). Separation of dynein species by high-pressure liquid chromatography. Methods Cell Biol *47*, 487-489.

115. Kagami, O., Takada, S., and Kamiya, R. (1990). Microtubule translocation caused by three subspecies of inner-arm dynein from Chlamydomonas flagella. FEBS Lett *264*, 179-182.

116. Kameshita, I., and H. Fujisawa. 1989. A sensitive method for detection of calmodulin-dependent protein kinase II activity in sodium dodecyl sulfate-polyacrylamide gel. *Anal Biochem*. 183:139-43.

117. Kamiya, R. (1988). Mutations at twelve independent loci result in absence of outer dynein arms in *Chlamydomonas reinhardtii*. J Cell Biol *107*, 2253-2258.

118. Kamiya, R. (2002). Functional diversity of axonemal dyneins as studied in *Chlamydomonas* mutants. Int Rev Cytol *219*, 115-155.

119. Kamiya, R., and Okamoto, M. (1985). A mutant of *Chlamydomonas reinhardtii* that lacks the flagellar outer dynein arm but can swim. J Cell Sci *74*, 181-191.

120. Kamiya, R., and Witman, G.B. (1984). Submicromolar levels of calcium control the balance of beating between the two flagella in demembranated models of *Chlamydomonas*. J Cell Biol *98*, 97-107.

121. Kamiya, R., Kurimoto, E., and Muto, E. (1991). Two types of *Chlamydomonas* flagellar mutants missing different components of inner-arm dynein. J Cell Biol *112*, 441-447.

122. Karki, S., and Holzbaur, E.L. (1999). Cytoplasmic dynein and dynactin in cell division and intracellular transport. Curr Opin Cell Biol *11*, 45-53.

123. Kathir, P., M. LaVoie, W.J. Brazelton, N.A. Haas, P.A. Lefebvre, and C.D. Silflow. 2003. Molecular Map of the *Chlamydomonas reinhardtii* Nuclear Genome. *Eukaryot Cell*. 2:362-79.

124. Kato, T., Kagami, O., Yagi, T., and Kamiya, R. (1993). Isolation of two species of *Chlamydomonas reinhardtii* flagellar mutants, *ida*5 and *ida*6, that lack a newly identified heavy chain of the inner dynein arm. Cell Struct Funct *18*, 371-377.

125. King, S.J., and Dutcher, S.K. (1997). Phosphoregulation of an inner dynein arm complex in Chlamydomonas reinhardtii is altered in phototactic mutant strains. J Cell Biol *136*, 177-191.

126. King, S.J., Inwood, W.B., O'Toole, E.T., Power, J., and Dutcher, S.K. (1994). The bop2-1 mutation reveals radial asymmetry in the inner dynein arm region of *Chlamydomonas reinhardtii*. J Cell Biol *126*, 1255-1266.

127. King, S.M., and Kamiya, R. (2009). Axonemal Dyneins: Assembly, Structure, and Force Generation. In: The *Chlamydomonas* Sourcebook: Cell Motility and Behavior, vol. 3, ed. G.B. Witman, Oxford: Academic Press, 131-208.

128. King, S.M., and Patel-King, R.S. (1995). The M(r) = 8,000 and 11,000 outer arm dynein light chains from *Chlamydomonas* flagella have cytoplasmic homologues. J Biol Chem *270*, 11445-11452.

129. King, S.M., Wilkerson, C.G., and Witman, G.B. (1991). The Mr 78,000 intermediate chain of *Chlamydomonas* outer arm dynein interacts with alpha-tubulin *in situ*. J Biol Chem *266*, 8401-8407.

130. Knippschild, U., A. Gocht, S. Wolff, N. Huber, J. Lohler, and M. Stoter. 2005. The casein kinase 1 family: participation in multiple cellular processes in eukaryotes. *Cell Signal*. 17:675-89.

131. Kon, T., Imamula, K., Roberts, A.J., Ohkura, R., Knight, P.J., Gibbons, I.R., Burgess, S.A., and Sutoh, K. (2009). Helix sliding in the stalk coiled coil of dynein couples ATPase and microtubule binding. Nat Struct Mol Biol *16*, 325-333.

132. Kotani, N., Sakakibara, H., Burgess, S.A., Kojima, H., and Oiwa, K. (2007). Mechanical properties of inner-arm dynein-f (dynein I1) studied with in vitro motility assays. Biophys J *93*, 886-894.

133. Koutoulis, A., G.J. Pazour, C.G. Wilkerson, K. Inaba, H. Sheng, S. Takada, and G.B. Witman. 1997. The *Chlamydomonas reinhardtii ODA*3 gene encodes a protein of the outer dynein arm docking complex. *J Cell Biol*. 137:1069-80.

134. Kuret, J., G.S. Johnson, D. Cha, E.R. Christenson, A.J. DeMaggio, and M.F. Hoekstra. 1997. Casein kinase 1 is tightly associated with paired-helical filaments isolated from Alzheimer's disease brain. *J Neurochem*. 69:2506-15.

135. Lechtreck, K.F., and S. Geimer. 2000. Distribution of polyglutamylated tubulin in the flagellar apparatus of green flagellates. *Cell Motil Cytoskeleton*. 47:219-35.

136. Lechtreck, K.F., and Witman, G.B. (2007). Chlamydomonas reinhardtii hydin is a central pair protein required for flagellar motility. J Cell Biol *176*, 473-482.

137. Lechtreck, K.F., Delmotte, P., Robinson, M.L., Sanderson, M.J., and Witman, G.B. (2008). Mutations in Hydin impair ciliary motility in mice. J Cell Biol *180*, 633-643.

138. Lefebvre, P.A., and C.D. Silflow. 1999. *Chlamydomonas*: the cell and its genomes. *Genetics*. 151:9-14.

139. L'Hernault, S.W., and J.L. Rosenbaum. 1983. Chlamydomonas alpha-tubulin is posttranslationally modified in the flagella during flagellar assembly. *J Cell Biol*. 97:258-63.

140. Li, G., H. Yin, and J. Kuret. 2004. Casein kinase 1 delta phosphorylates tau and disrupts its binding to microtubules. *J Biol Chem*. 279:15938-45.

141. Li, J.B., Gerdes, J.M., Haycraft, C.J., Fan, Y., Teslovich, T.M., May-Simera, H., Li, H., Blacque, O.E., Li, L., Leitch, C.C., Lewis, R.A., Green, J.S., Parfrey, P.S., Leroux, M.R., Davidson, W.S., Beales, P.L., Guay-Woodford, L.M., Yoder, B.K., Stormo, G.D., Katsanis, N., and Dutcher, S.K. (2004). Comparative genomics identifies a flagellar and basal body proteome that includes the BBS5 human disease gene. Cell *117*, 541-552.

142. Li, J.B., Lin, S., Jia, H., Wu, H., Roe, B.A., Kulp, D., Stormo, G.D., and Dutcher, S.K. (2003). Analysis of *Chlamydomonas reinhardtii* genome structure using large-scale sequencing of regions on linkage groups I and III. J Eukaryot Microbiol *50*, 145-155.

143. Lindemann, C.B., and Hunt, A.J. (2003). Does axonemal dynein push, pull, or oscillate? Cell Motil Cytoskeleton *56*, 237-244.

144. Lohler, J., H. Hirner, B. Schmidt, K. Kramer, D. Fischer, D.R. Thal, F. Leithauser, and U. Knippschild. 2009. Immunohistochemical characterisation of cell-type specific expression of CK1delta in various tissues of young adult BALB/c mice. *PLoS ONE*. 4:e4174.

145. Luck, D., Piperno, G., Ramanis, Z., and Huang, B. (1977). Flagellar mutants of *Chlamydomonas*: studies of radial spoke-defective strains by dikaryon and revertant analysis. Proc Natl Acad Sci U S A *74*, 3456-3460.

146. Lucker, B.F., R.H. Behal, H. Qin, L.C. Siron, W.D. Taggart, J.L. Rosenbaum, and D.G. Cole. 2005. Characterization of the intraflagellar transport complex B core: direct interaction of the IFT81 and IFT74/72 subunits. *J Biol Chem*. 280:27688-96.

147. Marshall, W.F. (2008a). The cell biological basis of ciliary disease. J Cell Biol *180*, 17-21.

148. Marshall, W.F. (2008b). Basal bodies platforms for building cilia. Curr Top Dev Biol *85*, 1-22.

149. Mastronarde, D.N., O'Toole, E.T., McDonald, K.L., McIntosh, J.R., and Porter, M.E. (1992). Arrangement of inner dynein arms in wild-type and mutant flagella of *Chlamydomonas*. J Cell Biol *118*, 1145-1162.

150. Meggio, F., Perich, J.W., Reynolds, E.C., and Pinna, L.A. (1991). A synthetic beta-casein phosphopeptide and analogues as model substrates for casein kinase-1, a ubiquitous, phosphate directed protein kinase. FEBS Lett 283, 303-306.

151. Merchant, S.S., Prochnik, S.E., Vallon, O., Harris, E.H., Karpowicz, S.J., Witman, G.B., Terry, A., Salamov, A., Fritz-Laylin, L.K., Marechal-Drouard, L., Marshall, W.F., Qu, L.H., Nelson, D.R., Sanderfoot, A.A., Spalding, M.H., Kapitonov, V.V., Ren, Q., Ferris, P., Lindquist, E., Shapiro, H., Lucas, S.M., Grimwood, J., Schmutz, J., Cardol, P., Cerutti, H., Chanfreau, G., Chen, C.L., Cognat, V., Croft, M.T., Dent, R., Dutcher, S., Fernandez, E., Fukuzawa, H., Gonzalez-Ballester, D., Gonzalez-Halphen, D., Hallmann, A., Hanikenne, M., Hippler, M., Inwood, W., Jabbari, K., Kalanon, M., Kuras, R., Lefebvre, P.A., Lemaire, S.D., Lobanov, A.V., Lohr, M., Manuell, A., Meier, I., Mets, L., Mittag, M., Mittelmeier, T., Moroney, J.V., Moseley, J., Napoli, C., Nedelcu, A.M., Niyogi, K., Novoselov, S.V., Paulsen, I.T., Pazour, G., Purton, S., Ral, J.P., Riano-Pachon, D.M., Riekhof, W., Rymarquis, L., Schroda, M., Stern, D., Umen, J., Willows, R., Wilson, N., Zimmer, S.L., Allmer, J., Balk, J., Bisova, K., Chen,

C.J., Elias, M., Gendler, K., Hauser, C., Lamb, M.R., Ledford, H., Long, J.C., Minagawa, J., Page, M.D., Pan, J., Pootakham, W., Roje, S., Rose, A., Stahlberg, E., Terauchi, A.M., Yang, P., Ball, S., Bowler, C., Dieckmann, C.L., Gladyshev, V.N., Green, P., Jorgensen, R., Mayfield, S., Mueller-Roeber, B., Rajamani, S., Sayre, R.T., Brokstein, P., Dubchak, I., Goodstein, D., Hornick, L., Huang, Y.W., Jhaveri, J., Luo, Y., Martinez, D., Ngau, W.C., Otillar, B., Poliakov, A., Porter, A., Szajkowski, L., Werner, G., Zhou, K., Grigoriev, I.V., Rokhsar, D.S., and Grossman, A.R. (2007). The *Chlamydomonas* genome reveals the evolution of key animal and plant functions. Science *318*, 245-250.

152. Million, K., J. Larcher, J. Laoukili, D. Bourguignon, F. Marano, and F. Tournier. 1999. Polyglutamylation and polyglycylation of alpha- and beta-tubulins during in vitro ciliated cell differentiation of human respiratory epithelial cells. *J Cell Sci*. 112 (Pt 23):4357-66.

153. Mitchell, D.R. (2003). Orientation of the central pair complex during flagellar bend formation in Chlamydomonas. Cell Motil Cytoskeleton *56*, 120-129.

154. Mitchell, D.R., and Kang, Y. (1991). Identification of *oda*6 as a *Chlamydomonas* dynein mutant by rescue with the wild-type gene. J Cell Biol *113*, 835-842.

155. Mitchell, D.R., and Rosenbaum, J.L. (1985). A motile *Chlamydomonas* flagellar mutant that lacks outer dynein arms. J Cell Biol *100*, 1228-1234.

156. Mitchell, D.R., and Sale, W.S. (1999). Characterization of a *Chlamydomonas* insertional mutant that disrupts flagellar central pair microtubule-associated structures. J Cell Biol *144*, 293-304.

157. Mitchell, D.R. (2009). The Flagellar Central Pair Apparatus. In: The *Chlamydomonas* Sourcebook: Cell Motility and Behavior, vol. 3, ed. G.B. Witman, Oxford: Academic Press, 235-248.

158. Morita, Y., and Shingyoji, C. (2004). Effects of imposed bending on microtubule sliding in sperm flagella. Curr Biol *14*, 2113-2118.

159. Myster, S.H., Knott, J.A., O'Toole, E., and Porter, M.E. (1997). The Chlamydomonas Dhc1 gene encodes a dynein heavy chain subunit required for assembly of the I1 inner arm complex. Mol Biol Cell *8*, 607-620.

160. Myster, S.H., Knott, J.A., Wysocki, K.M., O'Toole, E., and Porter, M.E. (1999). Domains in the 1alpha dynein heavy chain required for inner arm assembly and flagellar motility in Chlamydomonas. J Cell Biol *146*, 801-818.

161. Nakano, I., Kobayashi, T., Yoshimura, M., and Shingyoji, C. (2003). Central-pair-linked regulation of microtubule sliding by calcium in flagellar axonemes. J Cell Sci *116*, 1627-1636.

162. Nakazawa, Y., Hiraki, M., Kamiya, R., and Hirono, M. (2007). SAS-6 is a cartwheel protein that establishes the 9-fold symmetry of the centriole. Curr Biol *17*, 2169-2174.

163. Nicastro, D., C. Schwartz, J. Pierson, R. Gaudette, M.E. Porter, and J.R. McIntosh. 2006. The molecular architecture of axonemes revealed by cryoelectron tomography. *Science*. 313:944-8.

164. Nicastro, D., McIntosh, J.R., and Baumeister, W. (2005). 3D structure of eukaryotic flagella in a quiescent state revealed by cryo-electron tomography. Proc Natl Acad Sci U S A *102*, 15889-15894.

165. Nonaka, S., S. Yoshiba, D. Watanabe, S. Ikeuchi, T. Goto, W.F. Marshall, and H. Hamada. 2005. De novo formation of left-right asymmetry by posterior tilt of nodal cilia. *PLoS Biol*. 3:e268.

166. Nonaka, S., Y. Tanaka, Y. Okada, S. Takeda, A. Harada, Y. Kanai, M. Kido, and N. Hirokawa. 1998. Randomization of left-right asymmetry due to loss of nodal cilia generating leftward flow of extraembryonic fluid in mice lacking KIF3B motor protein. *Cell*. 95:829-37.

167. Oda, T., Hirokawa, N., and Kikkawa, M. (2007). Three-dimensional structures of the flagellar dynein-microtubule complex by cryoelectron microscopy. J Cell Biol *177*, 243-252.

168. Oiwa, K., and Sakakibara, H. (2005). Recent progress in dynein structure and mechanism. Curr Opin Cell Biol *17*, 98-103.

169. Okagaki, T., and Kamiya, R. (1986). Microtubule sliding in mutant *Chlamydomonas* axonemes devoid of outer or inner dynein arms. J Cell Biol *103*, 1895-1902.

170. Okita, N., Isogai, N., Hirono, M., Kamiya, R., and Yoshimura, K. (2005). Phototactic activity in Chlamydomonas 'non-phototactic' mutants deficient in Ca2+-dependent control of flagellar dominance or in inner-arm dynein. J Cell Sci *118*, 529-537.

171. Olmsted, J.B. 1981. Affinity purification of antibodies from diazotized paper blots of heterogeneous protein samples. *J Biol Chem*. 256:11955-7.

172. Omori, Y., Zhao, C., Saras, A., Mukhopadhyay, S., Kim, W., Furukawa, T., Sengupta, P., Veraksa, A., and Malicki, J. (2008). Elipsa is an early determinant

of ciliogenesis that links the IFT particle to membrane-associated small GTPase Rab8. Nat Cell Biol *10*, 437-444.

173. Omoto, C.K., and Brokaw, C.J. (1985). Bending patterns of Chlamydomonas flagella: II. Calcium effects on reactivated Chlamydomonas flagella. Cell Motil *5*, 53-60.

174. Omoto, C.K., Gibbons, I.R., Kamiya, R., Shingyoji, C., Takahashi, K., and Witman, G.B. (1999). Rotation of the central pair microtubules in eukaryotic flagella. Mol Biol Cell *10*, 1-4.

175. Omran, H., Kobayashi, D., Olbrich, H., Tsukahara, T., Loges, N., Hagiwara, H., Zhang, Q., Leblond, G., O'Toole, E., Hara, C., Mizuno, H., Kawano, H., Fliegauf, M., Yagi, T., Koshida, S., Miyawaki, A., Zentgraf, H., Seithe, H., Reinhardt, R., Watanabe, Y., Kamiya, R., Mitchell, D., and Takeda, H. (2008). Ktu/PF13 is required for cytoplasmic pre-assembly of axonemal dyneins. Nature *456*, 611-616.

176. O'Toole, E.T., Giddings, T.H., McIntosh, J.R., and Dutcher, S.K. (2003). Three-dimensional organization of basal bodies from wild-type and delta-tubulin deletion strains of Chlamydomonas reinhardtii. Mol Biol Cell *14*, 2999-3012.

177. Otto, E.A., B. Loeys, H. Khanna, J. Hellemans, R. Sudbrak, S. Fan, U. Muerb, J.F. O'Toole, J. Helou, M. Attanasio, B. Utsch, J.A. Sayer, C. Lillo, D. Jimeno, P. Coucke, A. De Paepe, R. Reinhardt, S. Klages, M. Tsuda, I. Kawakami, T. Kusakabe, H. Omran, A. Imm, M. Tippens, P.A. Raymond, J. Hill, P. Beales, S. He, A. Kispert, B. Margolis, D.S. Williams, A. Swaroop, and F. Hildebrandt.

2005. Nephrocystin-5, a ciliary IQ domain protein, is mutated in Senior-Loken syndrome and interacts with RPGR and calmodulin. *Nat Genet*. 37:282-8.

178. Parness, J., and S.B. Horwitz. 1981. Taxol binds to polymerized tubulin in vitro. *J Cell Biol*. 91:479-87.

179. Patel-King, R.S., and King, S.M. (2009). An outer arm dynein light chain acts in a conformational switch for flagellar motility. J Cell Biol *186*, 283-295.

180. Patel-King, R.S., Gorbatyuk, O., Takebe, S., and King, S.M. (2004). Flagellar radial spokes contain a Ca2+-stimulated nucleoside diphosphate kinase. Mol Biol Cell *15*, 3891-3902.

181. Pazour, G.J. 2004. Intraflagellar transport and cilia-dependent renal disease: the ciliary hypothesis of polycystic kidney disease. *J Am Soc Nephrol*. 15:2528-36.

182. Pazour, G.J., Agrin, N., Leszyk, J., and Witman, G.B. (2005). Proteomic analysis of a eukaryotic cilium. J Cell Biol *170*, 103-113.

183. Pazour, G.J., and Witman, G.B. (2000). Forward and reverse genetic analysis of microtubule motors in *Chlamydomonas*. Methods *22*, 285-298.

184. Pazour, G.J., and Witman, G.B. (2009). The *Chlamydomonas* Flagellum as a Model for Human Ciliary Disease. In: The *Chlamydomonas* Sourcebook: Cell Motility and Behavior, vol. 3, ed. G.B. Witman, Oxford: Academic Press, 445-468.

185. Pazour, G.J., Dickert, B.L., Vucica, Y., Seeley, E.S., Rosenbaum, J.L., Witman, G.B., and Cole, D.G. (2000). *Chlamydomonas* IFT88 and its mouse homologue, polycystic kidney disease gene tg737, are required for assembly of cilia and flagella. J Cell Biol *151*, 709-718.

186. Pazour, G.J., San Agustin, J.T., Follit, J.A., Rosenbaum, J.L., and Witman, G.B. (2002). Polycystin-2 localizes to kidney cilia and the ciliary level is elevated in orpk mice with polycystic kidney disease. Curr Biol *12*, R378-380.

187. Pazour, G.J., Sineschekov, O.A., and Witman, G.B. (1995). Mutational analysis of the phototransduction pathway of *Chlamydomonas reinhardtii*. J Cell Biol *131*, 427-440.

188. Pedersen, L.B., Geimer, S., and Rosenbaum, J.L. (2006). Dissecting the molecular mechanisms of intraflagellar transport in chlamydomonas. Curr Biol *16*, 450-459.

189. Perrone, C.A., Myster, S.H., Bower, R., O'Toole, E.T., and Porter, M.E. (2000). Insights into the structural organization of the I1 inner arm dynein from a domain analysis of the 1beta dynein heavy chain. Mol Biol Cell *11*, 2297-2313.

190. Perrone, C.A., Yang, P., O'Toole, E., Sale, W.S., and Porter, M.E. (1998). The Chlamydomonas IDA7 locus encodes a 140-kD dynein intermediate chain required to assemble the I1 inner arm complex. Mol Biol Cell *9*, 3351-3365.

191. Piperno, G. 1990. Functional diversity of dyneins. *Cell Motil Cytoskeleton*. 17:147-9.

192. Piperno, G., and Ramanis, Z. (1991). The proximal portion of *Chlamydomonas* flagella contains a distinct set of inner dynein arms. J Cell Biol *112*, 701-709.

193. Piperno, G., Huang, B., Ramanis, Z., and Luck, D.J. (1981). Radial spokes of *Chlamydomonas* flagella: polypeptide composition and phosphorylation of stalk components. J Cell Biol *88*, 73-79.

194. Piperno, G., Mead, K., and Shestak, W. (1992). The inner dynein arms I2 interact with a "dynein regulatory complex" in *Chlamydomonas* flagella. J Cell Biol *118*, 1455-1463.

195. Piperno, G., Mead, K., LeDizet, M., and Moscatelli, A. (1994). Mutations in the "dynein regulatory complex" alter the ATP-insensitive binding sites for inner arm dyneins in *Chlamydomonas* axonemes. J Cell Biol *125*, 1109-1117.

196. Piperno, G., Ramanis, Z., Smith, E.F., and Sale, W.S. (1990). Three distinct inner dynein arms in *Chlamydomonas* flagella: molecular composition and location in the axoneme. J Cell Biol *110*, 379-389.

197. Piperno, G., Siuda, E., Henderson, S., Segil, M., Vaananen, H., and Sassaroli, M. (1998). Distinct mutants of retrograde intraflagellar transport (IFT) share similar morphological and molecular defects. J Cell Biol *143*, 1591-1601.

198. Piperno, G., Z. Ramanis, E.F. Smith, and W.S. Sale. 1990. Three distinct inner dynein arms in *Chlamydomonas* flagella: molecular composition and location in the axoneme. *J Cell Biol*. 110:379-89.

199. Porter, M.E., and Sale, W.S. (2000). The 9 + 2 axoneme anchors multiple inner arm dyneins and a network of kinases and phosphatases that control motility. J Cell Biol *151*, F37-42.

200. Porter, M.E., Knott, J.A., Gardner, L.C., Mitchell, D.R., and Dutcher, S.K. (1994). Mutations in the SUP-PF-1 locus of *Chlamydomonas reinhardtii* identify a regulatory domain in the beta-dynein heavy chain. J Cell Biol *126*, 1495-1507.

201. Porter, M.E., Power, J., and Dutcher, S.K. (1992). Extragenic suppressors of paralyzed flagellar mutations in *Chlamydomonas reinhardtii* identify loci that alter the inner dynein arms. J Cell Biol *118*, 1163-1176.

202. Quarmby, L. (2009). Ciliary ion channels: location, location, location. Curr Biol *19*, R158-160.

203. Redeker, V., N. Levilliers, E. Vinolo, J. Rossier, D. Jaillard, D. Burnette, J. Gaertig, and M.H. Bre. 2005. Mutations of tubulin glycylation sites reveal cross-talk between the C termini of alpha- and beta-tubulin and affect the ciliary matrix in Tetrahymena. *J Biol Chem*. 280:596-606.

204. Redeker, V., N. Levilliers, J.M. Schmitter, J.P. Le Caer, J. Rossier, A. Adoutte, and M.H. Bre. 1994. Polyglycylation of tubulin: a posttranslational modification in axonemal microtubules. *Science*. 266:1688-91.

205. Roberts, A.J., Numata, N., Walker, M.L., Kato, Y.S., Malkova, B., Kon, T., Ohkura, R., Arisaka, F., Knight, P.J., Sutoh, K., and Burgess, S.A. (2009). AAA+ Ring and linker swing mechanism in the dynein motor. Cell *136*, 485-495.

206. Rolland, N., A. Atteia, P. Decottignies, J. Garin, M. Hippler, G. Kreimer, S.D. Lemaire, M. Mittag, and V. Wagner. 2009. Chlamydomonas proteomics. *Curr Opin Microbiol*. 12:285-91.

207. Rosenbaum, J. (2002). Intraflagellar transport. Curr Biol *12*, R125.

208. Rosenbaum, J. 2000. Cytoskeleton: functions for tubulin modifications at last. *Curr Biol*. 10:R801-3.

209. Rosenbaum, J.L., and G.B. Witman. 2002. Intraflagellar transport. *Nat Rev Mol Cell Biol*. 3:813-25.

210. Rupp, G., and Porter, M.E. (2003). A subunit of the dynein regulatory complex in Chlamydomonas is a homologue of a growth arrest-specific gene product. J Cell Biol *162*, 47-57.

211. Rupp, G., O'Toole, E., and Porter, M.E. (2001). The *Chlamydomonas* PF6 locus encodes a large alanine/proline-rich polypeptide that is required for assembly of a central pair projection and regulates flagellar motility. Mol Biol Cell *12*, 739-751.

212. Rupp, G., O'Toole, E., Gardner, L.C., Mitchell, B.F., and Porter, M.E. (1996). The sup-pf-2 mutations of *Chlamydomonas* alter the activity of the outer dynein arms by modification of the gamma-dynein heavy chain. J Cell Biol *135*, 1853-1865.

213. Sakakibara, H., Mitchell, D.R., and Kamiya, R. (1991). A *Chlamydomonas* outer arm dynein mutant missing the alpha heavy chain. J Cell Biol *113*, 615-622.

214. Sakakibara, H., Takada, S., King, S.M., Witman, G.B., and Kamiya, R. (1993). A *Chlamydomonas* outer arm dynein mutant with a truncated beta heavy chain. J Cell Biol *122*, 653-661.

215. Salathe, M. (2007). Regulation of mammalian ciliary beating. Annu Rev Physiol *69*, 401-422.

216. Sale, W.S., and Satir, P. (1976). Splayed Tetrahymena cilia. A system for analyzing sliding and axonemal spoke arrangements. J Cell Biol *71*, 589-605.

217. Sale, W.S., and Satir, P. (1977). Direction of active sliding of microtubules in Tetrahymena cilia. Proc Natl Acad Sci U S A *74*, 2045-2049.

218. Sale, W.S., Goodenough, U.W., and Heuser, J.E. (1985). The substructure of isolated and in situ outer dynein arms of sea urchin sperm flagella. J Cell Biol *101*, 1400-1412.

219. Saraiva, J.M., and M. Baraitser. 1992. Joubert syndrome: a review. *Am J Med Genet*. 43:726-31.

220. Satir, B., and Rosenbaum, J.L. (1965). The isolation and identification of kinetosome-rich fractions from Tetrahymena pyriformis. J Protozool *12*, 397-405.

221. Satir, P. (1963). Studies on Cilia. The Fixation of the Metachronal Wave. J Cell Biol *18*, 345-365.

222. Satir, P. (1967). Morphological aspects of ciliary motility. J Gen Physiol *50*, Suppl:241-258.

223. Satir, P. (1968). Studies on cilia. 3. Further studies on the cilium tip and a "sliding filament" model of ciliary motility. J Cell Biol *39*, 77-94.

224. Satir, P., and Christensen, S.T. (2007). Overview of structure and function of mammalian cilia. Annu Rev Physiol *69*, 377-400.

225. Satir, P., and Matsuoka, T. (1989). Splitting the ciliary axoneme: implications for a "switch-point" model of dynein arm activity in ciliary motion. Cell Motil Cytoskeleton *14*, 345-358.

226. Satir, P., and Sale, W.S. (1977). Tails of Tetrahymena. J Protozool *24*, 498-501.

227. Saunier, S., R. Salomon, and C. Antignac. 2005. Nephronophthisis. *Curr Opin Genet Dev*. 15:324-31.

228. Schmidt, M., G. Gessner, M. Luff, I. Heiland, V. Wagner, M. Kaminski, S. Geimer, N. Eitzinger, T. Reissenweber, O. Voytsekh, M. Fiedler, M. Mittag, and

G. Kreimer. 2006. Proteomic analysis of the eyespot of Chlamydomonas reinhardtii provides novel insights into its components and tactic movements. *Plant Cell*. 18:1908-30.

229. Scholey, J.M. 2008. Intraflagellar transport motors in cilia: moving along the cell's antenna. *J Cell Biol*. 180:23-9.

230. Scholey, J.M., and Anderson, K.V. (2006). Intraflagellar transport and cilium-based signaling. Cell *125*, 439-442.

231. Schuermann, M.J., E. Otto, A. Becker, K. Saar, F. Ruschendorf, B.C. Polak, S. Ala-Mello, J. Hoefele, A. Wiedensohler, M. Haller, H. Omran, P. Nurnberg, and F. Hildebrandt. 2002. Mapping of gene loci for nephronophthisis type 4 and Senior-Loken syndrome, to chromosome 1p36. *Am J Hum Genet*. 70:1240-6.

232. Scott, J.D. 2003. A-kinase-anchoring proteins and cytoskeletal signalling events. *Biochem Soc Trans*. 31:87-9.

233. Sharma, N., Berbari, N.F., and Yoder, B.K. (2008). Ciliary dysfunction in developmental abnormalities and diseases. Curr Top Dev Biol *85*, 371-427.

234. Shingyoji, C., Murakami, A., and Takahashi, K. (1977). Local reactivation of Triton-extracted flagella by iontophoretic application of ATP. Nature *265*, 269-270.

235. Sillibourne, J.E., D.M. Milne, M. Takahashi, Y. Ono, and D.W. Meek. 2002. Centrosomal anchoring of the protein kinase CK1delta mediated by attachment to the large, coiled-coil scaffolding protein CG-NAP/AKAP450. *J Mol Biol*. 322:785-97.

236. Smith, E.F. (2002a). Regulation of flagellar dynein by calcium and a role for an axonemal calmodulin and calmodulin-dependent kinase. Mol Biol Cell *13*, 3303-3313.

237. Smith, E.F. (2002b). Regulation of flagellar dynein by the axonemal central apparatus. Cell Motil Cytoskeleton *52*, 33-42.

238. Smith, E.F. (2007). Hydin seek: finding a function in ciliary motility. J Cell Biol *176*, 403-404.

239. Smith, E.F., and Lefebvre, P.A. (1996). PF16 encodes a protein with armadillo repeats and localizes to a single microtubule of the central apparatus in Chlamydomonas flagella. J Cell Biol *132*, 359-370.

240. Smith, E.F., and Lefebvre, P.A. (1997). PF20 gene product contains WD repeats and localizes to the intermicrotubule bridges in Chlamydomonas flagella. Mol Biol Cell *8*, 455-467.

241. Smith, E.F., and Sale, W.S. (1991). Microtubule binding and translocation by inner dynein arm subtype I1. Cell Motil Cytoskeleton *18*, 258-268.

242. Smith, E.F., and Sale, W.S. (1992a). Regulation of dynein-driven microtubule sliding by the radial spokes in flagella. Science *257*, 1557-1559.

243. Smith, E.F., and Sale, W.S. (1992b). Structural and functional reconstitution of inner dynein arms in *Chlamydomonas* flagellar axonemes. J Cell Biol *117*, 573-581.

244. Smith, E.F., and Yang, P. (2004). The radial spokes and central apparatus: mechano-chemical transducers that regulate flagellar motility. Cell Motil Cytoskeleton *57*, 8-17.

245. Snell, W.J. (1976). Mating in Chlamydomonas: a system for the study of specific cell adhesion. II. A radioactive flagella-binding assay for quantitation of adhesion. J Cell Biol *68*, 70-79.

246. Snell, W.J., Pan, J., and Wang, Q. (2004). Cilia and flagella revealed: from flagellar assembly in Chlamydomonas to human obesity disorders. Cell *117*, 693-697.

247. Sturgess, J.M., Chao, J., Wong, J., Aspin, N., and Turner, J.A. (1979). Cilia with defective radial spokes: a cause of human respiratory disease. N Engl J Med *300*, 53-56.

248. Summers, K.E., and Gibbons, I.R. (1971). Adenosine triphosphate-induced sliding of tubules in trypsin-treated flagella of sea-urchin sperm. Proc Natl Acad Sci U S A *68*, 3092-3096.

249. Summers, K.E., and Gibbons, I.R. (1973). Effects of trypsin digestion on flagellar structures and their relationship to motility. J Cell Biol *58*, 618-629.

250. Swiatek, W., Tsai, I.C., Klimowski, L., Pepler, A., Barnette, J., Yost, H.J., and Virshup, D.M. (2004). Regulation of casein kinase I epsilon activity by Wnt signaling. J Biol Chem 279, 13011-13017.

251. Takada, S., Wilkerson, C.G., Wakabayashi, K., Kamiya, R., and Witman, G.B. (2002). The outer dynein arm-docking complex: composition and characterization of a subunit (oda1) necessary for outer arm assembly. Mol Biol Cell *13*, 1015-1029.

252. Tang, W.J., C.W. Bell, W.S. Sale, and I.R. Gibbons. 1982. Structure of the dynein-1 outer arm in sea urchin sperm flagella. I. Analysis by separation of subunits. *J Biol Chem*. 257:508-15.

253. Tyler, K.M., Fridberg, A., Toriello, K.M., Olson, C.L., Cieslak, J.A., Hazlett, T.L., and Engman, D.M. (2009). Flagellar membrane localization via association with lipid rafts. J Cell Sci *122*, 859-866.

254. Vallee, R.B., Williams, J.C., Varma, D., and Barnhart, L.E. (2004). Dynein: An ancient motor protein involved in multiple modes of transport. J Neurobiol *58*, 189-200.

255. Wakabayashi, K., S. Takada, G.B. Witman, and R. Kamiya. 2001. Transport and arrangement of the outer-dynein-arm docking complex in the flagella of *Chlamydomonas* mutants that lack outer dynein arms. *Cell Motil Cytoskeleton*. 48:277-86.

256. Wakabayashi, K., S. Takada, M. Hayashi, J. Usukura, G.B. Witman, and R. Kamiya. 2002b. Structure and property of the outer-dynein-arm docking complex (ODA-DC) studied using recombinant proteins. *In* The Tenth International conference on the Cell & Molecular Biology of *Chlamydomonas*., Vancouver, Canada. 167.

257. Wakabayashi, K., S.M. King, and R. Kamiya. 2002a. Analysis of proteins interacting with the outer dynein arm docking complex (ODA-DC) from *Chlamydomonas* by chemical crosslinking. *Mol Cell Biol*. 13, supplement:184a.

258. Walczak, C.E., and Nelson, D.L. (1994). Regulation of dynein-driven motility in cilia and flagella. Cell Motil Cytoskeleton *27*, 101-107.

259. Wargo, M.J., and Smith, E.F. (2003). Asymmetry of the central apparatus defines the location of active microtubule sliding in Chlamydomonas flagella. Proc Natl Acad Sci U S A *100*, 137-142.

260. Wargo, M.J., Dymek, E.E., and Smith, E.F. (2005). Calmodulin and PF6 are components of a complex that localizes to the C1 microtubule of the flagellar central apparatus. J Cell Sci *118*, 4655-4665.

261. Wargo, M.J., McPeek, M.A., and Smith, E.F. (2004). Analysis of microtubule sliding patterns in Chlamydomonas flagellar axonemes reveals dynein activity on specific doublet microtubules. J Cell Sci *117*, 2533-2544.

262. Warner, F.D., and P. Satir. 1974. The structural basis of ciliary bend formation. Radial spoke positional changes accompanying microtubule sliding. *J Cell Biol*. 63:35-63.

263. Wilkerson, C.G., King, S.M., Koutoulis, A., Pazour, G.J., and Witman, G.B. (1995). The 78,000 M(r) intermediate chain of *Chlamydomonas* outer arm dynein is a WD-repeat protein required for arm assembly. J Cell Biol *129*, 169-178.

264. Wirschell, M., C. Yang, P. Yang, L. Fox, H.A. Yanagisawa, R. Kamiya, G.B. Witman, M.E. Porter, and W.S. Sale. 2009b. IC97 Is a Novel Intermediate Chain of I1 Dynein That Interacts with Tubulin and Regulates Interdoublet Sliding. *Mol Biol Cell*.

265. Wirschell, M., D. Nicastro, M.E. Porter, and W.S. Sale. 2009a. The regulation of axonemal bending. *In* The *Chlamydomonas* Sourcebook: Cell Motility and Behavior. Vol. 3. G.B. Witman, editor. Academic Press, Oxford. 253-282.

266. Wirschell, M., F. Zhao, C. Yang, P. Yang, D. Diener, A. Gaillard, J.L. Rosenbaum, and W.S. Sale. 2008. Building a radial spoke: flagellar radial spoke protein 3 (RSP3) is a dimer. *Cell Motil Cytoskeleton*. 65:238-48.

267. Wirschell, M., G. Pazour, A. Yoda, M. Hirono, R. Kamiya, and G.B. Witman. 2004. Oda5p, a novel axonemal protein required for assembly of the outer Dynein arm and an associated adenylate kinase. *Mol Biol Cell*. 15:2729-41.

268. Wirschell, M., Hendrickson, T., and Sale, W.S. (2007). Keeping an eye on I1: I1 dynein as a model for flagellar dynein assembly and regulation. Cell Motil Cytoskeleton *64*, 569-579.

269. Witman, G.B. (1986). Isolation of *Chlamydomonas* flagella and flagellar axonemes. Methods in Enzymology *134*, 280-290.

270. Witman, G.B. (1993). *Chlamydomonas* phototaxis. Trends Cell Biol *3*, 403-408.

271. Witman, G.B., Plummer, J., and Sander, G. (1978). *Chlamydomonas* flagellar mutants lacking radial spokes and central tubules. Structure, composition, and function of specific axonemal components. J Cell Biol *76*, 729-747.

272. Wong, W., and Scott, J.D. (2004). AKAP signalling complexes: focal points in space and time. Nat Rev Mol Cell Biol *5*, 959-970.

273. Yagi, T., Minoura, I., Fujiwara, A., Saito, R., Yasunaga, T., Hirono, M., and Kamiya, R. (2005). An axonemal dynein particularly important for flagellar movement at high viscosity. Implications from a new Chlamydomonas mutant deficient in the dynein heavy chain gene DHC9. J Biol Chem *280*, 41412-41420.

274. Yagi, T., Uematsu, K., Liu, Z., and Kamiya, R. (2009). Identification of dyneins that localize exclusively to the proximal portion of *Chlamydomonas* flagella. J Cell Sci *122*, 1306-1314.

275. Yamamoto, R., Yagi, T., and Kamiya, R. (2006). Functional binding of inner-arm dyneins with demembranated flagella of *Chlamydomonas* mutants. Cell Motil Cytoskeleton *63*, 258-265.

276. Yang, C., and Yang, P. (2006). The Flagellar Motility of Chlamydomonas pf25 Mutant Lacking an AKAP-binding Protein Is Overtly Sensitive to Medium Conditions. Mol Biol Cell *17*, 227-238.

277. Yang, P., and Sale, W.S. (1998). The Mr 140,000 Intermediate Chain of Chlamydomonas Flagellar Inner Arm Dynein Is a WD-Repeat Protein Implicated in Dynein Arm Anchoring. Mol. Biol. Cell *9*, 3335-3349.

278. Yang, P., and Sale, W.S. (2000). Casein kinase I is anchored on axonemal doublet microtubules and regulates flagellar dynein phosphorylation and activity. J Biol Chem *275*, 18905-18912.

279. Yang, P., D.R. Diener, J.L. Rosenbaum, and W.S. Sale. 2001. Localization of calmodulin and dynein light chain LC8 in flagellar radial spokes. *J Cell Biol*. 153:1315-26.

280. Yang, P., Diener, D.R., Yang, C., Kohno, T., Pazour, G.J., Dienes, J.M., Agrin, N.S., King, S.M., Sale, W.S., Kamiya, R., Rosenbaum, J.L., and Witman, G.B. (2006). Radial spoke proteins of Chlamydomonas flagella. J Cell Sci *119*, 1165-1174.

281. Yang, P., Fox, L., Colbran, R.J., and Sale, W.S. (2000). Protein phosphatases PP1 and PP2A are located in distinct positions in the *Chlamydomonas* flagellar axoneme. J Cell Sci *113 (Pt 1)*, 91-102.

282. Yang, P., Yang, C., and Sale, W.S. (2004). Flagellar radial spoke protein 2 is a calmodulin binding protein required for motility in Chlamydomonas reinhardtii. Eukaryot Cell *3*, 72-81.

283. Yang, P., Yang, C., Wirschell, M., and Davis, S. (2009). Novel LC8 mutations have disparate effects on the assembly and stability of flagellar complexes. J Biol Chem.

284. Zariwala, M., P.G. Noone, A. Sannuti, S. Minnix, Z. Zhou, M.W. Leigh, M. Hazucha, J.L. Carson, and M.R. Knowles. 2001. Germline mutations in an intermediate chain dynein cause primary ciliary dyskinesia. *Am J Respir Cell Mol Biol*. 25:577-83.

285. Zhai, L., P.R. Graves, L.C. Robinson, M. Italiano, M.R. Culbertson, J. Rowles, M.H. Cobb, A.A. DePaoli-Roach, and P.J. Roach. 1995. Casein kinase I gamma subfamily. Molecular cloning, expression, and characterization of three mammalian isoforms and complementation of defects in the Saccharomyces cerevisiae YCK genes. *J Biol Chem*. 270:12717-24.